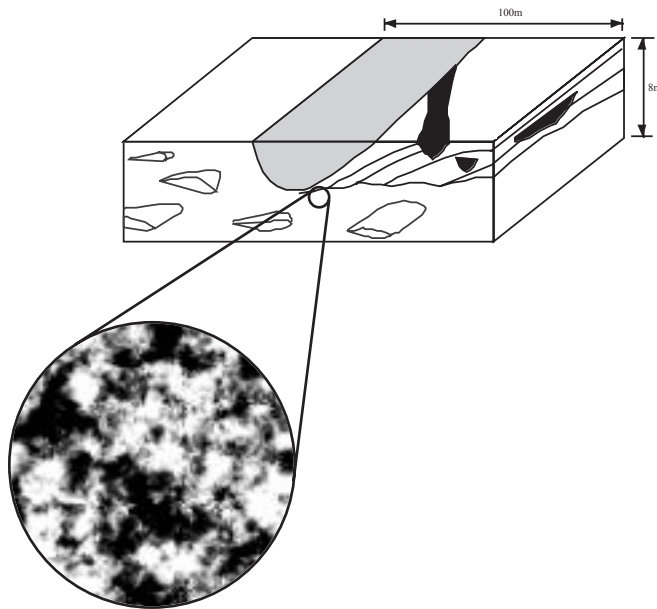


# Sedimentary Heterogeneity and Flow Towards a Well

Assessment of Flow Through Heterogeneous Formations



Joost Christiaan Herweijer

J.C. Herweijer, PO Box 967, Mt. Barker SA 5251, Australia, [Herwjc@gmail.com](mailto:Herwjc@gmail.com)

VRIJE UNIVERSITEIT

# **Sedimentary Heterogeneity and Flow Towards a Well**

Assessment of Flow Through Heterogeneous Formations

ACADEMISCH PROEFSCHRIFT

ter verkrijging van de graad van doctor aan  
de Vrije Universiteit te Amsterdam,  
op gezag van de rector magnificus  
prof.dr. E. Boeker,  
in het openbaar te verdedigen  
ten overstaan van de promotie commissie  
van de faculteit der aardwetenschappen  
op dinsdag 7 januari 1997 te 13.45 uur  
in het hoofdgebouw van de universiteit, De Boelelaan 1105

door

**Joost Christiaan Herweijer**

geboren te Utrecht

Promotor: prof.dr. J.J. de Vries

The conscientious review of this thesis by Prof.Dr. G. de Marsily (Université Paris VI) and Prof.Dr. G. Teutsch (Universität Tübingen) is gratefully acknowledged.

<b>GENERAL INTRODUCTION.....</b>	<b>1</b>
<b>1.1 INTRODUCTION</b>	<b>3</b>
<b>1.2 TECHNICAL PERSPECTIVE ON HETEROGENEITY</b>	<b>5</b>
<b>1.3 THE ROLE AND COSTS OF DATA IN DETERMINING HETEROGENEITY</b>	<b>8</b>
<b>1.4 SCOPE OF WORK</b>	<b>9</b>
<b>1.5 EXPECTATIONS</b>	<b>11</b>
<b>OVERVIEW OF LITERATURE AND METHODOLOGIES .....</b>	<b>13</b>
<b>2.1 PURPOSE AND SCOPE</b>	<b>15</b>
<b>2.2 SEDIMENTOLOGY: THE ARCHITECTURE OF HETEROGENEITY</b>	<b>15</b>
2.2.1 The importance of facies sequence and architecture	16
2.2.2 Geometries for sedimentary elements.	20
2.2.3 Models for Fluvial deposition	22
2.2.4 Hydraulic properties for sedimentary facies	26
2.2.5 Summary: the role of sedimentological data for fluid-flow models	27
<b>2.3 GEOSTATISTICAL MODELS FOR HETEROGENEITY</b>	<b>27</b>
2.3.1 Simulation of a gridded property using covariance structures	29
2.3.2 Modeling geological variability using geometrical shapes (objects)	43
2.3.3 Models based on genetic processes	45
2.3.4 Practical use of geostatistical models	46
<b>2.4 GEOSTATISTICS AND EFFECTIVE FLOW AND TRANSPORT PARAMETERS</b>	<b>49</b>
2.4.1 Effective hydraulic conductivity	51
2.4.2 Effective transport: macro-dispersion	53
2.4.3 Application of macro-dispersion concept: problems	56
2.4.4 Large-scale field experiments to assess macro-dispersion	58
2.4.5 Effective parameters versus geostatistical modeling	65
<b>2.5 USE OF PUMPING TESTS UNDER HETEROGENEOUS CONDITIONS</b>	<b>66</b>
2.5.1 Type-curves for heterogeneous formations	67
2.5.2 Use of drawdown derivative for aquifer diagnosis	69
2.5.3 Borehole flowmeter measurements to determine local conductivity	75
2.5.4 Geostatistical inversion of pumping test data	76
<b>EXAMPLE OF FLOW IN A HETEROGENEOUS AQUIFER: PUMPING TESTS AND TRACER TESTS AT COLUMBUS.....</b>	<b>79</b>
<b>3.1 INTRODUCTION</b>	<b>81</b>
<b>3.2 LOCATION AND HYDROGEOLOGICAL CONDITIONS</b>	<b>83</b>
<b>3.3 SEDIMENTOLOGY AND HETEROGENEOUS AQUIFER MODEL</b>	<b>84</b>
<b>3.4 FIELD PROGRAM</b>	<b>86</b>
3.4.1 Drilling wells following a "randomized" spatial distribution	86
3.4.2 Hydraulic (pumping) tests	88
3.4.3 Tracer Tests	94

<b>3.5 USING THE COLUMBUS FIELD DATA</b>	<b>98</b>
<b>INTERPRETATION OF PUMPING TESTS AT COLUMBUS.....</b>	<b>101</b>
<b>4.1 INTRODUCTION</b>	<b>103</b>
<b>4.2 PUMPING TEST ANALYSIS ASSUMING A LATERAL HOMOGENEOUS AQUIFER</b>	<b>104</b>
4.2.1 Analysis using delayed yield or delayed gravity drainage	105
4.2.2 Analysis based on the Theis equation	108
<b>4.3 ANALYSIS WITH TYPE-CURVES FOR LATERAL HETEROGENEITY</b>	<b>111</b>
4.3.1 Ring model (radial composite)	112
4.3.2 Strip model (linear composite)	114
4.3.3 Fractured rock (double-porosity) model	115
<b>4.4 ANALYSIS OF REGIONAL AND LOCAL CHANGES IN TRANSMISSIVITY</b>	<b>117</b>
<b>4.5 SMALL-SCALE MULTI-WELL PUMPING TESTS AND TRACER TESTS</b>	<b>121</b>
4.5.1 Analysis of the small-scale, multi-well, pumping tests	122
4.5.2 Analysis of the small-scale tracer tests	126
4.5.3 Low storage coefficients and highly permeable lenses	127
<b>4.6 CONCLUSION</b>	<b>128</b>
<b>GEOSTATISTICAL ANALYSIS OF THE COLUMBUS DATA .....</b>	<b>131</b>
<b>5.1 INTRODUCTION</b>	<b>133</b>
<b>5.2 ANALYSIS OF SPATIAL STATISTICS</b>	<b>133</b>
5.2.1 Uni-variate statistics of borehole flowmeter conductivities	135
5.2.2 Variograms for a Continuous Random Variable (Gaussian Field)	136
5.2.3 Indicator Variograms	138
<b>5.3 EFFECTIVE FLOW AND TRANSPORT PARAMETERS</b>	<b>139</b>
5.3.1 Averaging the Columbus conductivity data	140
5.3.2 Effective Dispersion (macro-dispersion)	145
<b>5.4 SUMMARY AND CONCLUSIONS</b>	<b>146</b>
<b>MODELS FOR PUMPING TESTS AND TRACER TESTS IN HETEROGENEOUS AQUIFERS COMPARABLE TO COLUMBUS .....</b>	<b>149</b>
<b>6.1 INTRODUCTION</b>	<b>151</b>
<b>6.2 FLOW AND TRANSPORT MODELING</b>	<b>152</b>
6.2.1 Setup of pumping test model	153
6.2.2 Setup of tracer test model	155
6.2.3 Modeling strategy	158
6.2.4 Type-curves for apparent macro-dispersivity	160
<b>6.3 FACIES MODEL FOR A COARSE-GRAINED POINTBAR</b>	<b>162</b>
6.3.1 Conceptual heterogeneity model and conductivity values	162
6.3.2 Results of pumping test model	164
6.3.3 Results of tracer test model	167
<b>6.4 A LOCAL OBJECT MODEL FOR CHUTE CHANNELS</b>	<b>170</b>
6.4.1 Description of the heterogeneity model	170

6.4.2 Results of pumping test model	171
<b>6.5 A GAUSSIAN MODEL FOR A COARSE-GRAINED POINTBAR</b>	<b>175</b>
6.5.1 Description of the heterogeneity model	176
6.5.2 Results of pumping test model	178
6.5.3 Results of tracer test model	183
<b>6.6 A NESTED-FACIES GAUSSIAN MODEL</b>	<b>190</b>
6.6.1 Description of the heterogeneity model	191
6.6.2 Results of pumping test model	192
6.6.3 Results of tracer test model	195
<b>6.7 DISCUSSION AND CONCLUSIONS</b>	<b>198</b>
<b>CONCLUSIONS AND PERSPECTIVE .....</b>	<b>203</b>
<b>7.1 SUMMARY OF RESULTS</b>	<b>205</b>
7.1.1 Reject Null Hypothesis: No single model describes a heterogeneous aquifer	208
7.1.2 Hypotheses: Heterogeneity can be derived from pumping test results	208
7.1.3 Hypothesis: Describing real variability requires a combination of models	211
7.1.4 Risk can more precisely be defined by constraining models	214
<b>7.2 SPECIFIC CONCLUSIONS AND OBSERVATIONS</b>	<b>214</b>
<b>7.3 GENERAL PERSPECTIVE</b>	<b>217</b>
<b>SAMENVATTING, CONCLUSIES EN PERSPECTIEF .....</b>	<b>219</b>
<b>8.1 SAMENVATTING</b>	<b>221</b>
8.1.1 De Nul Hypothese “Er is een éénvoudig model voor een heterogeen aquifer” werkt niet.	223
8.1.2 Hypothese: Heterogeniteit kan worden verwerkt in de pompproefanalyse	224
8.1.3 Hypothese: Een model voor heterogeniteit bestaat uit meerdere conceptuele modellen	227
8.1.4 Betere risico-analyse door inperking van variabiliteit	230
<b>8.2 PUNTSGEWIJZE CONCLUSIES EN OPMERKINGEN</b>	<b>231</b>
<b>8.3 EPILOOG EN PERSPECTIEF</b>	<b>234</b>
<b>SCREENING OF GEOSTATISTICAL RESERVOIR MODELS WITH PRESSURE TRANSIENTS .....</b>	<b>237</b>
<b>A.1 SUMMARY</b>	<b>239</b>
<b>A.2 INTRODUCTION</b>	<b>239</b>
<b>A.3 SEDIMENTARY HETEROGENEITY AND PRODUCTION TESTS</b>	<b>241</b>
<b>A.4 SIMULATION OF WELL TESTS FOR GEOSTATISTICAL MODELS</b>	<b>242</b>
<b>A.5 APPLICATIONS</b>	<b>243</b>
A.5.1 Case 1: A reservoir modeled using object techniques	244
A.5.2 Case 2: Horizon modeled with a Gaussian image	249
<b>A.6 CONCLUSIONS</b>	<b>258</b>
<b>REFERENCES .....</b>	<b>261</b>

<b>ACKNOWLEDGMENT.....</b>	<b>273</b>
<b>DANKWOORD.....</b>	<b>275</b>
<b>CURRICULUM VITAE.....</b>	<b>277</b>

## **CHAPTER 1**

### **GENERAL INTRODUCTION**

## 1.1 INTRODUCTION

Many practicing hydrogeologists intuitively realize that sedimentary heterogeneity can dramatically influence flow patterns and thus contaminant movement in sandy aquifers. Figure 1.1B shows an example of sedimentary heterogeneity. The different sedimentary facies have distinct hydraulic conductivities due to variations in granular texture and chemical diagenesis. Differences in conductivity cause preferential flow through the higher conductive material. This preferential flow affects the distribution of groundwater constituents such as contaminants or material injected to remove contaminants. It is now recognized that an inappropriate description of heterogeneity is

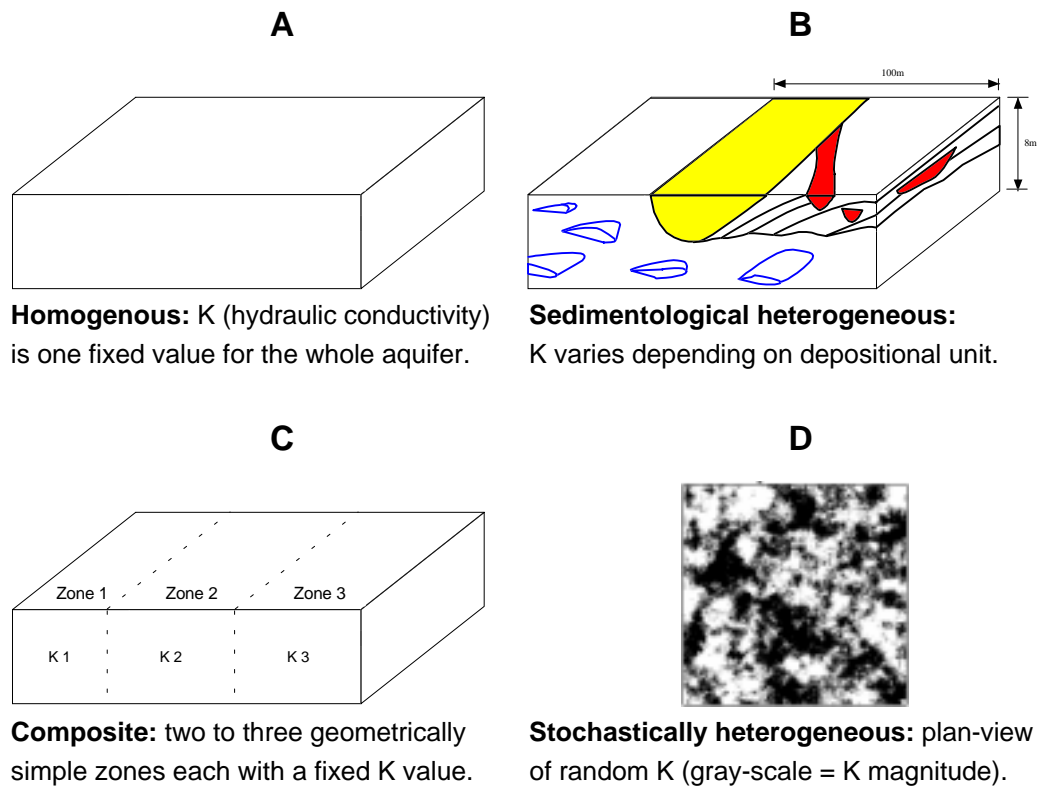


**Figure 1.1:** Homogeneous, composite, sedimentologically heterogeneous, and stochastically heterogeneous aquifer models.

often responsible for improperly designed, subsurface remediation systems such as pump-and-treat systems (Haley et al., 1991) and contaminant containment systems.

Sedimentological models, describing the depositional history of sands, are available for detailed description of heterogeneity, but are not often applied in hydrogeological studies. Their limited use is caused by the lack of reliable sedimentological field data, along with proven methods using sedimentological data efficiently and effectively to describe flow in heterogeneous aquifers. The application of sedimentology in hydrogeology seems caught in a vicious circle: lack of field data; limited use; no evidence of effectiveness; limited confidence in applicability; and no incentive to collect field data. This dissertation attempts to break this vicious circle.

Practical examples of the effects of heterogeneity on contaminant cleanup are: low conductivity geological heterogeneities that are not flushed by a specific pump-treat-inject cleanup, which was originally designed assuming homogeneity; and/or high conductivity zones causing fingers of a contaminant plume unforeseen by an analysis based on a homogeneous aquifer. The consequences of ignoring heterogeneity can cause serious political and economical complications (Parfit and Richardson, 1993). Unexpected migration of the contamination can result in extra costs and time for cleanup; additionally, it results in a loss of public confidence whether the problem is fully addressed or not. One apparently rigorous solution is an "over-design" catering to possible heterogeneity. Consequences of this "solution" can add large unnecessary expenses for cleanup while contributing to negative views about improper (over) spending for the environment. This dissertation presents research into field and modeling methods that realistically includes heterogeneity in the analysis of (contaminated) aquifers.

When designing this dissertation research, experience with petroleum geology and engineering offered valuable insights applicable to contaminant hydrogeology. Petroleum engineers deal with the removal of a valuable fluid (oil) from subsurface formations where it is trapped as pockets floating on and edged by worthless brine water. In the oil industry the primary objective is to produce all available oil and to avoid co-production of water. Neither objective is ever perfectly met. Generally only a part of the originally available oil volume is recovered, and significant amounts of water are co-produced at later stages of an oil field's production history. Geological heterogeneity is recognized as

an important variable determining the success of oil recovery (Weber, 1980). Oil can be left behind in isolated low permeable zones, and highly permeable zones can cause water to seek a preferential pathway towards production wells. History has taught the oil industry that underestimating heterogeneity can have important economical consequences for exploitation of a petroleum reservoir (e.g., Van Oert, 1988). It is now a well established practice to include heterogeneity when predicting reservoir performance.

Thus, there is clearly a broader of scope for sharing techniques between hydrogeology and petroleum engineering, notwithstanding the technical and cultural gap resulting from the different economical scales. In this dissertation an effort is made to bridge this gap. Petroleum engineering techniques are employed for hydrogeological purposes, and hydrogeological tools are used to address petroleum engineering problems.

## 1.2 TECHNICAL PERSPECTIVE ON HETEROGENEITY

Many methods available to hydrogeologists originate from the field of water resources assessment. Pumping tests are employed to determine well yield and the global hydraulic head response of aquifers given certain production stresses. Generally it has been sufficient to determine parameters for an equivalent homogenous (Figure 1.1B), or simple structured, aquifer consisting of several layers or zones (Figure 1.1C). For modern contaminant hydrogeology applications, however, not only the (average) hydraulic response is of interest, but also the tortuous geometry of flow paths that determines solute transport (see for example Herweijer et al., 1985). This dissertation elaborates the use of pumping test data to characterize these flowpaths, given a realistic heterogeneity based on sedimentary models. The facts that field pumping test data often do not follow the rules of the simplified models and that sedimentary heterogeneity might be responsible, have been previously recognized (see for example Kruseman and De Ridder, 1990). Table 1.1 summarizes these two different perspectives: pressure drawdown prediction for an effective homogeneous aquifer, and non-uniform pathway determination for a “realistic” heterogeneous aquifer.

Predictive tools, such as groundwater flow models, generally consist of a limited amount of large zones (homogeneous or composite model, see Figure 1.1A and Figure

**Table 1.1:** Different perspectives on a pumping test

	Water Resources	Contaminant Hydrogeology
Objective	Prediction of pressure drawdown	Determination of contaminant pathways
Aquifer description	Effective homogeneous	“Realistic” heterogeneous
Results	Single (average) values for hydraulic parameters	Spatial distribution of hydraulic parameters
Single-well test	Well-yield, aquifer-scale transmissivity	Local-scale transmissivity
Borehole flowmeter	Productive zones of a well	Hydraulic conductivity that represents a small scale
Multi-well test	Aquifer transmissivity, storage coefficient	Connectivity, heterogeneity model

1.1C) that are considered homogeneous and have uniform average properties. It is often assumed that these large homogeneous zones are adequate descriptors for an aquifer’s structure and behavior. Since this assumption is so widely accepted, most modeling methods are based on it. This fundamental assumption is formulated in this dissertation as a null hypothesis and much of this research attempts to determine its validity.

#### **Null Hypothesis:**

If one of the models (modeling methods depicted in Figure 1.1) fits to a limited set of field data (for example, a pumping test), then we have obtained an aquifer description that is reliable for a variety of predictions pertinent to the behavior of that aquifer.

Were no single model able to accurately describe a heterogeneous aquifer, then the rejection of this null hypothesis leads to two other hypotheses about dealing with multiple models (see Figure 1.1) and pumping tests:

**Hypothesis - 1:**

If different composite models can be found which fit the data of an aquifer's pumping test, then that heterogeneous aquifer can be characterized by reconciliation of the different composite models, along with its known sedimentological or other geological features.

**Hypothesis - 2:**

If the aquifer's pumping test data show a spatial variability that can not be fit with a homogeneous or composite model, then heterogeneity is a likely cause and these pumping test data can be used to predict contaminant flow which is predominantly a function of heterogeneity.

The fact that most groundwater flow and transport models consist of a limited number of large homogeneous zones with uniform average properties (see Figure 1.1C), is a similar perspective to traditional pumping test analysis: prediction of average flow; and disregard of non-uniform flow paths that sedimentary heterogeneities can cause. Contaminant transport is modeled by superimposing mechanical dispersion on these average flow patterns in turn representing tortuous flow paths through a heterogeneous medium. This approach was originally designed for laboratory columns of porous material and was generalized to aquifers. Field applications (e.g., Fried, 1979) and theoretical work (Matheron and de Marsily, 1980) have raised doubt as to whether or not the flow effects of sedimentary aquifer heterogeneity are appropriately covered.

In the more recent literature, macro-dispersion concepts (e.g., Gelhar, 1986) have been introduced to alleviate these concerns. These macro-dispersion models, however, are based on a restricted stochastic model that is not yet properly related to the reality of sedimentary heterogeneity. Field tracer tests (Boggs et al., 1992; Rehfeldt et al., 1992)

and transport models based on detailed sedimentological field data (Jussel, 1992) indicate that macro-dispersion may not correctly represent the impact of sedimentary heterogeneity on flow and transport.

Were the Null Hypothesis to be rejected, one realizes that for reliable modeling of groundwater flow and transport, multiple models should be considered. These multiple models should straddle different techniques for heterogeneity modeling, such as methods based on: sedimentological input (Figure 1.1B); methods based on stochastic conductivity fields (Figure 1.1D); and/or combinations of these. As such an ensemble of models is created that encompasses a broader and more realistic inclusion of aquifer heterogeneity, as opposed to the above described macro-dispersion concept. In this framework, field measurements can be used to select those models of the ensemble that fit the field data, as opposed to attempting to develop a single model that fits the field data. This leads to the following hypothesis:

**Hypothesis-3:**

If the objective is to make reliable, risk based, predictions using heterogeneous models, then one can not assume that a single conceptual model is perfect, and it is essential to use a range of possible concepts for aquifer heterogeneity models.

**1.3 THE ROLE AND COSTS OF DATA IN DETERMINING HETEROGENEITY**

Correct decisions can only be made after a multi-disciplinary assessment of the problem under investigation. A cost-benefit analysis similar to those in the oil industry, can uncover the relative value of different types of data. No data or method provide perfect understanding of an aquifer. A range of uncertainty remains for the prediction of aquifer behavior, like plume migration and cleanup efficiency. Therefore the most valuable data are those that contribute the most in narrowing predictive uncertainty.

This dissertation specifically focuses on the role of sedimentological data in conjunction with detailed pumping tests. The sedimentological data provide a three-dimensional framework for the composition of the subsurface. Sedimentological data

offer a relatively inexpensive way of using well data for predictions that stretch beyond the immediate vicinity of a well. However, sedimentological data are conceptual (not hard, but subjective) and do not provide a perfect subsurface description. Extra costs are involved in collecting sedimentological data. This goes often at the expense of collecting a larger quantity of data (more wells), or another type of data, such as geochemical data, that appear to be of similar importance to solving the issue under investigation.

The following example illustrates the choices often faced when designing cost effective prediction procedures. A contamination problem has been detected. Drilling several observation wells has roughly defined the extent of the contamination plume. To follow up, a certain fixed budget is available, allowing ten extra un-cored wells to be drilled for plume definition and migration monitoring. Many studies have shown that for heterogeneous cases, a large number of wells does not guarantee proper detection and complete removal of a contaminant plume (e.g., Boggs et al., 1992; Parfit and Richardson, 1993).

In contrast, the same budget can be allotted for five cored wells, including detailed description of the sediments. These data can be used to build a sedimentological model that offers a good opportunity to investigate lateral contaminant spreading, or at least the risks and uncertainty involved. Results presented in this dissertation may help to choose between hard data points and a global sedimentological model. At this moment the trade-off is often in favor of investment in more hard data points, rather than conceptual sedimentological knowledge. This dissertation proposes that a broad scope exists for closer integration of sedimentology into hydrogeological practice.

#### **1.4 SCOPE OF WORK**

This dissertation is an attempt to literally break ground for the above mentioned combination of field methods and modeling techniques to determine sedimentary heterogeneity and its consequences for groundwater flow. Multi-well pumping tests, classically used to determine average aquifer parameters, are employed to assess heterogeneity. This study presents a combination of tracer tests conducted in conjunction with multi-well pumping tests. These field data provide qualitative conclusions regarding

the possibility of predicting non-uniform tracer flow using multi-well pumping tests. The field experiment was conducted in 1989 and 1990 by the Tennessee Valley Authority (TVA) at the Columbus groundwater test site (Mississippi, USA). The shallow aquifer at this test site consists of strongly heterogeneous fluvial sands. This site has been used for several large-scale, natural gradient, solute transport, field experiments under the umbrella of what is known as the macro-dispersion experiment (MADE, Boggs et al., 1992). The pumping tests and forced gradient tracer tests presented in this dissertation were mainly conducted on a one hectare plot (the 1-HA test site) directly adjacent to the location of the MADE tracer tests.

As a follow up to the field work, numerical models are developed to simulate the pumping tests and the tracer tests. Several options for flow modeling are assessed with model input ranging from deterministic sedimentological geometries to property maps based on geostatistical models. The results of the various types of models are compared with the field observations. However, no attempt is made to perfectly match the field data. Rather, an analysis is made to determine which models capture specific trends in the field observations and which type of heterogeneity in each model is the cause. The resulting geostatistical models allow assessment of uncertainty in the aquifer response inherent to the uncertainty of sedimentological and hydraulic input parameters.

Geostatistics encompass all techniques, including deterministic sedimentology, for developing maps and three dimensional models of spatially variable properties. The advent of numerical techniques fueled by ever increasing, inexpensive, computing power, has made many geostatistical tools available. Each geostatistical modeling technique has pertinent assumptions that do not necessarily suit the studied case. A subjective decision has to be made as to which geostatistical modeling technique is the most appropriate given a certain heterogeneous aquifer. Thus, not only are geostatistical models used to validate the applicability of field tests in predicting non-uniform transport, but the field tests are also needed to validate the (choice of the) geostatistical modeling technique.

The principle of using pressure transients induced by pumping tests to analyze fluid-flow pathways in the subsurface, is generalized for use in petroleum reservoir engineering. A flow model is presented to investigate single-well test responses for strongly heterogeneous oil reservoir models based on geostatistical techniques. One application of such models is to test whether a modeled well test response corresponds

with field data. Multi-well pumping tests (pressure interference tests and/or three-dimensional pressure diffusion) are used in an approximate analysis of flow pathways in a heterogeneous reservoir. This approach compares two partially related processes, single-phase pressure diffusion and multi-phase flow (oil and water). Note the similarity to the use of multi-well pumping test results in predicting tracer transport.

### **1.5 EXPECTATIONS**

This dissertation presents and evaluates the results of field tests. The link between these test results and sedimentological phenomena will be revealed as completely as possible. Some alternative ways for interpretation are presented especially with respect to the pumping tests. In turn, this allows practitioners to detect heterogeneity and thus flow paths for solute transport by simple means.

This research study also presents an effort to model the field behavior. The primary aim of this modeling effort is to show that pumping test data can be used to describe solute transport (first breakthrough and peak breakthrough) characteristics of a heterogeneous aquifer. The models used are inspired by, but not exact reproductions of, the Columbus data set. The aim of this modeling effort is not necessarily to exactly reproduce measured data. Rather it is intended as an analysis of how important trends observed in the field can be adequately reproduced, and also what data and geostatistical techniques are the key to success. The main lesson drawn from this dissertation is how, and to what extent, a naturalistic phenomenological method (sedimentology) helps in understanding and modeling the hydraulic behavior of a natural heterogeneous aquifer.

## **CHAPTER 2:**

### **OVERVIEW OF LITERATURE AND METHODOLOGIES**

## 2.1 PURPOSE AND SCOPE

The purpose of this chapter is to review previously published work pertinent to the three main focuses of this dissertation: sedimentology, geostatistics, and pumping tests. Without exhaustively reviewing these topics, the following provides a, mostly non-mathematical, perspective of subsequently used methods. Sedimentological architecture related to depositional processes is the basis for understanding heterogeneity. Quantitative sedimentology allows sedimentological data to be used for constructing a coherent, three-dimensional, aquifer model of hydraulic conductivity. Geostatistical models can generate three-dimensional aquifer models that include uncertainty inherent in the sparsely available data. Effective parameters, such as average hydraulic conductivity and macro-dispersion, are discussed from a geostatistical perspective. Results are discussed of major, large-scale, field experiments conducted to assess solute transport in heterogeneous aquifers. Pumping test analysis is traditionally focused on homogeneous or composite systems (also see Figure 1A and 1C). A review is provided of how these "conventional" analysis methods interfere with strong heterogeneity. The borehole flowmeter method is discussed as a means of converting a single, well test transmissivity into a local-scale conductivity.

## 2.2 SEDIMENTOLOGY: THE ARCHITECTURE OF HETEROGENEITY

Hydraulic measurements on the local-scale can easily vary by several orders of

**Table 2.1:** Some simple sequence types in a sedimentary model predictability decrease downwards in this table.

Type of Sequence	Example Textural Sequence
gradual transitional	coarse - fine or fine - coarse
cyclic transitional	coarse - fine alternation
cyclical erosive features	coarse eroded in fine
chaotic erosive features	coarse eroded in fine
trends change after erosion	any sequence

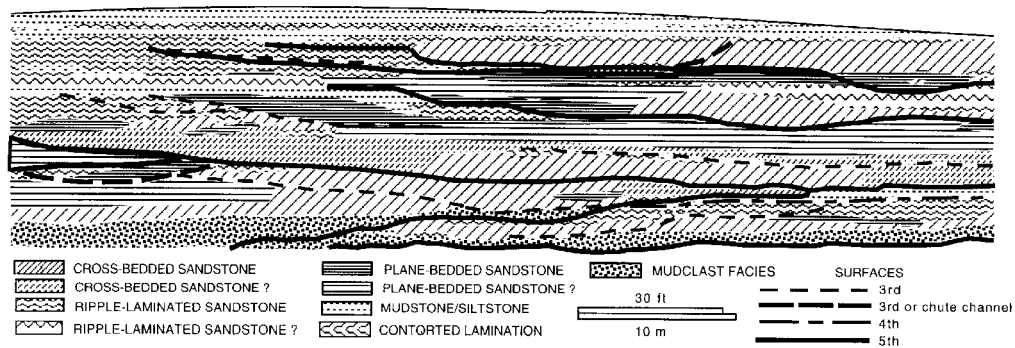


**Figure 2.1:** Example outcrop map of lithofacies (from Doyle and Sweet, 1995).

magnitude. It is hard to discern whether this variation reflects a large-scale trend, or is just a small-scale variability. Hydraulic measurements on a larger scale (pumping tests) are generally non-unique lumped averages. This implies that different spatial arrangements allow for the same effective behavior with respect to the pumping test, but not the same behavior with respect to another flow process, such as the migration of a solute. A sedimentological model is an indispensable added value allowing the establishment of a spatial framework for hydraulic conductivity; this is of preeminent importance for robust prediction of flow like the migration of a contaminant.

On a very small-scale (centimeter), hydraulic conductivity is related to textural characteristics of sand, such as grain size and sorting (e.g. Ridder and Wit, 1965). These textural characteristics are the result of a complex depositional process that determines the spatial arrangement of units (lithofacies) with similar textural and, consequently, hydraulic characteristics. Thus, effective hydraulic behavior on any practical field-scale (by definition larger than the centimeter scale), is dominated by the large-scale spatial arrangement of these units.

### 2.2.1 The importance of facies sequence and architecture

A simplified example of a schema describing what type of sequences can be expected in time and, hence, in space (vertical and horizontal), is shown in Table 2.1. Table 2.2 provides an example classification for fluvial sediments as proposed by Miall

**Table 2.2A:** Lithofacies classification (after Miall, 1988).

Code	Lithofacies	Sedimentary Structures	Interpretation
Gms	Massive, matrix-supported gravel	Grading	Debris-flow deposits
Fm	Massive or crudely bedded gravel	Horizontal bedding, imbrication	Longitudinal bars, lag deposits, sieve deposits
Gt	Gravel, stratified	Trough cross-beds	Minor channel fills
Gp	Gravel, stratified	Planar cross-beds	Longitudinal bars, deltaic growths from older bar remnants
St	Sand, medium to very coarse, may be pebbly	Solitary or grouped trough cross-beds	Dunes (lower flow regime)
Sp	Sand, medium to very coarse, may be pebbly	Solitary or grouped planar cross-beds	Linguoid, transverse bars, sand waves (lower flow regime)
Sr	Sand, very fine to coarse	Ripple marks	Ripples (lower flow regime)
Sb	Sand, very fine to very coarse, may be pebbly	Horizontal lamination, parting or streaming lineation	Planar bed flow (upper flow regime)
Sl	Sand, very fine to very coarse, may be pebbly	Low-angle (<10 degrees) cross-beds	Scour fills, washed out dunes, antidunes
Se	Erosional scours with intraclasts	Crude cross-bedding	Scour fills
Ss	Sand, fine to very coarse, may be pebbly	Broad, shallow scours	Scour fills
Fl	Sand, silt, mud	Fine lamination, very small ripples	Overbank or waning flood deposits
Fsc	Silt, mud	Laminated to massive	Backswamp deposits
Fef	Mud	Massive with freshwater mollusks	Backswamp pond deposits
Fm	Mud, silt	Massive, desiccation cracks	Overbank or drape deposits
C	Coal, carbonaceous mud	Plant, mud films	Swamp deposits
P	Carbonate	Pedogenic features	Paleosol

(1988). Lithofacies (Table 2.2A) are the principle components that can be obtained from rock samples (cores, outcrops, also see Figure 2.1). From a lithofacies assemblage one can interpret the type of architectural elements that can subsequently be related to a geometry (right column of Table 2.2B).

Note that the same lithofacies occur for several different elements. For example, lithofacies *St* (Sand, medium to very coarse, may be pebbly) can occur in channels, sandy bedforms, and downstream accretion macroforms. This non-uniqueness implies that properly diagnosing a sedimentary environment requires a combination of lithofacies and their sequence of occurrence, including the type of transition and the bounding surfaces

**Table 2.2B:** Architectural elements in fluvial deposits (after Miall, 1988)

Element	Symbol	Principal lithofacies	Geometry and relations
Channels	CH	Any combination	Finger, lens, or sheet; concave-upward erosional base; scale and shape highly variable; internal secondary erosion surfaces common
Gravel bars and bed forms	GB	Gm, Gp, Gt	Lens, blanket; usually tabular bodies; commonly interbedded with SB
Sandy bed forms	SB	St, Sp, Sh, Sl, Sr, Se, Ss	Lens, sheet, blanket, wedge; occurs as channel fills, crevasse splays, bar tops, minor bars
Downstream accreting macroform	DA	St, Sp, Sh, Sl, Sr, Se, Ss	Lens lying on flat or channeled base, with convex upward third-order internal and upper bounding surfaces
Lateral accretion deposit	LA	St, Sp, Sh, Sl, Sr, Se, Ss, less commonly G and F	Wedge, sheet, lobe; characterized by internal lateral accretion surfaces
Sediment gravity flow	SG	Gm, Gms	Lobe, sheet; typically interbedded with GB
Laminated sand sheet	LS	Sh, Sl, minor St, Sp, Sr	Sheet, blanket
Overbank fines	OF	Fm, Fl	Thin to thick blankets; commonly interbedded with SB; may fill abandoned channels

(see Table 2.1 and the right column of Table 2.2B). The non-uniqueness also implies that there is no one-to-one relation between lithofacies and hydraulic conductivity. Conductivity patterns typically follow sedimentary patterns in a diffuse mode, and geostatistical characterization (Section 2.3.1) solely based on conductivity (i.e., lithofacies) measurements, may fail to diagnose these conductivity patterns. The implication for geostatistical modeling of this non-uniqueness, is that a two or more step modeling procedure is preferred from a sedimentological point of view; first modeling of architectural elements takes place, followed by fine-scale, conductivity, infill models.

Thus, on the field-scale it is easy to envisage two or three separate scales of nested sedimentary heterogeneity and even more complex, hydraulic conductivity patterns. In contrast Gelhar's (1986) suggestion, the separation of the scales, may not be clear at all (also see Section 2.3.1 and Section 2.4). Tables 2.1 and 2.2 show that chaos, structure, transition, and erosion are intermingled causing complex combinations of different rock types. Thus, describing heterogeneity using a single (mathematical) formalism, appears

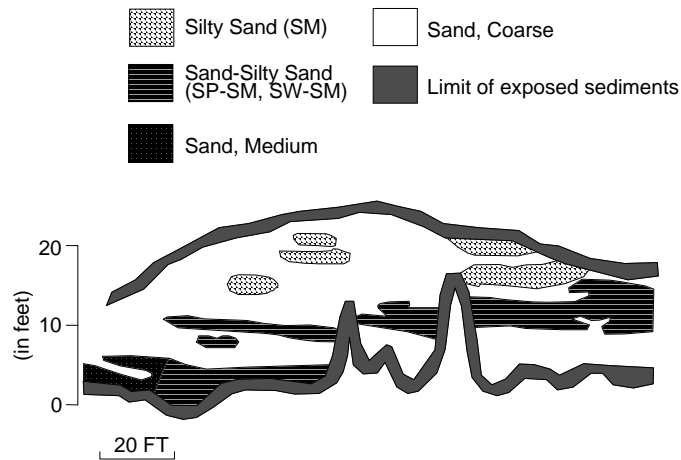


**Figure 2.2A:** Example outcrop used for quantitative sedimentological characterization (Excavation in Bentley Terrace, after Wu et al., 1973).

incorrect. Empirical modeling procedures are preferred that incorporate, as much as possible, different types of information regarding geometry and distribution of architectural elements (see Section 2.3). The schema proposed by Miall (1988) may not directly transfer to every case. It is important to stress, however, that the general methodology of identifying lithofacies and their associations prevails as a tool to unravel the sedimentological subsurface architecture.

Sedimentology has traditionally been a qualitative discipline; it provided mostly conceptual models and rarely quantitative data, such as dimensions and hydraulic properties of sedimentological units. This approach has been reversed over the last decade in conjunction with the increasing popularity of geostatistical models for subsurface heterogeneity (see Section 2.3). For petroleum engineering applications a strong trend emerged using sedimentological data for quantification of subsurface heterogeneity (for an overview see Bryant and Flint, 1993). The following summarizes some of the quantitative sedimentological data that is currently available.

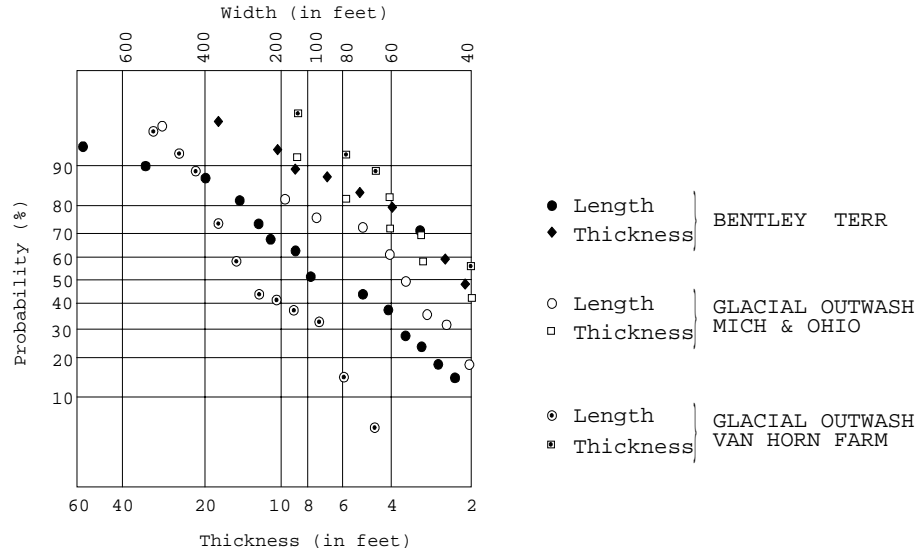


**Figure 2.2B:** Width-Thickness data derived from terrace and outwash deposits (after Wu et al., 1973; see also Figure 2.2A).

**2.2.2 Geometries for sedimentary elements.**

Montadert (1963) has been one of the first to present measurements on an outcrop of a shaley sandstone as a quantitative analog for reservoir heterogeneity. The sand shale section that he presented has been used by several researchers as a model for oil reservoirs or aquifers (e.g. Desbarats, 1987, 1990). Figure 2.2A shows one of several outcrops studied by Wu et al. (1973). They present data pertaining to the width and thickness of sedimentary structures in Mississippi terrace deposits (Figure 2.2B). Combined with estimated hydraulic conductivities, these data were the basis for an object-based probabilistic model (see also Section 2.3.2) used to estimate seepage under dams in the Mississippi (Wu et al., 1973).

On the basis of modern river data Leeder (1973) identified a relationship between the width and thickness of fluvial channels. Especially for meandering channels, a power

relation could be obtained providing an easy means to calculate width from thickness using the following relation:

$$w = 6.8 h^{1.34} \dots\dots\dots (2.1)$$

w = bankful width (m); h = bankful depth (m)

This data base has been enhanced and generalized for other types of fluvial channels, and now also include data from ancient rivers obtained from outcrops (Fielding and Crane, 1987; Bryant and Flint, 1993). These data are frequently used for object based, geostatistical models (Section 2.3.2) aimed at modeling oil reservoirs comprised of fluvial sediments. Swanson (1993) provides examples of how this type of data is used in a more deterministic framework of oil reservoir characterization. For practical application, it is often difficult to separate channel belts from individual channels when one is limited to down-hole data of ancient sediments (Budding et al., 1988; Lorenz et al., 1985).

Joseph et al. (1993) present a quantitative description of delta-lobe sediments. They present a detailed three-dimensional model obtained from sedimentological descriptions along several perpendicular cliffs combined with infill core holes. This model has been used as a “truth case” to test geostatistical modeling techniques (see Section 2.3.3). Weerts and Bierkens (1993) present a variogram analysis of the thickness of overbank deposits that occur as discontinuous stringers between channel sands in a the large Rhine-Meuse Valley in the Netherlands. Jussel (1992) and Jussel et al. (1994a; 1994b) present detailed sedimentological descriptions of coarse, fluvio-glacial gravel studied in Huntwangen, Switzerland. This description follows the advancing face of a gravel exploitation pit, resulting in a unique detailed data-set of the three-dimensional, spatial distribution of unconsolidated sedimentary facies and related lithologies.

Another important issue is determining directional trends from sedimentary structures. For shallow modern sediments, directional trends can often be determined from geomorphological features. A detailed analysis for ancient formations can be based on an analysis of sedimentary dips representing various types of cross-bedding and related to sedimentary transport directions. Geophysical, well-logging tools are available to measure sedimentary dips, but applications are mostly confined to consolidated

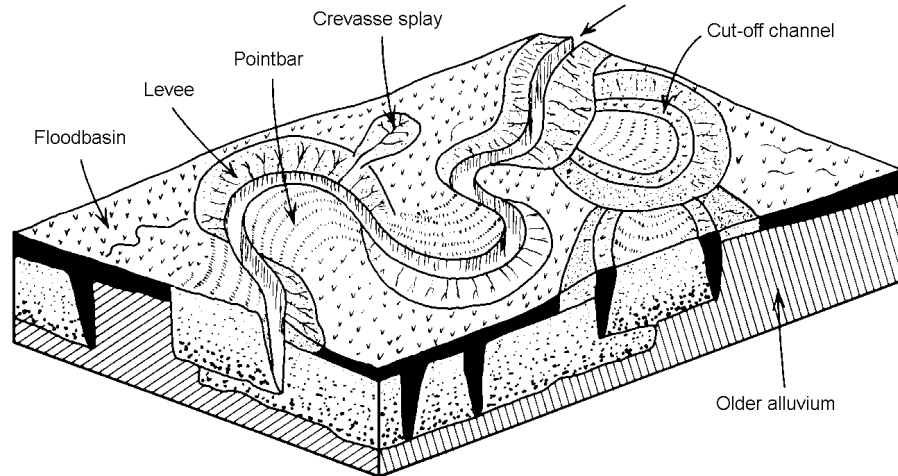


**Figure 2.3:** Traditional model for channel/pointbar deposition (from Freeze and Cherry, 1979).

sediments found at greater depth (Höcker et al., 1990). Moreover, the interpretation of local-scale dips towards directional trends, is not unambiguous (Herweijer et al., 1990). Further development of this technique requires considerable research (Bryant and Flint, 1993).

### 2.2.3 Models for Fluvial deposition

The following two sections provide short summaries for two major categories of fluvial deposits pertinent to the architecture of the shallow unconfined aquifer at the Columbus, groundwater, test site.

#### *Pointbar deposits*

Figure 2.3 shows the classical model for the sedimentation of sands in a channel/pointbar system. The pointbar is the inner bend of the meandering active channel where the majority of deposition occurs. The grain size of the deposited sands ranges from

medium-coarse at the edge of the active channel, to very-fine at a distance from the channel. Due to outward channel migration, a typical vertical sequence at a specific location shows a fining upward trend, with clay drapes occurring in the top half of the sequence.

Occasional breakout through the channel edge causes the deposition of crevasses. A crevasse consists of a relatively coarse feeder channel, along with a lobe of fine to very fine material. During high flood stage regular overflowing of the channel edges causes the deposition of fine levee material parallel to the outer bend outside the active channel. Cut-off or abandoned channels are partly filled with very coarse material (in transport at cut-off) and less coarse material, as fine as clay, deposited at suspension from the oxbow lake. All material is deposited in a flood plain consisting of fine material (clay) that shows terrestrial signs, like roots from vegetation and drying cracks.

At Columbus geomorphological and air photo data indicate that the upper half of the aquifer was deposited by a meandering channel/pointbar system. On the pointbar side, however, the grain size of the gravely sands is coarser than would be predicted by the classical pointbar model. The observed abrupt changes in the vertical sequence and the absence of the typical fining upward trend, point to more catastrophic depositional events. Such events resulted in an uneven sand distribution and more chaotic occurrence of gravel lenses and clay drapes (Collinson and Thompson, 1989).

Figure 2.4 shows a cross section (A) and an aerial view (B) representative of two

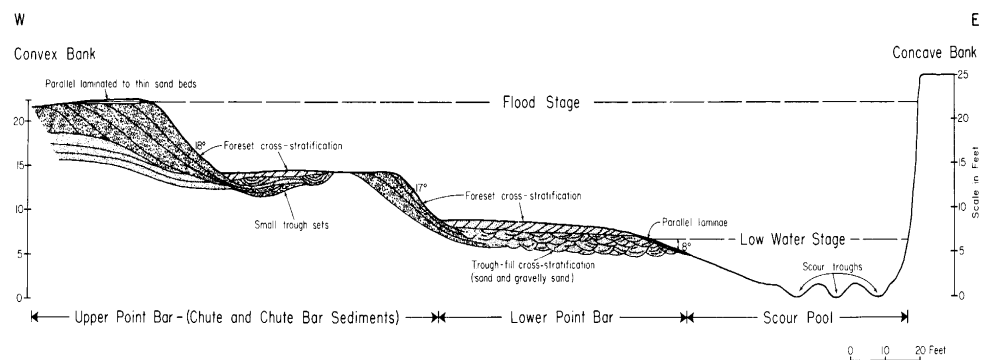


**Figure 2.4A:** Cross section of a modern coarse grained pointbar (from McGowen and Garner, 1971).

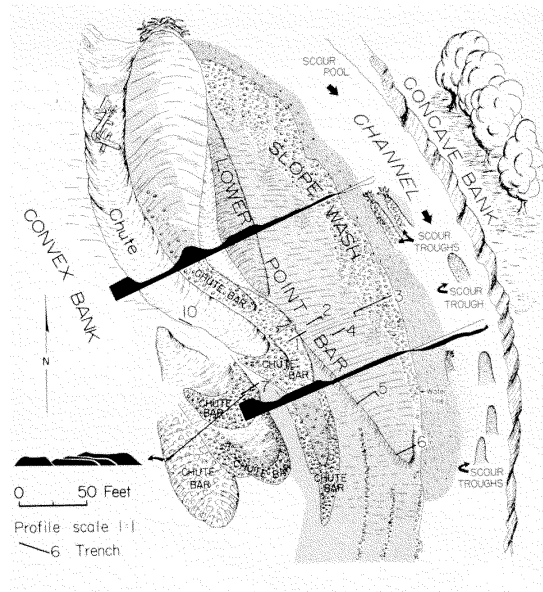


**Figure 2.4B:** Areal view of a modern coarse grained pointbar (from McGowen and Garner, 1971).

modern pointbars of the Amite River in Louisiana described by McGowen and Garner (1971). This cross section shows a three-tier system: channel floor; lower pointbar; and upper pointbar. At low water stage only the channel and a small part of the lower pointbar is active and under water. In compliance with the classical pointbar model, coarse sand is deposited in the channel and finer sand is deposited in the area of the active lower pointbar.

During the infrequent, high water (flood) stage, the entire pointbar becomes active. During these catastrophic events, small chute channels suddenly break through the upper pointbar depositing very coarse, gravely material as chute bars (shown on the left of Figure 2.4B). When the flood recedes, the chute channels are abandoned; from the stagnant water in these chute channels, a clay drape is deposited. The following dimensions of these chutes are given by McGowen and Garner (1971): depth 1.2 to 1.5 m; width 5 to 7 m; and length 30 to 150 m. Investigating similar sediments from the Upper Congaree River in South Carolina, Levey (1978) indicates the following

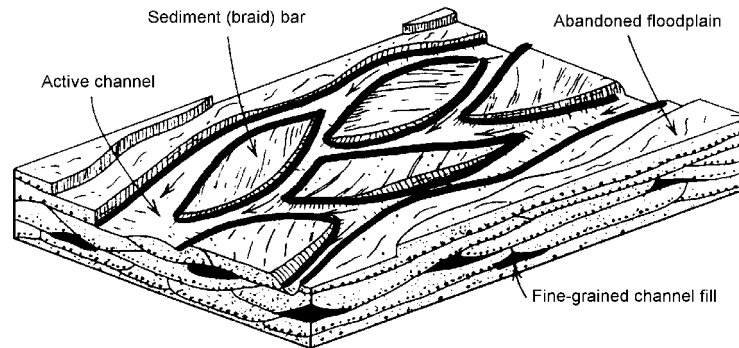


**Figure 2.5:** Model for braided river deposition.

dimensions for chute channels: depth 0.3 to 1 m; and width 3 m. He indicates for chute bars: width 2 to 8 m; and length 10 m to 100 m. Clearly, when considering the scale of this project test site, these deposits are major heterogeneities with a large potential impact on groundwater flow and contaminant transport.

#### *Braided River Deposits*

A braided stream model implies an irregular pattern of coarse gravely lenses deposited as braid bars at high flow stage and alternating with finer sediments deposited in the channels at low flow stage. Patterns can drastically change during a single, large, run-off event. Figure 2.5 shows a schematic diagram representing braided river deposition. Detailed studies of braided stream deposits are less common than those of pointbars (Reineck and Sing, 1986). Levey (1978) points out the similarities between chute channel and bar deposition on upper pointbars and braided stream depositions. These findings support the gradual transition at the Columbus, 1-HA, test site from coarse-grained, pointbar sediments to braided stream sediments. The rapidly changing bar and channel patterns result in units that are laterally smaller than the chute channels and chute bars presented earlier.

#### 2.2.4 Hydraulic properties for sedimentary facies

Oil field wells are regularly cored and a wealth of case specific, conductivity data is available based on measurements for (plug) samples from these cores. Weber (1980) and Weber and van Geuns (1989) summarize the approach for relating the conductivity data to sedimentary facies and architectural elements. This approach allows qualitative assessment of lateral continuity of conductivity on the basis of the facies to which plugs belong. Given the large distance between oil wells, however, there is limited, detailed, quantitative data on the lateral variation of conductivity.

Most studies that combine conductivity measurements with detailed sedimentological description, employ a mini-(air)-permeameter (Eype and Weber, 1971). This tool allows systematic *in situ* conductivity measurements on exposed material. Goggin et al. (1986) present measurements on an ancient Eolian sandstone. They present an extensive geostatistical characterization for these deposits (also see Section 2.3.1). They conclude that on a 100 m-scale, three nested orders of conductivity heterogeneity can be discerned. The largest two of these *nested-scales* are related to specific, dune, stratification patterns determining the permeability distribution. The smallest scale can be considered “noise”.

The variograms presented show a periodic- or hole-effect. This typical variogram behavior is related to repetitive or cyclic deposition (Table 2.1) and deviates from variograms normally used to describe heterogeneous conductivity fields (also see Section 2.3.1). Thus, when an aquifer straddles several facies, it is not completely valid to assume stationarity which implies a statistically homogeneous aquifer.

Jordan and Pryor (1992) present a detailed sedimentological investigation of a Mississippi meander deposit accompanied by mini-permeameter conductivity measurements. They conclude that depositional processes largely determine conductivity patterns. Davis et al. (1991) present mini-permeameter and sedimentological investigations of Rio Grande sediments that are exposed in large outcrops. They also find a distinct relation between the spatial conductivity distribution and sedimentary patterns. Variograms presented also show a periodic behavior or hole-effect.

### 2.2.5 Summary: the role of sedimentological data for fluid-flow models

Sedimentology is a tool for analyzing heterogeneous structures relevant to fluid-flow related to the depositional history of unconsolidated formations and rocks. It allows one to determine the analogy between subsurface formations and superficial material that can be inspected in detail (i.e., as well exposed outcrops or modern depositional systems). Appropriate sedimentological data allow one to reconstruct how subsurface material was transported and under which conditions it was deposited. Using this knowledge a geometrical model of architectural elements lumping together several lithofacies, can be established. A quantitative sedimentological model can be established if, likewise the current practice in petroleum geology, empirical relations for geometry dimensions are available from a "library" allowing selection of a data-set representative of the subsurface formation studied.

Field data from detailed outcrop studies combined with *in situ* hydraulic conductivity measurements, show a strong correlation between the conductivity distribution and depositional trends. For a subsurface application a quantitative correlation between lithofacies, can always be obtained from well (core) data. This relation, however, solely represents the local (point-support) scale.

Sedimentology is a practical and cost-efficient tool allowing one to obtain a spatial model based on these sparse, point-support, conductivity data. Sedimentology is based on simple data (i.e., rock samples; cores; trenches; and/or air-photos) and serves as valuable additional information for conductivity measurements. The latter is in contrast to unbiased measurements on a very dense grid. Both the geometrical model and the lithology versus hydraulic property relation, have a considerable uncertainty range; an uncertainty that is reflected by an integrated geostatistical model.

## 2.3 GEOSTATISTICAL MODELS FOR HETEROGENEITY

Most geologic information is available in qualitative form or, at best, in one- or two-dimensional quantification, such as vertical sequences from wells and outcrop-face descriptions. Geostatistical models are the only way to create a full three-dimensional representation that integrates geological and/or hydraulic information for every point in

the model space. Geostatistical models also include the uncertainty inherent in sparse subsurface information.

Traditionally, information gaps are bridged by interpolation of properties and geological horizons. A single unique representation of the subsurface is created. This yields a smooth structure that is unrealistic when comparing it to natural irregularity. Kriging is such an interpolation method. Although rooted in a specific geostatistical formalism, it is limited to a single optimal interpolation representing average reality while including error to cover uncertainty.

In contrast, geostatistical modeling aims at creating more than one possible representation of the subsurface with irregularity based on statistical characteristics of the subsurface. These characteristics are condensed in a limited set of parameters, for example the spatial covariance function. The subsurface is recreated in a model that has a random component reflecting the unknown fluctuation of the property or shape modeled. Different representations can be created based on the same characteristic parameters. This multiplicity is a measure of the uncertainty inherent in incomplete knowledge of the subsurface.

Two main categories of geostatistical models are distinguished:

- 1- **Pixel or grid models** based on a random function, mainly defined by a covariance function (variogram); this random function can be, for example, hydraulic conductivity (continuous) or facies number (discrete)
- 2- **Object models** based of geometrical shapes (objects) randomly distributed in space; for each object a size is drawn from an empirical probability density function that characterizes the facies represented by that object.

All geostatistical modeling procedures have two stages:

- 1- **Characterization:** statistical characteristics are derived from basic data (i.e., local property measurements; analog data such as outcrops; or simply one's best estimate based on general geological expertise).

- 2- **Simulation:** construction of a model that honors the statistical characteristics determined in stage one, well data if available, and additional constraints.

During the second stage several different representations can be constructed that honor the same statistical characteristics and constraining well data. These different, but equally possible, representations are called realizations. A geostatistical model can be analyzed to determine a certain property (e.g. volume) or hydraulic performance (e.g. drawdown in an area surrounding a well and/or first breakthrough of a tracer) of the model. Such an analysis has to be repeated for a number of different realizations. This procedure is known as the Monte Carlo procedure; it yields a result distribution for a property or a performance characteristic that covers a relevant expected value and an uncertainty range.

In the following sections some important concepts and techniques are discussed that have been published in the field of geostatistical heterogeneity modeling. These techniques have been applied in hydrogeology and petroleum engineering. Additionally, the macro-dispersion concept will be discussed; it is very closely related to the Gaussian covariance models (presented in the following sections).

### 2.3.1 Simulation of a gridded property using covariance structures

The covariance structure (also known as correlation structure or semi-variogram) is the second statistical moment of a spatial distribution. It is the spatial equivalent of the standard deviation of the well known, Gaussian (normal), probability, density function. For a specific property, Gaussian distributed values can be generated on a grid given a variogram and honoring given well data (conditioning data). This conditional simulation of a Gaussian field for a continuous variable (i.e., hydraulic conductivity), has been the traditional method of choice (Journel and Huijbregts, 1978). If the distribution is non-Gaussian, a “normal score transform” is used prior to the conditional simulation to make it Gaussian, followed by a back transform after the simulation (Deutsch and Journel, 1992). Matheron et al. (1987) and Journel and Alabert (1988) present methods that allow one to simulate gridded values of a discrete variable (i.e., a hydraulic conductivity class

or a facies indicator). Hewett (1986) simulates a continuous variable using a fractal method. Isaaks and Srivastava (1989) present a practical overview of theory and applications covering a suite of grid-based, covariance, characterization techniques. Deutsch and Journel (1992) provide an overview of numerical implementations and a computer software library pertinent to geostatistical characterization and simulation techniques.

The above mentioned simulation methods should not be confused with Kriging (Journel and Huijbregts, 1978), which is a widely used geostatistical interpolation method. Kriging is an optimal estimation on a grid of a Gaussian distributed property, given a limited number of data-points and a certain covariance structure. For every grid-point Kriging yields a single unique estimation of the average reality. This smooth average reality rarely coincides with reality. In contrast realizations of a geostatistical model obtained through simulation are rugged (not smooth) and could be close to reality.

*Variogram: definition, determination by simple means, and models*

All of the grid-based techniques require characterization of a data-set using a variogram. The variogram is a measure of a property's variability between pairs of data-points. The variogram is a function of the "distance between pairs", or lag. For a certain fixed lag, the variogram function-value is the variance of all possible pairs with that fixed lag-distance. When data are sparse, as is often the case, it is impossible to have a significant number of pairs with small lag-distances. In those cases a variogram has to be inferred from common geological knowledge (soft data) and/or measurements conducted for analogous systems. When sufficient data are available a variogram can empirically be determined. The latter is usually limited to the case for vertical variograms estimated from data along a well-bore. Horizontal variograms can seldom be accurately estimated from hard data (e.g., conductivity measurements), so additional soft data (e.g., qualitative geological descriptions) are mostly used.

The next procedure is a simplified schema illustrating the calculation of an experimental variogram. Suppose that a large number of spatially distributed

measurements is available for a property (i.e., hydraulic conductivity for a large number of spatially distributed wells), the procedure consists of the following steps:

- 1- Determine all lag-distances between well-pairs.
- 2- Make a table of  $\Delta K$  (difference of conductivity) for each of these pairs.
- 3- Rank the table according to lag-distances.
- 4- Divide the table in groups with similar lag-distances and number of pairs.
- 5- Calculate for each group the average lag-distance.
- 6- Calculate for each group the variance of  $\Delta K$ .
- 7- Plot variogram: variance of  $\Delta K$  from 6 versus lag-distance from 5.

Since values close together are fairly similar, a group based on pairs with a certain small distance will have a small variability. Thus, this group will be narrowly distributed and will have a small variance. Assuming that values at larger distances are less related, groups for larger distances will exhibit more variability and, thus, a larger variance. To assess anisotropy of a spatial distribution, variograms are calculated independently in

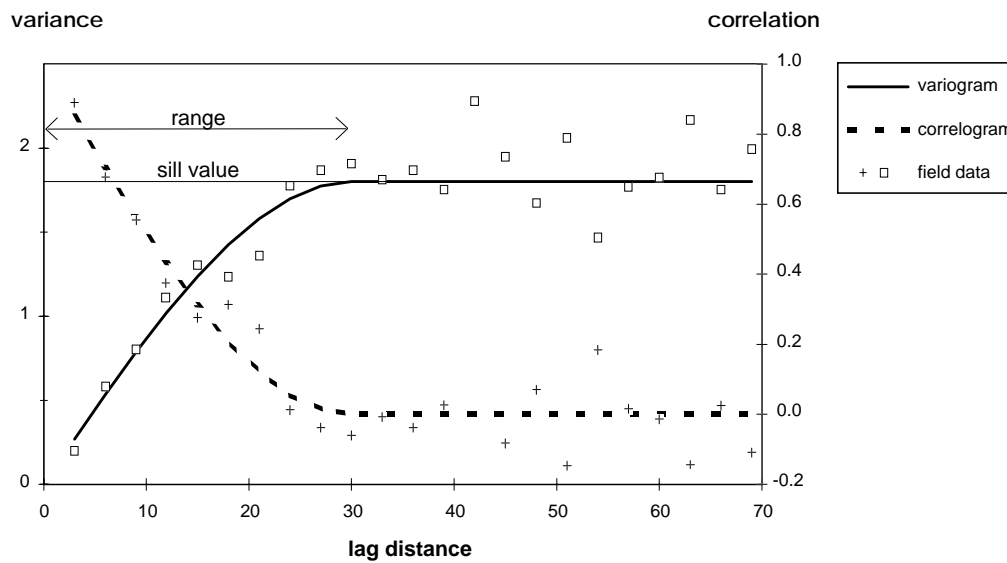


**Figure 2.6:** Example of variogram and correlogram (spherical model).

several directions (vertical and horizontal). An exhaustive variogram is a contour plot of variograms calculated in multiple directions (Isaaks and Srivastava, 1989). Exhaustive variograms are only calculated for extremely detailed data-sets, for example a seismic attribute obtained from a three-dimensional seismic survey (Haas and Dubrule, 1994).

In order to efficiently use the variogram for Kriging and simulation procedures, several analytical models have been proposed. Figure 2.6 shows an example of a spherical variogram. Most models show asymptotic behavior of the variance for increasing lag-distance, a feature that corroborates most experimental variograms obtained from field data. The asymptote, the sill, is the variance of all data pairs, regardless of the lag-distance. The lag-distance for which a constant (semi-)variance value is reached, is called the range.

A correlogram value is one minus the normalized variogram value (divide by sill value). The correlogram can be read as the probability to find a similar value at a certain lag-distance. This probability is 1 for lag-distance 0, and this probability approaches 0 for large lag-distances.

The correlation length is defined as the lag for which the correlogram reaches the value  $1/e$ , for example when the variogram reaches the value  $\sigma^2(e-1)/e$  (where  $\sigma$  = sill value,  $e$  = exponential). A formal definition of the variogram along with a detailed presentation of variogram models can be found in several handbooks, such as Journel and Huijbregts (1978), de Marsily (1986), or Isaaks and Srivastava (1989).

#### *Variograms (and co-variograms) of a discrete variable (Indicator)*

The above demonstrated variogram is pertinent to a continuous random function. All values possible for a property (i.e., hydraulic conductivity) are lumped in a single analysis. Flow in a natural geological system, however, can be determined by the spatial continuity of a small fraction of the subsurface. For example, very coarse, sand facies or tight shale streaks, can dominate flow-patterns, while volumetrically being unimportant. Journel and Alabert (1988) demonstrate for a large rock sample that spatial continuity is different for different, extreme (low/high), property values. They propose the indicator

**Table 2.3:** Anisotropic range for indicator variograms representing different architectural elements in a Turbidite sandstone oil reservoir (after Alabert and Massonat, 1990).

Direction	Channel	Lobe	Slump	Laminated facies
N20E	250 m	500 m	100 m	750 m
N110E	50 m	250 m	100 m	750 m
Vertical	12 m	8 m	16 m	17 m

method of conducting a separate spatial characterization focusing independently on different parts of the property value spectrum.

This indicator characterization implies transforming the data-set in a binary system so that property values above a threshold become 1, below the threshold they become 0. Subsequently, a variogram can be determined for this binary field. The transformation and variogram determination can be repeated for different thresholds (each threshold corresponds to an indicator). This procedure yields different indicator variograms for the different thresholds. Thus, different portions of the permeability spectrum have their own measure of spatial continuity. These determined variograms describe the probability to find a value above a given threshold and at a certain distance from another value above the same threshold. If more than one threshold is involved, the probability of a value above Threshold A, and at a certain distance of a value above Threshold B, could be reviewed resulting in cross-variograms for indicators. For practical reasons, however, these cross-variogram are neglected. As discussed later, this missing information causes some inconsistency in the simulation procedure.

The indicator approach described above is consistent with the geological fact that different facies-units (reflecting different, hydraulic, conductivity ranges) may have an essentially different, spatial continuity. For example highly conductive, fluvial channels may have a very different, spatial continuity compared to low conductive, lobe-shape crevasse (also see Section 2.2.3). As mentioned by Journel and Alabert (1988), the indicator formalism allows translation of this geological knowledge into indicator variograms that differ per facies.

This is a more flexible and realistic method of inferring variograms from indirect geological data, compared to the Gaussian method discussed earlier which requires information from different facies be condensed into a single variogram. Alabert and Massonat (1990) give a comprehensive application of this methodology (Table 2.3). Indicator variograms are estimated for several facies of very different shapes in a geologically complex oil field. Johnson and Dreiss (1989) use indicator variograms to characterize hydro-stratigraphic units in a large alluvial valley fill.

*A variogram: only a partial characterization*

The variogram is the second moment of a spatial distribution. Only a Gaussian field is fully characterized by the first moment (mean) and the second moment (covariance). For other distribution types a variogram can be calculated, but may not contain sufficient information for a full description of the random field. This effect is comparable to the fact that a standard deviation can be determined to characterize a skewed bi-modal distribution. On the basis of this standard deviation only, this distribution would be approximated by a Gauss curve, which is a fairly fruitless approximation.

Deutsch (1992) gives an example of a bombing model variogram. This bombing model consists of randomly sized circles dropped in random locations. A variogram derived from such a model looks very similar to those obtained from a normal Gaussian random field, even though the bombing model obviously violates the assumption of continuous random function, underlying a Gaussian random field.

Another problem is that the variogram models traditionally used, are often insufficient to incorporate typical nested structures encountered in sedimentary deposits. Much field data (e.g. Goggin et al., 1986; Davis et al., 1991; Johnson and Dreiss, 1989) show variograms that rise to a sill value that subsequently descends and rises again (Figure 2.7). This is known as a hole-effect and indicates that variance between the measurements is maximal for a certain distance, but becomes smaller for larger distances. This type of variogram is explained by a repetitive facies sequence ( $A_1-B_1-A_2-B_2-A_3$ ). Repetition (exact or diffuse) is a phenomenon that often occurs in nature, especially for vertical sequences.

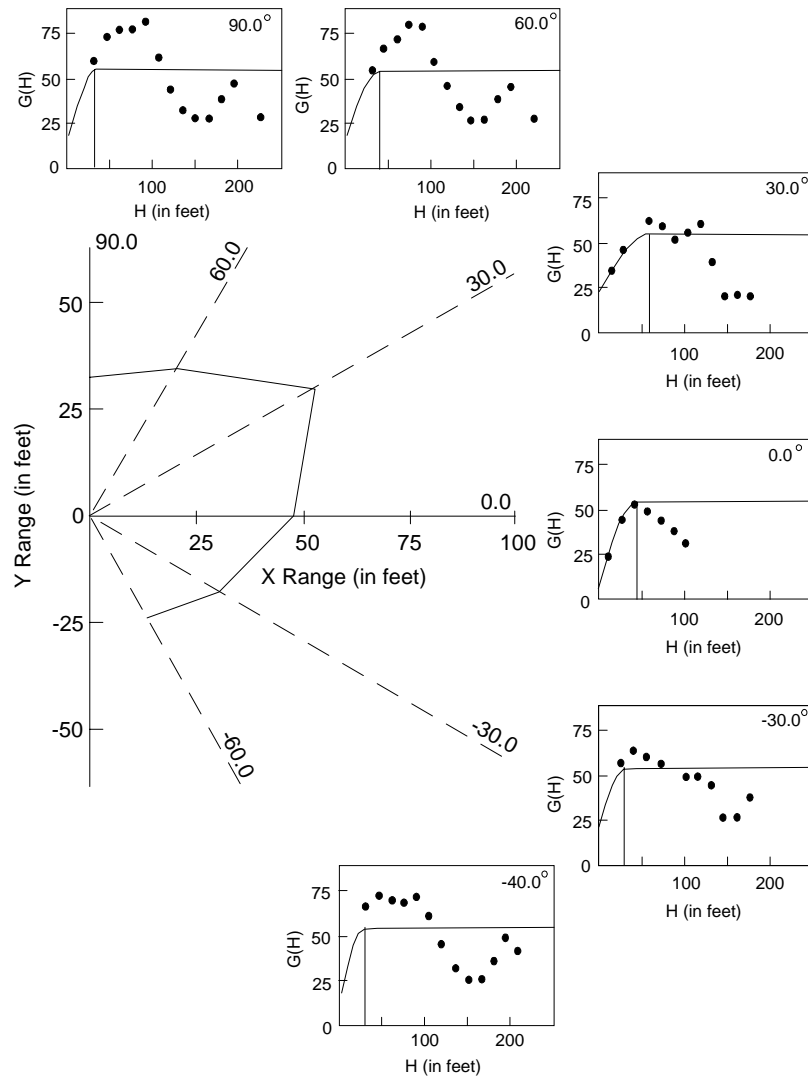


**Figure 2.7:** Example of field measured variograms for several directions. Note the hole-effect (after Goggin et al., 1986).

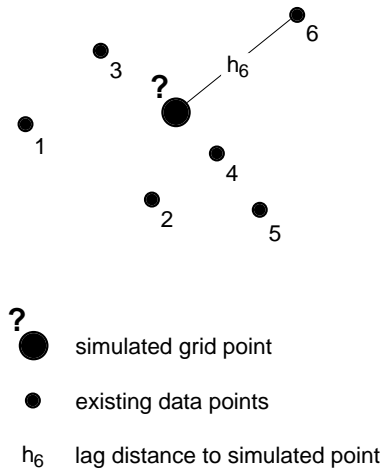
Measurements of a property (i.e., hydraulic conductivity) may differ greatly for close distances (one measurement in A, the other in B). For larger distances quite a few measurement pairs may be AA or BB, and thus, yield a higher correlation. A clear

example of such a repetitive deposit is a braided river valley fill. Not surprisingly, Rehfeldt et al. (1992) observe a hole-effect in these types of deposits. Variograms with a hole-effect are mostly neglected for two reasons. First, the error of estimation increases for larger lags of a variogram where the hole-effect occurs. Therefore, the hole-effect is mostly judged mathematically insignificant and can be considered as an artifact of the data. Second, hole-effect variograms are inconvenient for simulation; therefore, they are not incorporated in most simulation software (for an exception, see Ababou et al., 1994). It is important to stress that neither of these reasons is a compelling motivation to neglect the hole-effect which well matches typical geological features.

Another serious problem is that the variogram represents the statistical variation of a random field, the statistical properties of which do not change within the area of interest. This principle is called stationarity, and is often hard to justify. Since geological units do not follow the same statistical rules all the time, sharp breaks and/or gradual changes are very common on every scale. The problems are circumvented by recognizing a trend (Rehfeldt et al., 1992), and/or by identifying units that are statistically homogeneous (Gelhar, 1986).

Problems occur when using the same data, a hydraulic property measurement for example, to identify both trend and variation. It is difficult to identify what belongs to the trend and what belongs to the variation. If the trend is emphasized too much, variability is lost. Consider, for example, fitting a data-set with a polynomial trend and using the residuals to determine the variogram. If a high order, polynomial trend is fitted, this trend will cover much more of the variability than a low order, polynomial trend. Consequently, a very different variogram will be found. Thus, additional geological data are indispensable for recognizing units and trends. This raises the question of whether these additional data in themselves are not largely sufficient to characterize heterogeneity. The latter implies that variograms are only useful to fill in remaining variability or add noise to interpolation.

The weakness of the variogram method is strongly expressed in applications that allow only a single variogram. Macro-dispersion (which will be discussed in Section 2.4.2), is such a case. An example of a much more flexible approach, is conditional simulation of facies indicators combined with Gaussian simulations to fill in the hydraulic



Determine from variogram and lag the co-variance for all combinations: simulated point - data point

Use the data point values and these co-variances to develop a linear set (Kriging) equations and solve for the mean and variance of the Gauss distribution of the value at the grid point to be simulated.

Randomly draw a value from this Gauss distribution.

Add the value just drawn as a 7th data point.

Chose randomly a new grid point to be simulated.

**Figure 2.8:** Schema of a Gaussian sequential simulation. Right column lists procedure to simulate a new grid-point using data at six existing points (data or earlier simulated points).

conductivity variability within the facies. In the next sections basic techniques for conditional simulation will be presented.

### *Simulation of Gaussian fields*

A Gaussian field for a variable like hydraulic conductivity, is explained following the currently most popular approach of sequential simulation. Figure 2.8 shows a few initial (conditioning) data-points; for this example a conductivity value, which is measured in six wells. The probability density function for the value at the newly simulated grid-point, is a Gauss distribution. The mean and variance for this Gauss distribution is calculated (by Kriging) from the existing data-values and the covariances associated with the distances between these existing data-points and the new simulation point. These covariances are determined from the variogram by entering the appropriate lag for each pair of an existing data-point and the new simulation point. The so obtained Gauss distribution is used to draw a random value for the new simulation point. The latter is a complement of Kriging which employs this distribution only to estimate a mean and a

variance at the new point. Each simulated point is considered a new data-point, and as such, incorporated in the remainder of the simulation.

For a Gaussian spatial distribution the Gauss distribution for the new simulation point value, can be exactly developed from data by Kriging. Thus, the sequential simulation is theoretically exact. In numerical implementations, however, many practical considerations can cause errors (Gomez-Hernandez and Cassiraga, 1992; Deutsch and Journel, 1992). One of the most important techniques in avoiding artifacts is to choose a random path through the grid. As the simulation advances, too many new data-points (the previously simulated ones) have to be incorporated in the calculation. Computational efficiency is gained by defining a search neighborhood radius to limit the number of data-points considered.

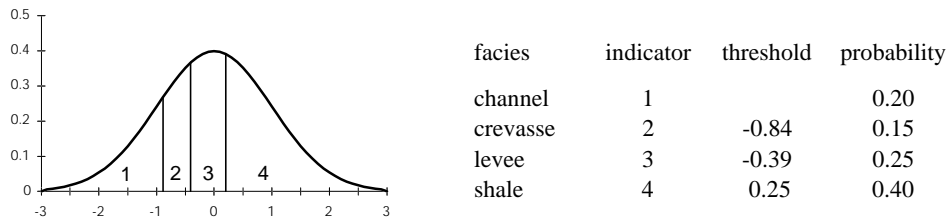


**Figure 2.9:** Gaussian, probability, density function subdivided in four facies by three thresholds.

#### *Simulation using the truncated Gaussian method*

To simulate a geological facies distribution it is necessary to simulate a discrete function. This function consists, for example, only of the numbers 1, 2, 3, and 4 indicating a facies. Matheron et al. (1987) introduced this method of truncated Gaussian simulation. A Gaussian field with a prescribed covariance is simulated using a technique similar as described above. This Gaussian field is normalized (average 0; standard deviation 1).

Subsequently thresholds are defined. When the simulated Gaussian value is below a threshold, a certain facies number is assigned. Above the threshold the next facies

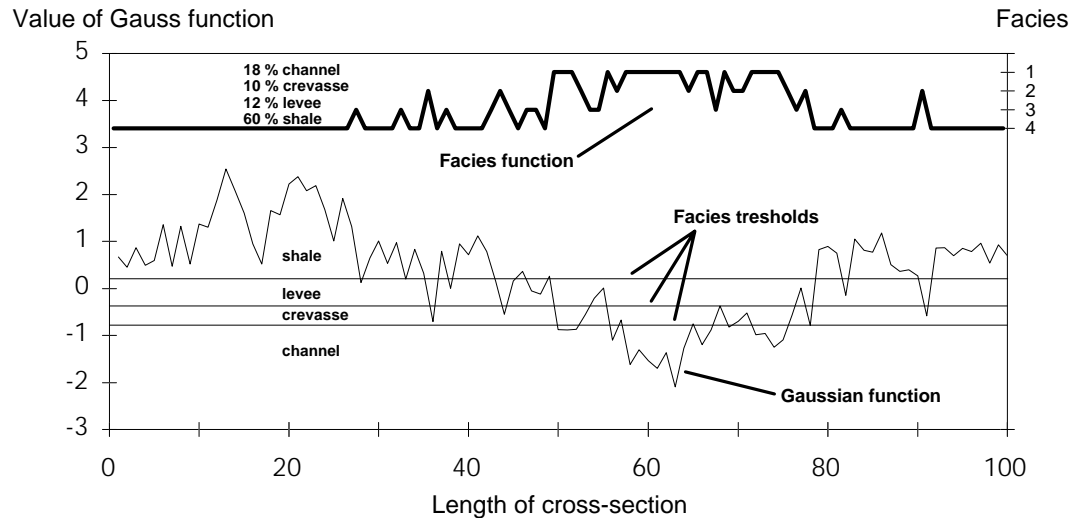


**Figure 2.10:** Cross sectional simulation of four facies using the truncated Gaussian method.

number is assigned. Figure 2.9 shows such a Gaussian distribution. The area under the curve is subdivided with three thresholds. The four areas under the Gaussian curve represent the four facies and are, respectively, a measure for the probability that a facies occurs. Over the whole model this probability of occurrence for a facies is similar to the volumetric proportion of that facies. In this example the facies represent four, traditional, fluvial facies, respectively: channels; crevasse lobes deposited as breakouts of the channel; levee overbank deposits parallel to the channel; and flood plane shale as a background (also see Section 2.2.3).

Figure 2.10 shows a one-dimensional example of a Gaussian spatial distribution. The thresholds concur with the subdivision of the Gauss curve in Figure 2.9. If the Gaussian value is above the shale threshold, the discrete function value becomes 4, indicating shale. If the Gaussian function is above the crevasse threshold the discrete function becomes 3, indicating crevasse. The upper curve in the Figure 2.10, the discrete function of the facies indicator, is derived by systematically applying all thresholds. This upper curve is a geological cross section. The discrepancy between the facies proportions in Figure 2.9 and the probabilities in Figure 2.10, are caused by the limited length of this

model in respect to the range of the Gaussian function (100 versus 25). As a result there is an inadequate sampling of the distribution.

The truncated Gaussian method has been extensively tested (Ravenne and Beucher, 1988). Facies simulations were made for an outcrop of fluvio-deltaic sandstones based on limited information, only two vertical sections for a 1,000 m long cliff face. The results of these simulations were found to compare well with the original outcrop description based on numerous, closely spaced, sedimentological records. A commercial three-dimensional software package based on this method is available (IFP, 1990) and used in the petroleum industry.

The truncated Gaussian method is a simple, theoretically elegant, method for modeling discrete facies distributions. A strength of this method is the possibility that facies proportions vary for different horizontal planes and for different vertical cross sections in the model. Using this option, geological bias can be included in the modeling procedure. The variable proportions per layer and per section imply that the thresholds used to derive the facies from the Gaussian distribution (Figure 2.9) are changed. It should be noted that significant changes in facies proportions can result in a variogram of the resulting facies map that severely differs from the intended variogram used in modeling the Gaussian field.

The thresholds applied to a continuous variable, imply that facies transitions occur exclusively to the class above and below. Other facies transitions are excluded. In the above example of the truncated Gaussian method (see Figures 2.9 and 2.10), there are always transitions from facies channel (1) to facies crevasses (2), and never a direct transition from channel (1) to shale (4). This transitional behavior correctly represents facies systems that are based solely on specific transitions from one facies into another (Table 2.1). The truncated Gaussian method, however, is less appropriate for facies systems that include alternate sequences, for example due to erosion. Another weak point of this method is that a single variogram defines the lateral continuity of very differently sized facies. The latter is not corroborated by common sedimentological wisdom (Section 2.2) that different architectural elements (Table 2.2) can have very different shapes (channels, lobes, blanket-sheet). The issue of different variograms for different facies is addressed by the indicator approach discussed in Section 2.3.1 and the next section.

*Simulation using the Indicator method*

The sequential simulation of an indicator stochastic field is conceptually similar to the previously discussed, sequential simulation of a Gaussian field (Section 2.3.1). However, the covariances used to estimate the distribution of the simulated point value, are drawn from the different indicator variograms. Consider a four-facies simulation for the data-points and simulation point given in Figure 2.8 (facies 1, 2, 3 and 4).

The procedure for an indicator simulation is similar to that described in Figure 2.8. For the second step, however, covariances obtained from the indicator variograms are used. For example: data-point 6 is facies 1, and the covariance in the simulated point is derived from the indicator variogram for facies 1, using only the existing data and previously simulated points for facies 1; data-point 5 is facies 2 (crevasse), and the covariance in the simulated point is derived from the variogram and existing points for facies 2. Hence, the different spatial continuity of each different facies (see for example Table 2.3) is accounted for.

The drawback of this non-parametric, discrete variable approach, is that the assumption of a Gaussian distribution in the simulated point is not justified. Nevertheless, the probability density distribution for the facies value of the simulated point, is estimated using Kriging equations and is analogous to the Gaussian simulation discussed in Section 2.3.1. As a result, the cumulative probability density often exceeds 1, and an empirical normalization is required. The cumulative probability exceeds 1, because only the positive probability to have facies  $i$  at a certain distance of locations with the same facies  $i$ , is accounted for; but the negative probability to have facies  $i$ , because another facies  $j$  is at a certain distance away, is not accounted for. Theoretically, it is possible to develop indicator variograms describing the correlation between facies  $i$  and  $j$ , but for practical reasons, this is generally omitted.

The indicator method is theoretically less elegant than both Gaussian methods previously discussed. However, flexibility is gained to assign different geological facies their own appropriate correlation structure (variogram). Thus, a better description of spatial continuity characteristics for independent facies is obtained. Desbarats (1987) applied indicator simulation to reconstruct a sandy-shale sequence map obtained from detailed outcrop investigation. Alabert and Massonat (1990) applied indicator simulation

to an oil reservoir consisting of Turbidite channels and lobes with facies of very different characteristic lengths (also see Table 2.3).

#### *Simulation using fractal methods*

Mandelbrot (1967) can be credited with bringing a specific brand of geostatistical modeling to wide attention. He showed that a rugged geometry, like a natural coastline, can be characterized using a peculiar problem that occurs when measuring its total length. The total length measured depends on the scale used for measurement or the length of the measuring device. Mandelbrot defines the fractal dimension to characterize ruggedness, as well as several simple procedures to create a rugged curve with a given fractal dimension. With statistical noise added these fractal procedures allow creation of hypothetical coastlines with striking similarity to realistic ones.

Scale dependence of measurements has been recognized for many natural shapes and property distributions, including subsurface shapes and properties. Dispersion of tracer flow, for example, has been found to increase with an increasing scale of experiment (Fried, 1979). Burrough (1983) shows that a random function created using a fractal dimension, is essentially a Gaussian random function with a power-law variogram (also see Section 2.3.1). The latter implies that the variance rises as a power function of the lag-distance. The concept of variation ever increasing with scale, corroborates well with geological knowledge that every increase of scale introduces new heterogeneity.

Hewett (1986) has applied fractal methods to the modeling of spatially variable hydraulic properties in oil reservoirs. This method is conceptually very simple and requires the following steps in recursion:

- 1- Obtain a value in the middle of two data-points by linear interpolation.
- 2- Add a random perturbation to the mid-point value.
- 3- Add the mid-point value as a data-point.
- 4- Repeat Step-1 for the resulting two pairs of data-point.
- 5- Reduce magnitude of the random perturbation with each recursive step.

This efficient method has been successfully applied to model heterogeneous oil reservoirs. A disadvantage is that the model is built in a horizontal direction. Vertical sequences do not honor any specific variogram. At a certain scale, the power-law variogram is also difficult to relate to specific geological information. The fractal variogram implies growing variability for a scale-cascade of geological processes (i.e., grains; cross beds; bars; channels; valley-fills; or basin-fills). If one step of this cascade dominates the model, then the sill-type variograms used in previously discussed methods, are more suitable for including with specific information in geological discussions.

### **2.3.2 Modeling geological variability using geometrical shapes (objects)**

The object technique is widely used in the oil industry and is also known as Boolean or discrete models. These models are often applied to "labyrinth" reservoirs (Weber and van Geuns, 1989) consisting of modest fractions of isolated facies deposited in background material. These facies can be shale streaks (Haldorsen and Lake, 1982) or sand bodies (Budding et al., 1988). Each of these shales or sand bodies is modeled as a single "object" with a shape approximated by a simple geometry; fluvial channels, for example, are approximated by half-ellipsoids, rectangular, or sinusoidal shapes. Figure 2.11 is an example of different types of fluvial sand bodies modeled against a shale background. The dimensions of the objects are obtained from statistical distributions derived from outcrop studies or from experience acquired on more densely drilled fields. A thickness distribution can be obtained from case-specific well data. The width of the objects is inferred from their thickness using width-thickness relationships (see, for example, Figure 2.2). Geological constraints other than simple width-thickness relationships, can also be taken into account. These constraints, or interaction rules, cover vertical succession, transitions, and erosion.

The procedure of these models generally is as follows:

- 1- Randomly select location in model area.
- 2- Select one of the facies to be modeled.
- 3- Randomly select dimensions and orientation from specified distributions.
- 4- Generate a new facies objects.
- 5- Apply erosion or interaction rules with already existing facies object.
- 6- Compare overall fraction of different facies with stop-criterion.
- 7- Continue with the next object or stop.

This method is conceptually simple and attractive for geologists given the intuitive resemblance between facies units and objects. Numerical implementations can be very fast. The weak side of this method is that often inconsistencies are encountered. For instance, close well spacing causes difficulties in generating random objects with sizes larger than the well spacing, if the simulations are to be conditioned by the wells. The interaction rules are very difficult to implement in numerical schemes; results are often disappointing from a geologist's point of view. A practical overview of various applications of object models, is given by Haldorsen and MacDonald (1987). An early hydrogeological application of object models analyzing seepage in heterogeneous sediments, has been reported by Wu et al. (1973).

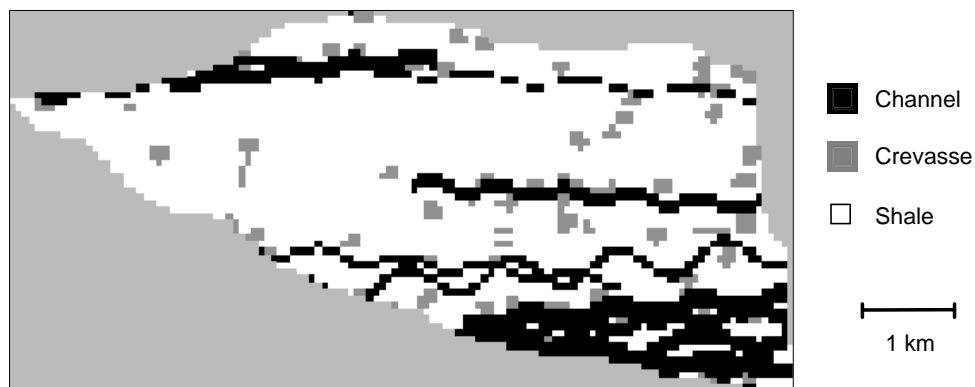


**Figure 2.11:** Object model of an oil reservoir consisting of fluvial sediments (plan).

A special category of object models is the GOCAD modeling approach. Computer Aided Design techniques are used to deterministically generate three-dimensional, geological objects in space (Wietzerbin, 1994; Wietzerbin and Mallet, 1993). Using a perturbation method statistical realizations are derived from this deterministic realization. Geological inconsistencies can subsequently be manually corrected. This method emphasizes the efficient creation of an ensemble of geologically correct scenarios, rather than abiding statistical laws.

### 2.3.3 Models based on genetic processes

The following models are based on simulation of physical sedimentary processes combined with a stochastic perturbation. The methods published are case specific and their practical applications are limited. Joseph et al. (1993) simulate a deltaic complex by deposition of mega fore-sets. The position of the deposition is a probabilistic function varying both the sea level and seafloor topography during deposition. The sea level variation is a parameter that can be obtained from sequence stratigraphy analysis (e.g. Bryant and Flint, 1993). The seafloor topography is recalculated by the model after deposition of each lobe. This method is strongly dependent on the initial seafloor topography data that are difficult to estimate for a subsurface formation.

Webb and Andersen (1993) use a random-walk algorithm to simulate a static network of braided streams. Using this topography, discharges through the branches are calculated. These discharges are converted to local velocities and related to deposition of a facies that concurs with the local hydrodynamic energy level (Tetzlaff and Harbaugh, 1989). To obtain a vertical pattern the sequence is repeated for several cycles of deposition. This methodology has been extensively tested using data from several modern environments. Koltermann and Gorelick (1992) simulate a several kilometer wide alluvial valley fill. Representative climatologic data are used, while distributions for water and sediment discharge are derived from modern analogs. During the modeling hydrodynamic energy levels are estimated, and sedimentation of different clastic facies is simulated as a function of this hydrodynamic energy level.

### 2.3.4 Practical use of geostatistical models

The following section presents field applications of geostatistical models. In the petroleum literature a large number of case studies have been published. In contrast, hydrogeologists have paid less attention to geostatistical modeling, mainly because of the stochastic analytical solutions that have been published for transport in heterogeneous media (see Gelhar, 1986 or Dagan, 1989). Another factor discouraging hydrogeologists' use of geostatistical models, is the limited availability of detailed sedimentological data.

Teutsch et al. (1990) present an indicator geostatistical model for hydraulic conductivities of an alluvial valley fill for an experimental field site in Germany. This geostatistical model is used to analyze the results of tracer experiments conducted at that site. Poeter and Townsend (1991) present an example of an alluvial aquifer. They also present a geostatistical model for which heterogeneous hydro-stratigraphic units are created using the indicator technique; this model is used for the assessment of spreading radioactive pollutants.

In the petroleum industry the use of geostatistical models has been twofold: first for determination of static volumes (reserves); and second for input of dynamic, fluid-flow, simulation studies to predict production behavior of a field. Budding et al. (1988), as well as Haldorsen and McDonald (1987), present object models that are analyzed to determine the oil/gas reservoir volume that can be removed/drained given a certain well spacing. Results of these calculations are used to predict the potential of producing extra oil by drilling (in-fill) wells in existing oil fields. Alabert and Modot (1992) calculate for several, pixel-based, geostatistical models the connected pore volume given a permeability threshold. This technique is applied to an oil reservoir consisting of Turbidite channels and lobes for which Gaussian, truncated Gaussian, and indicator geostatistical models are created. Their conclusion is that the choice of the modeling procedure is an important factor for connectivity. Thus, when applying a geostatistical method, choosing a method coherent with available geological knowledge, is equally as important as hard input data.

Alabert and Modot (1992) also introduce the connectivity length as a measure of the relative ease for fluid to flow from well to well. Connectivity is defined as the path length between two wells given a conductivity threshold (see Section 2.3.4 and Alabert

and Modot, 1992). The highest degree of connectivity (length) implies that there is a straight path between two wells given a certain permeability threshold. A low degree of connectivity implies that there are no conductivities above the threshold on the direct line between the two wells. Thus, the shortest well-to-well path becomes tortuous; and/or the connectivity (length) becomes larger than the well-to-well distance and infinitely large if no connection can be made given the conductivity threshold. For heterogeneous aquifers a conductivity threshold in the middle of the conductivity spectrum can be selected. Subsequently, it can be quantified which well-pairs have good connections, for example direct high conductivity paths, versus well-pairs that have indirect (longer) paths or no connection (at the selected conductivity level).

The inherent problem of detailed geostatistical models is the very large number of gridblocks that often makes numerical fluid-flow models beyond current computer capabilities. Thus, the grid needs to be reduced implying that the effective properties of many small gridblocks of the geostatistical model can be lumped in a single large gridblock. This result can be obtained through analytical determination of effective properties (also see Section 2.3.5) or local-scale numerical models (Gomez Hernandez, 1991; King et al., 1993; IFP, 1990). Giudicelli et al. (1992) present a full, field, fluid-flow simulation and a local-scale simulation for a Turbidite channel oil field. The geostatistical model consists of several nested models based on Gaussian and indicator techniques covering, respectively, lab-scale hydraulic properties and field-scale facies (Alabert and Massonat, 1990). Results of these simulations confirm the impact of geology on non-uniform flow and the validity of the geostatistical approach. It is shown, however, that the large level of grid size reduction has a significant impact on the simulation results.

Emmanuel et al. (1987) present flow simulations based on fractal geostatistical models. A three step simplification procedure is followed to make the simulation feasible. First two-phase flow of oil and water is simulated in full detail for a limited number of fractal geostatistical cross sections. Next stream-tubes for steady state flow between wells are calculated based on average reservoir properties. In the second step, the effective two-phase flow in the heterogeneous cross sections, is projected along the stream tubes; then these results are accumulated to determine the production of the wells. This methodology appears to be successful, because it includes heterogeneity in forecasts

of a full field response that lumps the performance of multiple wells. However, the performance of individual wells is matched only conceptually. Heterogeneity effects in individual wells realistically reflect those trends observed in the field, but not necessarily for the same well. Thus, this methodology seems to include the right level of heterogeneity, but not necessarily in exactly the right place.

Keijzer and Kortekaas (1990) present a fluid-flow simulation for three realizations of an object model for a part of the North Sea Brent oil field. This field consists of highly, conductive, fluvial channels and low conductive crevasses that generate complex connectivity patterns between wells. Using an analytical averaging approach a coarse grid is determined from the detailed geostatistical model. Without significant history matching a fluid-flow simulation of one of the three realizations, properly reproduces field performance and individual performance of the significant producer wells. A conventional, homogeneous, layer-cake, flow model was developed parallel to this geostatistical study. This conventional flow model requires unrealistic parameter calibrations to match the observed field history, while individual well performance is poorly simulated. The authors conclude that a more realistic geological description in the geostatistical model, is responsible for the good simulation results.

Damsleth et al. (1990) present a hybrid model combining the object approach for facies and the pixel approach for hydraulic properties. In contrast to the previously presented flow modeling studies, a systematic stochastic experiment is conducted involving 45 realizations for different property and facies patterns. They conclude that breakthrough times vary between all realizations, but all breakthrough times are shorter than the breakthrough time found for a homogeneous case. They also conclude that variability of facies patterns, is more significant for fluid-flow than the variation of small-scale, hydraulic properties.

It seems that the geological empirical approach followed by the oil industry has been successful in modeling heterogeneity and its impact on flow. This is in contrast with the more theoretical approach followed in hydrogeology (see next section) that seems difficult to relate with field data (also see Sections 2.4.4 and 2.4.5). The availability of several different methods for geostatistical modeling, each having strong and weak points, is a definite advantage. Another advantage is the possibility of nesting different models on different scales concurring within a sedimentological model. The appropriate

geostatistical modeling approach can be selected given: previous experience; available data; objectives for static or dynamic characterization; and, last but not least, availability of good software.

#### 2.4 GEOSTATISTICS AND EFFECTIVE FLOW AND TRANSPORT PARAMETERS

Hydrologists have successfully explored stochastic solutions of the flow and transport equation (for a summary see Dagan, 1986 and 1989; Gelhar, 1986; Neuman, 1982). Under certain assumptions, expressions have been developed that relate the effective flow and transport parameters (i.e., effective hydraulic conductivity and macro-dispersivity) to the variogram of the logarithmic hydraulic conductivity. All these methods pertain to solving a stochastically formulated Darcy flow-equation relating the (spatial) distributions of hydraulic conductivity, head, and flux. Under the assumption of a flow pattern, the stochastic partial differential equation can be solved; in other words, for a given (spatial) distribution of conductivity, the distribution of hydraulic heads is obtained. The distribution of hydraulic heads can be transformed into a distribution of flow velocity. The distribution of flow velocity is used to solve a stochastic version of the solute advection equation to obtain the spatial distribution of solute concentration.

For the whole category of stochastic solutions following the schema described above, the results obtained are not spatial distributions, but statistical moments that characterize these distributions. Only the first moment (mean, average) and the second moment (covariance, variogram) are considered, while higher moments are neglected. Practically, this means that a field observed, conductivity distribution is condensed in two parameters describing the spatial, probability, density function of which the field K-data are a realization. Solving the stochastic equations, as described above, yields the first two moments that characterize the probability density function of head and concentration. Unlike a geostatistical model, this solution does not yield a specific realization of the parameter of interest, but rather describes an average of an ensemble of realizations. Thus, similar to Kriging (Section 2.3.1), average heterogeneity is modeled, but not field specific heterogeneity.

More specifically, the assumptions necessary to apply the stochastic solutions are the following:

- 1- The logarithm of hydraulic conductivity is normally (Gaussian) distributed, and has a small standard deviation.
- 2- The hydraulic conductivity field is stationary, which implies that its statistical properties do not change in space. This assumption has been weakened by requiring only the variogram of the conductivity field not to change in space.
- 3- Ergodicity is assumed implying that the hydraulic conductivity field of a single aquifer represents, in a statistical sense, the average of multiple different realizations of statistically similar aquifers. Thus, a single aquifer is a chain of sub-aquifers with statistically similar heterogeneity, but without heterogeneity on a level larger than the sub-aquifer. Practically, this means that heterogeneity only occurs below a threshold scale that is a good deal smaller than the scale of the problem considered. Heterogeneity between this threshold scale and the problem scale, is not accounted for.

It is important to note that in the prolific literature on stochastic hydrology, the validity of the above assumptions has never been confirmed with factual field data. Young et al. (1991) show for the Columbus test site that log-normality and stationarity can not be assumed for the conductivity of fluvial deposits at that site. Also, the above assumptions are contradicted by the fact that conductivity is related to sedimentary facies. As discussed in Section 2.2, sedimentary facies occur on any scale as the result of different depositional processes that create a specific texture and, hence, different hydraulic properties. The facies architecture is a mixture of well, defined, gradual successions and erosive events occurring on a cascade of many scales. Contrary to suggestions made by Gelhar (1986), it is difficult to identify a single threshold scale that separates random variation from non-stationary trends. Thus, it is wrong to attribute the same statistical properties to a specific subsurface volume (second assumption) and to exclude new levels of heterogeneity above a certain scale threshold (third assumption).

2.4.1 Effective hydraulic conductivity

The determination of effective (average) hydraulic conductivity pertains to the procedure that relates local-scale conductivity values to conductivity values representative for a larger scale. This relation, for example, has to be established when comparing a permeability obtained through a well test, with permeabilities that are derived from borehole (core) samples. Effective permeability is also very important when flow models are made that have grid cells covering a much larger volume than the volume for which conductivity measurements are available. Effective conductivities are intrinsically related to the spatial arrangement of the local conductivities to be averaged, as well as to the temporal and spatial flow patterns in the averaged volume. As stated by

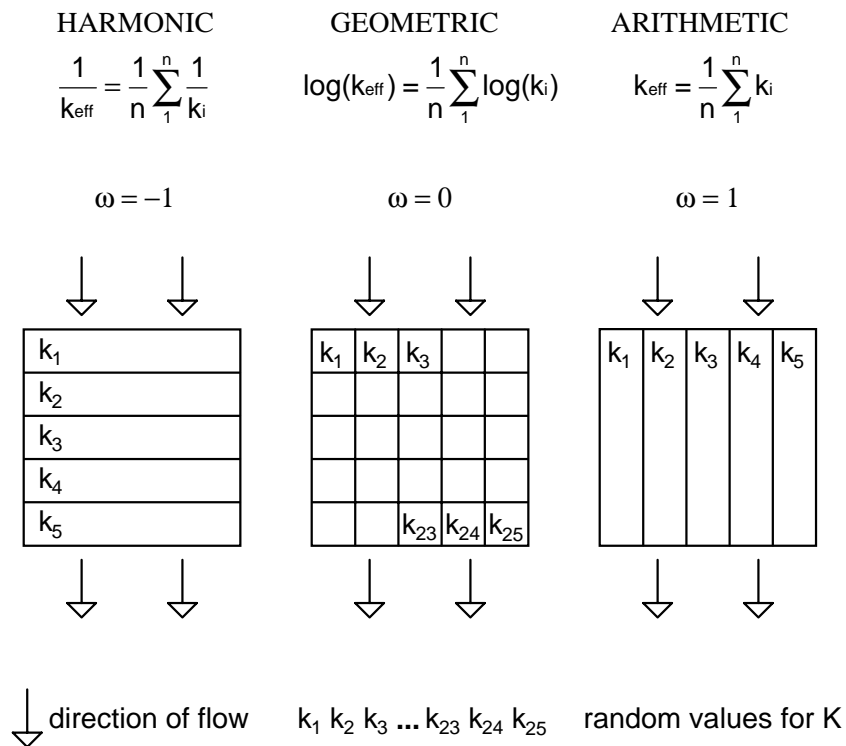


**Figure 2.12:** Basic scalar methods for averaging spatial heterogeneous K-values.  
 $k_1 \dots k_n$  are local-scale K measurements,  $\omega =$  power-exponent in the interval  $[-1,1]$

Weber and van Geuns (1989), the method of averaging is intrinsically related to the architecture of sedimentary facies to which the local conductivities are related (also see Section 2.2). This notion, however, is mostly absent in the literature dealing with averaging methods.

There are three methods of conductivity averaging that have traditionally been used (Figure 2.12). The harmonic and arithmetic averaging method are based on the well known, electrical analog from a current through a series of serial and parallel conductors, respectively. The logarithmic, or geometric, average has been empirically established as a correct method of averaging log-normally distributed conductivities in a non-layered heterogeneous medium. Warren and Price (1961) and Matheron (1967) have validated that the geometric average is the average for uniform linear flow through a two-dimensional field of isotropic, log-normally distributed, conductivity values. These three methods can be generalized using the power-average equation (Equation 2.2, also see: Journel et al., 1986; Alabert, 1989; Desbarats, 1992a).

$$K_{\text{eff}}^{\omega} = \frac{1}{n} \sum_{i=1}^n K_i^{\omega} \dots\dots\dots(2.2)$$

$k_1 \dots k_n$  are local-scale K measurements,  $\omega$  = power-exponent in the interval [-1,1]

For steady state linear flow in three-dimensional, spatially isotropic, correlated media, several different theoretical approaches (Dagan, 1989) yield relations of the form:

$$K_{\text{eff}} = K_{\text{Geo}} (1+C.\sigma_{\ln K}^2) \dots\dots\dots(2.3)$$

The constant C (in equation 2.3) is equal to 0 for the two-dimensional isotropic case (Matheron, 1967), while C is equal to 1/6 for the isotropic, three-dimensional, case (Gutjahr et al., 1978; Dagan, 1979). Gelhar and Axness (1983) provide an extension of this relation for the three-dimensional anisotropic case. Desbarats (1992a) empirically confirms that this relation, practically, can be represented by a power-average for  $\omega = 1/3$

(Equation 2.2). His numerical experiments cover several correlation lengths and pertain to linear flow from one-side to the opposite side of a cube. He observes that the relation deteriorates when the conductivity distribution covers more than 2 orders of magnitude on a natural log-scale (equal to 1 order of magnitude on a 10 log-scale). The validity of a power-average using  $\omega = 1/3$  for the general case of three-dimensional uniform flow, has also been documented by King (1989) and Noetinger (1994).

Ababou and Wood (1990), Naff (1991), and Desbarats (1992b) provide different formulas for the effective permeability for radial, steady, state flow. Desbarats (1992b) shows some numerical experiments for which the formulas provided by Ababou and Wood (1990) and Naff (1991) do not yield a correct result. The applicability of the formula proposed by Desbarats (1992a, 1994) to well tests, is problematic, given transient flow during a well test versus stationary flow considered in his formula. The heavily weighted inclusion of near well conductivities in the average (Desbarats, 1992a), is in contradiction with the concept of a ring-of-influence (Butler, 1990; Oliver, 1990).

More recent work has focused on the tensor character of effective conductivity in spatial anisotropic media. The traditional representation of anisotropic conductivity is limited to the three diagonal tensor elements ( $K_{xx}$ ,  $K_{yy}$ ,  $K_{zz}$ ). Gomez Hernandez (1991) shows that after an averaging procedure, the effective conductivity tensor for a large volume has non-diagonal terms. These non-diagonal terms represent tortuous flowpaths through the averaged medium. For example,  $K_{zx}$  allows evaluation of flow in the z-direction due to a hydraulic head gradient in the x-direction. This situation occurs when the non-averaged volume contains a barrier for flow in the x-direction forcing flow downward in response to a hydraulic head gradient in the x-direction. This tensor averaging has not yet been widely used nor tested, mainly because of the lack of numerical flow models that include a complete conductivity tensor. Some recent work on this matter has been also presented by Indelman and Dagan (1993a, 1993b, 1993c).

#### 2.4.2 Effective transport: macro-dispersion

Warren and Skiba (1964) introduced the term "macroscopic dispersion" to cover dispersion of fluid-flow as a result of large-scale, hydraulic conductivity heterogeneities.

Their results were based on numerical fluid-flow models for a model grid filled with random conductivities. Gelhar and Axness (1983) used spectral analysis to derive an expression for the macroscopic dispersion as a function of the spatial covariance (variogram) of a heterogeneous conductivity field. Similar to traditionally used Fickian dispersion, macro-dispersion is inserted in a diffusion equation as a velocity dependent, diffusion coefficient. It is characterized by  $\alpha$ , the dispersivity (dispersion length). If the three assumptions (listed at the beginning of Section 2.4) are satisfied, the following relationships between dispersivity and variogram parameters exist:

For an exponential variogram (Gelhar and Axness, 1983):

$$\alpha = \sigma_{\ln K}^2 \cdot \lambda \dots\dots\dots(2.4)$$

For a spherical variogram (Neuman et al., 1987):

$$\alpha = 0.375 \cdot \sigma_{\ln K}^2 \cdot r \dots\dots\dots(2.5)$$

$\lambda$  is correlation length, and  $r$  is range (also see Section 2.3.1)

An alternative approach to assess macro-dispersion is to relate the spatial moments of a plume to the statistical moments of the spatial conductivity distribution (for a summary, see Dagan, 1989). The zero-order and the first two, spatial, plume moments are defined as follows (at time  $t$ ;  $x$  is spatial vector; integration over relevant space):

$$0 \text{ total mass:} \quad M = \int C(x,t) dx$$

$$1 \text{ center of mass (i coordinate):} \quad \bar{X}_i = \frac{1}{M} \int x_i \cdot C(x,t) dx$$

$$2 \text{ moment of inertia tensor (i,j=1,2,3):} \quad \bar{X}_{ij} = \frac{1}{M} \int (x_i - \bar{X}_i) \cdot (x_j - \bar{X}_j) \cdot C(x,t) dx$$

$$\text{moments (0, 1 and 2) of concentration plume } C(x,t) \dots\dots\dots(2.6)$$

Under the previously listed assumptions, and for a uniform linear flow field, the first and second statistical moments (mean and variogram) of the heterogeneous, spatial, conductivity distribution, can be derived from the first and second spatial moment of a plume. Thus, the plume spatial moments can be used to determine the effective conductivity, as well as the effective dispersion (and hence, macro-dispersivity for asymptotic cases) without knowing the underlying conductivity distribution (Dagan, 1989). The mean conductivity can be calculated simply by applying Darcy's equation to the advection of the center of mass (the first moment) of the plume. The effective dispersivity is calculated from the second plume moment using the following relation (Dagan, 1989):

$$D_{ij} = \frac{1}{2} \frac{dX_{ij}}{dt} \dots\dots\dots(2.7)$$

Both macro-dispersion and the related method of moments can be viewed in the light of the previously discussed, Gaussian, geostatistical models (see Section 2.3.1). First suppose that a large number of Gaussian conductivity realizations is available, and that transport of a tracer plume has been modeled for each of them. Subsequently, the plumes from all realizations are averaged in one single plume. This single plume represents many realizations and is properly described by macro-dispersion and moments method. Alternatively, a second approach can be followed by creating a Gaussian geostatistical model much larger than its correlation length (its basic unit of heterogeneity). For this single realization, transport of a plume is modeled over a sufficiently large length (multiple correlation lengths) in order to obtain asymptotic flow behavior. Also for this case, macro-dispersion and/or the method of moments, describe the plume. Frind et al. (1987), for example, show numerical experiments that confirm this second option. These two options illustrate the previously discussed assumption of ergodicity, meaning a single, but large enough, realization represents a large number of realizations. The other two assumptions (normality and stationarity) prescribe use of a Gaussian model with a single, spatially invariant, variogram.

### 2.4.3 Application of macro-dispersion concept: problems

As it stands today the macro-dispersivity concept has not yet been routinely applied to practical problems. A very limited number of field experiments has been conducted to verify its applicability (also see Section 2.4.4). Several studies have been conducted using hypothetical, but realistic, aquifer analogs. These analogs were inferred from geological outcrop data or from maps of modern environments. Numerical, tracer test experiments were conducted for these aquifer analogs.

Desbarats (1987) modeled tracer flow through an aquifer inferred from a realistic example of a sand-shale sequence. A geostatistical model based on indicator variograms, is used to produce realizations of the aquifer. He indicates that it is impossible to reproduce modeled tracer flow using the macro-dispersivity concept. Desbarats and Srivastava (1991) use a modern fluvial topography as an analog for aquifer transmissivity of a hypothetical aquifer. Although this hypothetical aquifer does not fit with the assumptions (discussed at the beginning of Section 2.4), they conclude that estimates of macro-dispersivity based on the variability of conductivity, concur well with estimates based on plume spreading in the tracer model. However, they also show that the applicability of macro-dispersivity is limited to predicting the general average trend of tracer breakthrough. Early breakthrough time and peak levels predicted by macro-dispersion, are subjected to severe errors, even at large distances from the source. In turn this poses serious problems for practical application of macro-dispersion, since early breakthrough and peak level are often more important issues of a contamination problem when compared with average plume behavior.

On the basis of sedimentological field data (also see Section 2.2.2) presented by Jussel (1992) and Jussel et al. (1994a, 1994b), a hypothetical aquifer is assembled using an object geostatistical model (2.13). Tracer flow is modeled for this hypothetical aquifer; then macro-dispersivities are determined from the model results and compared with results from formulas developed by Gelhar and Axness (1983) and Dagan (1989).

The transport behavior found by Jussel (1992) reflects, typically, the two nested-scales of heterogeneity. For transport distances less than five meters (5 m), macro-dispersivity values concur with values predicted by Dagan's theory using the covariance structure of the Gaussian random field within the sand and gravel lenses. Subsequently,

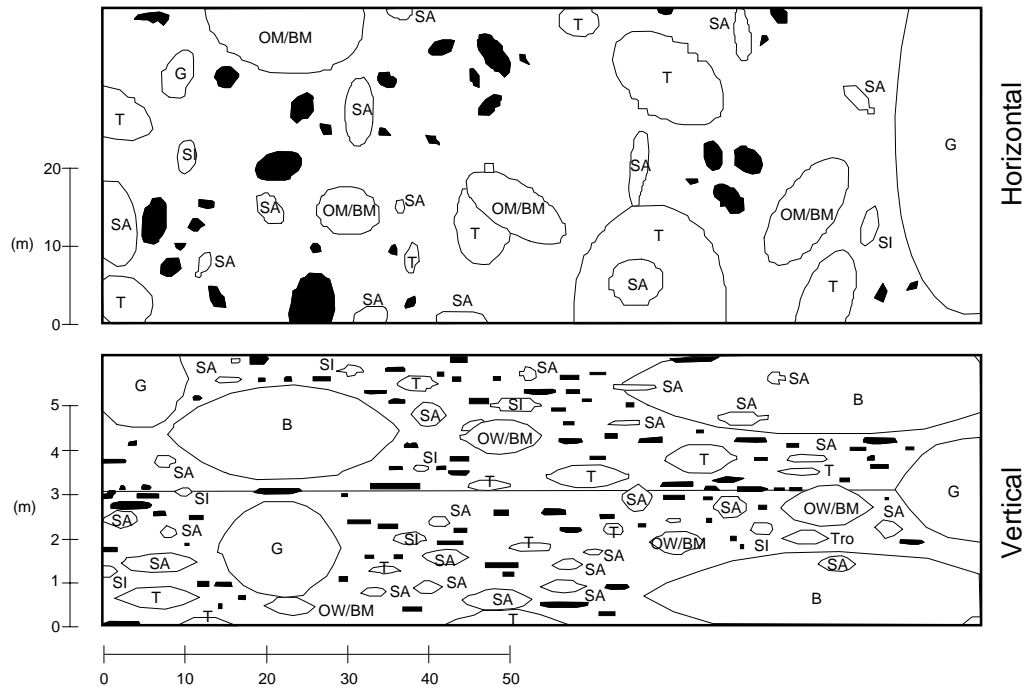


**Figure 2.13:** Object model for hypothetical gravel aquifer (after Jussel, 1992).

the effective dispersivity becomes larger and starts to approach the Dagan curve based on the covariance structure of the whole aquifer. The scale of the experiment is only larger, by a factor of 5, than the whole aquifer's correlation length. Therefore, macro-dispersivity values never approach the asymptotic value predicted by Dagan's theory. The latter could be possible if the scale of the experiment covered many more correlation lengths (10-20). However, at that scale the next level of aquifer heterogeneity probably becomes effective.

Thus, application of macro-dispersion to hypothetical, though geologically realistic, cases, raises concerns whether or not the concept is reliable enough to solve practical problems (e.g. breakthrough of a pollutant or a peak level of a plume). The next section discusses the limited field experience available for macro-dispersion and reveals further issues about the applicability of macro-dispersion.

#### 2.4.4 Large-scale field experiments to assess macro-dispersion

Field tests are the only way to validate the potential application of macro-dispersion in solving practical, contamination, transport problems. Most, existing, field, dispersivity data, however, should be treated with extreme caution (Gelhar et al., 1992). Only recently have large-scale, controlled, field experiments been conducted with the precision required to meet the above stated objective. The following discussion of large-scale, field experiments pertains to conservative solute transport and detection of subsurface heterogeneity covering large time-scale and spatial-scale. Known quantities of tracer are released and three-dimensionally monitored for a several year period.

##### *The Borden experiment*

A long term, natural gradient, solute transport experiment was conducted at the Canadian Forces' Borden Base (Mackay et al., 1986). Different conservative and reactive tracers were injected and monitored more over a three year period. The aquifer is: phreatic; approximately six meters (6 m) thick; underlain by an impermeable clay layer; and consists of sandy sediments with hydraulic conductivity values ranging from  $10^{-5}$  to  $10^{-6}$  meters per second (m/s). The objective of the tracer experiment was to study physical, chemical, and micro-biological processes controlling groundwater transport. The three-dimensional monitor network consisted of more than 250 wells equipped with multilevel samplers and drilled in an 120 m long by 20 m wide area.

The Borden experiment is the first, good quality, data base for geostatistical studies regarding solute transport in groundwater. Studies pertinent to aquifer heterogeneity and macro-dispersion are presented by Freyberg (1986) and Sudicky (1986). The variance of  $^{10}\log K$  (hydraulic conductivity) is approximately 0.3, indicating a variability of less than an order of magnitude. Sudicky calculates a macro-dispersion coefficient of 0.5 m for the Borden aquifer, a value that is consistent with the plume observed in the field. The latter is presented as a confirmation of the applicability of the macro-dispersion theory. However, this conclusion might not be transferable to more complex structured aquifers in contrast to projections proposed in the above mentioned articles. The Borden aquifer

consists of mainly, parallel bedded, clean, well sorted, fine to medium, grained sand (Mackay et al., 1986). This indicates only a modest level of heterogeneity.

#### *The Cape Cod experiment*

Another large-scale experiment was conducted at Cape Cod (Massachusetts, USA). Leblanc et al. (1991) present a general overview of this natural gradient, tracer experiment. Reactive and non-reactive tracers were injected and monitored during 18 months using a three-dimensional network of multi-level sampler wells. The aquifer consists of glaciofluvial sand and gravel sediments. The results of a pumping test indicate an average hydraulic conductivity of 0.001 m/s. Results from borehole flowmeter tests and permeameter tests, indicate that the conductivity varies 1 order of magnitude. After 460 days the non-reactive bromide plume has migrated 280 m, and is very elongated (approximately 90 m long by 15 m wide).

Garabedian et al. (1991) present an analysis of the spatial distribution of a non-reactive bromide tracer. A good mass-balance error was observed for this tracer. Of the original amount of released tracer, between 85% and 105% was consequently captured by the monitoring network. The flow velocity calculated from the migration of the center of mass of this tracer plume, concurs well with hydraulic gradients derived from piezometer observations and with the average hydraulic conductivity. From the longitudinal variance of the plume (the longitudinal second moment), a longitudinal dispersivity of 0.96 m was calculated. This value was found to be in reasonable agreement with a macro-dispersivity value of 0.5 m independently calculated from the local conductivity measurements.

Using the transverse moments, dispersivities of 0.018 m (horizontal) and 0.0015 m (vertical) were calculated. Both values do not concur with the value (essentially 0) calculated from the observed conductivity distribution and the steady state, flow field. The horizontal transverse mixing is explained by non-steady state, flow effects. Goode and Konikow (1990) present a method to calculate mixing due to these transient effects. The vertical mixing is explained by initial, density, contrast effects and recharge effects.

It is concluded that the tracer plume migration is well predicted by: the hydraulic gradient; the analysis of tracer-plume moments; and the macro-dispersivity analysis of local-scale conductivity measurements. This conclusion is similar to the conclusion

derived from the large-scale, natural, tracer experiment at the Borden site, even though the aquifer at Cape Cod has very different, hydraulic properties. In their conclusions Leblanc et al. (1991) and Garabedian et al. (1991) state that this extends the positive conclusion regarding the general applicability of the macro-dispersion concept. However, it should be noted that this conclusion is biased, because both aquifers have a very similar level of (absent) heterogeneity, although the average properties differ. Both the fine-medium sand of the Borden aquifer and the coarse-sands to gravels of the Cape Cod aquifer, are classified as clean, while low anisotropy ratios indicate the absence of meter-scale shale streaks or channelized deposits.

*The MAcro-Dispersion Experiment (MADE) at the Columbus test site*

This experiment was designed to test macro-dispersion concepts in an aquifer more heterogeneous than Borden and Cape Cod (Boggs et al, 1992). At Columbus Air Force Base (CAFB, Mississippi, USA) a shallow, unconfined, sand-gravel aquifer was selected for a long duration, natural gradient, tracer experiment. Four conservative tracers were injected. Movement of these tracers was monitored during 20 months using 258 observation wells each equipped with multi-level samplers. For characterization of the spatial, hydraulic, conductivity distribution, 2,187 measurements were conducted using a borehole flowmeter (Rehfeldt et al., 1992; also see Section 2.5.3). This systematic use of the borehole flowmeter for hydraulic conductivity measurements, was the novelty of this project. In addition to the MADE experiment, another test site, the 1-HA test site, was selected at CAFB in order to investigate in more detail pumping tests in a strongly heterogeneous aquifer. Results of these pumping tests are presented, analyzed, and modeled in the following chapters.

The CAFB site has been an excellent fulfillment of the wish "to define the limitations of existing theories and expand our understanding of highly heterogeneous media" (Gelhar, 1986). Hydraulic conductivity values stretch over four ( $^{10}\log$ ) orders of magnitude (Rehfeldt et al., 1992), and a distinct geological pattern could be identified (Herweijer and Young, 1991; Section 2.2.3 and Section 3.3). Figure 2.14A shows the extent of the observation well network and hydraulic head data. Figures 2.14B and 2.14C show the plume's horizontal and vertical extent (300 m x 75 m x 8 m) after 20 months

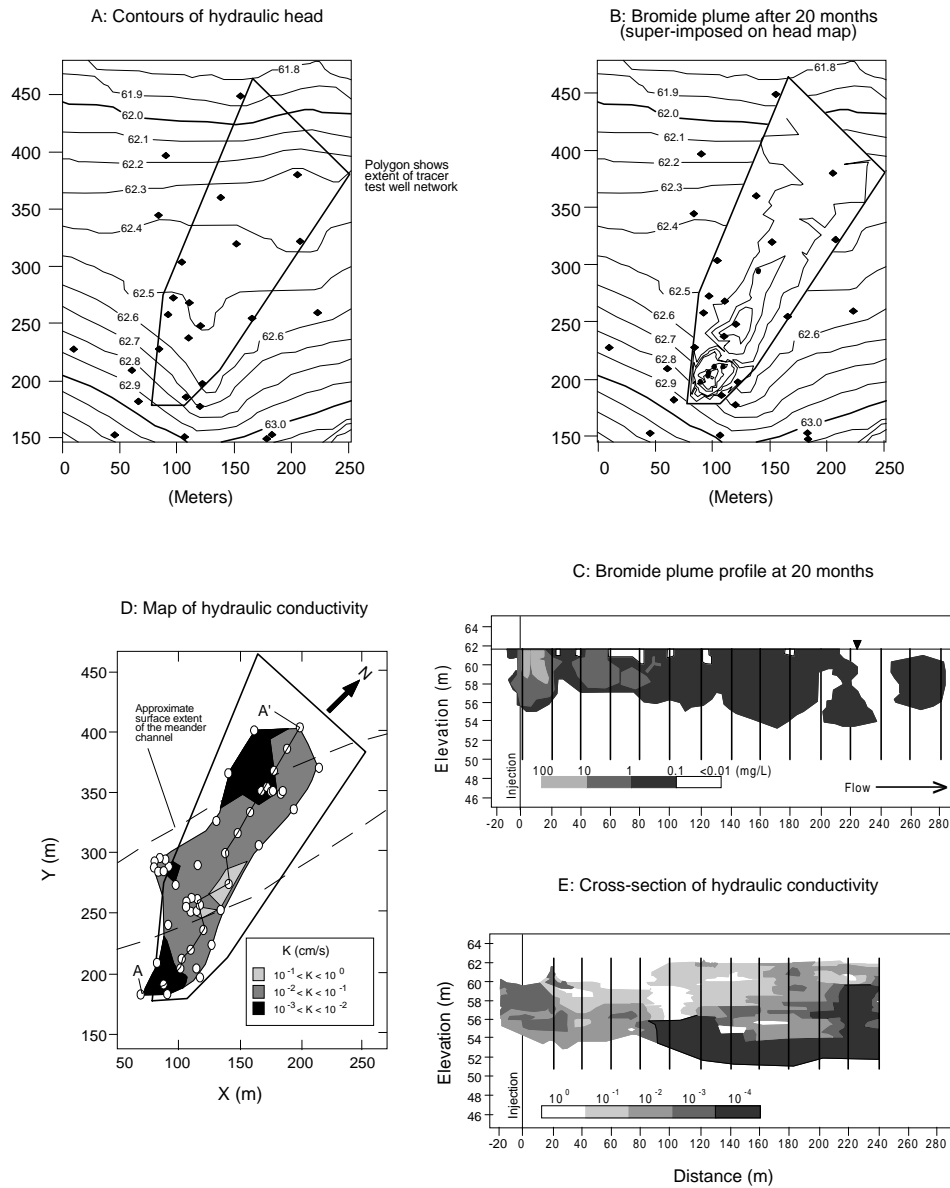


**Figure 2.14:** Observations from the MADE experiment conducted at Columbus Air Force Base (after Boggs et al., 1992, Adams and Gelhar, 1992 and Rehfeldt et al., 1992).

Figures 2.14D and 2.14E show the horizontal and vertical, hydraulic, conductivity distribution. A buried meandering channel (Figure 2.14C) cuts across the observation network and is traversed by the plume. The analysis of the tracer data dramatically reveals severe heterogeneous conditions. Macro-dispersivity values based on the plume extension, are 5-10 m (Adams and Gelhar, 1992). These values do not coincide with the range of 1.5 -1.8 m for the macro-dispersivity derived from the spatial, hydraulic, conductivity distribution (Rehfeldt et al., 1992). A serious problem occurs with the mass-balance of the conservative tracer (Boggs and Adams, 1992).

The question is, what causes the ambiguous macro-dispersivity values and tracer mass escaping the well network. Rehfeldt et. al. (1992) give several arguments indicating that the channel crossing the site of the MADE tracer experiment, has no significant impact on plume development. The observed non-stationairity at this location of the channel, is addressed using a polynomial trend removal. The authors conclude, however, that the proper trend can only be discerned using the tracer data. They admit that the latter makes the trend removal approach rather fruitless in predicting transport in the absence of detailed, tracer, test data, as is commonly the case. They conclude that trends should be identified from "hydraulic head distribution and major geologic features", leaving the question open as to why the meandering channel and existing head data (Figure 2.14A), have not been used for such an analysis. As presented in this dissertation, design, analysis and modeling of pumping tests conducted at the 1-HA test site, have been fully driven by an approach combining geology and drawdown response.

#### *The Horkheim experiment*

Teutsch et al. (1990) present results from a field experiment that includes, similar to the work presented in this dissertation, pumping tests and a forced-gradient tracer test. The test site is in an alluvial valley in Horkheim, in south Germany. It is comprised of highly heterogeneous, Neckar River sediments, comparable to those sediments found at the Columbus site. Local values for hydraulic conductivity were found to range over several orders of magnitude.

Ptak and Teutsch (1994) summarize different methods used for evaluation of the local hydraulic conductivity. Borehole flowmeter conductivities are compared with

conductivity values obtained using a permeameter and grainsize (sieve) analysis. They conclude that borehole flowmeter conductivities, used as input for macro-dispersion calculations for the Cape Cod and MADE experiments, may not fully represent the local-scale variability. The two reasons are: (1) the pumping test transmissivity representative of a larger scale (also see Section 6.5.2), is used to scale the flowmeter conductivities; and (2) the limited sensitivity of the impeller flowmeter biasing towards the higher conductivity values. As discussed in Section 2.5.3 and Chapter 3, these problems can be partly overcome by using a sensitive, electromagnetic, flow-measurement device and by using a pumping test with a limited investigation zone.

The macro-dispersivities obtained from the different methods assessing local-scale, hydraulic, conductivity, range from 5.8 m (for the flowmeter data) to 17.1 m (for the sieve-analysis data). These values are similar to the values found for Columbus, but significantly higher than the values found for Borden or Cape Cod. The macro-dispersivity based on the conductivity data, compares well with the values derived from the tracer experiments conducted at the Horkheim test site (Ptak and Teutsch, 1994). As predicted by practice (e.g. Gelhar et al., 1992) and theory (e.g. Dagan, 1989), macro-dispersivity increases with the length-scale of the tracer experiment. Contrary to this theory, no asymptotic behavior is observed at the scale of the experiment. Schad and Teutsch (1994) present pumping test results for the Horkheim test site. In a very similar fashion to the Columbus pumping tests, Schad and Teutsch conclude that these pumping test results are useful for a semi-quantitative diagnosis of heterogeneity.

#### *Summary of conclusions from field experiments*

In summary, four, large-scale, field experiments were aimed at practically testing the macro-dispersivity concept. In two cases, Borden and Cape Cod, macro-dispersion estimated from conductivity measurements, compares well with the macro-dispersion estimated from tracer migration. In these two cases the macro-dispersion estimated from tracer migration, reaches an asymptotic value; a positive conclusion is drawn regarding the practical use of macro-dispersion in predicting solute transport. The values for dispersivity, however, are low, just above the values considered to represent granular effects at the column-scale. This observation is also corroborated by geological

observations that only a single, clean, sandy/gravelly facies is involved. Thus, conclusions about the applicability of macro-dispersion based on these experiments, are limited to cases involving a similar low level of heterogeneity.

The two other test sites, the MADE and the Horkheim sites, are much more heterogeneous. For these test sites conductivity ranges over several ( $^{10}\log$ ) orders of magnitude, a fact indicating the presence of different low and high conductivity facies. In both cases macro-dispersion fails to reach an asymptotic value; therefore, its use in predicting tracer migration is doubtful.

In the case of the MADE site, the plume migration is also potentially severely impacted by a sudden (erosive) non-stationarity. This specific non-stationarity is not recognized, and the macro-dispersivity is obtained by detrending conductivity data (Rehfeldt et al., 1992). This detrending also eliminates an unspecified portion of the heterogeneity. Thus, the obtained macro-dispersivity is rather meaningless; it is no surprise that it does not fit very well with the value obtained from tracer migration data.

In contrast the Horkheim site seems to be a more stationary case. Macro-dispersion values obtained from the spatial distribution of conductivity data, fit reasonably well with the tracer migration data. Both the MADE and Horkheim cases do not meet the original three assumptions (see beginning of Section 2.4) regarding macro-dispersion. Thus, the problems encountered in predicting plume migration using macro-dispersivity are, no surprise.

It is remarkable that geological data are mainly considered a secondary issue, and are, consequently, not used as serious input for describing heterogeneous flow at these test sites. Leblanc et al. (1991) show a photograph of sediments constituting the Cape Cod aquifer. The photograph seems to be comprised of gravel-sand crossbed-sets roughly measuring 1 m (length). If this is heterogeneity typical for the scale of the tracer test, then the macro-dispersivity of 0.96 m observed from plume migration, could have been inferred from the typical length of these sedimentary structures. The latter is an approach consistent with the original relation between dispersion length and typical heterogeneity, such as grain size (see, for example, Fried, 1979).

Rehfeldt et al. (1992) show a geologic facies map representing the MADE aquifer. This facies map shows sand and gravel lenses measuring from 1 m to more than 7 m in length. Contrary to the macro-dispersivity obtained from mathematically, detrended,

conductivity data (Rehfeldt et al., 1992), the facies length-scale coincides with the macro-dispersion calculated from tracer migration (Adams and Gelhar, 1992). Moreover, the location map of the MADE site (Boggs et al., 1992) shows that the site is located close to a modern meandering river. Based on this observation, it is also predictable that there is a possible presence of a non-stationarity in the form of an abandoned meander. Results of sedimentological investigations could be major input for detrending, and could then allow one to properly remove the non-stationarity prior to geostatistical analysis (Young et al., 1991; Rehfeldt et al., 1992).

#### 2.4.5 Effective parameters versus geostatistical modeling

Both results from hypothetical aquifer studies and field experiments, indicate that the macro-dispersion concept has a very limited range of applicability. This prevailing problem is the mismatch between the assumptions underlying macro-dispersivity (see beginning of Section 2.4) and the geological reality appearing in sedimentological studies and/or specific field data. Macro-dispersion condenses all heterogeneity into a simple variogram, while excluding nested types of heterogeneity known to exist in sedimentology (see Section 2.2). Nested heterogeneity has a strong impact on solute transport (e.g. Jussel, 1992). This nested-scale behavior explains the discrepancy of macro-dispersion values found at the MADE site. The macro-dispersivity value of 1.5 m based on conductivity measurements (Rehfeldt et al., 1992), represents small-scale heterogeneities. The value of 5 -10 m reported by Adams and Gelhar (1992) and based on the observed plume, could be influenced by large-scale heterogeneities (or non-stationarities), such as the buried channel crossing the site (Herweijer and Young, 1991), and/or extra mixing could have occurred due to transient flow effects (Goode and Konikow, 1990).

In the best case, macro-dispersion can be used to describe average behavior (plume moments), but fails to predict practical aspects of solute transport, such as the time of first breakthrough and/or the peak concentration. This average behavior entails the average of multiple realizations or an ergodic (spatial) average when the scale of the solute transport is much larger than the heterogeneity scale. This geostatistically, averaged, solute, transport behavior should be compared to Kriging which also produces

the average of multiple realizations as an optimal estimate (map) for the spatial distribution of a variable.

Solute transport simulation for an ensemble of realizations in a geostatistical model, provides many more options. Such a model can be built using sedimentological knowledge, either by choosing a model based on multiple variograms of non-parametric variables (facies indicators), or an object model, or a genetic model. This inclusion of sedimentology dominates the petroleum industry's geostatistical modeling. Compared to systematic conductivity measurements necessary in establishing reliable variograms, sedimentological data can be inexpensively obtained. The Cape Cod and MADE experiments show that simple sedimentological data provide the same insight that is inferred from macro-dispersion. Processing many realizations of a geostatistical model, offers the possibility of addressing questions that do not relate to average behavior, such as risks of: quick breakthrough and/or peak levels exceeding a certain threshold.

Several cases have been reported of a proper match between oil production data and flow simulations of a geostatistical model for heterogeneous reservoirs that includes sedimentological data (e.g. Keijzer and Kortekaas, 1990). These matches were obtained without a major calibration effort, indicating that geostatistical models properly capture non-uniform flow patterns in heterogeneous fields. These successful practical applications are in contrast with the experience obtained with macro-dispersion. The latter appears to be a very problematic concept, even when much data are available such as in the field experiments previously discussed. Due to this, practical applications of the macro-dispersion concept are very limited.

## 2.5 USE OF PUMPING TESTS UNDER HETEROGENEOUS CONDITIONS

It has long been realized that the conventional approach of explaining pumping test response with an idealized type-curve model, disregards heterogeneity (King Hubbert, 1941; Muskat, 1949; Boulton, 1963). Problems arising from analyzing complex drawdown plots with type-curves, fall into two categories. First, it may be difficult to obtain a good fit using type-curves based on idealized aquifer models. These mis-fit problems, however, may provide useful information regarding heterogeneity. Second, good fits are possible, but a wide range of seemingly inconsistent values for the hydraulic parameters from different pumping tests and/or observation wells may be obtained.

Complex drawdown-curves, such as those for delayed gravity drainage (Neuman, 1972), a multi-layer case (Hemker, 1984; Hemker and Maas, 1987), and/or a linear strip (Butler and Liu, 1991; Bourgeois et al., 1993), provide many degrees of freedom and may result in a good fit that not necessarily provides a geologically valid solution. Especially for single-well tests, a non-uniqueness problem may occur; the same drawdown-curve may be produced by different sets of hydraulic parameters. Therefore, the choice for a certain type-curve model should be strongly governed by geological knowledge (Massonat and Bandiziol, 1991).

In the next sections several interpretation concepts are reviewed. Since the Columbus aquifer is unconfined, major attention has been paid to concepts for analyzing unconfined aquifer pumping tests. The use of the drawdown derivative, a concept originating from the petroleum engineering literature, is discussed. This method emerged over the past decade as a major tool for analyzing well test data focused on model and heterogeneity diagnosis (Ehlig-Economides, 1988).

### 2.5.1 Type-curves for heterogeneous formations

The Theis equation (Theis, 1935) can be used to analyze pumping tests under the assumption that groundwater flow is essentially horizontal; thus, vertical flow components can be neglected. One of the problems in applying the Theis solution to unconfined aquifers, is that this equation ignores the reduction of the saturated thickness occurring close to the pumping well. Jacob (1963) has shown that for this reason, the Theis solution should be used only after a correction factor has been applied to the drawdown data.

The Theis equation cannot provide type-curves that reproduce S-shaped curves, often observed in unconfined aquifers. The delayed yield theory (Boulton, 1954, 1963) explains the S-shape curves by assuming that in an unconfined aquifer, water is released from two storage components: first a volume released instantaneously when the aquifer head is dropped and removed from elastic storage coefficient of an equivalent confined aquifer; secondly, a volume that increases with time and is related to  $S_y$ , the specific yield. Streltsova (1972) shows that delayed yield for an unconfined aquifer can be approximated by water released from an aquitard overlying a confined aquifer. The aquitard has a zero (0) transmissivity and a storage coefficient equal to its specific yield.

The vertical resistance of the aquitard is smaller, by a factor of three, than the vertical resistance of the aquifer. The delayed gravity drainage theory (Neuman, 1972, 1974, 1975) assumes that the unconfined aquifer is a compressible system in which the water table is a moving material boundary. Air entry effects and unsaturated flow are disregarded. Although the theories based on delayed yield and delayed gravity drainage differ, Neuman (1975) shows that for fully penetrating wells the different methods produce identical values for the parameters  $T$ ,  $S$ , and  $S_y$ .

Streltsova (1988) gives type-curves for the general two-layer model and shows that the Neuman type-curve is a special case. Gringarten (1982) shows that the drawdown response for a fractured (double porosity) aquifer is exactly similar to the drawdown response caused by delayed yield. The latter similarity is illustrated by Reeves et al. (1984). Using a double porosity, fracture-flow model, they simulate drawdown-curves matching field drawdown data observed in an unconfined aquifer.

Barker and Herbert (1982), as well as Butler (1988) show that changes in transmissivity with radial distance can cause pseudo S-shaped, drawdown responses. Butler and Liu (1991) show the effect of linear changes in transmissivity. It is possible to envisage that delayed yield curves not showing a good horizontal segment, might be largely affected by radial and, especially, linear transmissivity contrasts. Typical examples of such curves can be found in Prickett (1965) and Neuman (1975).

Thus, the S-shaped type-curve can be explained by: multi-layer effects; fractures; unconfined effects; and, partly, by radial and linear, conductivity contrasts. Therefore, one should be extremely cautious when dealing with heterogeneous unconfined aquifers, because all these may occur: the multi-layer situation; pseudo fractures (highly conductive sediment streaks); lateral conductivity contrasts; and unconfined effects. In the latter case, one should also consider using Theis type-curves, or comparable methods, for extracting trends related to aquifer heterogeneity, complementary to the Neuman type-curve analysis.

Mis-fits to Theis type-curves, draw more attention to aquifer heterogeneity than good fits to the Neuman curves. These good fits using Neuman type-curves, are relatively easy to obtain given the large number of fitting parameters. The resulting values for hydraulic parameters, however, are often difficult to relate to actual aquifer conditions. Moreover, the Cooper-Jacob straight line method, which is based on the Theis equation, has been shown in several cases to be a robust tool for identifying lateral transmissivity

changes in an aquifer (Butler, 1990). This use of the Cooper-Jacob straight line is similar to the derivative method (Ehlig-Economides, 1988) that is widely used in the petroleum industry (also see Section 2.5.2). For a specific field case where significant heterogeneity is suspected, an appropriate interpretation approach is to use several drawdown-curve models. From fits, mis-fits, and dispersion of obtained hydraulic parameters, an impression of the heterogeneity effect can be distilled.

**2.5.2 Use of drawdown derivative for aquifer diagnosis**

In the last decade petroleum well test interpretation has paid much attention to diagnosing heterogeneous flow systems using the derivative method (for a summary, see Ehlig-Economides, 1988). In the hydrogeological literature only a few applications have been reported (Butler and Liu, 1991). Correct calculation of the drawdown time-derivative, requires extremely accurate drawdown measurements. This can be costly for shallow aquifers, and sometimes difficult, for example due to atmospheric influences.

The principle of using the derivative of drawdown with respect to the logarithm of time, is a generalization of the Cooper-Jacob, straight, line method. This method can be applied to the infinite, acting, radial, flow case (i.e., the zone of influence delivering most of the well's flow, is radial in an apparent homogeneous aquifer). The derivative to logarithmic-time, in this case, becomes constant after a while (stabilization, i.e. the Cooper-Jacob slope). This can be simply derived from the fact that the drawdown for an observation well at radial distance r, can be approximated (Cooper and Jacob, 1946) by:

$s = \frac{2.30 \cdot Q}{4 \cdot \pi \cdot KH} \cdot \log \frac{2.25 \cdot KH}{r^2 \cdot S} \cdot t \dots\dots\dots(2.7)$								
$\text{and, } \frac{ds}{d(\log t)} = \frac{2.30 \cdot Q}{4 \cdot \pi \cdot KH} \dots\dots\dots(2.8)$								
$\text{thus, } KH = \frac{2.30 \cdot Q}{4 \cdot \pi \cdot \Delta s} \text{ where } \Delta s = \frac{ds}{d(^{10} \log t)} \dots\dots\dots(2.9)$								
<table style="width: 100%; border: none;"> <tr> <td style="width: 50%;">s = drawdown</td> <td style="width: 50%;">Q = rate</td> </tr> <tr> <td>K = hydraulic conductivity (m/s)</td> <td>H = aquifer thickness</td> </tr> <tr> <td>r = radial distance</td> <td>S = storage coefficient</td> </tr> <tr> <td>t = time/t<sub>0</sub></td> <td>Δs = Cooper-Jacob slope or derivative stabilization level</td> </tr> </table>	s = drawdown	Q = rate	K = hydraulic conductivity (m/s)	H = aquifer thickness	r = radial distance	S = storage coefficient	t = time/t <sub>0</sub>	Δs = Cooper-Jacob slope or derivative stabilization level
s = drawdown	Q = rate							
K = hydraulic conductivity (m/s)	H = aquifer thickness							
r = radial distance	S = storage coefficient							
t = time/t <sub>0</sub>	Δs = Cooper-Jacob slope or derivative stabilization level							

Calculating the transmissivity from this derivative stabilization, is nothing else than determining the straight line slope on the Cooper-Jacob semi-log plot, and then using the well known, Cooper-Jacob formula (Equations 2.8 and 2.9). Figure 2.15 shows drawdown-curves obtained using a numerical model for a pumping test in a homogeneous aquifer. Figure 2.15A is a plot of drawdown on a log-log-scale. Figure 2.15B is a semi-log (Cooper-Jacob) plot, while Figure 2.15C is a plot of the drawdown derivative on a log-log plot. The derivative stabilization after 200 seconds, yields directly the Cooper-Jacob slope value of 0.062 m/s that can then be used in Equation 2.9 to calculate the transmissivity (KH). The sharp rise of the derivative for the modeled drawdown-curve at  $t = 4 \times 10^6$  seconds, represents the rise of drawdown due to the numerical model's no-flow boundaries. This rise is on the log-log drawdown plot and is barely discernible, and on the semi-log plot it is only apparent more than half a log-cycle later.

The above example shows that for a homogeneous aquifer, the use of the derivative is analogous to the Cooper-Jacob, straight, line method. For a more complex aquifer, the analysis of the derivative can be very helpful for a detailed analysis of flow systems during the pumping test. For example, consider an aquifer consisting of two, concentric, transmissivity zones. In this case the derivative first becomes constant (a first Cooper-Jacob slope) and reflects the transmissivity of the inner zone. After a transitional period, the derivative becomes constant again (a second Cooper-Jacob slope), but now at a value reflecting the transmissivity of the outer zone. For the Neuman, delayed yield, type-curve shown in Figure 2.16, the derivative first becomes constant at a value reflecting the aquifer transmissivity. Subsequently, the derivative dips to a minimum reflecting the flattening on the drawdown-curve; then it climbs back to the same constant value of the early-time representing the aquifer transmissivity.

If flow towards a well is considered, in or close to a linear zone (channel or dike), then for early-time this channel contributes most of the well flow, while the drawdown can be approximated (see e.g. Kruseman en de Ridder, 1990, p. 281) by:

$$s = \text{constant} \cdot \sqrt{t} \quad (2.10)$$

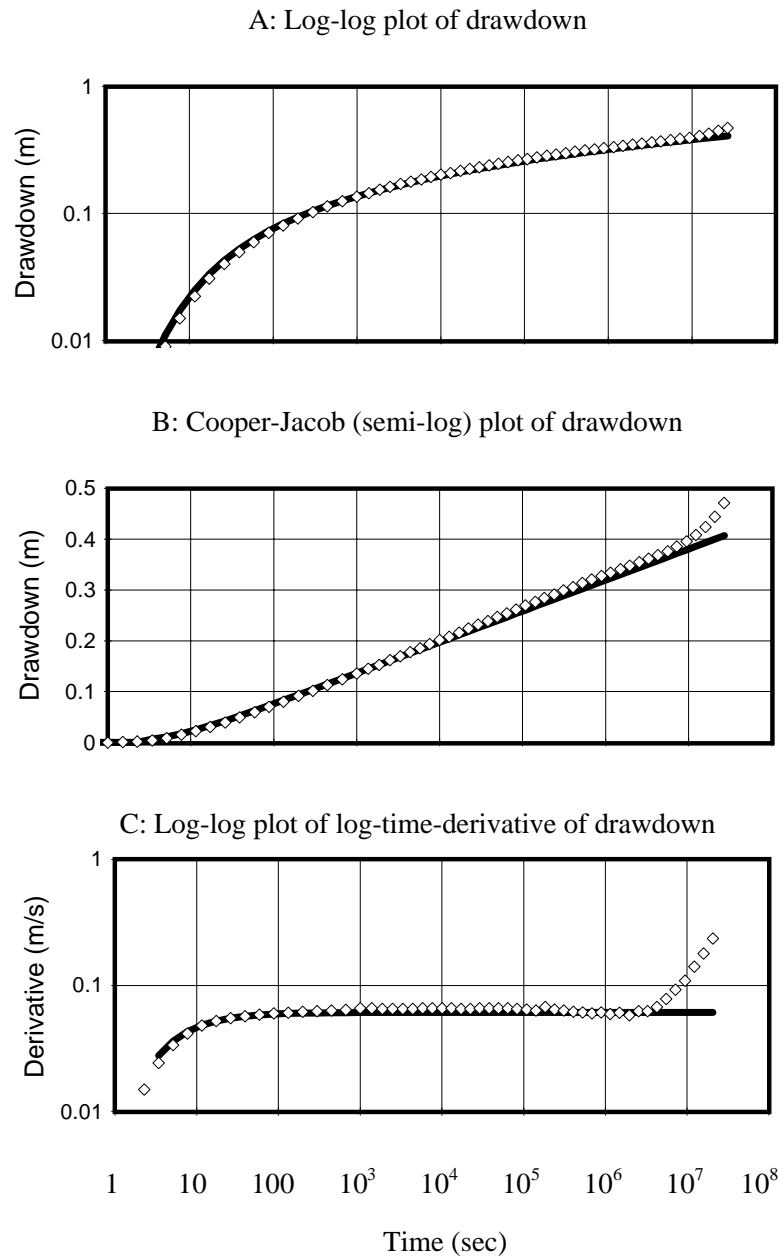


**Figure 2.15:** Example drawdown and derivative for a homogeneous aquifer. This type-curve (line) compared to data from pumping test model (diamonds).

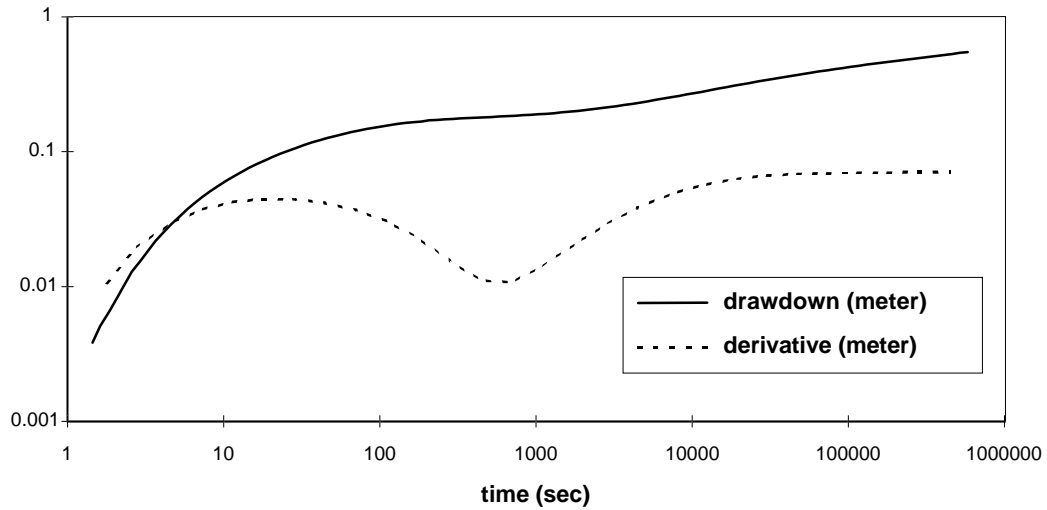


**Figure 2.16:** Drawdown and derivative for a Neuman type-curve.

parameters:  $Q = 0.002 \text{ m}^3/\text{s}$ ;  $T = 2.3 \cdot 10^{-3} \text{ m}^2/\text{s}$ ;  $S = 4.2 \cdot 10^{-4}$ ;  $S_y = 0.07$ ;  $\beta = 0.03$ .

Hence, the derivative will be:

$$\frac{ds}{d(\log \cdot t)} = \frac{0.5}{2.3} \cdot \text{constant} \cdot t^{0.5} \dots\dots\dots(2.11)$$

This implies a straight line (slope = 0.5) for both the drawdown and the drawdown derivative on a log-log plot. This, so called, half-slope can be used to identify a linear flow regime. Similarly, the occurrence of a quarter-slope (slope = 0.25 on a log-log plot), often following the half-slope, can be derived. The quarter-slope occurs for both the drawdown, as well as the drawdown derivative and represents bilinear flow: linear from a matrix to a channel or dike; and also linear from the channel or dike towards the well.

The derivative is most useful for analysis of drawdown-curves that do not easily fit one, simple, type-curve model and where the zone of influence passes through several different geometries. If the conditions underlying the drawdown approximations (see above formulas), are temporarily valid, then the derivative signature allows one to diagnose, respectively, a homogeneous or linear (channel or dike) aquifer. This diagnosis

is only valid for the time that the derivative shows the typical signature; a time period which should be converted into a spatial extent using the zone of influence during that time period. A distinct feature with a derivative signature, may not show up at all, if there is not any time period for which the zone-of-influence covers this feature exclusively<sup>1</sup>.

The following example covers a fairly complex geometry which can be partly resolved using the derivative method. Figure 2.17 shows an example case of a drawdown on a log-log and a semi-log plot, as well as the drawdown derivative on a log-log plot. The drawdown derivative (Figure 2.17C) shows a first stabilization reflecting radial flow in the zone close to the well, and subsequently a half-slope on both the log-log drawdown plot (Figure 2.17B) and the derivative plot (Figure 2.17C), which indicates that linear flow in a channel occurs. After the zone of influence has passed the outer edges of the finite length channel, the flow regime becomes radial again, while the derivative stabilizes at a value reflecting the outer zone transmissivity. The drawdown curves shown in Figure 2.17 are based on a simulated, single-well, pumping test for two, rectangular, high K channels crossing each other in a perpendicular direction at the well-bore.

The derivative plot reveals three flow regimes (i.e., radial high K, linear, and radial low K) that are hard to discern on both, conventional, drawdown plots (Figure 2.17A and 2.17B). Thus, the analysis of the log-time drawdown derivative, is extremely useful for heterogeneous aquifers where drawdown inherently does not fit (and should not be fitted) with a single (simple or complex) type-curve model. The limitation is that the middle flow period in Figure 2.17 (between 0.3 - 5 hr) allows one to diagnose some sort of linear flow (a channel or a dike), but the actual geometry (two perpendicular channels crossing at the well-bore) remains unresolved by this single-well test.

Over the past decade the petroleum industry has intensively used the derivative method to diagnose flow regimes, such as: double-porosity; two-layer; reservoir limits; (Ehlig-Economides, 1988). In recent literature effects caused by lateral sedimentological

---

<sup>1</sup> Butler (1990) gives an overview on the zone of influence of a pumping test. He defines this zone as a “concentric ring of material that continually increases in width as it moves away from a pumping well”. This definition involves a moving inner and outer boundary; this is different from commonly used definitions which only consider the outer boundary. It explains why in a heterogeneous setting the type of aquifer seen by the test can change constantly. The radius of the inner boundary is  $\sqrt{0.1Tt/S}$ , the radius of the outer boundary is  $\sqrt{14.8Tt/S}$ .

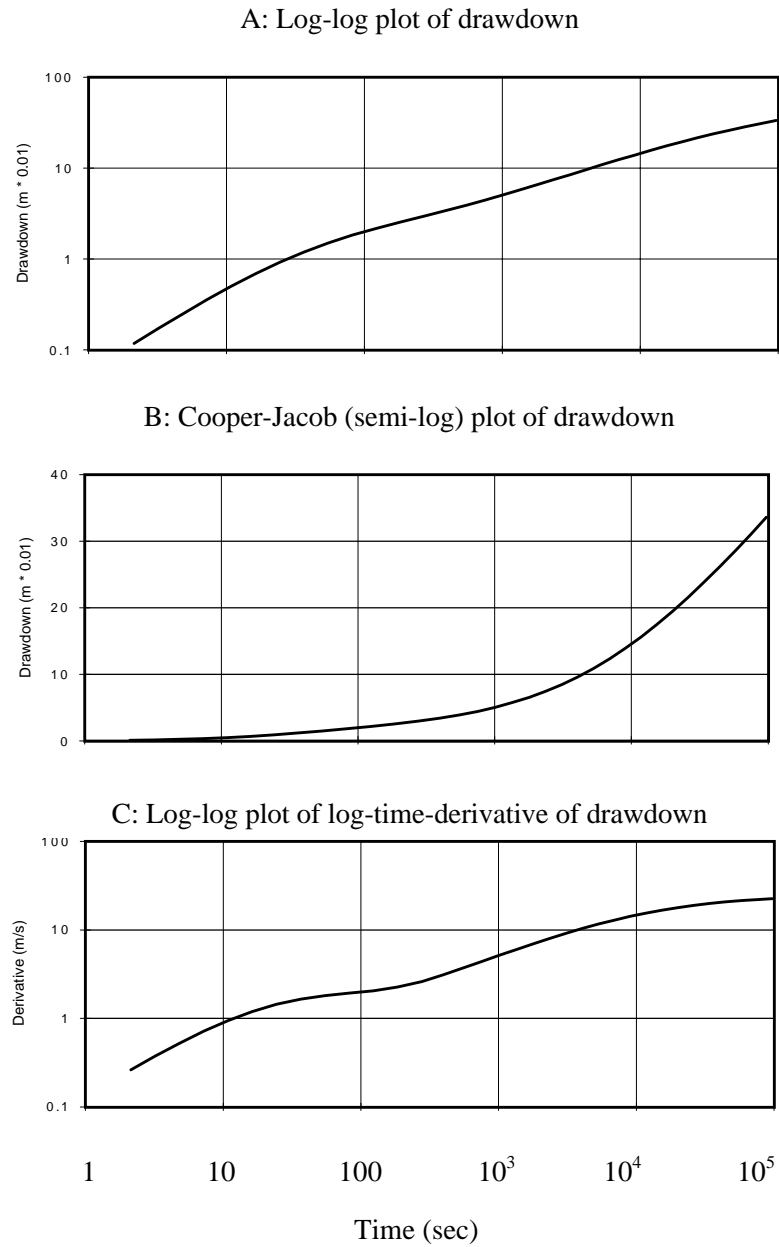


**Figure 2.17:** Drawdown and derivative for single-well test in a heterogeneous aquifer. Pumped well is located in the center of two crossing finite length high-K channels.

heterogeneity, have been more scrutinized (Massonat and Bandiziol, 1991; Bourgeois et al. 1993; Massonat et al., 1993).

### 2.5.3 Borehole flowmeter measurements to determine local conductivity

A depth profile of the hydraulic conductivity representative of a local area around the well-bore, can be obtained by using a borehole flowmeter to measure the contributions of the different layers in relation to the total rate withdrawn or injected. The borehole flowmeter method is typically conducted in conjunction with a single-well test. Hydraulic conductivities for individual layers are obtained by splitting the total transmissivity proportionally to the layer flow-rates. Figure 2.18 conceptually shows the use of borehole flowmeter for the calculation of vertical profile of horizontal conductivity. Several authors (e.g., Rehfeldt et al., 1989; Moltz et al., 1989) discuss the application of this technique, analyzing data obtained using an impeller borehole flowmeter. A very sensitive, electromagnetic, borehole flowmeter is discussed by Young and Pearson (1990) and Moltz and Young (1993).

The borehole flowmeter is a unique method that obtains small-scale conductivity values from a well test. There are, however, the following two limitations. First, the calculation of individual layer conductivity values, assumes infinite extending layers; this assumption is often contradicted by heterogeneity revealed by borehole flowmeter measurements (e.g. Rehfeldt et al., 1992). Second, a detailed interpretation of the pumping test is required to establish a reliable transmissivity value at the well-bore. A large-scale pumping test, as used by Moltz et al. (1989), gives an average aquifer transmissivity that does not reflect local heterogeneity around individual wells (see Section 5.3 and Section 6.5.2). In case of severe heterogeneity, it is often impossible to obtain a proper transmissivity around a well, especially when the Cooper-Jacob equation is applied for the whole pumping period (Rehfeldt et al., 1989b). Due to both limitations it can be stated that the borehole flowmeter properly reflects vertical contrasts of horizontal conductivity in a well, but that a significant error might be introduced when quantitatively comparing borehole flowmeter conductivity observed in different wells.

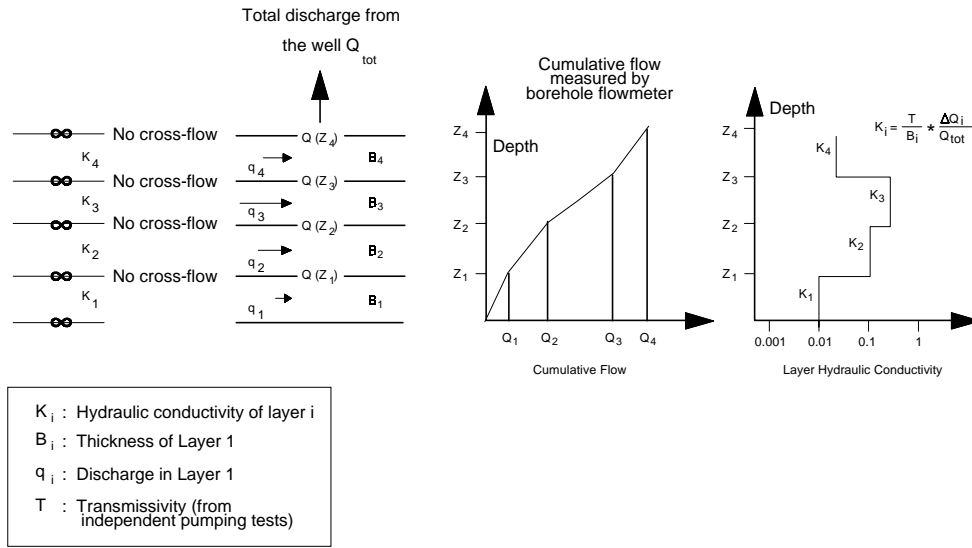


**Figure 2.18:** Determination of layer conductivities using borehole flowmeter measurements

#### 2.5.4 Geostatistical inversion of pumping test data

Alabert (1989) conducted numerical flow simulations for a suite of different geostatistical models. Based on these results, he presents the relationship between pumping test conductivity for a single-well test and specific geostatistical parameters. Deutsch (1992) employs the so called simulated annealing method (Deutsch and Journel, 1992) to create a geostatistical model that fits certain pumping test data. In this method an initial geostatistical model is created independent of the pumping test data, but based on geological evidence. Subsequently, this model is changed step-wise, without changing its geostatistical character, until its pumping test response fits observed data. This procedure is repeated for several different realizations. The result is a special (sub-)set of realizations of the geostatistical model constrained by the pumping test. Constraining the geostatistical model by using the pumping test data, helps to narrow the variability of

hydraulic behavior of interest (i.e., oil production for the case presented by Deutsch (1992)).

The main problem of this procedure is that the geostatistical model undergoes thousands of updates; for each of these updates a pumping test response has to be calculated. Conducting a numerical flow simulation for each update, is obviously too cumbersome to be cost effective; one has to revert to an averaging procedure to relate an effective model conductivity to the effective conductivity from the pumping-response. This averaging procedure imposes a strong *a priori* assumption for the pumping test. The averaging procedures employed assume: an *a priori*, radial, flow pattern; a certain radius-of-influence (Oliver, 1990); and, thus, a pseudo, homogeneous, pumping test response.

Deutsch (1992) employs a radial flow model and a power-average. The power-exponent is obtained by comparing the average of a few realizations with pumping test results obtained by numerical flow modeling. Sagar (1993) and Sagar et al. (1993) present more sophisticated averaging schemes that involve a different procedure for radial and angular averaging. Both these assumptions are rather limited given field observed well test responses for heterogeneous media that often indicating non-radial flow patterns. Simple averaging schemes for non-radial flow patterns, are not readily available, a fact limiting the above outlined approach.

Another inversion method involves the method known as the "pilot point method" (Marsily et al., 1984). Using a gradient method the transmissivity is optimized for a limited amount of "pilot points" in a model. The pilot points are selected at locations where the transmissivity is most sensitive, given the pumping test data available. For all other grid-points, transmissivity values are obtained through Kriging. Thus, the solution is not a geostatistical heterogeneous case, but rather a geostatistical average representing the pumping test. Sanchez Villa (1993) presents a geostatistical modeling procedure based on the same method. For an initial realization the pilot points are optimized. Subsequently, realizations are created that include the original data and the pilot point data (including an error) as conditioning points. Applications of this method have been limited to multi-well, pumping, test data (Marsily et al., 1984; Fasanino et al., 1986)

## **CHAPTER 3:**

### **EXAMPLE OF FLOW IN A HETEROGENEOUS AQUIFER: PUMPING TESTS AND TRACER TESTS AT COLUMBUS**

### 3.1 INTRODUCTION<sup>1</sup>

In hydrogeology as in most other scientific disciplines, (field) experimental data are important and an ultimate benchmark in testing theories and numerical procedures. Usually it is extremely hard to exactly reproduce theoretical predictions. Depending on the severity of the problems, one either has to decide to refine the data quality or ultimately consider alternative theoretical concepts. For a natural science, like hydrogeology, major attention has to be paid to the latter, in other words, an alternative hypothesis has to be formulated based on the field experimental work.

Often the logic is reversed: analytical theories are postulated; tested against numerical experiments; and, subsequently, field experiments are only conducted to validate theories and considered disappointing when problems with theoretical concepts occur. Obviously, numerical validation only implies that a mathematical schema is implemented correctly while still representing a hypothetical theory.

A very important issue ought to be comparison of theoretical approaches to field data from controlled experiments. These should be designed not only to validate the theory, but also to challenge the theory, potentially becoming a source of inspiration for new concepts. These field experiments are expensive; therefore, funding is scarcely available for tracer tests (see Section 2.4.4) and practically unavailable for pumping tests. Even controlled field data are often imperfect; they include significant errors and uncertainty. As a result, the popularity of numerical experiments versus field experiments, is understandable, though not defensible.

For the subject of this dissertation, data are needed specifically in order understand the relationship among heterogeneity, pumping test response, and solute (tracer) transport. This implies that several different types of data have to be available: geological data to understand the origin of heterogeneity; pumping test data; and solute transport (tracer) data to describe subsurface fluid pathways. Research has been conducted at the Tennessee Valley Authority's (TVA) groundwater test site at Columbus Air Force Base. The investigations of the shallow unconfined aquifer are part of TVA's groundwater program and, for the most part, fit this dissertation's research requirements. This site has

---

<sup>1</sup> Parts of this chapter are derived from papers jointly authored with S.C. Young.

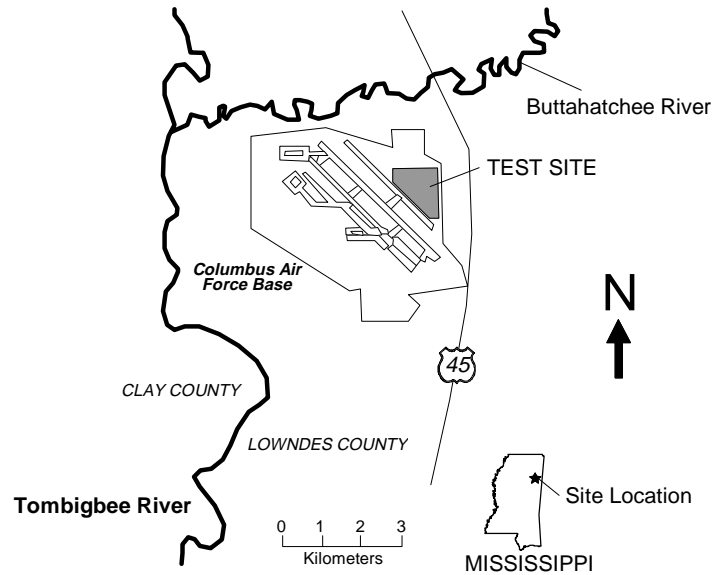


**Figure 3.1:** Location map of test site.

been used since 1986, for a natural, gradient, tracer experiment (MADE, see Section 2.4.4). In 1989, parallel to this experiment, a large number of pumping tests, along with several, forced-gradient, tracer tests were conducted. These tracer tests were conducted on a small, one hectare, subset, test site at Columbus (Young 1991a, 1991b); this site was named the 1-HA test site. This uncontaminated site was chosen as an analog for a case requiring recovery or containment of a pollutant, it is also a case where aquifer heterogeneity becomes very important in evaluating the risks and strategies of recovery/containment.

The ideas behind this test program were: (1) To demonstrate the variability in outcome of standard pumping tests; and (2) to develop practical methods for detection of preferential solute transport pathways in a heterogeneous aquifer. Demonstration of the variability of pumping test response, has not, traditionally, been brought to hydrogeologists' attention, since researchers have always been eager to show uniformity and conformity with idealized models. Contrary to these traditional approaches, this test

program was designed to capture heterogeneity, hence creating a large variety of results. The tests results of the Columbus 1-HA test site, have been an invaluable inspiration and guideline in approaching the problem of quantification of subsurface heterogeneity presented in the following chapters. This chapter's next sections present part of the field data relevant to material presented in the later chapters.

### 3.2 LOCATION AND HYDROGEOLOGICAL CONDITIONS

The 1-HA test site is located on 25 hectares of the TVA Columbus Groundwater Research Test Site on the Columbus Air Force Base in Mississippi (USA). The site is approximately 6 km east of the Tombigbee River and 2.5 km south of the Buttahatchee River; it lies above the 100-year flood plain of both rivers (Figure 3.1). The unconfined

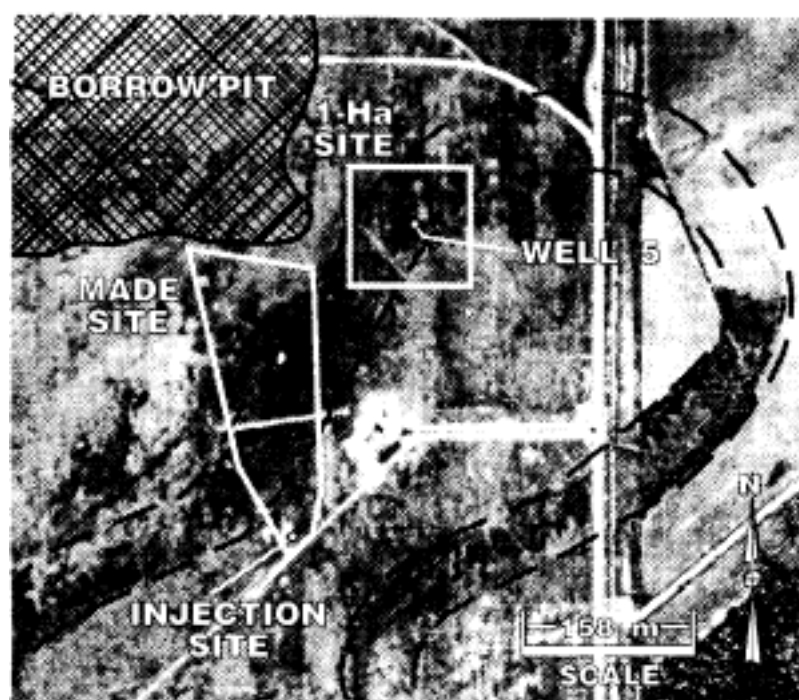


**Figure 3.2:** Air photograph of the Columbus test site.

upper aquifer is composed of approximately 10 meters of Pleistocene and Holocene fluvial deposits, primarily consisting of irregular lenses of poorly sorted to well sorted sandy-gravel and gravely-sand.

Groundwater levels across the Columbus Research Test Site have been monitored since 1985, using single-staged and multi-staged monitor wells. The phreatic surface seasonally fluctuates two to three (2-3) meters. The horizontal gradient varies from approximately 0.02 (low water table) to 0.05 (high water table). Erratic occurrence of upward and downward vertical gradients, have been observed throughout most of the site. These vertical gradients are related to the heterogeneities causing a complex flow pattern. Rainfall at the site averages 144 cm annually.

### 3.3 SEDIMENTOLOGY AND HETEROGENEOUS AQUIFER MODEL

The test site is located in an alluvial valley of the Tombigbee River. The valley is filled with coarse-grained, gravely, fluvial sands deposited during the Pleistocene and

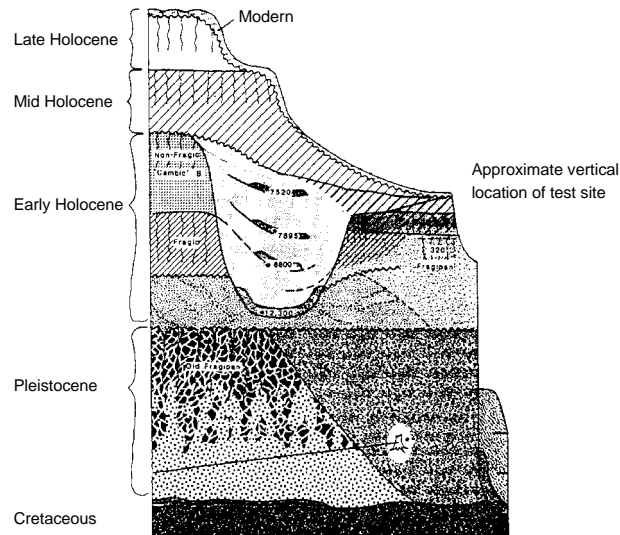


**Figure 3.3:** Conceptual sedimentological model for Tombigbee Valley fill (from Muto and Gunn, 1986). Note that the vertical scale is approximately 12 m.

Holocene. Air photographs (Figure 3.2) show traces of a former river meander. The width of this meander is approximately 75 m. using the width-thickness relation for highly, sinuous, meandering rivers (Leeder, 1973, also see equation 2.1), a meander fill thickness of 6 m is estimated. As shown later, the borehole, flowmeter, conductivity measurements indicate a contrast at 4 - 5 m depth that can be related to the channel deposit. Both the information from the width-thickness relation and the borehole flowmeter logs, strongly contradict the hypothesis proposed by Rehfeldt et al. (1992); their hypothesis is that the meander is only a superficial phenomenon. The 1-HA test site lies on the inner edge of this channel or the pointbar. The upper three meters (3 m) of the aquifer are exposed in gravel pits near the site; these are described by Rehfeldt et al. (1989) as a heterogeneous architecture of sand and gravel lenses ranging in length from 1 m to 8 m.

Muto and Gunn (1986) present a comprehensive description of the depositional history of the entire Tombigbee Valley. They based their interpretation (Figure 3.3) on numerous field data including trenches, core holes, and air photographs. According to this work, braided streams dominated the area during the Pleistocene. Larger meandering streams developed during the end of the Pleistocene, occasionally cutting deeply into the older deposits. Depositional models for the sands at the test site were evaluated in order to characterize the occurrence and the dimensions of gravel lenses and clay drapes. Given the regional model of Muto and Gunn (1986) and the site specific data, two depositional models are emphasized: deposition on the pointbar of a meandering stream; and braided stream deposition (see Section 2.2.3).

The coarse-grained, pointbar, depositional model for the upper part of the aquifer, implies a trend from coarse gravely sediments in the northwest, close to the former channel, to slightly finer material in the center and southeast area of the site. However, elongated coarse-gravel lenses do occur in the center and southeast of the site in the form of chute channels and chute bars. The direction of the meander infers that these lenses are oriented southwest to northeast. This sedimentological model predicts that these lenses are longer than 10 m and 2 to 7 m wide. The lenses may be capped and tailed (to the northeast) by thin clays. Since the position of the braid bars and braided channels is less stable than in meandering river deposits, the braided stream model for the lower half of the aquifer, predicts a more regular structure of alternating gravely lenses (braid bars) and

clay/silt infills for the braided channels. These lenses should be less extensive laterally than in the upper part of the aquifer.

### 3.4 FIELD PROGRAM

The field program consisted of three phases: (1) placement of wells; (2) a wide variety of hydraulic (pumping) tests; and (3) tracer tests. The following sections summarize the most important aspects of this field program.

#### 3.4.1 Drilling wells following a "randomized" spatial distribution

Initially, an important point of concern was the design of an optimal well network. The purpose of the field data is to systematically show variability. As a result, various conflicting needs must be satisfied. Information on the short-range spatial variability of a property (i.e., conductivity), requires closely spaced wells. However, to map this property sufficient aerial coverage requires an evenly spaced network. Formulated in geostatistical terms, a variogram requires a certain number of closely spaced wells to determine the variance for short-range lags, while Kriging (mapping) requires sufficient coverage of evenly spaced wells over the whole area.

Warrick and Myers (1987) present a procedure that optimizes a network for empirical determination of a variogram. Olea (1984) outlines criteria for choosing an optimal sampling network for Kriging. Considering the guidelines given by these authors, a computer model was developed (Herweijer, 1989) to generate, analyze, and optimize well networks. This program receives as input the number of: existing wells; new wells to improve the data-set for Kriging; and wells to improve the data-set for variogram determination. Figure 3.4 shows the selected, optimal, well network. Figure 3.5 graphically illustrates for this well network, the distribution of the number of well-pairs as a function of lag (inter-well) distances and the azimuth of the connecting vector. Since not all wells were drilled at the same time, the well planning model was re-run several

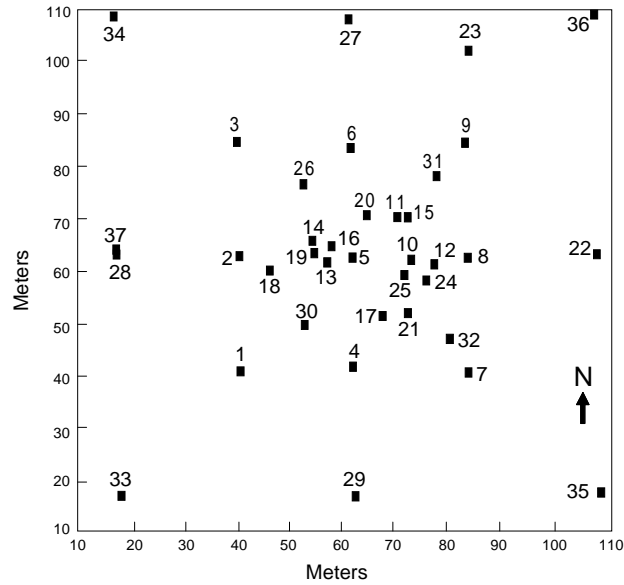


Figure 3.4: Well network at the 1-HA test site.

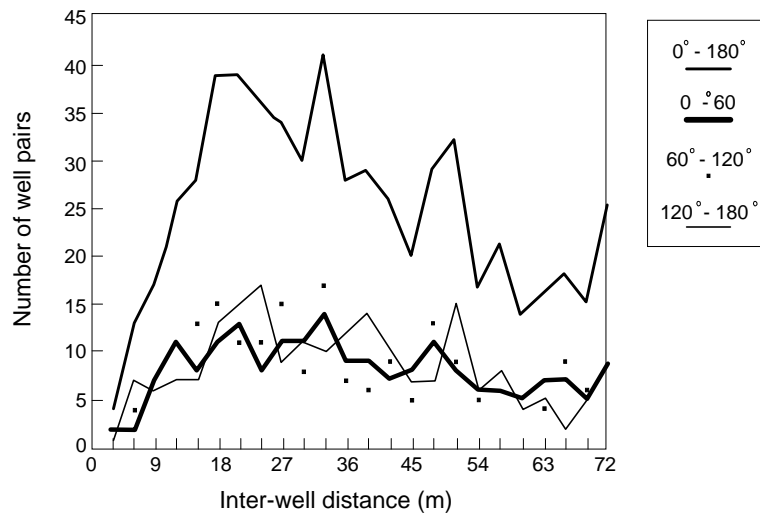


Figure 3.5: Number of well pairs versus inter-well distance (lag). Upper curve represents all well pairs, lower three curves represent well pairs with a connecting vector in three 60 degree sectors.

times, using the earlier drilled wells as fixed input. Initially nine wells are fixed to form the inner grid. Later, an additional eight wells are dedicated to form the outer grid. All other wells are positioned randomly.

### 3.4.2 Hydraulic (pumping) tests

In order to characterize the three-dimensional distribution of conductivity, a suite of single-well pumping tests, multi-well pumping tests, and borehole flowmeter measurements, was conducted at the test site. Through various test designs (i.e., varying from a 1-minute slug-test to a week long, multi-well, pumping test), different radii-of-influence concurring with different scales, are addressed. As a consequence the conductivities obtained from these test represent the average of various aquifer volumes.

**Table 3.1:** Overview of multi-well pumping tests.

Test	Pumped well	Rate l/min	Duration hr	Date	Observation wells equipped with pressure transducers <sup>1</sup>	Remark
AT1	5	68	144	May-89	2, 4, 6, 8, 15, 17, 18, 25, 30 <sup>2</sup>	Cyclic pumping
AT2	5	68	144	Jun-89	1-32 (rotating schedule)	
AT3	5	112	144	Jul-89	1, 2, 4, 6, 8, 14, 17, 20, 25, 26, 30, 31 <sup>2</sup>	
AT4	16	35	12	Oct-91	5, 13, 14, 19	injection
AT5	16	12	12	Oct-91	5, 13, 14, 19	
AT6	16	35	12	Oct-91	5, 13, 14, 19	
AT7	16	12	12	Oct-91	5, 13, 14, 19	injection
AT8	12	24	12	Jun-92	8, 10, 15, 17, 24, 25	
MADE1	PW1 <sup>2</sup>	62	72	Mar-85	7 wells <sup>3</sup>	
MADE2	PW2 <sup>2</sup>	208	192	Jul-85	7 wells <sup>3</sup>	
SC1	12	60	2.3	Jul-89	8, 10, 12, 13, 15, 17, 21, 24, 25, 31, 32	
SC2	13	77	1	Jun-89	5, 13, 14, 16, 18, 19	
SC3	16	81	2.3	Jul-89	5, 10, 11, 13, 14, 16, 17, 18, 19, 20, 25, 26	
SC4	19	34	0.8	Apr-89	13, 14, 16, 19	
SC5	24	34	1	Apr-89	10, 12, 25	
SC6	25	77	1	Jun-89	10, 12, 21, 24, 25, 32	
SC7	31	55	2.5	Jul-89	8, 9, 10, 11, 12, 15, 16, 17, 20, 25, 26, 31	

<sup>1</sup> Locations on Figure 3.4.

<sup>2</sup> For most other wells water levels were hand-measured.

<sup>3</sup> Wells are outside one-hectare test site, locations are on Figure 3.2.

In the following subsections the pumping tests of these various scales, are discussed in a sequence of descending scale for a full spectrum of scales ranging from large to small.

*Large-scale and small-scale, multi-well pumping tests*

Table 3.1 lists all multi-well pumping<sup>2</sup> tests at the 1-HA site. Ten pumping tests with pumping durations greater than 12 hours, were conducted in the Columbus aquifer. Eight of the tests were conducted on the 1-HA test site (see Figure 3.4). Of these eight tests, three of the tests involved pumping Well-5 (AT1-AT3) for about six days, while monitoring all 37 wells in the 1-HA test site. For AT1 and AT3, nine observation wells had pressure transducers for any given time interval, while the remaining wells were monitored manually with an electric tape. For AT2 a cyclic pumping, or pulse test, nine pressure transducers were shifted every two days. Hence, a total of 27 wells had continuous measurements for two days. For the pumping tests at Well-16 (AT4 - AT7), the pumping well (16) and the four closest wells had pressure transducers. For pumping test AT8, the pumping well (12) and the six closest wells had pressure transducers.

At the adjacent MADE site, two pumping tests had durations greater than 12 hours. The MADE1 pumping test included 12, partially-penetrating, observation wells along three rays extending outward from Well PW1. Four of the wells were monitored with pressure transducers; the remaining wells were monitored manually with an electric tape. The MADE2 pumping test included 15, partially-penetrating, observation wells. Five of these wells were monitored with pressure transducers; two of them were monitored with chart recorders, while the remaining wells were monitored manually with an electric tape (Boggs et al., 1990; Boggs et al., 1992).

Seven, small-scale, multi-well, pumping tests were carried out involving two-well clusters; each cluster had one pumping well and several observation wells within a radius of 6 m. The primary purpose of these tests was to determine the: variability of the calculated conductivities; and storage coefficients among combinations of a single pumping well and different observation wells at approximately the same distance. For these two clusters, tracer tests were also conducted (see Section 3.4.3).

---

<sup>2</sup> Pumping test is general terminology and also covers tests for which water is injected.

Figure 3.6 shows the difference in well layout for the large-scale, multi-well, pumping tests in comparison with the small-scale, multi-well, pumping tests. The short duration small-scale tests aim at analyzing the variety of responses to similarly laid out tests conducted at different locations. Each response represents a focused area between the pumping well and the observation well. Depending on heterogeneity, these responses can vary dramatically.

#### *Single-well tests at different scales*

A single-well test involves pumping a well while measuring drawdown in that same well. The single-well test provides a relatively inexpensive possibility of obtaining a transmissivity representative for an area surrounding that well. The extent of this area, or its radius-of-influence (see for example Butler, 1990 and Oliver, 1992), depends on many factors, such as the conductivity and heterogeneity surrounding the well and the time interval for which the test is analyzed. The main objective of the single-well tests conducted at the Columbus 1-HA test site, was to obtain accurate local values of the transmissivity. In turn these values were used to calculate layer K-values using the

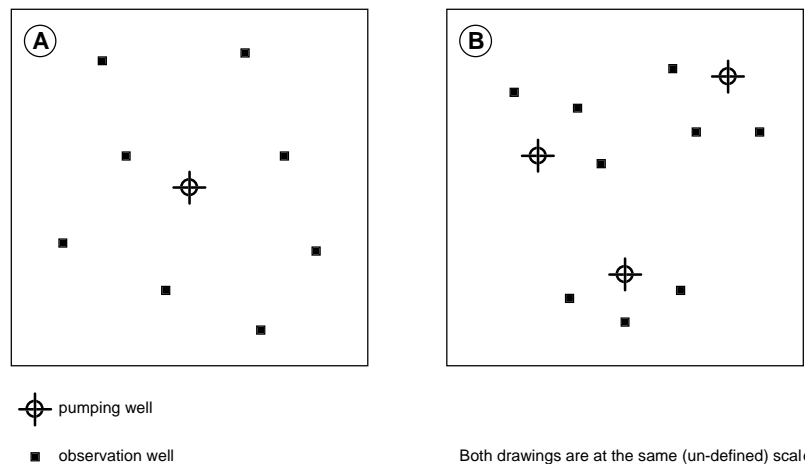


**Figure 3.6:** Example well layout for a large-scale, multi-well, pumping test (A) and small-scale, multi-well, pumping tests (B).

borehole flowmeter (see Section 3.4.2). In order to investigate the influence of a test design, five different types of single-well tests were performed for the test site's wells:

- 1- A falling head slug-test (23 l displaced volume);
- 2- A short duration (2 min) pump test at 34 l/min;
- 3- A moderate-rate (22 l/min) injection test (duration 45 min);
- 4- A low-rate (15 l/min) pumping test (duration 30 min);
- 5- A high-rate (60 l/min) pumping test (duration 30 min).

Figure 3.7 shows four types of single-well tests and the range of values obtained for 37 wells. Both the slug-tests (not displayed in Figure 3.7) and the short (2 minute) duration tests yielded conductivities far below the values of the large-scale pumping tests. This reduced conductivity is probably caused by damage during drilling and installation; this is known as a negative skin effect (see Earlougher, 1977; Faust and Mercer, 1984). Additionally, Figure 3.7 ranks all wells by the injection test transmissivity. It is obvious

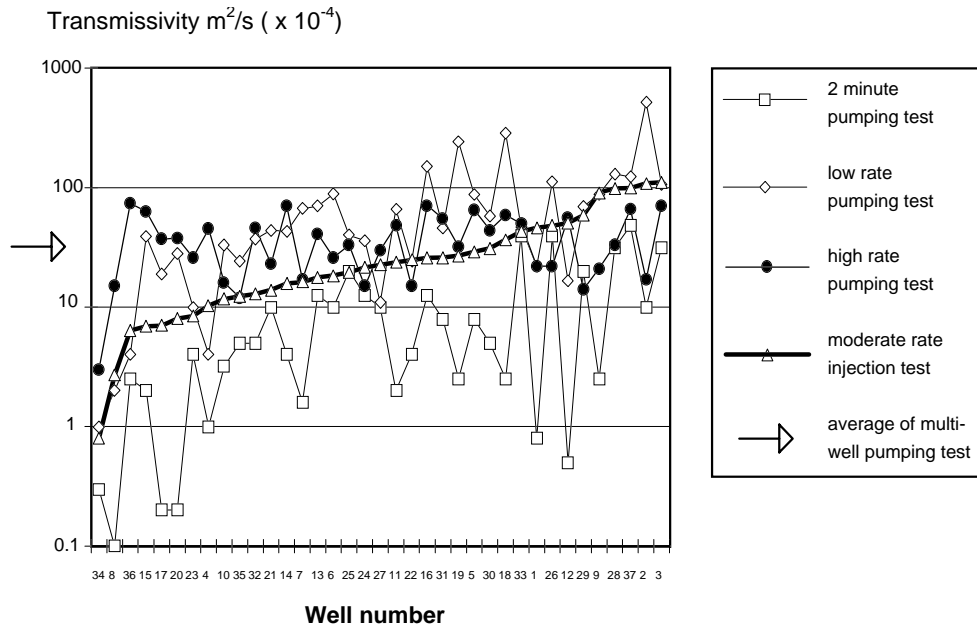


Figure 3.7: K-values obtained using different hydraulic (pumping) test.

that the results from the other tests only partially follow this ranking. The short duration test yields values that are systematically lower than the injection test values. The low-rate pumping tests show roughly the same trend as the injection test. The high-rate tests show significantly less variation and their values are always around the value obtained from the large-scale multi-well tests (indicated by the arrow).

The differences among the results of the tests with different rates, can be attributed to the fact that the aquifer is unconfined and, therefore, its total transmissivity changes with the drawdown created during the test. Especially thin, highly conductive layers just below the water table, can cause a significant reduction in transmissivity for a test that dewateres that layer in the direct vicinity of the pumped well. Young (1991a, 1991b) presents a comprehensive discussion of results and pitfalls when interpreting these tests. The fact that interpreting the same test at a different time-scale yields very different results, is further discussed in Section 4.4. The moderate rate injection test results were used to determine borehole flowmeter conductivities.

#### *Borehole flowmeter test results*

A conductivity depth profile representative of the localized area around the wellbore, can be obtained during a single-well test by using a borehole flowmeter to measure contributions of different subsurface layers to the total flow-rate withdrawn or injected. Conductivities for the individual layers are obtained by splitting total transmissivity obtained from a pumping test, proportionally to the layer's flow-rates. As discussed in Section 2.5.3, this requires a transmissivity correctly representing the summation of local-scale conductivity multiplied by thickness.

However, in the case of a heterogeneous aquifer, there may not be a simple relationship between that transmissivity and the vertical sum of local-scale conductivities (also see Sections 4.4 and 6.5.2). This heterogeneity effect introduces a significant error in addition to the instrument error. Several authors (e.g., Moltz et al., 1989) discuss the application of this technique by analyzing data obtained using an impeller borehole flowmeter. At the 1-HA test site a newly developed (Young and Pearson, 1990), highly sensitive, electromagnetic borehole flowmeter, was successfully applied.

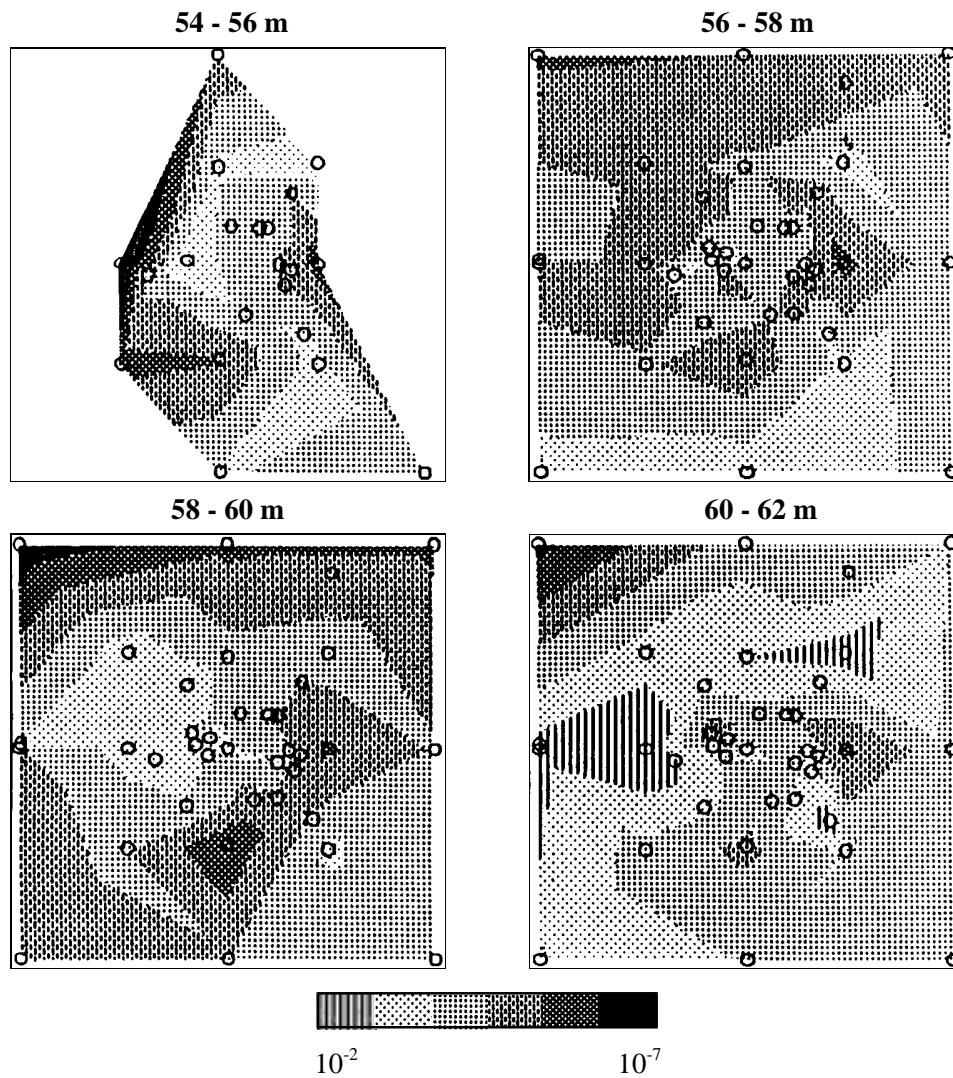


**Figure 3.8:** Maps of depth averaged  $^{10}\log(K)$ , for four depth intervals (indicated in meter above MSL). Circles denote well locations.

Figure 3.8 shows four maps obtained by depth averaging the measurements over two meter (2 m) thick intervals. The trend observed in the upper two layers concurs with the main geologic structure (the buried channel discussed in Section 3.3). Figure 3.9 shows a three-dimensional display of vertical logs of the borehole flowmeter

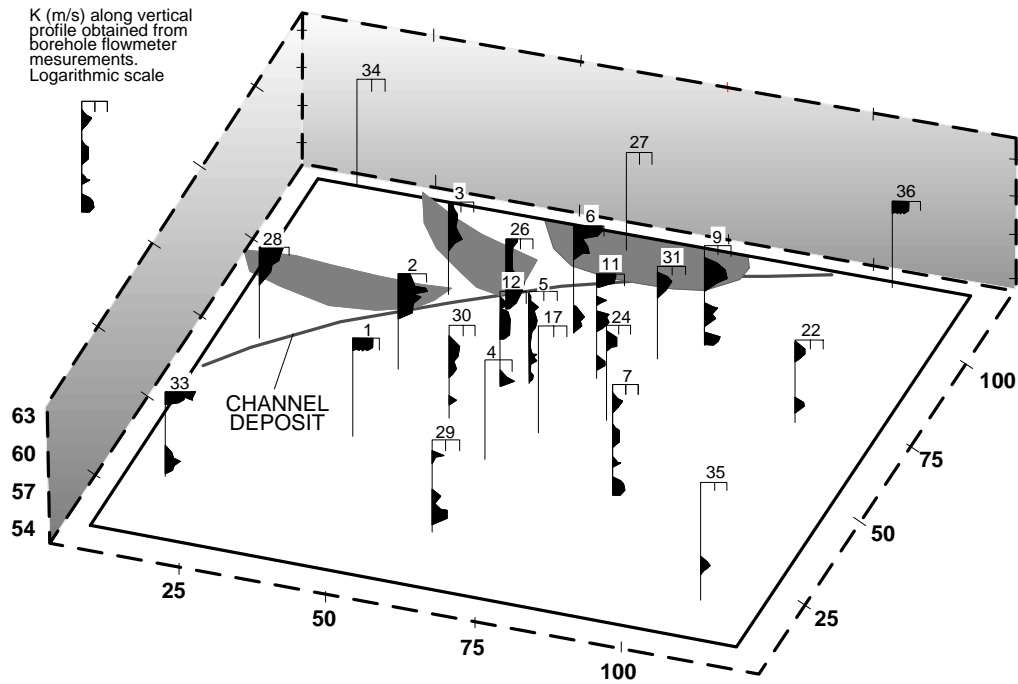


**Figure 3.9:** 3D diagram viewed from above, of  $K$  value greater than  $7 \cdot 10^{-4}$  m/s at selected wells. The contours are the interpreted outline of the buried meander. Scale is logarithmic, left is  $7 \cdot 10^{-4}$  m/s, right is  $7 \cdot 10^{-2}$  m/s.

conductivity. The borehole flowmeter results are an indirect indicator of both the geologic layering within the system and the relative properties of the layers. The borehole flowmeter profiles enable one to determine the aquifer's structure pertinent to its main parameter of interest, the conductivity, while avoiding costly, continuous, soil sampling on a per well basis. The borehole flowmeter conductivities are further discussed in Chapter 5 and are used as data for the geostatistical models discussed in Chapter 6.

### 3.4.3 Tracer Tests

A series of tracer tests was carried out on scales ranging from 3 to 100 m using a Br and Cl tracer. The next sections will briefly present two, small-scale, tracer tests (TT1

and TT2), and a large-scale tracer test (TT-large). Table 3.2 gives an overview of these tracer tests. In these tests water was injected in a tracer release well and withdrawn in equal portions from tracer observation wells. Tracer injection was started when the drawdown reached a steady state. Tracer breakthrough was monitored using multi-level samplers located at 1.5 meter intervals. The two, small-scale, tracer tests discussed, involved clusters of closely drilled wells (4-6 m) for which small-scale, multi-well, pumping tests had been conducted. The relationship between the tracer test results and the results from analyzing these pumping tests, are presented in more detail in Chapter 4. The large-scale tracer test involved injection at the central well (used as the pumping well for the large-scale pumping tests); using a 5-spot configuration, water was withdrawn from the four corner wells of the densely drilled middle section of the test site (Figure 3.4).

#### *Small-scale tracer tests*

For small-scale, tracer Test-1, tracer was injected in Well-16 and breakthroughs were observed in four wells (Well-5, Well-13, Well-14, and Well-19). Figure 3.10 shows the borehole flowmeter profiles observed during this tracer test and during previous single-well tests. Lenses at two levels (56 m MSL and 59-60 m MSL) can be readily correlated between all the wells, except Well-5. Breakthrough occurred within 100 minutes in all wells, except Well-5. This fits well with the good correlation of the borehole flowmeter profiles (Figure 3.10) indicating continuous high conductivity lenses.

For small-scale tracer Test-2, tracer was injected in Well-12 and breakthrough was observed in four wells (Well-8, Well-10, Well-24, and Well-25). Figure 3.11 shows the

**Table 3.2:** Overview of tracer tests

Test	Injection well	Rate m <sup>3</sup> /s	Duration	Date	Withdrawal and observation wells equipped with vertically distributed samplers	Pumping test <sup>1</sup>
TT1	16	0.0006	12 hr	Apr-90	5, 13, 14, 19	SC3
TT2	12	0.0005	12 hr	Apr-90	8, 10, 24, 25	SC1
TT-large	5	0.0018	60 day	May-90	1, 3, 7, 9 + samplers at almost all other wells	AT1 - AT3

<sup>1</sup> Corresponding pumping test (see Table 3.1).

borehole flowmeter profiles observed during this tracer test and during previous single-well tests. Compared with tracer Test-1, breakthrough takes significantly more time (200 minutes or more) for nearly the same distance between injection and observation wells. The vertical, borehole flowmeter profiles (Figure 3.11) indicate large vertical contrasts in conductivity. However, the high conductivity intervals can not be correlated among the wells as easily as those in the cluster used in tracer Test-1 (see Figure 3.10). This explains the relative delay in tracer breakthrough compared to tracer Test-1.

#### Large-scale tracer test

The large-scale tracer test involved injecting tracer in the central Well-5 (160 l/min)

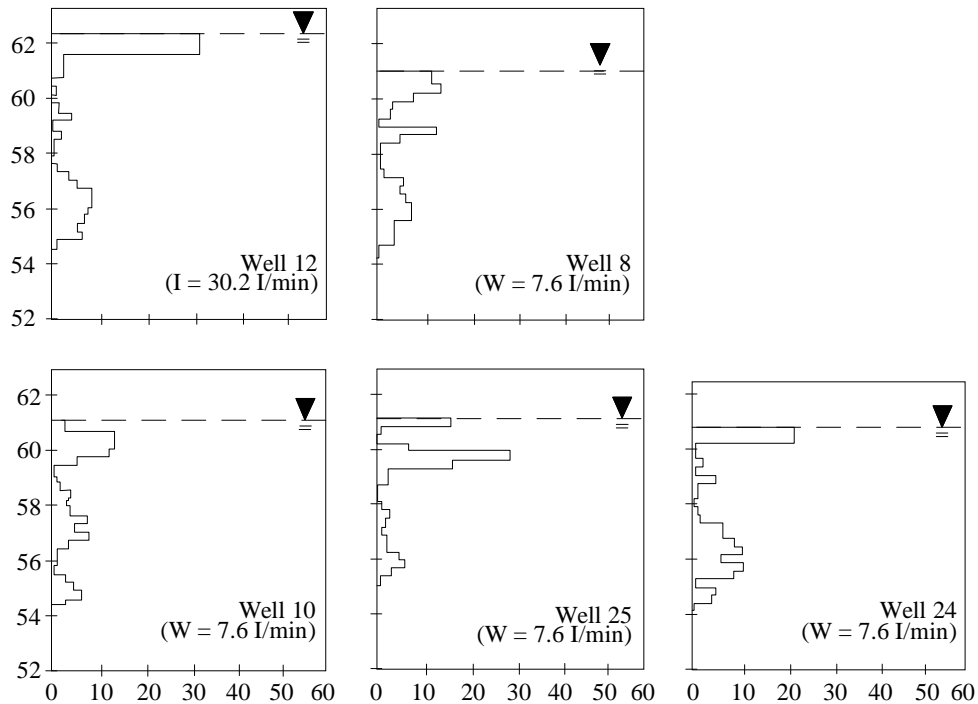


**Figure 3.10:** Vertical borehole flowmeter profiles for tracer Test-1. Vertical axis is elevation (m above MSL), while horizontal axis is percent of total flow.

and withdrawing from the four corner wells Well-1, Well-3, Well-7, and Well-9) of the inner 1-acre network. At approximate, steady state, injection/withdrawal, a 20,000 liter slug of 1500 mg/l Cl tracer was introduced. Thereafter, tracer movement was monitored for a maximum of 165 hours. Using electrical conductivity probes a qualitative insight was obtained in tracer movement (first breakthrough and peak breakthrough) in the network between the injection and withdrawal wells. Using a specially constructed probe in the fully penetrating wells, samples were collected representing different depths. Figure 3.12 shows an example of tracer breakthrough at Well-11, positioned half-way between the injection well and northeast corner Well-9. First breakthrough in Well-11 occurs in the upper zone; after a double-peak there appears to be a decrease of the tracer concentration (electrical conductivity). The other levels in Well-11 do not show the descending tail of the breakthrough curve.

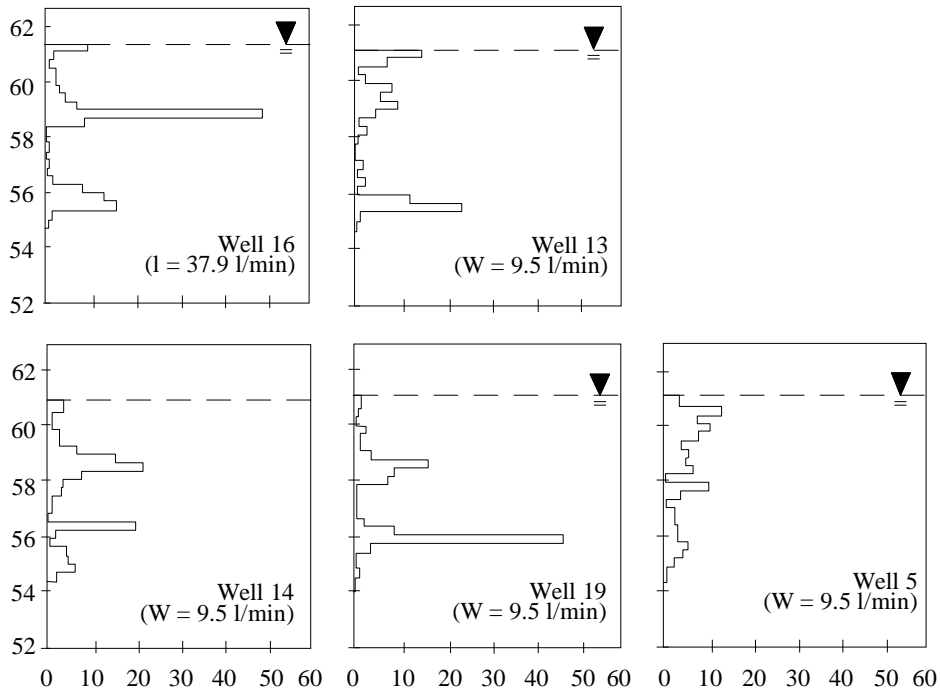


**Figure 3.11:** Vertical borehole flowmeter profiles for tracer Test-2. Vertical axis is elevation (m above MSL), and horizontal axis is percent of total flow.

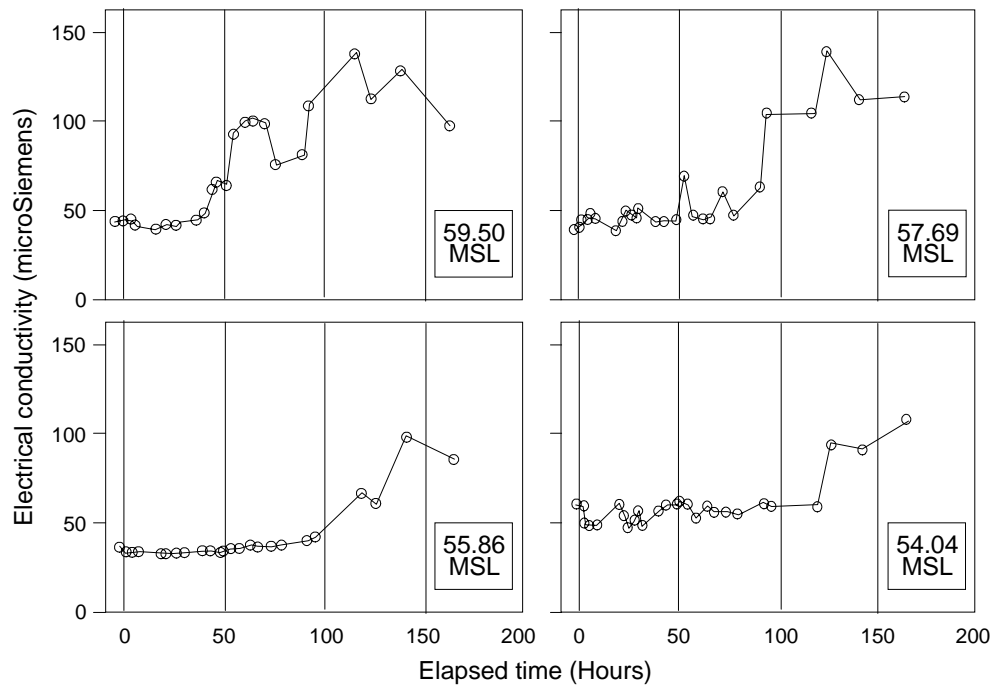


**Figure 3.12:** Tracer breakthrough at four different levels in Well-11 during the large scale tracer test.

Figure 3.13 shows the times of peak breakthrough for all the wells in the network. The tracer travels preferentially to the northwest corner Well-3 and along the upper portion of the aquifer.

### 3.5 USING THE COLUMBUS FIELD DATA

Thanks to the extensive field program at Columbus, a good reference data-set demonstrating heterogeneity is available. A good mix of head (pressure) drawdown data (pumping tests), transport data (tracer tests), detailed hydraulic conductivity measurements, and sedimentological data, is available. These data underlay most of the analysis methods and modeling approaches presented in the next chapters. It should be noted that the data are only used in a qualitative manner; in other words, no analysis method is attempted that aims at a direct quantitative duplication of field data.

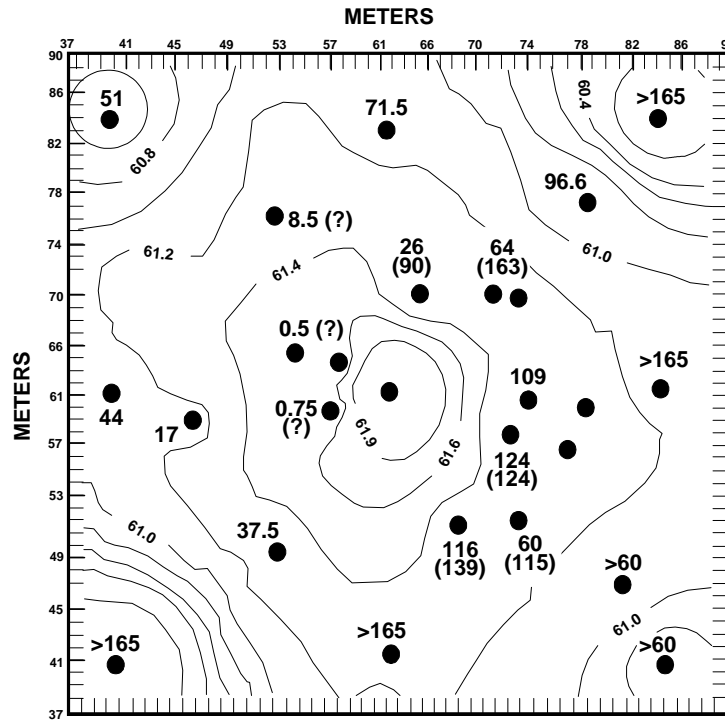


**Figure 3.13:** Tracer breakthrough across the well network during large scale tracer test. Contours depict water table (m). At each well the time (hr) of first breakthrough in the upper portion of the aquifer is depicted (in parenthesis the breakthrough time for the lower portion).

**CHAPTER 4:**

**INTERPRETATION OF PUMPING TESTS AT COLUMBUS**

#### 4.1 INTRODUCTION<sup>1</sup>

When a multitude of pumping test data is available for a certain area, two types of “problems” can arise when simultaneously analyzing the drawdown plots with type-curves. First, it may be difficult to obtain a good fit using type-curves based on idealized, homogeneous, aquifer models. Secondly, a wide range of seemingly inconsistent values for hydraulic parameters from different pumping tests and/or observation wells, may be obtained. Especially, the latter “problem” was encountered in a heterogeneous aquifer comprised of fluvial sediments at Columbus Air Force Base (CAFB), Mississippi. The Columbus field data (see Chapter 3) provide an unique opportunity to investigate the effects of aquifer heterogeneity on pumping test results.

Traditionally, the objective in analyzing pumping test data is to obtain hydraulic parameters (conductivity and storativity) representing a relatively simple hydrogeologic model. Using this hydrogeologic model and the hydraulic parameters which resulted from matching the pumping test data, water level responses are predicted for various stress regimes. For issues such as contaminant transport prediction, however, insight is required in the tortuous geometry of flowpaths and, consequently, the variability of hydraulic conductivity. Thus, one should take into account all geological knowledge about heterogeneity and then reconcile several, possible, hydrogeological, heterogeneity models. A suite of different models should be employed to explain the observed drawdown behavior, including the “problematic” variability of responses. Therefore, conclusions may be based on different models, and possibly on incomplete fits; an example of this is when a certain model is only applicable for a certain time interval of the pumping test. No model is a perfect rendition of the complicated heterogeneous “reality”.

This chapter shows that careful analysis of drawdown-curves from multi-well pumping tests at Columbus, yields both information concerning aquifer heterogeneity, as well as the possible geometry of hydraulic connections among wells that is actually consistent with the Columbus aquifer's sedimentological model.

---

<sup>1</sup> Parts of this chapter are derived from papers jointly authored with S.C. Young.

**Table 4.1:** Parameters used for pumping test analysis (Neuman, Theis, Ring, Strip).

Parameter	Explanation	Unit (SI)
t	time since pumping started	s
r	distance between pumping and observation well	m
s	drawdown	m
H	thickness of aquifer	m
Q	rate	m <sup>3</sup> /s
T	transmissivity	m <sup>2</sup> /s
K <sub>h</sub> , K <sub>v</sub>	horizontal and vertical hydraulic conductivity	m/s
S	elastic storage coefficient	
S <sub>y</sub>	specific yield	
β	$(r^2 K_v) / (H^2 K_h)$	

#### 4.2 PUMPING TEST ANALYSIS ASSUMING A LATERAL HOMOGENEOUS AQUIFER

The pumping test data collected at the two test sites, were interpreted using several different approaches. All drawdown responses measured by pressure transducers, were analyzed using Neuman's equations for delayed gravity drainage (Neuman, 1975); the Theis equation (Theis, 1935); and the Cooper-Jacob straight line method (Cooper and Jacob, 1946). Manually measured drawdown-curves were analyzed only with the Cooper-Jacob straight line method (Cooper and Jacob, 1946), because their early-time response was insufficient to support type-curve matching. Table 3.1 presents a listing of all pumping tests. In addition Table 4.1 presents all relevant symbols and abbreviations for hydraulic parameters used in the next sections. The AT2 drawdown data (resulting from cyclic pumping) could only be analyzed using the Theis equation. An important issue concerning the different methods for evaluating the results, is discerning which analysis (or combination of analyses) yields results that are useful in unraveling the aquifer's heterogeneous model.

#### 4.2.1 Analysis using delayed yield or delayed gravity drainage

Neuman type-curves were fitted to field drawdown data using an interactive, "manual" fit procedure based on computer generated type-curves. This procedure was conducted for all observation wells monitored during the large-scale pumping test using pressure transducers (see Section 3.4.2). Most of the resulting fits are good when only the drawdown is considered. Figure 4.1 shows an example of field drawdown data and a fit with a Neuman type-curve. The type-curve derivative was calculated after the matching procedure, and shows, for this case also, a good fit. The flattening of the drawdown-curve (and the descent of the derivative curve) at late-time, indicates recharge by a rainfall event.

Figure 4.2 shows a type-curve fit with more complications. The derivative indicates some marked deviations between the field drawdown data and the type-curve. An improved fit with a Neuman type-curve, however, is difficult, because the transmissivity is fixed by the late-time part of the curve. Therefore  $S$ ,  $S_y$ , and  $\beta$  were adjusted until a reasonable fit (of the drawdown) is obtained.

Even more complications are shown in Figure 4.3 including the fact that the rather

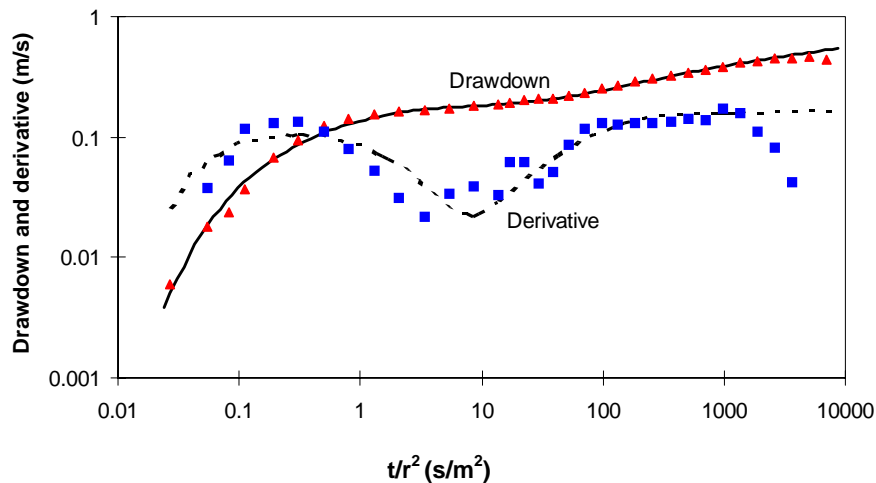


**Figure 4.1:** Drawdown and drawdown derivative for AT3, observation Well-20.

$r = 8.53 \text{ m}$ ;  $Q = 0.002 \text{ m}^3/\text{s}$ ;  $T = 2.3 \cdot 10^{-3} \text{ m}^2/\text{s}$ ;  $S = 4.2 \cdot 10^{-4}$ ;  $S_y = 0.02$ ;  $\beta = 0.03$ .

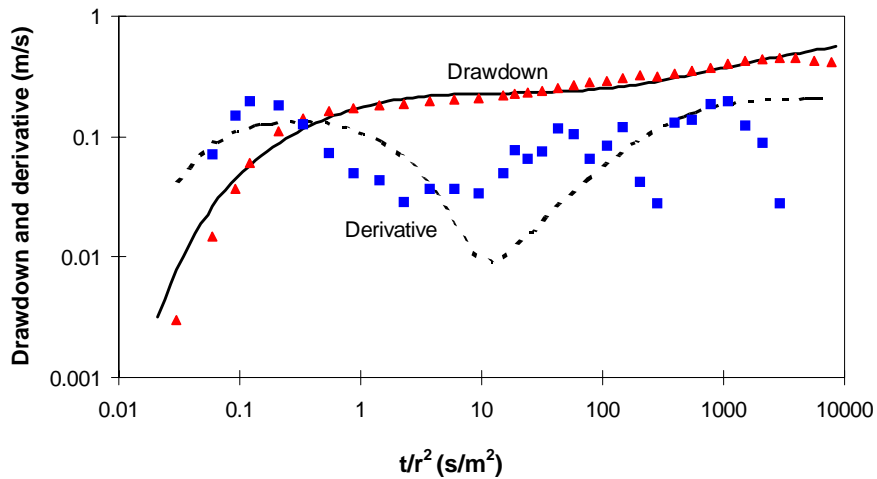


**Figure 4.2:** Drawdown and drawdown derivative for AT3, observation Well-14.

$$r = 8.14 \text{ m}; Q = 0.002 \text{ m}^3/\text{s}; T = 1.8 \cdot 10^{-3} \text{ m}^2/\text{s}; S = 3.1 \cdot 10^{-4}; S_y = 0.07; \beta = 0.03$$

low drawdown values, limit the accuracy of the field data's derivative calculation. The delayed yield effect of the derivative (the V-shaped decline and rise of the derivative), is difficult to recognize on the field data derivative. A rather high value for  $\beta$  is needed to obtain a good fit with a Neuman type-curve.

An evaluation of the appropriateness of the Neuman method should include not only the goodness of the type-curve fit, but also the consistency in the calculated parameters. Figure 4.4A shows that a consistent set of transmissivity values was obtained from the seven, constant-rate, pumping tests. However, the range in the parameters, related to the aquifer's storage properties (Figures 4.4B and 4.4C), raises questions about the validity of these results.

The set of  $S$  values estimated from the pumping test data raises three concerns (also see Figure 4.4B). First, the observed range of a three order magnitude, is inconsistent with the premise of a homogeneous aquifer. Second, the MADE2 results show that  $S$  varies inversely with the radial distance between pumping and observation wells. Third, numerous  $S$  values are larger than  $10^{-3}$ ; this would be the upper range for the elastic

storage coefficient for the saturated thickness of the Columbus aquifer ranging from 6.5 to 9 meters.

The set of estimated  $S_y$  values presents two additional concerns (also see Figure 4.4C). First, the two order of magnitude range is inconsistent with the assumption of a homogeneous aquifer. Secondly, the MADE2 results show that  $S_y$  varies inversely with the radial distance from the pumping wells.

Although the Neuman type-curves reasonably match the drawdown-curves and

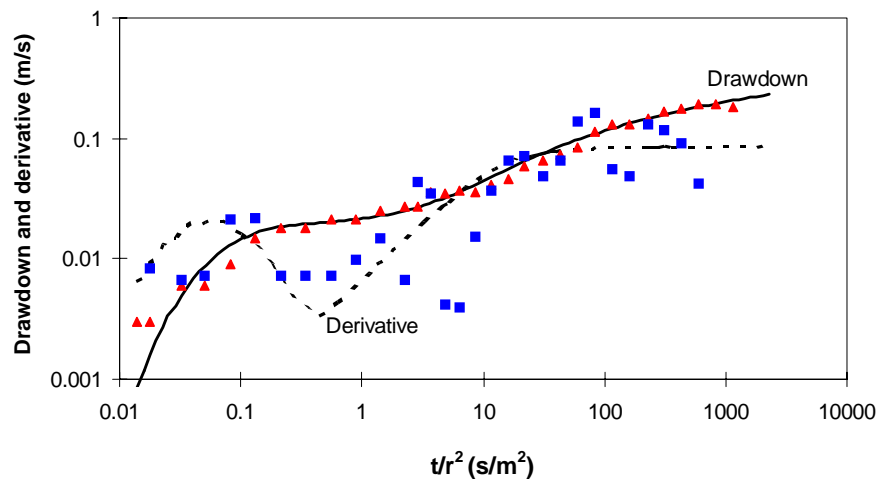


**Figure 4.3:** Drawdown and drawdown derivative for AT3, observation Well-4.

$$r = 21 \text{ m}; Q = 0.002 \text{ m}^3/\text{s}; T = 4.3 \cdot 10^{-3} \text{ m}^2/\text{s}; S = 5.7 \cdot 10^{-4}; S_y = 0.04; \beta = 0.6.$$

produce consistent transmissivity values, the trends and the magnitude of the  $S$  and  $S_y$  values are not consistent with either the delayed gravity drainage theory or the expected storage properties of a sand and gravel aquifer. The variability in  $S$  and  $S_y$  indicates aquifer heterogeneity, but there are no interpretative methods for translating this variability back to the heterogeneous structure of the aquifer.

In Section 4.3 two alternative models, the ring model and the strip model, will be employed to address the impact on the drawdown-curves of large-scale trends in the

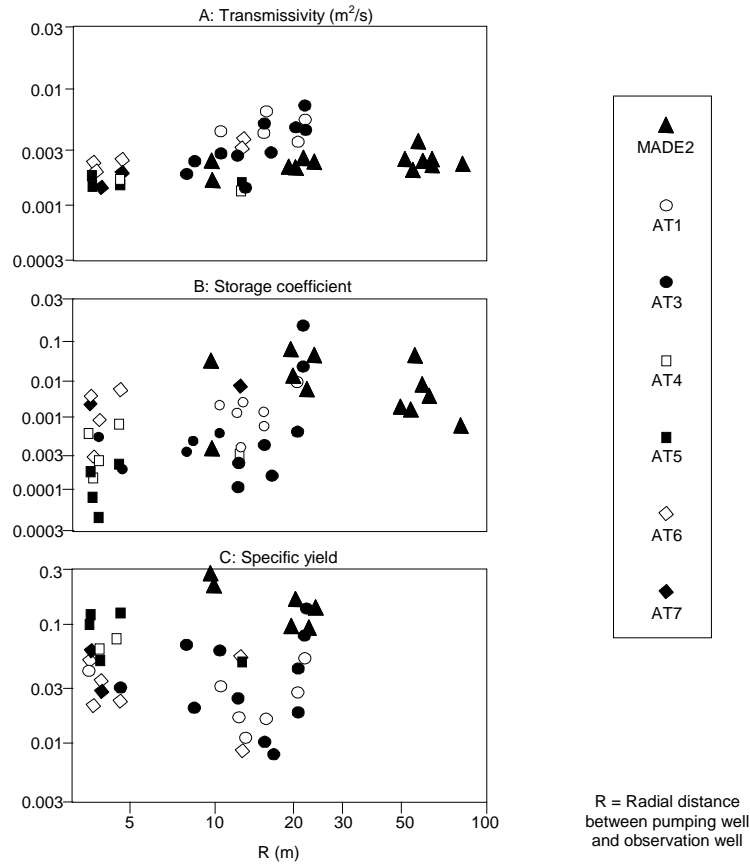


**Figure 4.4:** Results from Neuman type-curve fits for different pumping tests.

transmissivity field. The next section and Section 4.4 focus on developing a simple approach to collectively analyze the results of drawdown-curves in order to extract information about the nature of vertical and/or aerial heterogeneity in the aquifer.

#### 4.2.2 Analysis based on the Theis equation

If delayed gravity drainage is not the primary cause for the non-Theisian behavior at Columbus, then Theis type-curves, or comparable methods, may be more useful than

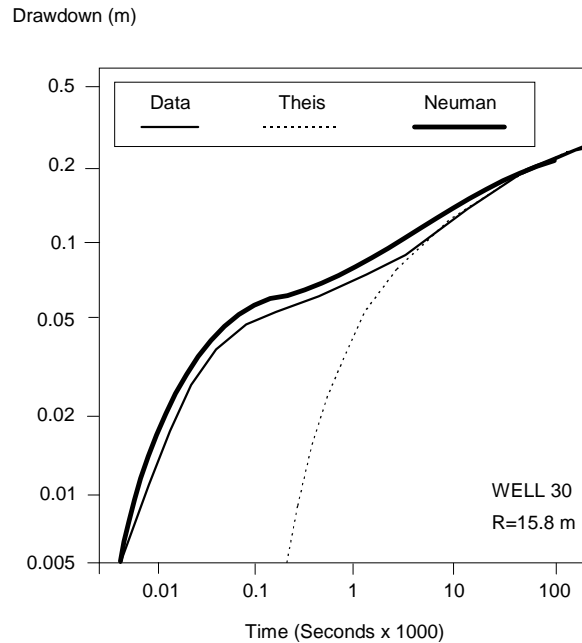


**Figure 4.5:** Example of Theis and Neuman type-curve fit.

Neuman type-curves for extracting trends related to aquifer heterogeneity. Misfits to Theis type-curves draw more attention to aquifer heterogeneity than do the good fits to Neuman type-curves. Moreover, the Cooper-Jacob, straight line method which is based on the Theis equation, has been shown to be useful for identification of lateral transmissivity changes (Butler, 1990). In an unconfined heterogeneous aquifer where the effects of delayed gravity drainage or aquifer heterogeneity on drawdown-curves are uncertain, it is prudent to compare results from both the Neuman type-curve analysis and analysis based on the: Theis equation; type-curve fit; or Cooper-Jacob, straight line method. Before applying the Theis equation, however, its use needs to be justified.

The importance of delayed gravity drainage in permeable, coarse-grained, unconfined aquifers is open to debate and is also site dependent. Akindunni (1987) studied, via numerical simulations, unsaturated/saturated groundwater flow to a well in an unconfined sandy aquifer. He shows that gravity drainage can occur sufficiently and quickly, so that its impact on the drawdown response is negligible. His numerical simulations show that the drawdown-curves in some unconfined aquifers match the Theis

curve, for all practical purposes. Akindunni's theoretical sandy aquifer has an average hydraulic conductivity of  $6 \cdot 10^{-4}$  m/s and an air entry value of 0.02 m. These values are similar to those estimated for the Columbus aquifer. At the 1-HA test site the effective hydraulic conductivity of the aquifer is  $6 \cdot 10^{-4}$  to  $1.1 \cdot 10^{-3}$  m/s based on the results of the large-scale aquifer tests and the borehole flowmeter tests (see section 2.5). Air entry values were calculated from grainsize information from Columbus soil data (Boggs et al., 1990) using a procedure published by Mishra et al. (1989). From these calculations the air entry value is estimated to be as low as a few centimeters.

On the basis of the similarity between the Columbus aquifer and Akindunni's theoretical sandy aquifer, it is inferred that delayed gravity drainage is possibly insignificant at Columbus. It should be noted that the issue of delayed gravity drainage or delayed yield is very much open to debate. Results from other work (Narasimhan and Ming Zhu, 1993; Nwankor et al., 1992) contradict the findings using Akkidunni's model results. Nevertheless it is worthwhile considering the Theis equation as an alternative to Neuman's method for interpreting pumping tests at the Columbus site.

Jacob's correction factor for drawdown ( $s_{\text{corr}} = s - s^2/2H$ ) in an unconfined aquifer (Kruseman and de Ridder, 1990, p 101), was used to adjust all field drawdown-curves analyzed with the Theis solution. All Theis curve fits were performed automatically with WELLTEST, a TVA program to match type-curves using non-linear least squares. Figure 4.5 shows a Theis fit for test AT3. These results show that the Theis curve poorly fits the early-time drawdown data (first one percent of duration), but fits reasonably well the rest of the drawdown data. Figure 4.6 demonstrates the good fits typically obtained between the Theis curves and the AT2 drawdown data for cyclic pumping.

The Cooper-Jacob Straight Line (CJSL) method (Cooper and Jacob, 1946) is based on the same, simple, aquifer model, as the Theis method. The CJSL method is appropriate once  $t > r^2 S/0.04T$  (Cooper and Jacob, 1946) -- a time after which a semi-log plot of the Theis solution represents a straight line. As discussed in Section 2.5.2, the occurrence of a straight line on the semi-log plot, is equivalent to a horizontal segment of the derivative curve. Moderate changes of the derivative, without the occurrence of a straight line, can represent lateral changes of aquifer transmissivity. Sharp changes of the derivative, typically represent a more complex aquifer model, such as a delayed yield model (e.g. Figure 4.1) or the effects of boundaries or heterogeneities. For test AT4 and

test AT7, the interval from 3,400 to 34,000 seconds, was used for the CJSJL method. For test AT1 and test AT3, the time interval differs for each observation well, but includes at least ninety-five percent (95%) of the data used for the Theis and Neuman fits. The slopes of the semi-log plots were obtained from a linear regression analysis.

Figure 4.7 compares the results of the CJSJL, the Neuman, and the Theis analyses for the multiple tests conducted at Well-5 and Well-16. In general the different methods provide similar parameter estimates. Good agreement exists between the mean and standard deviation for the transmissivity, as well as the storage coefficient values for those tests conducted at Well-5. The agreement at Well-16 is poorer. For test results at Well-16 (AT4 through AT7), fitting the Neuman curves produces average transmissivity and storage coefficient values that are one-half to four-times the respective values produced by the Theis curves.

#### 4.3 ANALYSIS WITH TYPE-CURVES FOR LATERAL HETEROGENEITY

Interpretation of drawdown data at Columbus was extended to drawdown-curves

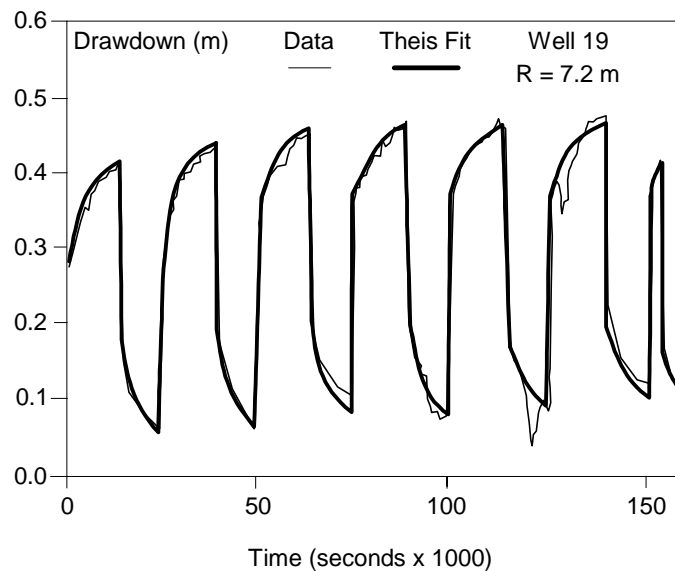


**Figure 4.6:** Example of Theis type-curve fit for pulse-test AT2.

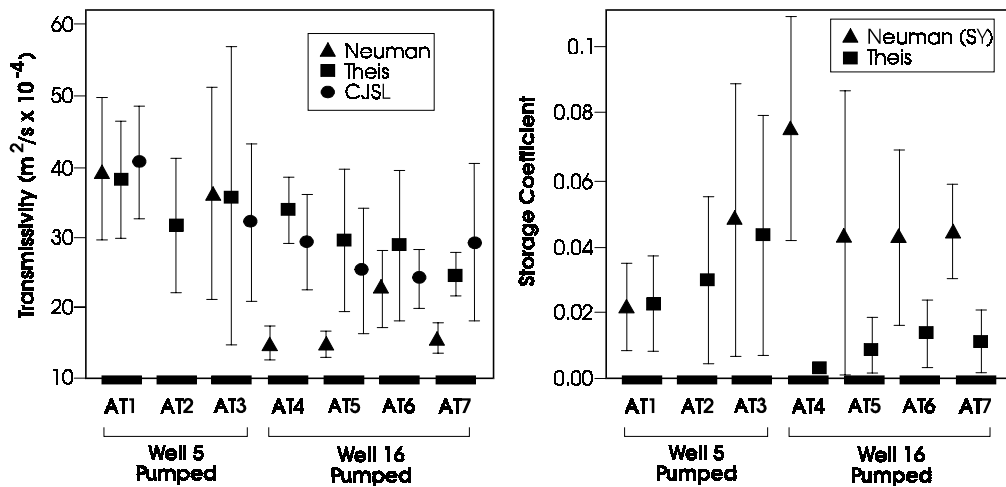


**Figure 4.7:** Calculated ranges of transmissivity and storage coefficients for different type-curve fits for the aquifer tests conducted at Columbus.

for idealized zonal patterns in the aquifer's hydraulic structure. A large degree of freedom exists when matching field data with these zonal type-curves. At least one extra parameter has to be estimated in comparison with the Neuman delayed gravity drainage analysis. Therefore, type-curve fitting should be guided by an *a priori* insight to the heterogeneity that might cause certain drawdown behavior. It is obvious that the sedimentological information (see Chapter 3) is indispensable in this respect.

#### 4.3.1 Ring model (radial composite)

Liu and Butler (1990) published a program to generate drawdown curves for a confined aquifer consisting of three concentric ring shaped zones around the pumping well that have different transmissivity and storage properties. Figure 4.8 shows a fit of the ring model (also called radial composite) to field drawdown data from pumping tests at the Columbus site. For simplicity a two-ring model has been fitted. This fit should be compared with Figure 4.3 that shows the same field data fitted with a Neuman delayed yield type-curve. A reasonable fit is obtained, for early-time better than could be obtained

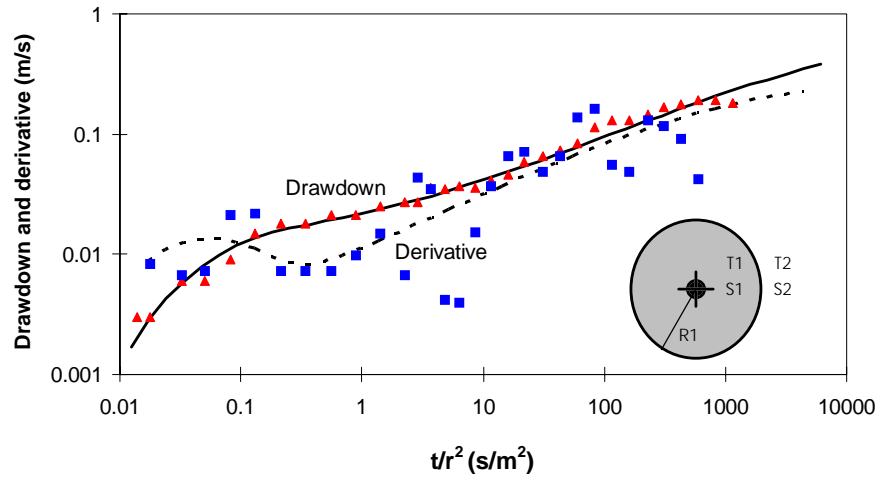


**Figure 4.8:** Drawdown and drawdown derivative for AT3, observation Well-4.

$r = 21$  m;  $Q = 0.002$  m<sup>3</sup>/s;  $T1 = 2.5 \cdot 10^{-2}$  m<sup>2</sup>/s;  $S1 = 1 \cdot 10^{-3}$ ;  $R1 = 50$  m;  $T2 = 1.5 \cdot 10^{-3}$  m<sup>2</sup>/s;  $S2 = 0.2$  (compare Figure 4.3)

with a Neuman curve, but for very late-time the fit is a bit less accurate. The late-time data are, however, influenced by a recharge event (also see Figure 4.1).

The parameters obtained seem reasonable, but also raise some questions. The storage coefficient obtained for the outer ring (S2), is in good agreement with a value that one would expect for an unconfined aquifer (approximately the effective porosity). The storage coefficient for the inner ring (S1), is rather low and might include some release from elastic storage. This lateral storage contrast effectively represents a delayed yield effect (from the outer ring). There is also a rationale for exploring the increase in the storage coefficient with the distance, because the pumping well is connected to the outer ring through highly permeable stringers (only several cm thick) comprising a small fraction of the aquifer volume. Both the depositional model and the results of small-scale pumping and tracer tests (Section 4.5), suggest that such stringers are plausible, although a lateral radial extension of 50 m is unlikely.

4.3.2 Strip model (linear composite)

Another lateral heterogeneity model is the strip (linear composite) model (Liu and Butler, 1990; Butler and Liu, 1991). As with the radial composite case, the spreading of the radius-of-influence from Zone-1 into Zone-2 is marked by changes in the semi-log slope. Figure 4.9 shows the strip model geometry and example drawdown-curves in a homogenous aquifer with an infinite linear strip of high transmissivity. However, there is no clear cut transition on any drawdown-curve indicating migration of the radius-of-influence from Zone-2 into Zone-3, because of the infinite nature of Zone-2. Rather, a gradually changing slope (derivative) occurs indicating drainage of the bulk of the aquifer through its highly conductive strip. This gradual increasing slope (derivative) is observed in some of the field data (Figures 4.2 and 4.3) after the derivative minimum.

This phenomenon is particularly difficult to fit with a Neuman curve. Consequently, it is very possible that flow is governed by a linear (channel) system in combination with a delayed gravity drainage system. Unfortunately, no type-curves are

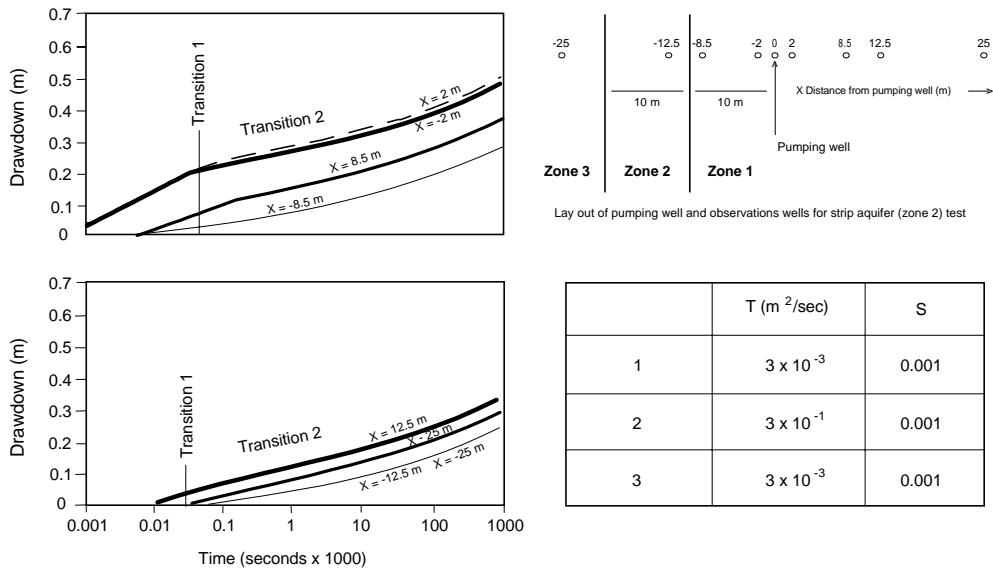


Figure 4.9: Example drawdown-curves for an aquifer with infinite linear strip of high transmissivity (zone 2).

available that combine delayed yield by fitting the descending part of the field-derivative with the linear strip model, and by fitting the gradually rising part of the field-derivative.

Due to the asymmetry in the aquifer heterogeneity relative to the pumping well, wells at the same radial distance from the pumping well can have very different drawdown responses, while wells with similar drawdown behavior can be at very different radial distances from the pumping well. For instance a more pronounced sigmoidal shape and greater drawdown, occurs in observation wells away from the strip (see Figure 4.9; compare  $X=8.5$  and  $X= -8.5$ ). Very similar drawdown responses occur in wells located within Zone-2 (the strip) and Zone-3, regardless of the distance to the pumping well (see Figure 4.9; compare  $X= -12.5$  and  $X= -25$ ). This type of asymmetry is often observed at Columbus and results in a dispersion of aquifer parameters when type-curves on the basis of conventional lateral homogeneous or radial symmetric models are used.

#### 4.3.3 Fractured rock (double-porosity) model

As discussed in Section 2.5.1, delayed yield type-curves are theoretically similar to double-porosity type-curves used when interpreting pumping tests in fracture-matrix aquifers. Thus, the Columbus field data could be analyzed using type-curves representing a small, highly conductive, fracture network (high conductive sediments) in a matrix (low

**Table 4.2:** Additional parameters for pumping test analysis with the Kazemi method.

Parameter	Explanation	Unit (SI)
$K_m, K_f$	hydraulic conductivity of matrix and fractures	m/s
$S_m, S_f$	Storage coefficient for matrix and fractures	m/s
$n$	number of orthogonal fracture sets (1, 2, 3)	
$l$	characteristic length of matrix blocks	
$\alpha$	$4n(n+2)/l^2$	$1/m^2$
$\beta$	0 for early-time; for late-time: 1/3 for orthogonal and 1 for planar	
$\omega$	$S_f / (S_f + \beta S_m)$	
$\lambda$	$\alpha r^2 K_m / K_f$	

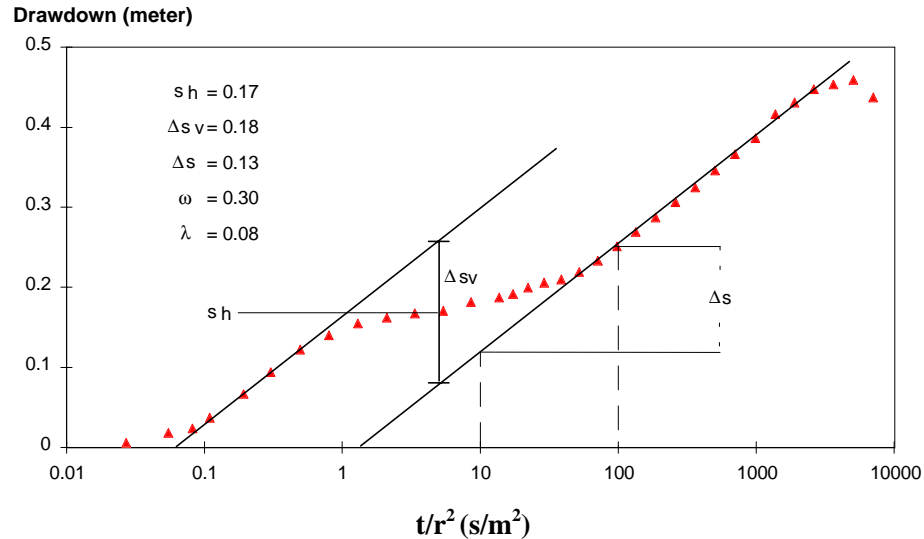


**Figure 4.10:** Drawdown for AT3, observation Well-20 (compare Figure 4.1).

$$r = 8.53 \text{ m}; Q = 0.002 \text{ m}^3/\text{s}; T = 2.8 \cdot 10^{-3} \text{ m}^2/\text{s}; S_f = 4.4 \cdot 10^{-4}; S_m = 0.012.$$

conductive sediments). Kazemi's method for double-porosity fractured aquifers (Kruseman and de Ridder, 1990, p. 251 and 254) is comparable to the previously discussed Neuman method. Fracture storage is the equivalent of elastic storage, while matrix storage is the equivalent of specific yield. Table 4.2 shows the parameters used in applying the Kazemi method (in addition to parameters listed in Table 4.1).

Two observation wells (Well-14 and Well-20) monitored during pumping test AT3, were sufficiently close to the pumping well to allow for a complete application of Kazemi's method. Figure 4.10 shows an example of this application of Kazemi's method for drawdown observed during aquifer test AT3 at Well-20.

Transmissivity, fracture, and a matrix storage coefficient were effectively found to be similar to the values obtained from the Neuman curve fit (see Figure 4.1). From the horizontal curve segment an inter-porosity flow coefficient ( $\lambda = 0.07\text{-}0.08$ ) was determined. This value can be explained as two sets of fractures (e.g. orthogonal horizontal and vertical). The fractures have a characteristic length of 10 m; the conductivity contrast between fractures and matrix is 300 (see Kruseman and de Ridder, 1990, formula 17.3, p. 252). These "fractures", of course, represent highly conductive sediment lenses (streaks). The conductivity contrasts observed using the borehole

flowmeter and the results of small-scale pumping and tracer tests (Section 4.5), suggest that such a model is plausible.

#### 4.4 ANALYSIS OF REGIONAL AND LOCAL CHANGES IN TRANSMISSIVITY

From the previous sections it can be concluded that five different methods of data analysis produce similar estimates for average, large-scale, aquifer transmissivity. The five methods, however, represent dramatically different aquifer models. Although these five methods produce interesting concepts regarding aquifer heterogeneity, none of them can be assumed to be fully correct. Therefore, as previously argued, extensive type-curve fitting using one (or all) of these methods, might be less useful. Good fits with type-curves having many adjustable parameters, may even draw attention away from heterogeneity and, thus, mislead an interpreter. As shown in Figure 4.4 such a complex type-curve fitting procedure, produces a wide range of parameter values in a case where drawdown data from many observation wells are available.

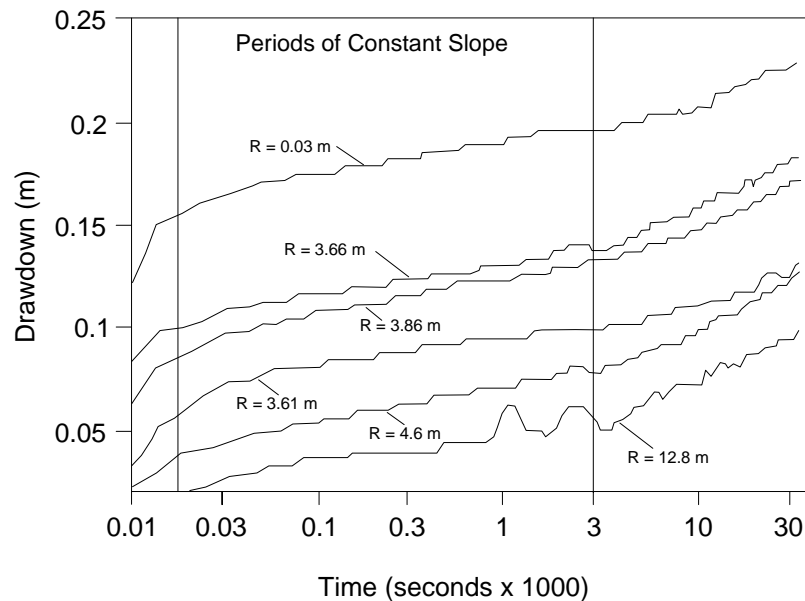


Figure 4.11: Drawdown data for AT4.

**Table 4.3:** Transmissivity values for aquifer test AT4 determined with CJSJL-method, slope 1 and T1 for 200 to 1,000 s; slope 2 and T2 for 3,400 to 34,000 s.

Observation well	r m	slope 1 m/s	T1 m/s <sup>2</sup>	slope 2 m/s	T2 m/s <sup>2</sup>
16	0.03	$1.6 \cdot 10^{-2}$	$6.9 \cdot 10^{-3}$	$3.3 \cdot 10^{-2}$	$2.9 \cdot 10^{-3}$
14	3.61	$1.4 \cdot 10^{-2}$	$7.9 \cdot 10^{-3}$	$2.7 \cdot 10^{-2}$	$3.9 \cdot 10^{-3}$
19	3.66	$1.5 \cdot 10^{-2}$	$7.4 \cdot 10^{-3}$	$4.4 \cdot 10^{-2}$	$2.5 \cdot 10^{-3}$
13	3.86	$1.8 \cdot 10^{-2}$	$6.2 \cdot 10^{-3}$	$3.9 \cdot 10^{-2}$	$2.8 \cdot 10^{-3}$
5	4.6	$1.7 \cdot 10^{-2}$	$6.5 \cdot 10^{-3}$	$4.5 \cdot 10^{-2}$	$2.5 \cdot 10^{-3}$
26	12.76	N/A	N/A	$4.2 \cdot 10^{-2}$	$2.6 \cdot 10^{-3}$

This dispersion of results indicates that heterogeneity exists, but does not provide proper insight into the actual variability or structure of the transmissivity field. It is shown in this section that there is a practical method for extracting information on heterogeneity from the drawdown-curves. A cornerstone of this method is interpreting the variable slope of the semi-logarithmic drawdown plot, a method equivalent to a careful evaluation of the drawdown derivative (Section 2.5.2).

Figure 4.11 presents the semi-logarithmic plots of the drawdown data for AT4. From these plots two, alternative, heterogeneity explanations are possible. The first explanation is that the delayed gravity drainage occurs slowly enough so that the three segments associated with an S-shaped Neuman curve, are identifiable in the drawdown data. The second explanation is that the segmentation is in response to a zonal variation of transmissivity; this is consistent with the previously discussed radial and strip models (Butler 1988; Butler and Liu, 1991).

With regard to the first explanation, one can divide the drawdown data on Figure 4.11 into three time periods that comprise a deformed S-shaped curve. In doing so, period one would end near 30 seconds, period two would last from about 30 to 3,000 seconds, while period three would begin near 3,000 seconds. Two problems arise in regard to these drawdown-curves and the theory of delayed gravity drainage. First, period two should plot as a horizontal line. Second, when the CJSJL method is applied, the drawdown-curve

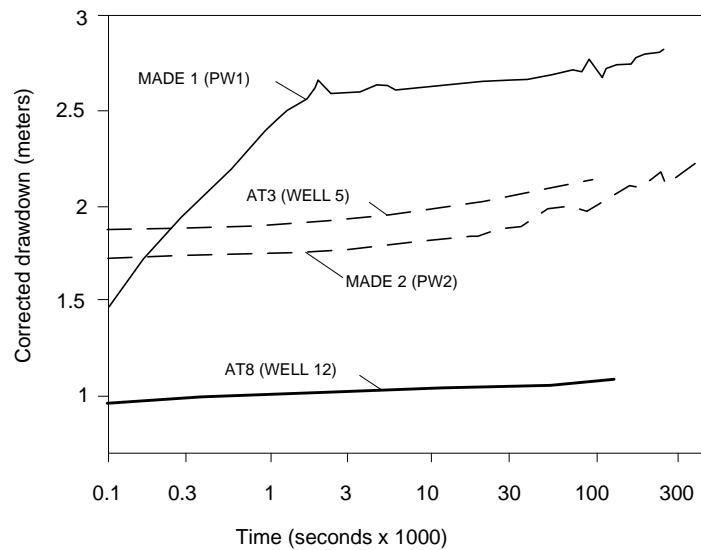


**Figure 4.12:** Drawdown for pumped wells of different pumping tests.

during stages one and three should plot with the same slope yielding the same transmissivity.

With regard to the second explanation, the previously discussed, radial and linear, strip model's results indicate that changes in the slope of the semi-log, drawdown-time plot can be caused by changes in the transmissivity field. The slope of the first linear segment suggests that during the initial 3,000 seconds, the ring-of-influence (see definition in Butler, 1990) passes through aquifer material with an effective transmissivity of about  $6.5 \cdot 10^{-3} \text{ m}^2/\text{s}$  (Table 4.1). After 3,400 seconds the ring-of-influence passes into aquifer material with an effective transmissivity of about  $3 \cdot 10^{-3} \text{ m}^2/\text{s}$ . This transition in transmissivity may be related to the boundaries of the buried river channel that crosses the 1-HA test site (also see Figure 3.2). Well-16 (the pumping well for AT4) is located in that buried river channel. If the channel contains highly conductive deposits of sands and gravel, then the ring-of-influence will begin in an initially high transmissivity zone and then move outward to a lower transmissivity zone.

To determine whether the correlation between the transmissivity trends and the boundaries of the river meander exist across the entire aquifer, CJSJL analyses were

performed on the drawdown data from the other four pumping wells. Figure 4.12 shows the drawdown-curves for the other pumping wells, while Table 4.3 provides the results of the CJSL analysis. On close examination, one can deduce that the location of the pumping well relative to the river channel, greatly affects the shape of the drawdown-curve and the calculated transmissivity trends. This deduction is based on the premise that the river channel contains highly conductive deposits; this premise is well supported by the results of single-well pumping tests and a large-scale, recirculating, tracer test at the 1-HA test site (Young, 1991a,b).

Based on the previous discussion, the CJSL analysis of drawdown data from pumping wells located in the river channel (Well-5, Well-16 and PW2), should produce a higher transmissivity at early-times than at late-times. Conversely, the CJSL analysis on drawdown data from pumping wells located outside the river channel (Well-12 and PW1), should produce a lower transmissivity at early-times than at late-times. The ring-of-influence associated with each pumping test at late-times, is large compared to the scale of the site's heterogeneity. Therefore at the late-times, the CJSL analysis produces similar transmissivity values for all the pumping tests.

Table 4.4 shows that the CJSL analysis produces a transmissivity of approximately  $2.5 \cdot 10^{-3} \text{ m}^2/\text{s}$  at late-times for all of the tests. Considerably higher transmissivity values are calculated at early-times for the three wells located in the former river channel. Considerably lower transmissivity values are calculated at early-times for the two wells

**Table 4.4:** Transmissivity values resulting from analyzing drawdown for pumped wells of different pumping tests. The early- and late-time transmissivity (respectively T1, T2) are determined with the CJSL-method.

Pumping Well	Test	Rate $\text{m}^3/\text{s}$	Period 1 s	T 1 $\text{m}^2/\text{s}$	Period 2 s	T 2 $\text{m}^2/\text{s}$
PW1	MADE1	0.0010	100-1800	$0.2 \cdot 10^{-3}$	2000-250000	$2.1 \cdot 10^{-3}$
PW2	MADE2	0.0035	100-8700	$1.0 \cdot 10^{-2}$	33000-500000	$1.7 \cdot 10^{-3}$
5	AT3	0.0019	100-2500	$9.9 \cdot 10^{-3}$	5600-100000	$2.3 \cdot 10^{-3}$
16	AT4	0.0006	100-2500	$6.3 \cdot 10^{-3}$	3400-35000	$2.9 \cdot 10^{-3}$
12	AT8	0.0004	171-30000	$2.7 \cdot 10^{-3}$	171-30000	$2.7 \cdot 10^{-3}$

located outside the former river channel (PW1 and 12, also see Figure 3.2). These results are consistent with the premise that transitions in the semi-log plots of the drawdown data, are caused by the ring-of-influence (see Section 2.5.2 and Butler, 1990) entering and leaving the permeable sediments in the former river channel. The difference in the results for Well-12 and PW1 are attributed to their geologic setting. Well-PW1 is on the outside of a former river channel meander and is, probably, located in more, fine-grained, overbank deposits than Well-12 located on the inside of a meander and, probably, in moderately, permeable, pointbar deposits.

#### **4.5 SMALL-SCALE MULTI-WELL PUMPING TESTS AND TRACER TESTS**

Small-scale pumping tests were conducted, in conjunction with tracer tests, to investigate the effects of localized, highly permeable lenses between well locations on the calculated values of T and S. The most likely region for these lenses, are the pointbar's chute deposits deposited during high flood stage as small channels cutting from the main channel through the medium-to fine-grained pointbar deposits (see Section 3.3).

For two clusters of wells, small-scale aquifer tests (see Section 3.4.2) were analyzed in detail. One well cluster (Well-5, -13, -14, -16, and -19) is located five meters (5 m) northwest of the center of the well network. The other well cluster (Well-8, -10, -12, -24 and -25) is located about ten meters (10 m) east of the center of the well network (see Figure 3.7). To assess the flow patterns within these well clusters and to better interpret the pumping test results, two tracer tests (Test-1 and Test-2) were conducted (see Section 3.4.3). Both tests involved pumping equal amounts of water from four observation wells and then injecting it into a well located 3 to 6 meters from the observation wells. Well-16 and Well-12 were used as injection wells. Once the water table profile achieved quasi-steady state, a bromide tracer pulse was administered and monitored using multi-level samplers located at 0.6 meter intervals in the observation wells and in the injection well (Young, 1991b).

4.5.1 Analysis of the small-scale, multi-well, pumping tests

The resulting drawdown-curves from the small-scale pumping tests were analyzed using the Theis equation. From the depositional model (see Chapter 3) it becomes evident that the aquifer materials and lenticular structures can change dramatically with distance and direction. These changes indicate that the hydraulic properties calculated at an observation well could be affected by the pumping well location.

In the next sections we will show how detailed interpretation of the pumping test results, can provide useful information regarding the degree of connectivity between wells. Connectivity is a measure of the relative ease for fluid to flow from well to well. It is defined as the path length between two wells, given a conductivity threshold (see Section 2.3.4 and Alabert and Modot, 1992). The highest degree of connectivity (length) implies that there is a straight path between two wells, given a certain conductivity threshold. For example, if a high-conductivity lens directly connects two wells, then the

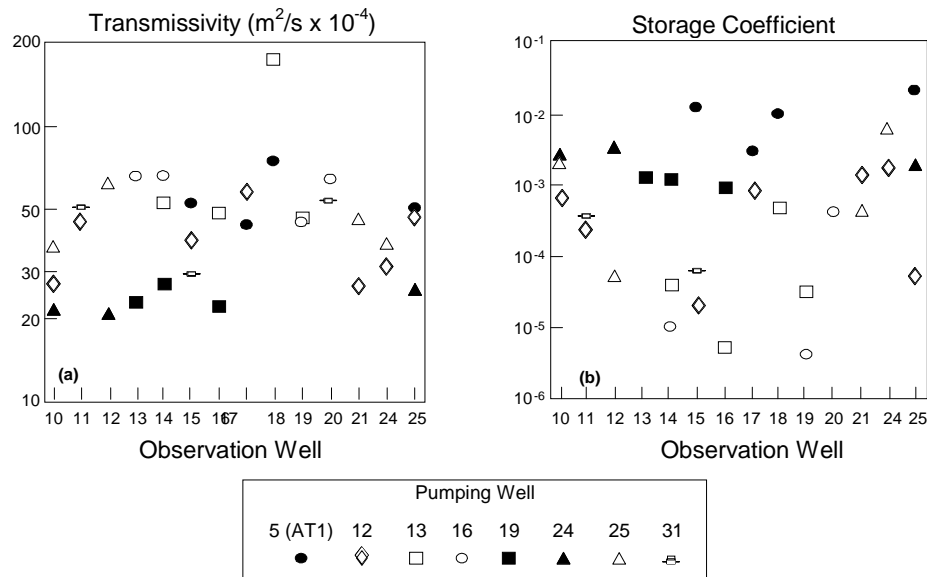
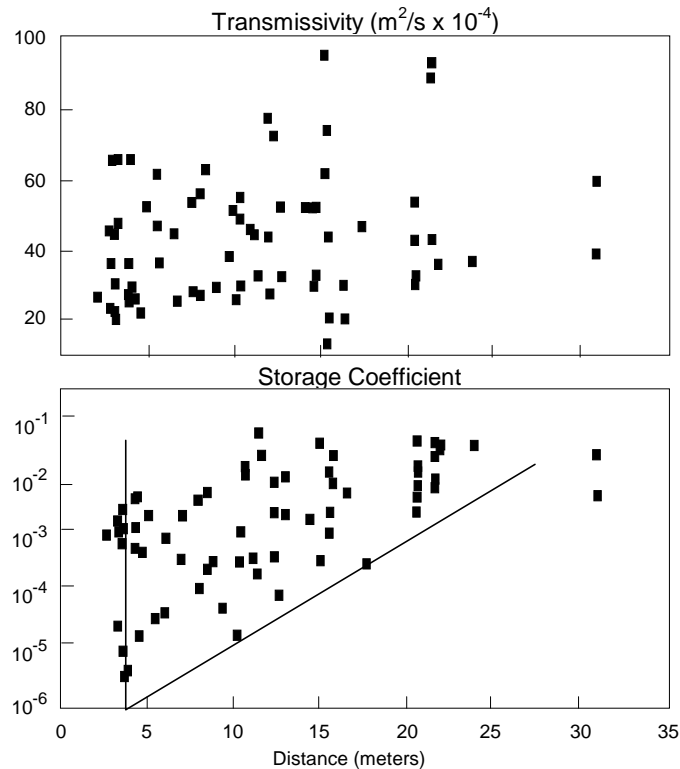


Figure 4.13: Transmissivity and storage coefficient determined for the same observation well and different pumping wells.



**Figure 4.14:** Transmissivity and storage coefficient as a function of the distance between pumped and observation well.

connectivity is high (short connectivity length), given a conductivity threshold just below the conductivity of the lens. For two wells not intersected by the same high-conductivity lens, connectivity is low (larger length). In the latter case the fluid has either to move a longer tortuous way through the high-conductivity material or it has to travel through lower conductive material.

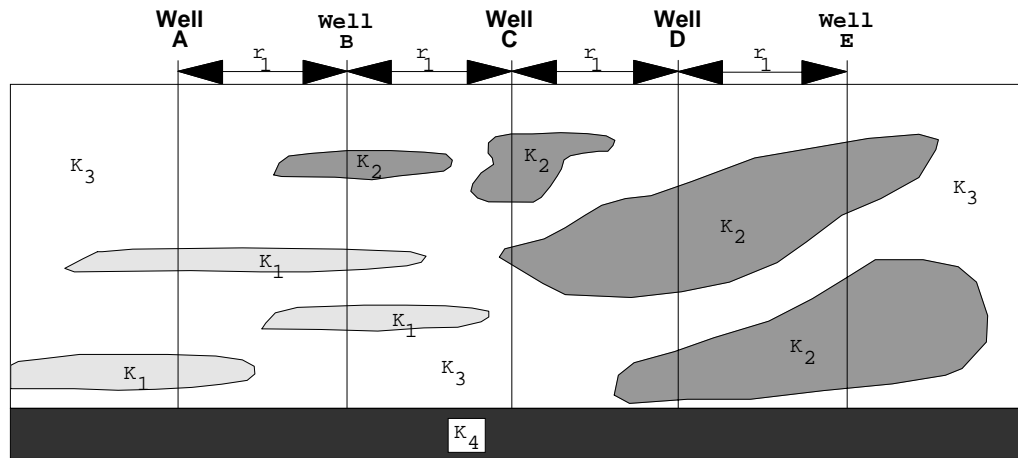
Figure 4.13 shows calculated transmissivity and storage coefficient values at selected observation wells for different aquifer tests. The transmissivity and storage coefficient values calculated using data from the same observation well, but for different pumping tests, typically vary by a factor of two and several orders of magnitude, respectively. Six of the eight tests had pumping rates that were within twenty percent (20%) of 68 L/min; the remaining two tests had pumping rates of 34 L/min.

Figure 4.14 shows the transmissivity and the storage coefficient values as a function of the distance between the pumping and the observation wells. These values were calculated from the drawdown-curves for: the seven, small-scale, pumping tests; test AT2; and the initial 10,000 seconds of tests AT1 and AT3. The large-scale pumping tests (AT1, AT2, and AT3) were included because they provide pumping-well / observation-well combinations that are complementary to the small-scale pumping tests.

In Figure 4.14, no trend is evident between transmissivity and distance (upper diagram), but there is a trend between storage coefficient and distance (lower diagram). Storage coefficients typically associated with unconfined aquifers (i.e., between  $10^{-2}$  and  $10^{-1}$ ) are consistently found only for well-pairs with distances greater than 20 meters. Well-pairs separated by a distance less than 10 meters have a storage coefficient range including small values, typically associated with confined aquifers (i.e., less than  $10^{-4}$ ), as well as intermediate values (i.e., between  $10^{-2}$  and  $10^{-4}$ ).

The delayed yield theory (Boulton, 1963) predicts an increase in the average storage coefficient with time, but not large variations in storage values at any given distance. Aquifer heterogeneity can explain both this trend and this variability. The hypothesis is that the low storage coefficients ( $10^{-6}$  to  $10^{-4}$ ) are calculated where the pumping and observation wells intersect the same, high, hydraulic conductivity lens. In that instance, the lens acts as a confined aquifer permitting head changes caused by pumping to rapidly propagate to the observation well. As discussed in detail later, this hypothesis is confirmed by the tracer tests and the borehole flowmeter profiles. These data confirm common, high, hydraulic conductivity lens(s) between an observation and a pumping well for which a low storage coefficient is calculated.

In order to explain the trend in the lower diagram of Figure 4.14, the fictitious aquifer shown in Figure 4.15 is employed to help in illustrating how high hydraulic conductivity lenses between a well-pair (pumping and observation well) affects the calculated storage coefficients. When pumping Well-B, the highly conductive lenses (K1) act temporarily as a confined aquifer and result in a very rapid, drawdown response in Well-A. Consequently, low storage coefficients would be calculated from drawdown data in Well-A when pumping Well-B. By comparison, quite a bit higher storage coefficients would be calculated from the drawdown in Well-C produced by the same pumping at



K is hydraulic conductivity:  $K_1 \gg K_2 \gg K_3$

**Figure 4.15:** Cross section of a fictitious aquifer with wells intersecting lenses of different conductivity.

Well-B. In the latter instance there is no high-conductivity pathway, so drawdown is much less rapid.

Since lenses have finite lengths and are not necessarily interconnected, the probability of obtaining low storage coefficients should generally decrease with increasing distance between the pumping and observation wells. This effect will be demonstrated in Section 6.4 using a numerical model of discrete lenses of finite length. The lenticular system and its interconnections can be compared to a fracture system around a well. This is consistent with the fact that a fracture type-curve could be fitted to some of the drawdown data from observation wells close to the pumped well (see also Section 4.3.3).

The vertical line in the lower diagram of Figure 4.14 indicates for a distance of 4 m, the range of storage coefficients is from  $10^{-2}$  to  $10^{-6}$ . This wide range indicates that some of the well-pairs spaced four meters apart are connected by a high hydraulic conductivity lens, while others are connected by a lens of moderate hydraulic conductivity, or may only be connected through the lower conductivity matrix. For distances greater than 20-m, the storage coefficient is larger than  $10^{-3}$ . This range indicates that high hydraulic

conductivity lenses with lengths greater than 20 m may not exist between any of the well-pairs.

The implication of the above is that calculated storage coefficients are affected not only by the physical and drainage properties of the different aquifer deposits, but also by the complex manner in which these materials are juxtaposed. The dependence of calculated storage coefficients on the inter-connectivity of high hydraulic conductivity lenses, is consistent with the depositional model. The coarse-grained chute deposits probably form many of the high hydraulic conductivity connections between well-pairs. Their width is restricted to about 7 m, while their length is considerably longer. However, the alternation of different, coarse-grained, depositional events with clay drapes, makes it unlikely that wells greater than 20 m apart are connected by one, continuous, high, hydraulic conductivity lens. The inter-connectivity length is also consistent with the "fracture" length results obtained from analyzing drawdown-curves with a double-porosity model (Section 4.3.3). This inter-connectivity length is also consistent with the variogram range obtained from spatial analysis of the local-scale (borehole flowmeter) conductivity measurements (Section 5.2.2).

#### **4.5.2 Analysis of the small-scale tracer tests**

The small-scale tracer tests were analyzed to investigate the conclusions concerning connectivity that emerged from the analyses of the small-scale pumping tests and the depositional model. The tracer monitoring confirmed preferential flow patterns along vertically narrow intervals, while the initial tracer breakthroughs typically occurred over a vertical-scale of about 0.6 m. A lower bound for the average hydraulic conductivity (flow-velocity), is calculated for the most permeable interval between the well-pairs using: the travel distance; the time of the peak tracer concentration; an estimate of the porosity for the high hydraulic conductivity lenses; and the measured average spatial hydraulic gradient between the injection and observation wells. A detailed discussion of these tests is beyond the scope of this dissertation, but can be found in Young (1991b). Young (1995) provides justification for calculation of the conductivity from tracer test data and shows a good comparison between these conductivity values and conductivity values from borehole flowmeter data.

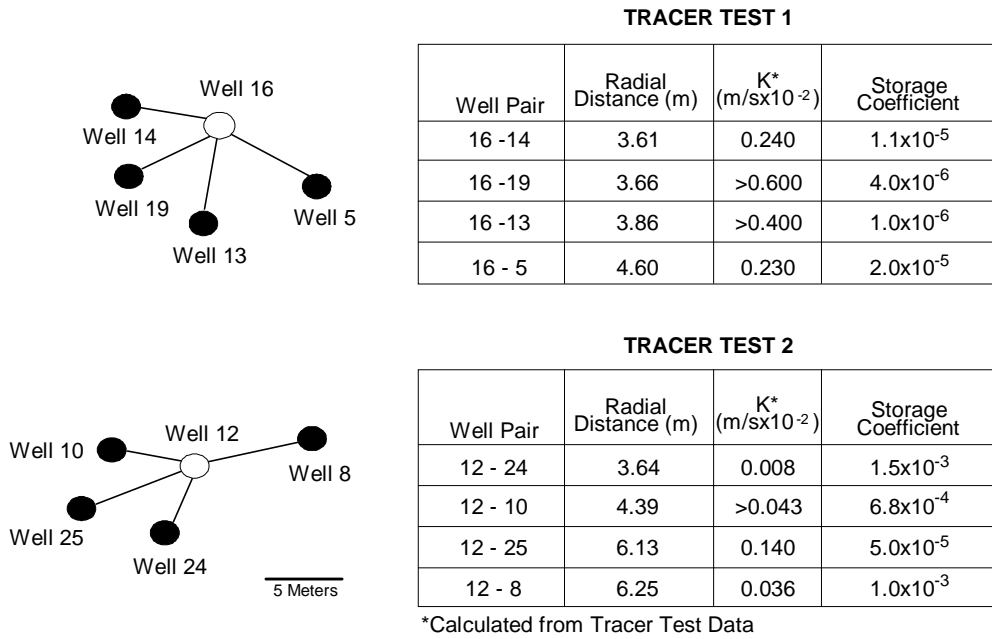


**Figure 4.16:** Comparison of storage coefficients and hydraulic conductivity (velocity) calculated from the peak travel time of small-scale tracer (Test-1 and Test-2).

**4.5.3 Low storage coefficients and highly permeable lenses**

The hydraulic conductivity values that were calculated for each well-pair from the tracer breakthrough can be used as an indicator for well connectivity. Figure 4.16 shows these tracer determined, hydraulic conductivities in combination with the storage coefficients were calculated for the same well-pairs from the small-scale multi-well tests. The storage coefficients for the wells from tracer Test-1 and Test-2, were calculated from drawdown data produced by pumping Well-16 at 81 L/min and by pumping Well-12 at 60 L/min, respectively. The well-pairs associated with tracer Test-1 have higher hydraulic

conductivity values (calculated from the tracer breakthrough time) and lower storage coefficient values than the well-pairs from tracer Test-2. The most significant result is the correlation between high, tracer-determined, hydraulic conductivities and the low storage coefficient values for each well-pair. This supports the explanation that low storage coefficients are produced where the pumping and observation wells are connected by a high hydraulic conductivity lens.

For tracer Test-2, it is important to compare the response of well-pairs 12-24 and 12-25. Both trends in the storage coefficient and the hydraulic conductivity values indicate: Well-25 is better connected hydraulically to Well-12 than is Well-24; although Well-25 is about 70% farther from Well-12 than Well-24. Because of the better connection, more drawdown occurred during the pumping test at Well-25 than at Well-24. Similarly, based on the tracer-determined hydraulic conductivities and the storage coefficient values, Well-13 and Well-19 are better connected hydraulically via a high hydraulic conductivity lens to Well-16 than is Well-14.

#### 4.6 CONCLUSION

Multi-well pumping tests were conducted in a highly, heterogeneous, unconfined, fluvial aquifer composed primarily of sand and gravel. The depositional model includes coarse, meandering, channel deposits and finer pointbar deposits intermingled with very coarse, chute channel deposits in the upper aquifer, while braided-stream deposits are in the lower aquifer. The integration of the sedimentological model and pumping test analysis allow one to assess possible zonal transmissivity changes and the occurrence of high-conductivity flowpaths between specific well-pairs.

The field data collected at the test site conclusively show that a pumping test in a heterogeneous aquifer can have many, different, drawdown responses. Nearly perfect curve-fits produced by application of the Neuman, delayed, gravity, drainage equations to drawdown data, can be misleading since aquifer heterogeneity may be a major cause of the S-shaped drawdown responses. Additionally, it is shown that field drawdown-curves can also be fitted with type-curves in a radial composite model representing lateral variability of hydraulic parameters. Finally, it is shown that even a double-porosity

("fractured" rock) model can be used to fit the field drawdown data. A typical length of 10 m was determined for these "fractures" (high-conductivity connections).

Simple analysis methods based on Theis type-curves and the CJSJL method were applied to different segments of the drawdown curve. These methods are practical for a large variety of drawdown behaviors and help to provide a characterization of possible zonation of transmissivity within the heterogeneous Columbus aquifer. The latter method is a simplification of the derivative method (Section 2.5.2) and is suitable when data quality and/or logistics prohibit application of the derivative method.

It is stressed that interpretation of pumping test data should include a variety of analytical (type-curve) models. Especially useful are the less well known, zonal, type-curve models (Butler, 1988; Butler and Liu, 1991), since these models are consistent with geological insights pointing to lateral changes of conductivity (transmissivity). The consistency of expert geological knowledge should at least have equal value and priority to the objective of good type-curve fits. The absence of good type-curve fits is not a failure of the method, but rather yields relevant information about unmet model assumptions (i.e., the presence of heterogeneity versus assumed homogeneity). For sufficiently accurate data, the variability of obtained parameters, is not an "error", but rather it is relevant information pointing to heterogeneity. The results presented in this chapter confirm that this approach allows assessment of lateral heterogeneity trends along with connectivity among/or between high-conductivity lenses. This obtained information is consistent with independent information from tracer tests and local-scale, borehole flowmeter, conductivity data. The heterogeneity characterization using detailed pumping tests, as described in this chapter, is valuable when designing and evaluating remediation systems, especially pump-and-treat, for heterogeneous aquifers.

## **CHAPTER 5**

### **GEOSTATISTICAL ANALYSIS OF THE COLUMBUS DATA**

## 5.1 INTRODUCTION

This chapter presents an analysis of the spatial distribution of the borehole flowmeter conductivity data collected at the Columbus one-hectare test site. The results of this analysis are compared with knowledge of the actual depositional system. The spatial distribution parameters obtained are used to determine effective conductivities based on local-scale measurements, which in turn are compared with the large-scale effective conductivities measured in the field from the different pumping tests. Thus, the applicability of several averaging techniques is tested while the practical averaging behavior of the different pumping tests is assessed. The geostatistical models presented in Chapter 6, are partly based on the parameters of the spatial conductivity distribution resulting from the analysis presented in this chapter. Thus, analyzing spatial statistics serves two purposes. First, by providing input to formulas one can determine average parameters, such as average permeability and/or macro-dispersivity. Second, by obtaining input for geostatistical models one is able to recreate images that represent the aquifer's heterogeneity.

As discussed in Sections 2.2 and 3.3, the spatial distribution of a hydraulic property, such as conductivity, is the result of various natural processes. Depositional processes play the main role in determining grainsize distribution and limits of genetic-units (i.e., a fluvial channel). For more or less consolidated sediments, geochemical processes may play a role in changing properties (i.e., cementation and clay diagenesis). Spatial statistical analysis provides, independently of these processes, a measure of the conductivity distribution. When the spatial characteristics are a correct measure, they should be consistent with the most dominant of the natural process as mentioned above.

## 5.2 ANALYSIS OF SPATIAL STATISTICS

The following sections present a basic geostatistical analysis of the borehole flowmeter conductivity data (see Sections 2.5.3 and 3.4.2) collected at the Columbus 1-HA test site. Note that these data do not satisfy *a priori* some basic assumptions underlying the applied methods. First, the conductivity obtained using the borehole flowmeter method is not a point measurement. Rather, the values obtained represent a

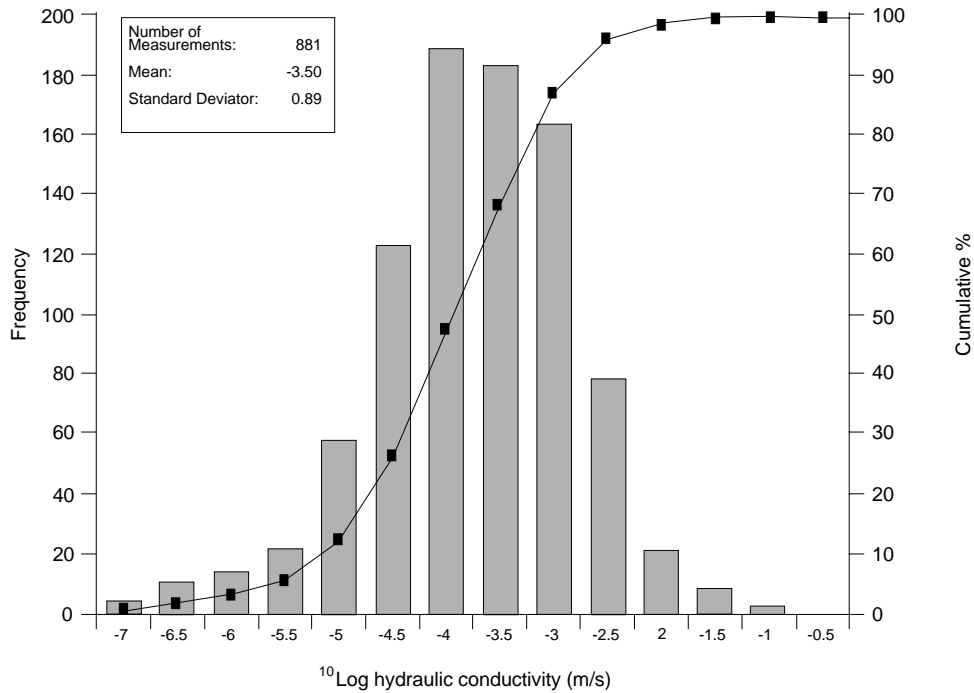


**Figure 5.1:** Distribution of  $^{10}\log$  hydraulic conductivity values derived from borehole flowmeter measurements conducted at Columbus.

certain radius-of-investigation, because the measurement is based on prorating the transmissivity of a single-well test. This well test has a considerable radius-of-investigation of several meters, possibly up to 25 m. Thus, the assumption that basic data are point values is not met. The later is an important prerequisite for geostatistical analysis based on the variogram method. Second, the assumption of stationarity (see Section 2.4) is not valid, because several different geological units occur with potentially different statistical properties. Earlier work at the Columbus test site (Young et al., 1991; Rehfeldt, 1992) shows that it had not been possible to establish a satisfactory mathematical trend. Therefore, an attempt is made to use the sedimentological units as a denominator to subdivide the test site into units that may have uniform statistical properties.

### 5.2.1 Uni-variate statistics of borehole flowmeter conductivities

An attempt is made to subdivide the into three groups reflecting the sedimentological facies recognized for the test site (i.e., channel, pointbar, and braided deposits). From the air-photo (Figure 3.2) it is obvious that, with respect to the deposits near the land surface, the site can be subdivided into two triangles: the northwest triangle occupied by channel deposits; and the southeast triangle occupied by pointbar deposits. From the sedimentological history it is inferred that at a certain depth braided river deposits occur (see Section 3.3). On the basis of an analysis of the of borehole flowmeter logs, a zone between 58 and 59 m MSL (roughly in the middle of the 8 m thick saturated zone) is considered a transition from braided to channel deposits. Thus, all sediments below 59 m MSL are considered braided deposits. For data-points between 58 and 59 m MSL no facies is identified.

Figure 5.1 shows the histogram for all logarithmic ( $^{10}\log$ ) conductivity data. Table 5.1 summarizes the distribution parameters for different facies. Inspection of the facies histograms suggests a reasonable approximation of a log-normal distribution for all cases. On the basis of the distribution parameters the pointbar and braided distribution cannot be distinguished. The channel conductivities are roughly 0.6 order of magnitude higher than the rest. As previously explained, it should be realized that these borehole flowmeter conductivities are not point measurements. Thus, the obtained conductivity distribution is relatively smooth. Therefore, when using this conductivity for geostatistical modeling, the

**Table 5.1:** Parameters for distribution of logarithmic conductivity (m/s).

Facies	$\mu^1$	$\sigma^2$	min	max	N
channel	-2.86	0.95	-5.00	-0.50	147
pointbar	-3.40	0.78	-5.59	-1.44	229
braided	-3.63	0.85	-6.70	-1.75	370
channel, pointbar	-3.19	0.89	-3.59	-0.50	376
all data	-3.49	0.94	-6.70	-0.50	881

<sup>1</sup> mean of  $^{10}\log$  conductivity

<sup>2</sup> standard deviation

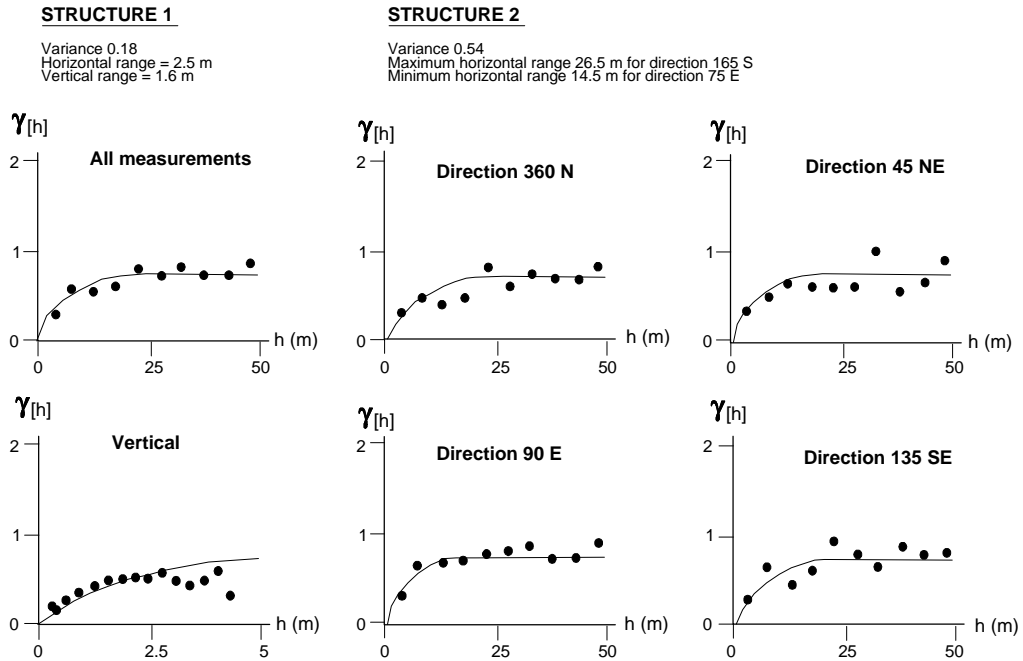


**Figure 5.2:** Experimental (crosses) and model (line) variograms for  $^{10}\log$  conductivity of braided sediments at the Columbus 1-HA test site.

$\gamma(h)$  = semi-variance as a function of lag distance  $h$

conductivity contrasts could be enlarged to some extent.

### 5.2.2 Variograms for a Continuous Random Variable (Gaussian Field)

Experimental variograms are determined for all the groups in the above mentioned table. A three-dimensional, spherical, variogram model is determined using the following strategy. Independently four directional variograms (respectively 90 E, 45 NE, 0 N and 315 NW) along with a vertical variogram, are fitted with an isotropic model. From these four isotropic directional variograms, both an anisotropy direction and a ratio are estimated. Using this anisotropy direction, a single anisotropic variogram model is simultaneously fitted to all experimental directional variograms, as well as the vertical variogram. Unfortunately, it appears that the spatial distribution of wells does not allow

one to separately determine accurate variograms for the channel and the point bar facies. Therefore, these two groups in the upper half of the aquifer, are lumped into one group (channel/pointbar).

Figure 5.2 shows the resulting variogram model fit for the braided facies in the lower half of the aquifer. The first structure has a very short correlation length and is, essentially, a nugget effect. This nugget occurs only for the horizontal data and could represent an error implicit to the borehole flowmeter method used for measuring conductivity. It is easy to envision that two wells, which are very close together, have different transmissivity values, and hence, different borehole flowmeter conductivities. These different transmissivities can result from differences in well construction and/or well damage. The only reproducibility tests that have been conducted for the borehole flowmeter, pertain to flow rates in the same well and, in turn, indicate a certain stability range for the instrument.

The double structure allows one to exactly honor exactly the well data in conditional simulations. A simple single structure (equal to the second structure), including a real horizontal nugget, is, however, an equally appropriate interpretation of the field conductivity data.

Table 5.2 lists the single structure variogram parameters obtained for the upper and lower part of the studied aquifer. Those values found are consistent with the geological model. The channel deposits show a relatively large anisotropy with an ESE azimuth that compares well with the channel direction on the air-photo (Figure 3.2). The braided deposits are only moderately anisotropic (anisotropy factor of 2) in a direction that corresponds with the main valley's direction. The latter corroborates sedimentological insights that braided deposits are deposited by straight streams on a relatively steep flood

**Table 5.2:** Variogram parameters.

Facies	$R^1$ -hor <sub>max</sub>	azimuth	$R^1$ -hor <sub>min</sub>	$R^1$ -ver	covariance	nugget
chan/pointb	29	74 ENE	7	1.3	0.55	0.12
braided	26	16 NNW	14	1.6	0.54	0.18

<sup>1</sup> Range of variogram

plane. These streams follow the main topographic drainage direction (N-S for the Tombigbee River system).

### 5.2.3 Indicator Variograms

In this section an initial attempt is made to determine indicator variograms. As discussed in Section 2.3.1, one or more conductivity thresholds need to be chosen. Conductivity values above the threshold are set to 1 while below the threshold are set to 0; an experimental variogram is calculated for these 0 and 1 data. The indicator variogram for a certain threshold expresses the correlation of conductivities above/below the threshold. In this way a high/low conductivity "facies" is correlated much easier without being confused by variations of conductivity in the range above/below the threshold. For the upper and lower half of the aquifer, the channel/pointbar, and the braided section respectively, a sensitivity is conducted calculating indicator variograms for the following series of five thresholds:

- Threshold 1: average log conductivity
- Threshold 2: average log conductivity + 1 standard deviation
- Threshold 3: average log conductivity + 2 standard deviations
- Threshold 4: average log conductivity - 1 standard deviation
- Threshold 5: average log conductivity - 2 standard deviations

For the braided portion of the aquifer, indicator variograms (Figure 5.3) can be interpreted as follows: the thresholds equal and above the average, do not show any correlation structure, while the thresholds below the average show a correlation structure with a 10-20 m correlation range. This is interpreted as: units with a conductivity less than or equal to the average, are floating in a matrix of uncorrelated average and/or greater conductivities. Note that the variograms for the extreme thresholds are not very significant. In these cases only a very limited number of data-points exceeds (or is below) the threshold; thus, the correlation is not based on a sufficient number of data-points.

For the channel/pointbar portion of the aquifer's upper half, the indicator variograms (Figure 5.3) can be interpreted as follows: for all thresholds less than or equal to the average, no correlation is apparent. Only the lowest threshold shows a small semi-variance for a length of 3 m, pointing to low conductivity units with a dimension between

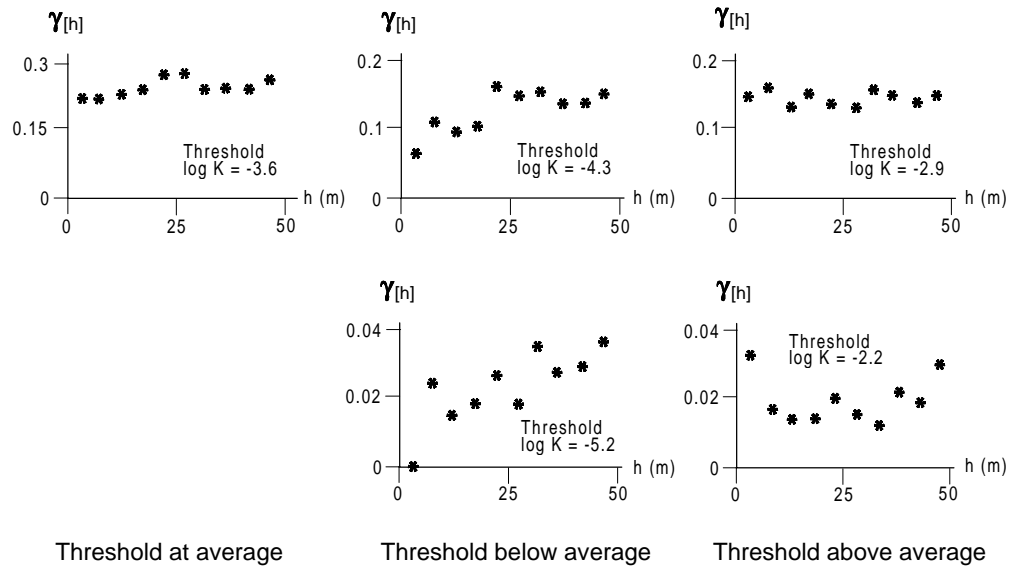


**Figure 5.3:** Experimental indicator variograms for braided facies for different thresholds (see text for explanation of thresholds).

$\gamma(h)$  = semi-variance as a function of lag distance  $h$

3 and 6 m. The thresholds above the average show a correlation structure with a range of roughly 25 m, (compare this with the previously presented Gaussian analysis). This is interpreted as high conductivity units (dimension 10-25 m) and low conductivity units (dimension 3-6 m) floating in a matrix of average conductivity.

### 5.3 EFFECTIVE FLOW AND TRANSPORT PARAMETERS

As discussed in Section 2.4, effective flow and transport parameters are related to the spatial distribution of conductivity. Effective parameters serve as what is known as an “up-scaling” operator to represent small-scale heterogeneity in a homogeneous model on a large-scale. For example, a heterogeneous model consisting of local-scale (point) measurements of conductivity (borehole flowmeter conductivities) is translated into a homogeneous model with a single value resulting from a large-scale pumping test.

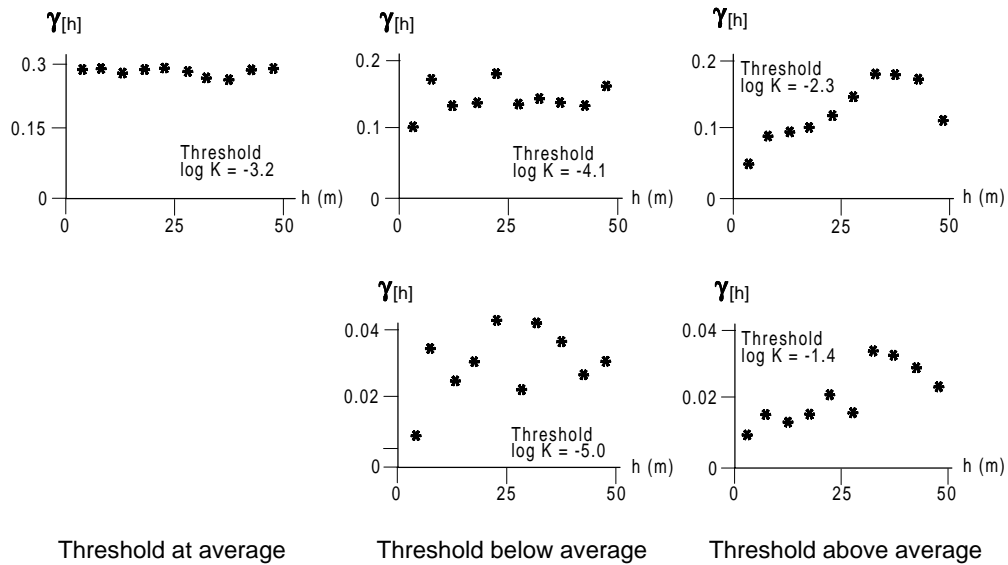


**Figure 5.4:** Experimental indicator variograms for combined channel/pointbar facies for different thresholds (see text for explanation of thresholds).

$\gamma(h)$  = semi-variance as a function of lag distance  $h$

In this section the previously calculated parameters of spatial distribution from the Columbus conductivity data, are used to determine effective parameters. The effective conductivity is compared with the results of pumping test. The forced-gradient tracer tests conducted at the 1-HA test site, do not allow a full comparison with macro-dispersivity values, because the theory underlying macro-dispersion is only derived for uniform linear flow and not for divergent/convergent radial flow.

### 5.3.1 Averaging the Columbus conductivity data

Using the traditional averaging formulas, the following averages are found for the different conductivity data measured at Columbus

conductivity from large-scale, multi-well, pumping test	$5.5 \cdot 10^{-4}$ m/s
harmonic average for all borehole flowmeter K measurements	$1.7 \cdot 10^{-5}$ m/s

geometric average for all borehole flowmeter K measurements	$3.2 \cdot 10^{-4}$ m/s
arithmetic average for all borehole flowmeter K measurements	$2.6 \cdot 10^{-3}$ m/s

In the next sections three averaging methods are studied that take the spatial heterogeneity more explicitly into account.

#### Power-average

As shown above, the value from the large-scale pumping test falls between the geometric and the arithmetic average. As discussed in Section 2.4, the geometric and arithmetic average are represented by the generalized  $\omega$  average for, respectively,  $\omega = 0$  and  $\omega = 1$  (also see Figure 2.11 and Equation 2.2). Figure 5.5 shows the results of the conductivity power-averages for the whole range of powers between -1 and 1. A value of  $\omega = 0.2$ , exactly reproduces the average aquifer conductivity obtained from the large-scale, multi-well, pumping test. This obtained value compares well with the values derived from numerical experiments and theory. Ababou and Wood (1990) theoretically

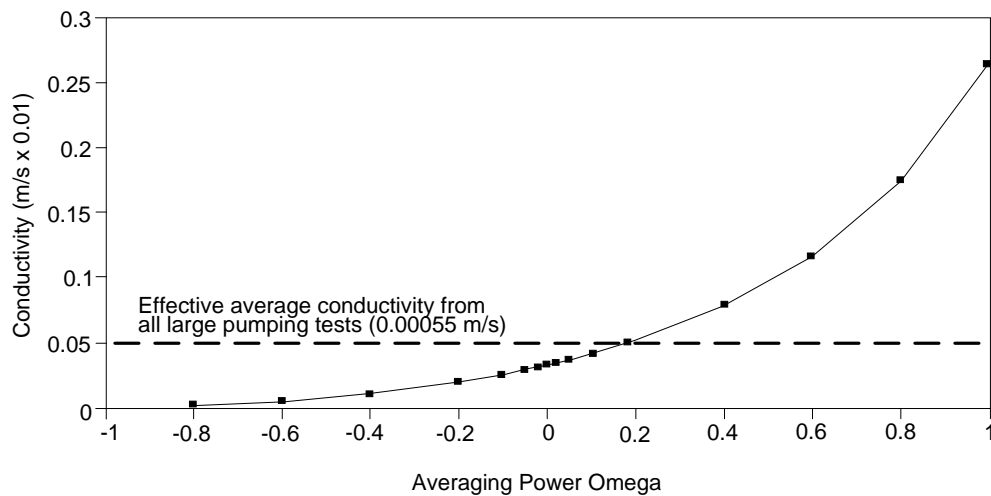


**Figure 5.5:** Power-average of borehole flowmeter conductivity as a function of the averaging power.

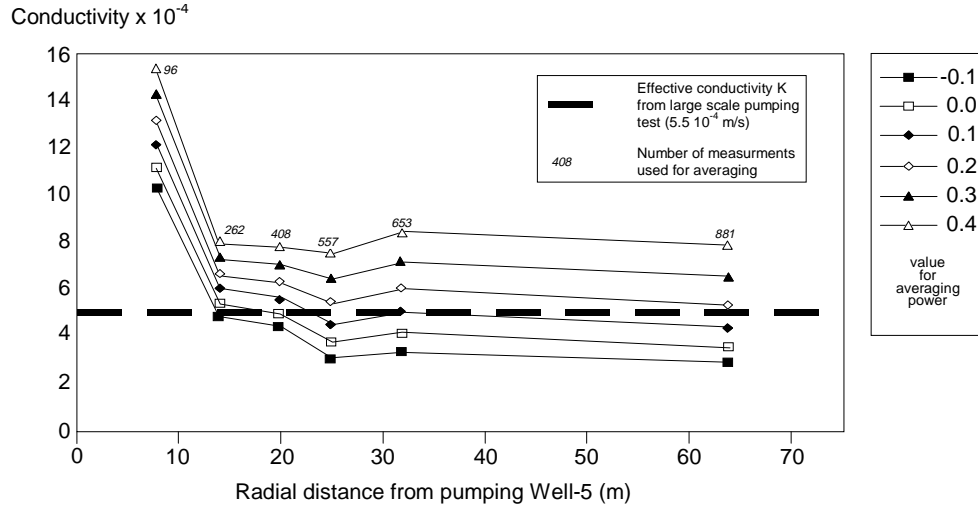


**Figure 5.6:** Power average of borehole flowmeter conductivity as a function of the radius of averaging (for several different power-exponents).

conjecture an  $\omega = 0.3$  value for steady state radial flow. Desbarats (1992a) finds a value of  $\omega = 1/3$  for finite cubic flow fields with isotropic conductivity, co-variance structure for up to 0.2 dimensionless, correlation length which is the ratio of correlation length and the length of the flow field.

Butler's (1990) formula (see Section 2.5.2) is applied to calculate the area of influence that in turn determines the results of a pumping test. The following parameters obtained from the analysis of the large-scale, multi-well, pumping test, were used:  $T = 5.0 \cdot 10^{-4} \text{ m}^2/\text{s}$ ;  $S = 0.05$ ; and  $t = 50,000 \text{ sec}$ . The inner and outer radius of the area of influence were estimated at 7 m and 85 m. Figure 5.6 shows the results for subsets of the total data-set. These subsets consist of all wells within a certain radial distance (radius of averaging) from the pumped well. Figure 5.6 shows that localized around the production well a zone of high conductivity exists. Consistent with the radius-of-influence calculated above, the 0.2 power-average of the borehole flowmeter conductivity data, represents the large-scale pumping only when the averaging area expands beyond a radius of 15 m. The fact that the average conductivity increases when wells at a radius between 25 and 32 meter are included, is explained by a high conductivity channel approximately 30 m distance from the production well (see Section 3.3).

The stability of the power-average with  $\omega = 0.2$ , is also investigated for subsets of a few randomly selected wells from the complete database of available wells. Four different subsets options are investigated:

- 5 wells excluding the pumping well
- 5 wells including the pumping well
- 10 wells excluding the pumping well
- 10 wells including the pumping well

For each of these options, the power-average conductivity (power-exponent = 0.2) is determined for 10 combinations of (5 or 10) wells forming a subset of the complete data-set. Table 5.3 shows distribution parameters obtained from the ensembles of realizations. When the pumping well is excluded the subset average, conductivities are distributed around the average conductivity of the total data-set (which equals the conductivity from the large-scale interference test). If the pumping well is included in the subset, then the average of subset conductivity is consistently too high. The reason for this is that the pumping well permeabilities are approximately a factor of four higher than the average for all measurements.

*Average based on Dagan's formula*

Dagan's formula (Section 2.4, Equation 2.3) yields an effective conductivity of  $5.6 \cdot 10^{-4}$  m/s. This value fits very well with the conductivity value obtained from the large-

**Table 5.3:** Distribution of average conductivities (in m/s) obtained for 10 different combinations of (5 or 10) wells that are a subset of the total data-set.

number of wells	pumping Well-5	average <-----of distribution of 10 power averages obtained for sub-sets----->	minimum	maximum	stand. dev.
5	excluded	$4.92 \cdot 10^{-4}$	$1.65 \cdot 10^{-4}$	$1.05 \cdot 10^{-3}$	$2.62 \cdot 10^{-4}$
10	excluded	$5.03 \cdot 10^{-4}$	$3.49 \cdot 10^{-4}$	$7.76 \cdot 10^{-4}$	$1.44 \cdot 10^{-4}$
5	included	$6.75 \cdot 10^{-4}$	$2.45 \cdot 10^{-4}$	$1.33 \cdot 10^{-3}$	$2.90 \cdot 10^{-4}$
10	included	$5.79 \cdot 10^{-4}$	$3.58 \cdot 10^{-4}$	$8.26 \cdot 10^{-4}$	$1.36 \cdot 10^{-4}$

scale, multi-well, pumping test, although Dagan's equation is theoretically only derived for small conductivity variations and uniform flow.

*Inverse distance weighted averaging*

The volumetric integral proposed by Desbarats (1992b) is approximated by a simple summation of all wells. An average conductivity of  $5.5 \cdot 10^{-4}$  m/s is determined when all wells are averaged, excluding the pumping well. This value fits well with the effective conductivity obtained from the multi-well pumping test. Note that the summation conducted is a rather poor representation of the areal integral underlying this type of average. For the average, excluding the production well, this is balanced by the well network (Figure 3.7) which shows some sort of a radial distribution of wells around the production well.

Although a good fit is obtained there are several concerns regarding application of this method. The omission of the pumping well conductivities is obviously in contradiction to the theory and intent of the Desbarats' (1992b) method. By including the pumping well, in one way or another way, the good fit between the pumping test value and the inverse distance weighted average would deteriorate. As shown in Section 5.3.1, the pumping well has a relatively high conductivity compared to the remainder of the field. Application of the inverse distance weighting schema would cause a significantly higher average value.

The omission of the pumping well is in agreement with the concept of a ring-of-influence (Oliver, 1990; Butler, 1990). This concept implies that conductivities in an inner ring around the pumping well, do not impact an effective conductivity obtained from a pumping test, when the effective conductivity is based on late-time, pumping test data. It should be noted that Desbarats (1992b) developed the concept of distance weighted averaging for a steady state, single-well test. Comparing this type of average with a transient pumping test, may not be valid. The latter, however, would indicate that there exists a significant difference between results obtained from a transient and steady state pumping test. This subject requires more attention.

Consequently, questions remain whether this method can be correctly applied to multi-well, pumping test data such as those from Columbus. An application published by Desbarats (1994) has shown good results when comparing core conductivities from a well with the interpretation of a single-well test conducted on that same well. For that application, however, the pumping well is assumed to be statistically similar to the remainder of the conductivity field (the principle of stationarity, see Section 2.4). The latter is typically not the case for the Columbus, multi-well pumping test data.

### 5.3.2 Effective Dispersion (macro-dispersion)

As discussed in Section 2.4.2 (Equation 2.4), macro-dispersivities can be calculated from the spatial, conductivity, distribution parameters calculated in Section 5.2. Note, however, that these calculations are approximate, because the distribution parameters greatly exceed the small conductivity range for which the theory was derived. Additionally, the spatial anisotropy observed is not considered in the theory of macro-dispersion. The following macro-dispersivity values were calculated based on the correlation lengths that emerged from the variogram analysis (Gaussian and indicator method):

macro-dispersivity of 53 m for correlation length 30 m  
macro-dispersivity of 47 m for correlation length 26 m  
macro-dispersivity of 25 m for correlation length 14 m  
macro-dispersivity of 9 m for correlation length 5 m

These values are very different from the range presented by Rehfeldt et al. (1992); those were derived from borehole flowmeter measurements conducted at the nearby MADE site (see Section 2.4.4). The significant discrepancy between the two ranges, is probably the result of detrending. The range of macro-dispersivity values (above) is more consistent with values reported by Adams and Gelhar (1992) that were based on the plume's moments.

#### 5.4 SUMMARY AND CONCLUSIONS

For the variogram to be meaningful for macro-dispersivity analysis, the data-set and the underlying conductivity field need to be stationary. In other words, the statistical properties should not change as a function of the position in the field (also see Section 2.4). Earlier work (Young et al., 1991; Rehfeldt et al., 1992) conducted at the Columbus test site indicates that the hydraulic conductivity field is non-stationary, because a trend occurs. That work also shows that attempts to obtain an unambiguous stationary field by a mathematical detrending, are not successful. In this dissertation an attempt is made to use sedimentological insight to split the data-set into stationary units. The scope of this exercise, however, is limited by the sparse sedimentological data available.

The upper part of the aquifer, the channel and pointbar deposits, appears to be significantly anisotropic. Correlation lengths are determined in the order of 30 m for the maximum (anisotropic) direction (ENE) and 7 m for the minimum anisotropic (NNW). It can not be distinguished whether this anisotropy should be primarily attributed to the channel, to the pointbar, or to the trend between the channel and the pointbar.

For the lower part of the aquifer a much less anisotropic structure is found. The maximum correlation length is 26 m (NNW direction) while the minimum correlation length is 14 m (ENE) direction. For both the upper and the lower part of the aquifer, respectively channel/pointbar and braided deposits, the co-variance of  $^{10}\log$ -conductivity is in the order of 0.8. The anisotropy directions are in agreement with the channel direction observed on the air-photo and the main direction of the valley that in turn determines the direction of the braided streams.

The indicator variogram analysis does not yield clear results. Some geological ideas could be confirmed by analyzing the indicator variograms for different thresholds. Note that for most practical applications (see Section 2.3.4) of the indicator method, variograms have been estimated using additional geological data (e.g. facies dimensions).

On the basis of this spatial analysis of the borehole flowmeter conductivities, effective parameters for flow and transport (effective conductivity and macro-dispersivity), are evaluated. Note that the conductivity variability is relatively high, compared with the small values for which the theory is derived. Several analytical methods yield good results for effective conductivity in comparison to the result of the

large-scale, multi-well pumping test. Using the power-average, a power-exponent  $\omega = 0.2$  was found, which fits well with theoretical and practical insights. The power-exponent 0.2 indicates that the borehole flowmeter conductivities certainly have a smaller support scale than the large-scale, multi-well test. It also indicates, however, that it is not completely correct to use the extreme power-exponent 1 (i.e. arithmetic proportioning) for determining these borehole flowmeter conductivities from a single-well test. This latter concern is further addressed in Section 6.5.2. In the case of the inverse distance weighted averaging (Desbarats, 1992b) some questions remain as to how to include conductivity data from the pumping well.

When subsets from the well data are considered, a significant variability appears among the average values for different subsets. The comparison of local conductivities, their spatial average, and field measurements of conductivity allows one to understand a data-set. Discrepancies between the average conductivity determined from a relative small set of small-scale measurements (e.g. borehole flowmeter data) and the large-scale average value (from a pumping test) should be duly noted. These discrepancies should not only be identified as potential errors, but geological information can be derived from these discrepancies. Weber and van Geuns (1989), show some empirical methods to incorporate geological information to resolve such discrepancies.

As shown in this chapter non-stationarity can be easily inferred from geological insights; its effect on the spatial analysis can be corrected by investigations into the relationship between facies and conductivity trends. This constitutes an alternative to the use of tracer test data to overcome de-trending problems encountered during geostatistical analysis (Rehfeldt et al., 1992). Further applications of pumping tests and averaging applied to geostatistical models is discussed in Appendix A.

**CHAPTER 6:**

**MODELS FOR PUMPING TESTS AND TRACER TESTS IN HETEROGENEOUS  
AQUIFERS COMPARABLE TO COLUMBUS**

## 6.1 INTRODUCTION

As stated in Chapter 1, it is very attractive to use relatively simple field data, such as a multi-well pumping test, to obtain realistic models for reliably predicting subsurface contaminant transport. The field data collected at Columbus indicate that preferential solute transport pathways due to sedimentary heterogeneity, can be diagnosed using multi-well pumping tests (see also Chapters 3 and 4). The following sections present several models of groundwater flow and tracer transport that are representative of the heterogeneous, Columbus, 1-HA test site. The objective of this modeling study is to test the stated hypothesis that multi-well pumping tests are discriminative in respect to solute transport. Within the framework of geostatistical modeling, pumping test data offer the possibility of selecting from an ensemble of models (realizations) created for a given set of geological and conductivity data. When the geostatistical input parameters cover an appropriate spectrum, this ensemble of realizations reflects not only the possible range of heterogeneity models, but also the uncertainty inherent to incomplete knowledge of the subsurface geology. If those realizations not matching the pumping test are rejected, the original uncertainty range is reduced (Deutsch, 1992)

This chapter includes a facies model, along with different types of geostatistical models that reflect the heterogeneity of the Columbus 1-HA test site. A geostatistical flow and transport modeling effort is presented which covers a large ensemble of model realizations. For all these aquifer models, both a pumping test under confined conditions and a two-well tracer test are modeled. The variety of pumping test and tracer test responses, is shown. The coherence between pumping test data and solute transport data is demonstrated. No effort was made to condition these models exactly to the Columbus data because this was considered a fruitless effort given: the scarce geological data available for specific wells (no cores were available for detailed analysis); and the limited accuracy of the pumping test data.

In order to clearly isolate the heterogeneity effect, unconfined conditions are ignored. An unconfined aquifer's pumping test response during early-time, follows the response of the equivalent confined aquifer. Therefore, conclusions based on the confined models can be compared to information derived from the early-time, field observed drawdown-curves at Columbus. Thus, the work presented here is intended to only show

the principle of relating multi-well pumping test results to tracer test results. Conclusions are limited to a qualitative replication of the results of the field experiments at the Columbus 1-HA test site.

## 6.2 FLOW AND TRANSPORT MODELING

The use of geostatistical techniques to create input for a flow model of a strongly heterogeneous aquifer, implies very detailed grids for hydraulic properties. Practical flow modeling applications mostly involve up-scaling (see Section 2.3.4). Effective (average) properties are, in general, calculated from several fine grid cells of the geostatistical model. For the modeling study presented in this chapter, however, the geostatistical model's fine gridding is fully maintained. In fact, the geostatistical model was designed to allow flow modeling without any reduction of the size of the grid.

Although the fine geostatistical grid remains unchanged, any numerical solution scheme distorts the spatial variability of the original input. This distortion pertains to determining inter-cell (or inter-node) hydraulic properties that are mainly obtained by averaging. No strict theoretical guideline exists for the correct grid resolution. A good rule is that a "unit length of heterogeneity" should be covered by "several" cells. For the Gaussian model the rule-of-thumb given by Desbarats (1990) was adhered to so that, at least, five grid cells should cover one correlation length. In order to obtain the same unknown distortion of the spatial variability of hydraulic properties, the grid size must be uniform over the whole model domain. Therefore, a regular square grid combined with a conventional Finite Difference technique, is appropriate. Refining the grid is acceptable, as long as a regular cell is exactly covered by a couple of refined cells. In that case the refined cells can all be assigned the hydraulic property of the specific regular cell replaced by the refined cells. For the "relatively" less, heterogeneous, facies, geological model, this fine gridding is maintained for reasons of consistency.

The U. S. Geological Survey Modular Groundwater Flow model MODFLOW (McDonald and Harbaugh, 1988) is used for pumping tests and the flow part of tracer tests. For tracer flow a stochastic, particle, tracking extension module for MODFLOW was developed. This particle tracking technique is published by Desbarats (1990).

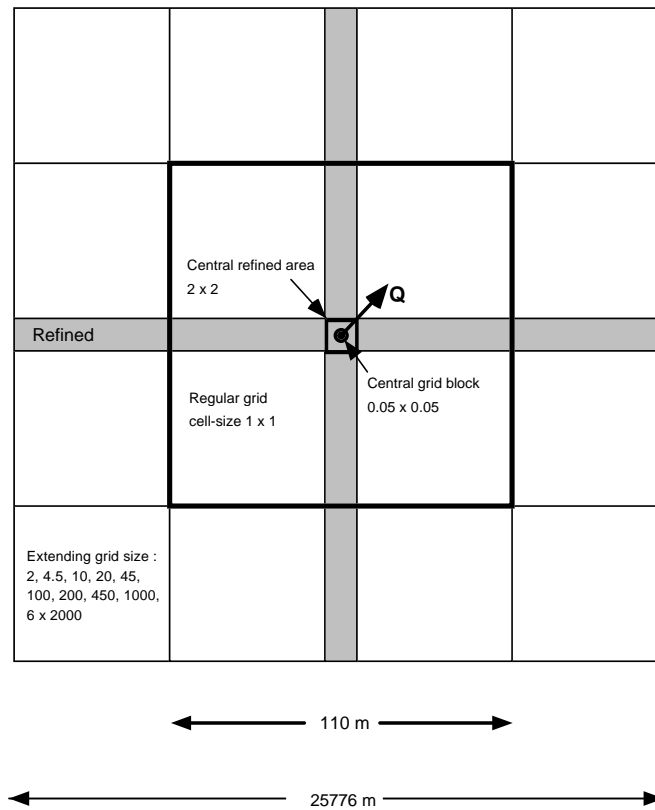


**Figure 6.1:** Grid layout for pumping test and tracer test model (all dimensions in meters). The grid size is 149 x 149 x 6 (rows-columns-layers). Note the different scales for the different areas of grid refinement.

### 6.2.1 Setup of pumping test model

Figure 6.1 shows the grid for the pumping test model. The middle area, represents the 1-HA test site. A four, six, or twelve layer confined aquifer is modeled. The grid consists of an inner section around the pumping well where cell sizes are refined to 0.05 m (the well-bore diameter). Between a distance of 1 meter to 55 meters from the well (in X and Y directions) the grid is regular with a cell size of 1x1 m<sup>2</sup>. This regular grid cell size is small enough to model heterogeneities accurately. At distances larger than 55

meters, the cell size is gradually increased to 2,000 meters (by a factor of at most 2.2). The model is bounded by closed boundaries at a distance 12,500 meters (in X and Y directions) from the pumping well.

The heterogeneous model is limited to the regular grid in the middle field of 110x110 m<sup>2</sup> that represents the 1-HA test site (see Figure 6.1). A single average conductivity value is assigned to the outer zone of extending grid cells. The influence of this average zone outside the middle field, starts around 1,000 seconds. This is the time for which the radius-of-influence (Butler, 1990) reaches 50 meters. The latter calculation is based on an a homogeneous aquifer with average properties. The radius-of-influence concept, however, is less applicable to heterogeneous models. Continuous high conductivity zones may extend to the outer zone. Drainage of the outer zone may commence prior to the inner zone being fully drained.

At the well all water is withdrawn from the upper well gridblock. The central well block is assigned a vertical conductance several (5-6) orders of magnitude larger than the surrounding aquifer. Vertical flow can occur within the well without any significant resistance. As a result, the contributions of the layers tapped by the well, will be dynamically established during the transient pumping test. This implicit well model avoids a static allocation of layer rates, but causes an extra computational burden. A correct simulation of the layer rates at the well, is necessary for accurately modeling both a single-well test (see Section 6.5.2) and the tracer recovery along the vertical of a well. By assigning a storage coefficient of 1 to the central gridblock (the pumping well), well-bore storage is correctly simulated (Butler, 1988, p 154).

A constant rate pumping test is simulated for a time period of 1,000,000 seconds (278 hours). Fifty-five (55) time-steps are simulated starting as small as 0.003 second and ending as large as 200,000 seconds. In order to check the accuracy of the pumping test simulations, the following series of test cases were run: homogeneous case (Theis solution); two radial zones of different K-values (radial composite "ring" case); a leaky aquifer; and an aquifer consisting of three linear zones with different K-values (Butler and Liu, 1991)). The simulated drawdowns and the derivative were compared with results from analytical solutions for these cases. These comparisons confirmed that the drawdown and its derivative are very accurately modeled for observation wells and that for the pumping well itself only a few minor errors occur.

### 6.2.2 Setup of tracer test model

The objective of the tracer test model is to characterize tracer flow between two wells of a multi-well pumping test, respectively the pumping well and a specific well serving as an observation well. A steady state MODFLOW run is conducted using the same conductivity data-set used in the pumping test model. At an observation well of the pumping test model, the pumped rate is re-injected. Contrary to the pumping well, no local refinement is applied for the injection well, but the layer injection rates are proportioned to the layer conductivities of that injection well. The latter is strictly valid only for a confined aquifer consisting of homogeneous layers with different conductivities. For the studied heterogeneous models, an error is introduced, because some unrealistic vertical redistributions of the tracer may occur close to the injection well. A constant porosity is assumed for the unconsolidated sediments.

For tracer flow, a stochastic model was used based on the Node-to-Node-Routing (NNR), particle tracking algorithm (Desbarats, 1990, 1991). This algorithm uses the steady state flow field modeled with MODFLOW (described above). The algorithm is based on moving particles from node to node, starting at the injection well until a destination (pumped well) is reached. The algorithm was implemented as an extension to the MODFLOW code<sup>1</sup>. A probabilistic procedure is used to select the next node where a particle residing at a certain node can move. The steady state flow field is used to determine the probability for each neighboring node to be the next node. After probabilistically selecting this next node, the total cell flux is used in determining both the velocity and the time necessary to make the node-to-node move. By accumulating this time for each particle, the total residence time can be determined. A large number of particles is moved one-by-one through the system.

The residence time distribution (RTD) obtained for this large ensemble of particles, represents a characteristic response and effectively represents the flow of a tracer slug through the system. The NNR procedure is essentially a simplified version of the “Random Walk” procedure for modeling of tracer flow (Prickett et al., 1981). The “Random Walk” procedure uses a Gaussian distribution based on the dispersion length to

---

<sup>1</sup> The author gratefully acknowledges the guidance obtained from Alexandre J. Desbarats to develop and test the NNR particle tracking extension for MODFLOW.

calculate random dispersive displacements. In contrast the NNR method uses the heterogeneous geostatistical conductivity field to generate inter-gridblock macro-dispersive displacements (see also Section 2.4.2),

As explained in detail by Desbarats (1990, 1991), the NNR algorithm is extremely effective in simulating tracer tests in strongly heterogeneous media. Also it introduces correct values for macro-dispersivity given certain geostatistical parameters for the conductivity field. Conventional tracer models that employ Finite Difference or Finite Element techniques in solving the concentration equation, generally show an unfavorable numerical behavior (i.e., instability or extreme inefficiency due to small grid size and/or small time-steps) for strongly heterogeneous geostatistical models; this is due to large conductivity contrasts between individual cells. Other conventional tracer models, such as the original “Random Walk” model (Prickett et al, 1981) involve interpolation of the velocity field at the subgridblock-scale between nodes. Subsequently particles are moved along the interpolated streamlines (e.g. Goode and Shapiro, 1991). This interpolation procedure requires relatively homogeneous or smoothly varying flow fields, and does not match the strongly heterogeneous flow fields resulting from the heterogeneity models considered in this dissertation.

For the above mentioned strongly heterogeneous flow fields the inevitable smoothing of the interpolation results in a bias for the tracer solution at the subgridblock-scale. As noted by Desbarats (1990) the perceived non-exactness of the NNR algorithm (Goode and Shapiro, 1991), only pertains to dispersion at the subgridblock-scale. Thus, a smoothing bias (conventional particle tracking) is traded for a dispersive bias (NNR). Goode and Shapiro (1991) indicate that the artificial (numerical) dispersion introduced by the NNR-method, is maximal 0.35 times the characteristic length of a grid cell. Desbarats (1990, 1991) has shown that this dispersive bias is negligible in comparison with the macro-dispersion deliberately introduced by the heterogeneity of a geostatistical model (see also Section 2.4.2 and 5.3.2). The smoothing bias introduces an unknown error dependent on the interpolation algorithm applied. This unknown smoothing error suppresses the macro-dispersion of the heterogeneous geostatistical conductivity field. The objective of the tracer modeling presented in this dissertation, is to study these heterogeneity effects and, therefore, this suppression is an undesired effect.

The NNR is a numerical transformation from the random permeability field to a random velocity field. The random velocity field is subsequently used for a stochastic solution of the mass transport equation. In this sense the NNR method is a numerical implementation of the concepts underlying the macro-dispersion theory (Section 2.4). In contrast to this theory, no idealized restrictions are imposed in respect to the statistical properties of the heterogeneous conductivity field. Given any model for heterogeneous conductivity, the only practical restriction is that the conventional flow (pressure-head) equation can be solved with sufficient detail and accuracy.

Thus, if a detailed geological model is constructed using geostatistical techniques on a fine-grid, the NNR method resolves all significant geostatistical detail. Given enough grid resolution compared to the correlation length of the conductivity field, a negligible amount of numerical subgridblock dispersion is added. Just as macro-dispersion represents the macro-scale heterogeneity (see also Section 2.4.2), this subgridblock dispersion can be seen as the result of some unknown heterogeneity on the subgridblock-scale. The subgridblock dispersion is preferred above an unknown smoothing error that is based on an assumed interpolation schema on the subgridblock-scale. Thus, this simple concept and this method's extreme efficiency, allow one to conduct tracer modeling based on large grids containing the best estimate of geological variability, in other words a detailed geostatistical model. The latter contrasts conventional tracer models based on a simplified heterogeneity model combined with a black box approximation of the detailed flow field (i.e., lump treatment of heterogeneity as dispersion). The apparent increase in work load when employing a geostatistical model, is balanced by avoiding conventional tracer modeling, considered by most to be a cumbersome time consuming task. The work load is truly shifted from the numerical transport-modeling effort to the geological and geostatistical conceptualization effort.

The MODFLOW extension that implements the NNR method was extensively tested prior to application to the geostatistical models developed for the Columbus 1-HA test site. The following test cases were investigated:

- 1- 2-D vertical slice model of five layers with different conductivities;
- 2- 3-D spatial uncorrelated random conductivity field;
- 3- 2-D horizontal spatial correlated Gaussian conductivity field.

For all these cases, flow is modeled between two different, constant head boundaries and two no-flow boundaries. At the constant head, particles are injected proportionally to the influx from the constant head boundary. For test Case-1, conductivities varied, stepwise per layer, over two orders of magnitude ( $3 \cdot 10^{-5}$ - $3 \cdot 10^{-3}$  m/s). The RTD for tracer breakthrough, is theoretically calculated from the different velocities for each of the five layers. The output from MODFLOW and the NNR tracer extension, accurately matches the predicted RTD. This test was originally run for an uniform grid. This uniform grid was changed to a strongly irregular grid in both coordinate directions without changing the layer geometry. The RTD from the latter model matches the RTD for the regular model, as well as the theoretically expected RTD. Thus, this validates the proper functioning of the MODFLOW-NNR extension for irregular grids.

For random conductivity fields, a theoretical macro-dispersion can be calculated for transport models of test Case-2 and Case-3. Desbarats (1990) presented a test case that is exactly replicated in test Case-2. The RTD and macro-dispersivity from the MODFLOW-NNR extension, are practically similar to the results and the simulated values given by Desbarats (1990). The macro-dispersivity differs slightly from the theoretical value. For larger residence times (the 1% slowest particles of the cumulative RTD) some deviation occurs. For test Case-3 of a correlated Gaussian conductivity field, a macro-dispersivity was found within 10% of the theoretically expected value. This deviation is not surprising given the fact that assumptions (e.g. infinite flow field, very small conductivity variation) of the underlying theory are not fully met.

### 6.2.3 Modeling strategy

To investigate in detail the pumping test response of heterogeneous aquifer models, the following modeling strategy was employed. During the pumping test, drawdown is recorded at the pumping well to obtain single-well test results, and is also recorded at several observation wells. The observation wells are arranged in circles around the pumping well (Figure 6.2). Each circle has eight observation wells at angular directions incrementing forty-five degrees ( $45^\circ$ ). For each observation well, drawdowns in all vertical layers of the model are independently recorded. It is impossible to model the

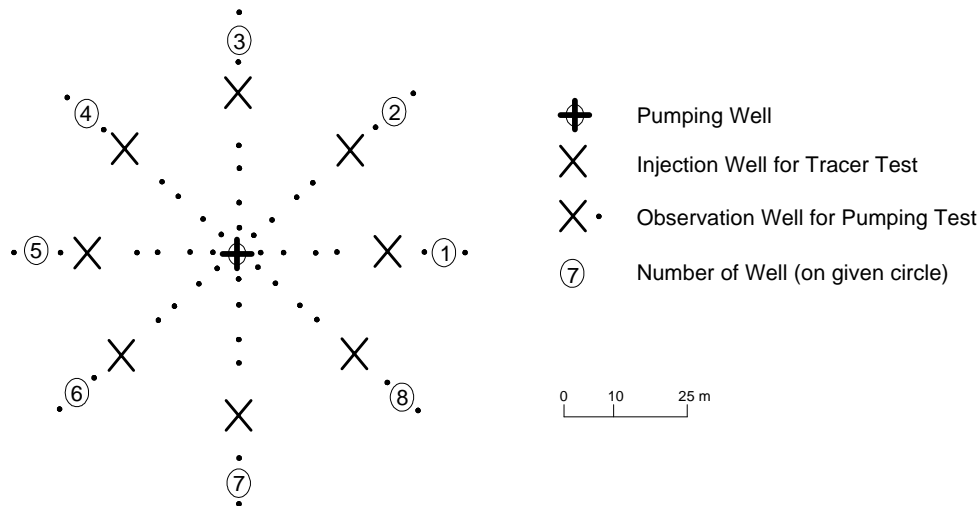


**Figure 6.2:** Well pattern used for pumping test model and two-well tracer test models. Note that each observation well is actually a nest with as many independent piezometers as model layers.

exact response of a fully penetrating observation well, because that would require grid refinement to the well-bore radius for each observation well. Therefore, the maximum, average, and minimum drawdown is analyzed for each series of independent vertical observation points that form a “well”.

For comparison with the tracer test results, the time is recorded for which the maximum drawdown exceeds a threshold. This time is called “drawdown breakthrough” time. The observation wells on the circle with a radial distance of 30 meters, were used to model tracer tests. A series of two-well, forced gradient, tracer tests was modeled. Each well on this circle was modeled as an individual tracer injection well, re-injecting water pumped from the central well; this central well was also used as pumping well for the pumping tests. Thus, for each geostatistical or deterministic, aquifer model of conductivity, the results from eight two-well tracer tests are available to characterize tracer flow from different directions towards the pumping well. The result of modeled tracer tests is the cumulative RTD. The breakthrough time for a fixed value on the initial part of this curve (e.g. the 15% value) was compared with the head-breakthrough time.

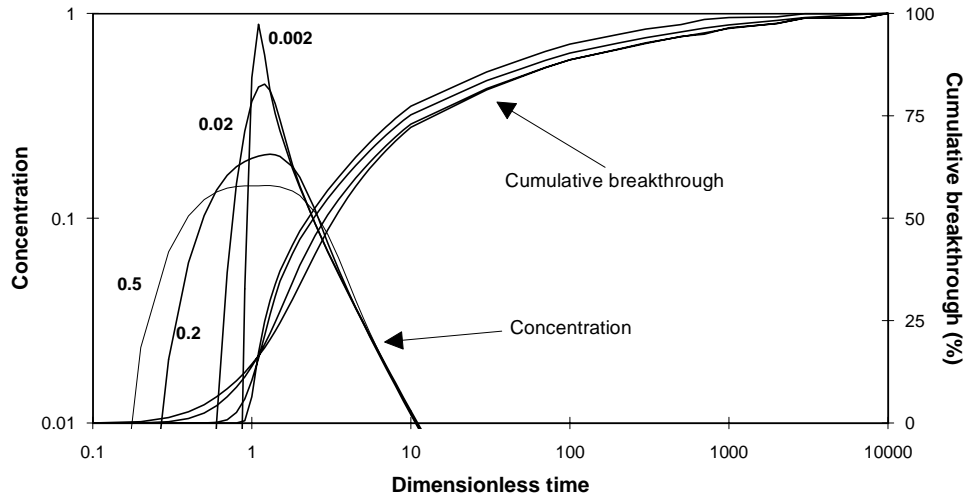


**Figure 6.3:** Dimensionless concentration breakthrough.

Bold labels represent dimensionless dispersivity for each breakthrough curve.

Dimensionless time = rate / (porosity x thickness x inter-well distance).

Dimensionless dispersivity =  $\alpha_L$  / inter-well distance.

For comparison among tracer tests, a series of percentiles is used (5-15-50-75%) to characterize the full breakthrough curve (see Figure 6.3).

#### 6.2.4 Type-curves for apparent macro-dispersivity

Apparent macro-dispersivities can be estimated from the breakthrough curves resulting from tracer advection through a strongly heterogeneous medium. To determine an apparent macro-dispersivity, a set of type-curves for the RTD is used (Figure 6.3). These type-curves were generated using an analytical model of a two-well tracer test (instantaneous injection of a tracer slug) in a homogeneous aquifer (Gelhar and Collins, 1971; Gelhar, 1982). Figure 6.3 shows that peak breakthrough occurs practically at dimensionless time 1. Figures 6.3 and 6.4 show that the time of 15% cumulative breakthrough also concurs with dimensionless time 1. Thus, the time when 15% cumulative breakthrough has occurred, is a good estimator for peak-breakthrough

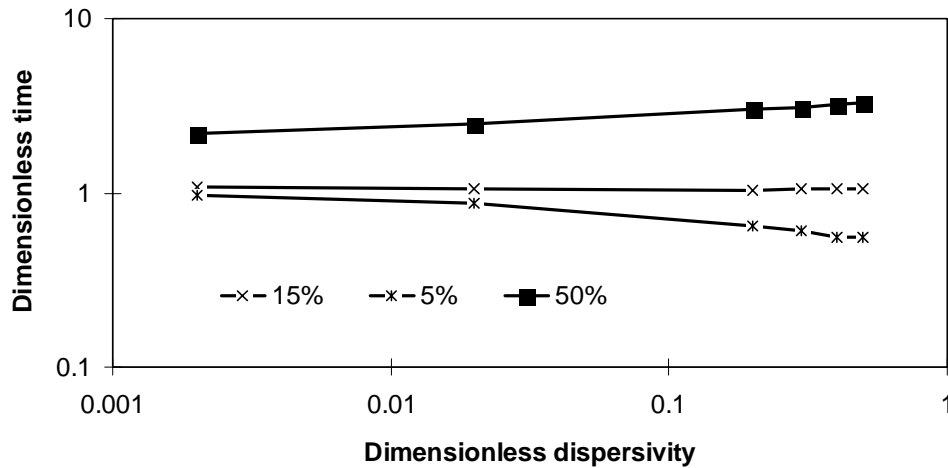


**Figure 6.4:** Relation between dispersivity and cumulative breakthrough time.

(dimensionless time = 1). Hence, the time of this 15% cumulative breakthrough can be used to calculate effective porosity. The difference in dispersivity can be inferred from the sigmoid shape of the cumulative curve; hence, the time lag between 5% and 50% cumulative breakthrough. This time lag ranges from a quarter log-cycle (small dimensionless dispersivity) to three-quarters log-cycle for dispersivity 0.5. The chart in Figure 6.4 can also be used to estimate dispersivity from this same time lag (5% to 50%). Note, the largest dimensionless dispersivity is half the inter-well distance. Attempts to quantitatively assess larger dispersivities, in the order of the inter-well distance, are considered fruitless.

This approximate estimation method, is not very practical for field application, because accurate measurements of the 50% cumulative breakthrough time are often not available. However, for RTD curves obtained by modeling a two-well tracer test for a heterogeneous geostatistical model, the above described methodology permits a reasonably accurate and efficient estimation of effective porosity and longitudinal dispersivity.

### 6.3 FACIES MODEL FOR A COARSE-GRAINED POINTBAR

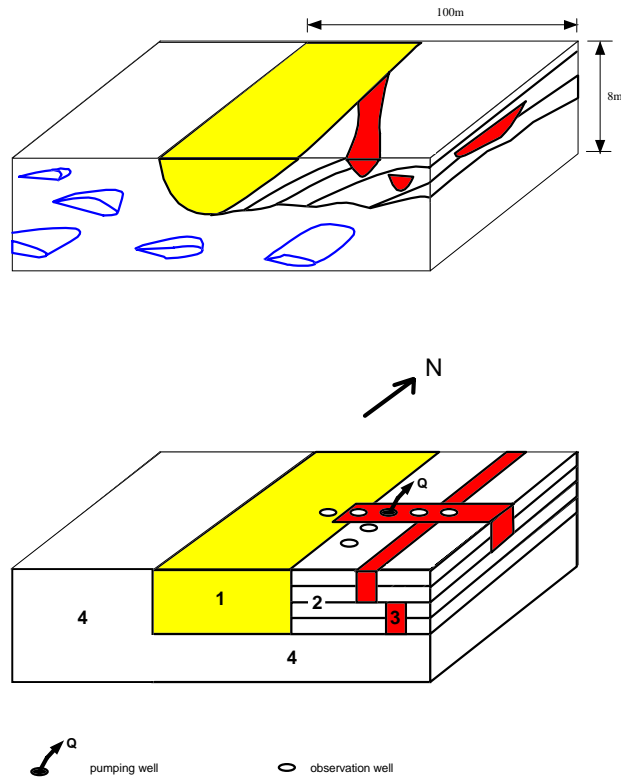
A simple facies model illustrates the effect of heterogeneity for pumping and tracer tests. This model represents the sedimentological model inferred for the Columbus 1-HA test site (see Chapter 3). It can be seen as a best guess for a possible model of the Columbus test site given limited geological data. In the formalism of geostatistical modeling, it can be seen as a possible realization from an ensemble of all possible geostatistical (deterministic, object, Gaussian etc.) models.

#### 6.3.1 Conceptual heterogeneity model and conductivity values

Figure 6.5 shows two block diagrams representing the coarse-grained pointbar model applicable to Columbus. The upper diagram shows a geometry of facies and architectural elements, that can realistically be expected; the lower diagram schematically shows a layout for a flow model. The main structures (channel and pointbar) are infinitely continued to the North and South. Due West from the channel the original braided deposits, also called terrace-deposits, are assumed and into these the channel/pointbar system has been eroded. The pointbar layers are chosen perfectly horizontal and are laterally connected to the main channel. This contradicts the upper diagram in Figure 6.5 which more realistically presents the true depositional structure indicating that the pointbar layers are slightly tilted ending on the eroded surface of the underlying braided terrace deposits. However, this pointbar structure is very difficult to discretize and, therefore, the simplified option is chosen for discretization. For the same convenience of

**Table 6.1:** Conductivities used in the facies model.

Facies	horizontal conductivity $K_h$		vertical conductivity $K_v$		$K_h/K_v$
	$^{10}\log$	m/s	$^{10}\log$	m/s	
channel	-3.0	$1.0 \cdot 10^{-3}$	-3.5	$3.3 \cdot 10^{-4}$	3
pointbar	-4.0	$1.0 \cdot 10^{-4}$	-5.5	$3.3 \cdot 10^{-6}$	30
chute channel	-2.0	$1.0 \cdot 10^{-2}$	-3.5	$3.3 \cdot 10^{-4}$	30
braided	-4.0	$1.0 \cdot 10^{-4}$	-4.5	$3.3 \cdot 10^{-5}$	3



	facies or architectural element	log-K measured			model
		min	med	max	
<b>1</b>	main meandering channel deposits	<b>1</b> -5.0	... -2.9	... -0.5	-3.0
<b>2</b>	pointbar deposits	<b>2</b> -5.6	... -3.4	... -1.3	-4.0
<b>3</b>	chute (cross-pointbar) channel deposits	<b>3</b>	no field observations		-2.0
<b>4</b>	braided stream deposits	<b>4</b> -6.7	... -3.6	... -1.8	-4.0

Figure 6.5: Sedimentological facies model and pumping test model schematization.

discretization, the chute channels are chosen, either parallel or perpendicular to the main channel. In this case the sedimentological model is not significantly compromised, since connections between the main channel and the chute channel are similar to the “realistic” upper diagram of Figure 6.5. The braided lower half of the aquifer is assumed to be homogenous.

Horizontal conductivities for the model are inferred from the field measured, borehole flowmeter conductivities. Table 6.1 presents the conductivity values in the three-dimensional block diagram (see also Figure 6.5) used for modeling the pumping test. For the channel and braided deposits the conductivity value has been chosen as a rounded value close to the logarithmic mean observed in the field data (see Section 5.2.1, Table 5.1). The chute channels are relatively conductive coarse-grained sediments intersecting the pointbar. Their existence is confirmed by borehole flowmeter data. They are small geometries; individual chute channels are difficult to pinpoint and trace. Therefore no specific conductivity data are available for the chute channels. Thus, the model value for the chute channels is based on high end values of the field data for pointbar conductivities. Consequently, the model value for the pointbar is biased to the lower end of the field observed pointbar conductivities.

*In situ* measurements of the vertical conductivity ( $K_v$ ) are not available. Likewise, for the chute channel conductivity, an intuitive choice has been made. The  $K_h/K_v$  ratio for the channel and braided sediments, is chosen rather low and close to the ratio found for measurements on core samples for unconsolidated sediments (de Ridder and Wit, 1965). This is motivated by the reworked and, thus, relatively homogeneous nature at that scale of these sandy/gravelly sediments. The pointbar and chute channel deposits represent a more cyclic depositional environment (Reineck and Sing, 1980). Thus, low hydraulic conductivity laminations and intercalations are assumed and in turn result in a low  $K_v$  and a larger  $K_h/K_v$  ratio of 30. The storativity is chosen uniformly at  $1.25 \cdot 10^{-4} \text{ m}^{-1}$ , yielding an elastic storage coefficient of  $1.0 \cdot 10^{-3}$  for the entire eight meter thick aquifer.

### 6.3.2 Results of pumping test model

Figure 6.6 shows the pumping test response of the facies model described in the previous section. Drawdown-curves are given for five observation wells on a circle with

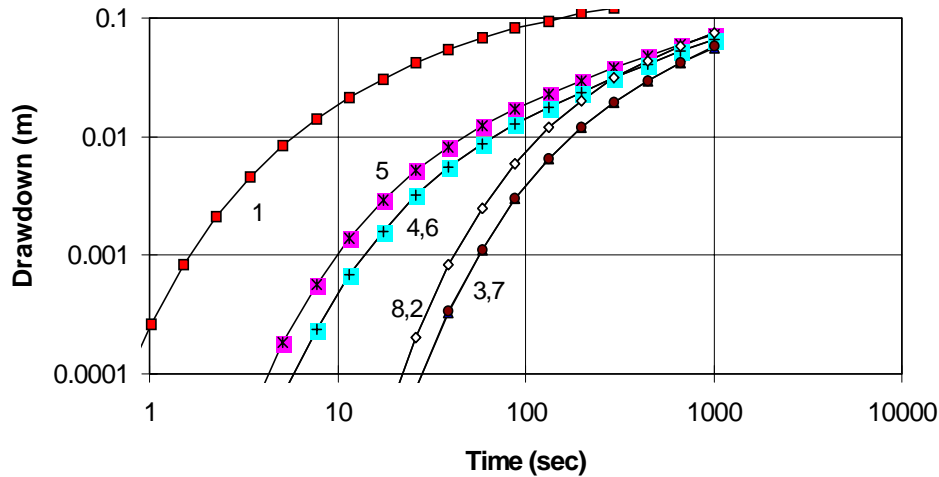


**Figure 6.6:** Drawdown response for 8 observation wells on a circle at  $R = 30$  meters (note that the drawdown-curves are practically identical for Well 2 and Well-8, along with Wells 3 and 7, and Wells 4 and 6).

radial distance 30 meters (see Figure 6.2). Well-1 located in the chute channel shows the earliest onset of the drawdown, followed by the two wells in the main channel (Wells 4 and 5). This difference in onset time of the drawdown-curve, is linked to the connection between pumping well and observation well. For observation Well-1 a direct connection through the very high transmissivity ( $2 \cdot 10^{-2} \text{ m/s}^2$ ), chute channel exists. For Wells 4 and 5 the connection combines the chute channel and the main channel ( $4 \cdot 10^{-3} \text{ m/s}^2$ ). For Wells 2 and 3 the connection consists of relatively low conductivity pointbar and braided material ( $8 \cdot 10^{-4} \text{ m/s}^2$ ).

As a result of different connectivity, a considerable shift occurs in the onset time of the drawdown-curve for the various observation wells. This has interesting implications when a type-curve is fitted. If one does not realize that the aquifer is heterogeneous and the test is of limited duration, it is a typical procedure to fit a Theis type-curve to the field data. The alternatives, such as the radial-composite and linear-composite type-curve (see Sections 2.5 and 4.3), also start out as a pure Theis curve; differences from the Theis curve occur mostly for late-time drawdown. Figure 6.7 shows that for the first 1,000

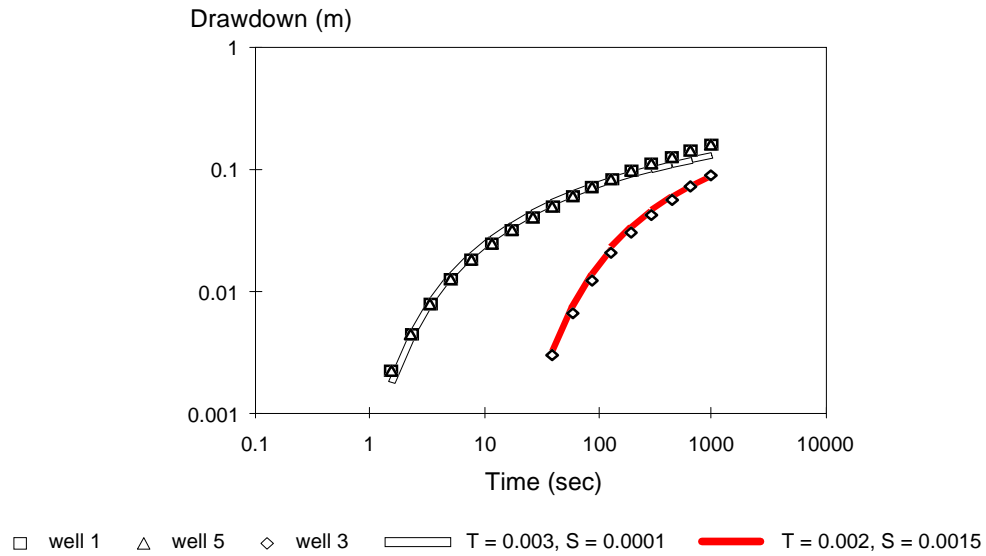


**Figure 6.7:** These curves fitted to early drawdown for curves selected from Figure 6.6.

seconds, appropriate fits can be achieved using a Theis curve. The transmissivity values for the fitted Theis curves only differ by a factor 1.5. However, the storage coefficients obtained from the fitted Theis curves differ by a factor of 15 which is more than one order of magnitude. This range of storage coefficient values reflects the range of the onset time of the drawdown-curve. Thus, this apparent difference in storage coefficients is caused by the modeled heterogeneity which is not recognized by Theis type-curve interpretations. This heterogeneity consists of a high conductivity connection between pumping and observation well.

The apparent differences in storage coefficient resulting from unrecognized heterogeneity when using the type-curve model in interpretation, concur with the results obtained from analyzing the Columbus pumping test data. Section 4.5.3 demonstrates that field data showed a relation between the high conductivity connections between pumping and observation well, and the apparently low storage coefficients indicating a relatively early onset of the drawdown.

### 6.3.3 Results of tracer test model

Figure 6.8 shows cumulative RTD's for five two-well tracer tests. As discussed in Section 6.2.3, the pumped well of these tracer tests corresponds with the pumped well of the pumping tests. The injection wells (see Figure 6.2, Wells 1 through 5 at radial distance  $R = 30$  m) correspond with the pumping tests' observation wells; their drawdown-curves are shown in Figure 6.6. Comparison of the pumping test results and the tracer test results (Figures 6.6 and 6.8), reveals that there is a good correlation between drawdown breakthrough time (time when drawdown first exceeds 0.001 m) and cumulative tracer breakthrough time (time when breakthrough first exceeds a certain percentage). The first response for both pumping and tracer test occurs at Well-1 directly connected to the pumping well by the high conductivity chute channel. For Wells 4 and 5, both drawdown and tracer breakthrough follow approximately one log-time cycle later. After another half log-time cycle, drawdown and tracer breakthrough follow in Wells 2 and 3. Figure 6.9 shows this relation is a simple straight line: increase of logarithmic tracer breakthrough time with an increase of logarithmic drawdown breakthrough time. This relation is valid for times of 5%, 15%, and 50% tracer cumulative tracer breakthrough; but it is not valid for 75% cumulative tracer breakthrough. Thus, the drawdown breakthrough time is an excellent indicator characterizing the first 50% of the tracer breakthrough, in other words the initial and peak breakthrough.

Comparison of Figure 6.8 with the two-well tracer test type-curves (Figure 6.3), reveals that mostly non-dispersive transport occurs. The steep ascent of the curves indicates a virtual dispersion-free front as it breaks through. The differences in initial breakthrough translate mainly in differences in effective porosity, that is when a homogenous isotropic aquifer is assumed. Due to their position outside the main channel, as well as the chute channel, Wells 2 and 3 are the least impacted by heterogeneity. The tracer response at these two wells is very similar to the tracer response for a homogeneous isotropic model (based on the same modeling procedure presented in Section 6.2.2).

For the heterogeneous model, the peak breakthrough of Well-1 is at approximately five days, thus it is earlier by a factor of 20 than that of the homogeneous model. This shift in peak breakthrough for this heterogeneous case, indicates that the effective

porosity is smaller by a factor of 20 than that of the bulk drainable porosity. Therefore, if the connected bulk drainable porosity, for example, is 30%, the observed effective porosity for this heterogeneous case would be 1.5%. Thus, channeling through heterogeneous pathways that only make up a fraction of the aquifer, causes an apparent reduction of effective porosity when interpretations are based on a homogeneous isotropic model. The apparent differences in effective porosity for the different tracer tests conducted in the same heterogeneous aquifer, indicate that for different well-pairs, flow is channeled through different fractions of the aquifer.

The relative flattening of the cumulative breakthrough for Well-4, indicates a slowdown of breakthrough pace relative to the homogeneous solution. It indicates the presence of two systems: one with a relatively rapid breakthrough; and the other with a slower system. The rapid system has streamlines through the better conductive channel. The slower system has streamlines through the low conductive pointbar. All these observations concerning the time of initial breakthrough and the shape of the

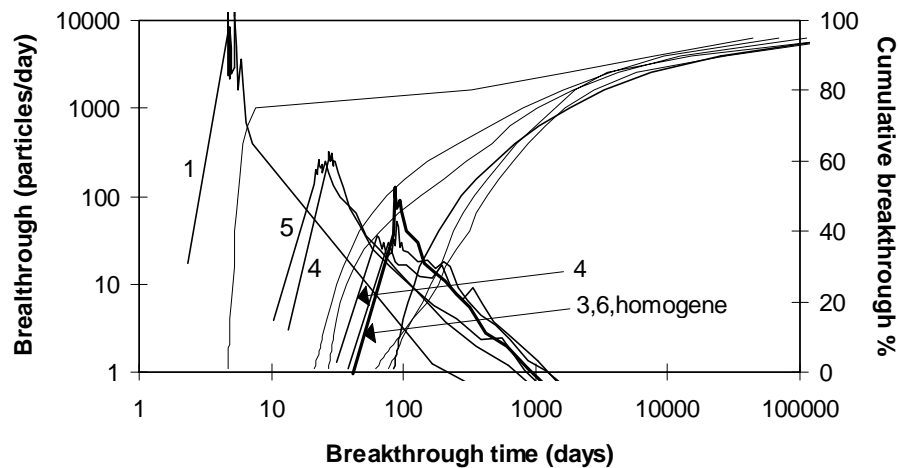


**Figure 6.8:** Cumulative breakthrough for five two-well tests in facies model (numbers indicate wells where tracer is injected). The breakthrough curve for Wells 2 and 3 are practically equivalent to breakthrough curves modeled for a homogeneous aquifer.

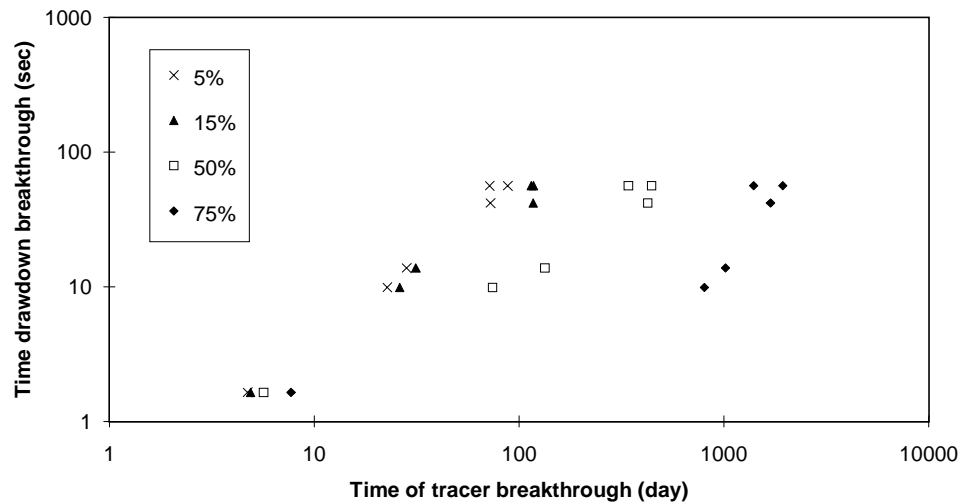


**Figure 6.9:** Cumulative tracer breakthrough versus drawdown breakthrough.

breakthrough curve, are fully consistent with the conductivity patterns from the facies model. It is obvious that in this case, it is senseless to determine macro-dispersion as an effective property. Along the same line, it is senseless, considering the effective porosity as an aquifer property determined from a tracer test, rather than a correction for undescribed heterogeneity.

No attempt was made to replicate the breakthrough data observed during the large-scale, 5-spot, tracer test (Section 3.4.3). However, on a qualitative basis the responses shown in Figure 6.8, compare reasonably well with breakthrough patterns observed during that test (see also Figure 3.13). In the model, the first well, located in the highly conductive chute channel, breaks through after a few days. The second group of model wells, located in the more permeable channel, break through somewhat later (around 20 days). The third group of model wells, located on the low conductive pointbar, does not break through until approximately 100 days. The field data show: after about two days, the northwest (NW) corner well broke; at two and a half days (2.5) the opposite (SE) corner was approached by tracer front visible in intermediate wells; and the two other corners (NE and SW) were far from breakthrough at the end of the seven day monitoring.

**Table 6.2:** Input parameters for object model of chute channels embedded in pointbar (also see Figure 6.10).

	Width (m)			Length (m)			Azimuth	
	Min	Min	Tolerance	Min	Min	Tolerance	Min	Max
Case 1	3	6	1.5	20	30	5	45 NE	135 SE
Case 2	5	10	2.5	40	60	10	45 NE	135 SE

<sup>1</sup> Minimum (min) and maximum (max) of uniform distribution range from which the width and length are sampled.

<sup>2</sup> Tolerance specifies the minimum clearance between the pumping well and the edge of an individual channel .

Thus, the very skewed pattern of sudden breakthroughs at significantly different times, is reasonably well reproduced. The difference in absolute values between the model and the field data, can, in part, be explained by the higher injection rate in the field, along with the different geometry modeled for the 5-spot field tracer test versus the four independent two-well tracer tests.

#### 6.4 A LOCAL OBJECT MODEL FOR CHUTE CHANNELS

From Section 4.5 one or more chute channels embedded in a pointbar matrix, emerges as a good and simple conceptual model explaining the apparent variability of storage coefficients obtained from interpretation of pumping tests conducted at the Columbus 1-HA test site. As a first step towards geostatistical generalization, a simple object model (Section 2.3.2) for modeling pumping test is presented.

##### 6.4.1 Description of the heterogeneity model

A computer program was developed to generate MODFLOW input for four rectangular chute channel bodies (objects) with one per layer. All these channel objects cross the pumping well. The dimensions (length and width) and the direction of the sand bodies, are randomly selected from a uniform distribution that specifies ranges. The height is fixed to one model layer (2 m). Figure 6.10 shows a schematic plan view of the

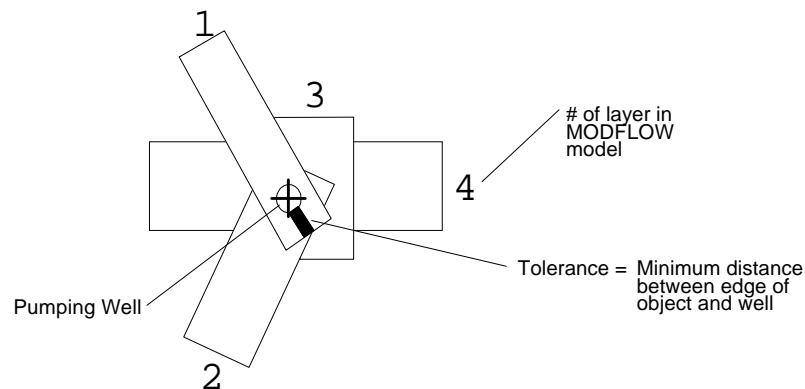


**Figure 6.10:** Schematic plan view of object model.

resulting geometry and the definition of the input parameters. Table 6.2 shows the input data for two analyzed cases. Each chute channel object is assigned a constant conductivity of  $10^{-2}$  m/s; the pointbar matrix is assigned a constant conductivity of  $10^{-4}$  m/s (see Table 6.1). For both cases, five different realizations were created by varying only the random number sequence used to select the channel objects' geometrical parameters (see Figure 6.10 and Table 6.2). Thus, each realization represents a statistically equi-probable architecture of four chute channel bodies intersecting the pumping well.

#### 6.4.2 Results of pumping test model

Figure 6.11 shows the drawdown response for a single realization of Case-1 for the local object model. The drawdown is plotted for several circles of observation wells (see Section 6.2.3 and Figure 6.2). For a radial distance of 10 meters, the early part of the drawdown-curves spread out over approximately 1.5 log-cycle. As demonstrated previously, observation wells penetrating chute channels show a quicker response than those not penetrating chute channels. When interpreted with the Theis method (while ignoring heterogeneity), this translates into apparent storage coefficients ranging over

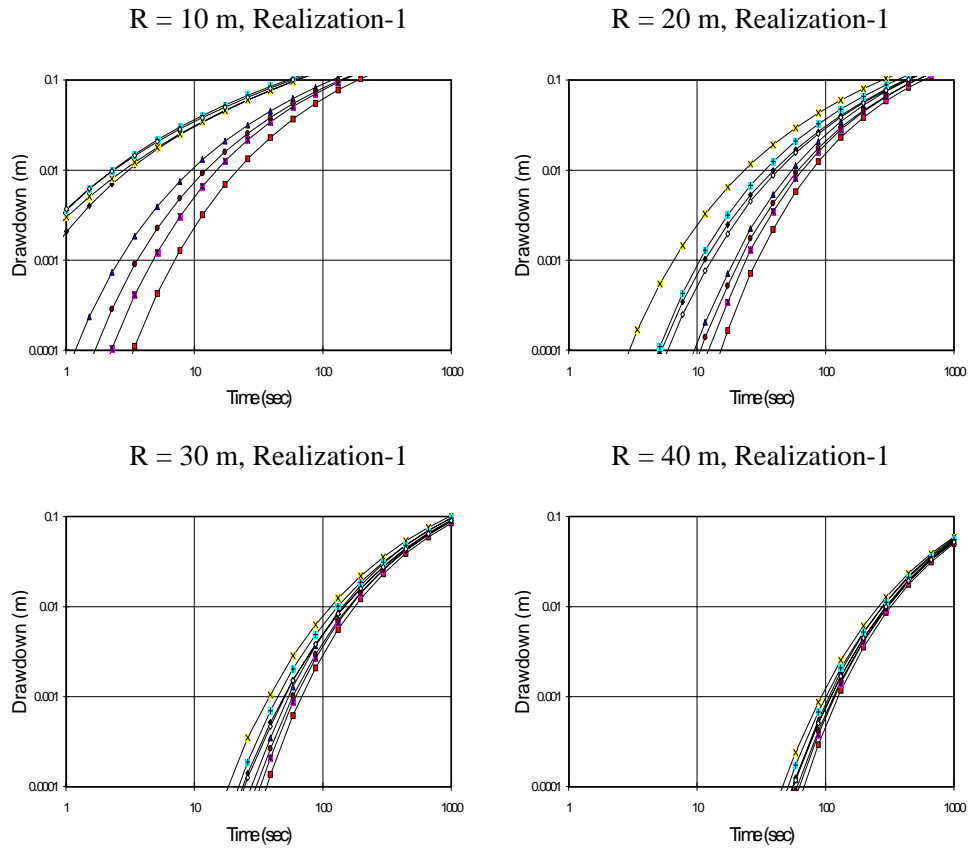


**Figure 6.11:** Drawdown for wells at radial distance 10, 20, 30 and 40 meters for Realizations-1 of the Boolean model (Case-1).

nearly two orders of magnitude (see also Section 6.3.2). For increasingly large radial distances, this range of early-time drawdown response diminishes. For radial distances of 30 meters and larger, the range is practically negligible. A single storage coefficient value would be the result of fitting these curves to all drawdown responses. This 30 meter threshold coincides, not surprisingly, with the maximum length of the high, hydraulic conductivity, chute channels.

Figure 6.12 presents the results for observation Wells 1 and 2 (respectively at azimuth 90 E and 45 NE) for five different realizations of Case-1. The time range for the

drawdown onset is comparable to the range observed on a circle around the pumping well within a single realization. Figure 6.13 shows results for wells on a circle within a single realization of Case-2. For radial distances of 40 and 50 meters, a considerable range of early-time drawdown responses still occurs; it is much more than shown in Figure 6.11 for Case-1. This is the result of the larger lengths of the chute channel bodies (up to 60 meters) used in this case. These larger lengths translate into a larger probability that observation wells at large distances are directly connected by a high conductivity pathway to the pumping well.

Thus, these two "random chute channel" models predict a trend for the range of onset time for drawdown, versus the radial distance of observation well. This trend reflects whether a high conductivity object (chute channel) connects the pumping well and the observation well. If analyzed using a Theis curve (still ignoring heterogeneity), this range of onset time translates into a range for the apparent storage coefficient<sup>2</sup>. For small radial distances, a large range (more than one order of magnitude) of apparent storage coefficients, is predicted by the model (see Figure 6.11). For radial distances larger than the unit heterogeneity length, all drawdown-curves indicate approximately the true value for the storage coefficient that is input to the flow model. This trend for apparent storage coefficient, versus radial distance (for Case-1 with an object length of about 30 meters), can be compared to a similar trend obtained from the pumping tests conducted at the 1-HA test site (Figure 4.13).

As discussed in Section 6.2.3, the observation wells are nests consisting of four piezometers penetrating the four model layers. At a greater distance from the well, it is unlikely that for each model layer a chute channel crosses a piezometer at a single location. Thus, a different drawdown response may be expected along the vertical of an observation well (piezometer nest in the model). Figure 6.14 shows for a single realization of Case-1, the vertical difference (maximum drawdown difference between

---

<sup>2</sup> Strictly spoken, conventional interpretation in disregard of the heterogeneity would result in a high diffusivity (high ratio transmissivity/storage). This reflects partly the heterogeneous reality of a highly conductive zone between pumping and observation well. Fitting a Theis (or related analysis), however, biases the transmissivity estimate towards the late-time period of the pumping test and the storage estimate towards the early-time part of the pumping test. Therefore a bundle of curves converging to a similar late-time response (see figure 6.13 and 6.14 at  $R = 40$  m) results in fairly similar transmissivities and dissimilar storage coefficients.

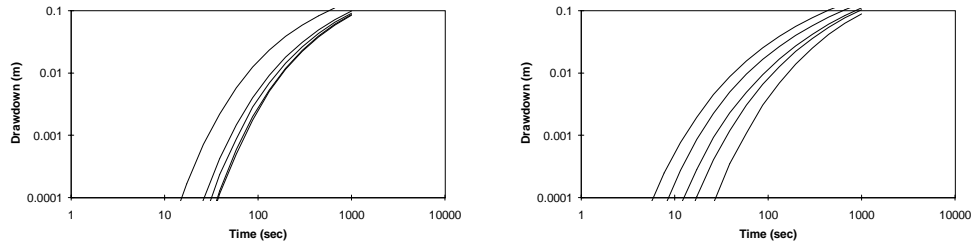


**Figure 6.12:** Pumping test response of Well-1 (left) and Well-2 (right) both at the same radial distance ( $R=20$  m) for 5 realizations of object model Case-1.

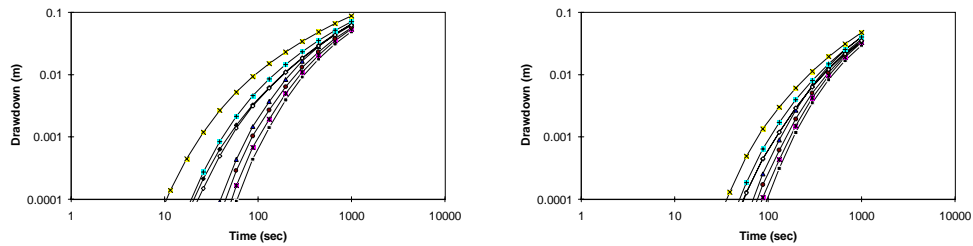


**Figure 6.13:** Pumping test response for circles at  $R = 40$  m (left) and  $R = 50$  m (right) for a single realization of object model Case-2.

two layers of the model) at the location of observation well nests with a radial distance of 20 meters.

Vertical gradients develop with different magnitudes and different timing. The differences result from the presence and/or absence of a chute channel at or near a certain observation nest. If the observation nests are, in reality, fully penetrating wells (as is the case at the Columbus 1-HA test site), then vertical flow in the well-bore can be expected. This vertical flow, occurring in some wells and not in others, has indeed been observed during borehole flowmeter surveys conducted during the pumping tests at the Columbus 1-HA test site. It should be noted that this vertical flow also occurs in solutions for multi-layer confined aquifers (Streltsova 1972 and 1988) and in the related Neuman (1975) delayed gravity drainage solution for unconfined aquifers. In these solutions, however, vertical flow occurs only at intermediate-time and disappears during late-time. For the random chute channel model and after an initial phase, the vertical flow is steady state,

even at times beyond 1,000 seconds (the maximum time shown in Figure 6.14). Thus, persistent vertical flow in observation wells is an excellent indicator for heterogeneity at or close to the observation well and/or pumping well.

### 6.5 A GAUSSIAN MODEL FOR A COARSE-GRAINED POINTBAR

As a further geostatistical generalization, aquifer models are used with conductivity values that vary from cell to cell. The conductivity is generated as a random variable following a Gaussian spatial distribution with a given covariance (also see Section 2.3.1). The conductivity grids are generated using the sequential simulation program published by Deutsch and Journel (1992). The essential parameters used to create these grids, are the correlation range (length of lateral continuity) and the distribution of the conductivity values. As shown in Chapter 5, the correlation range is especially difficult to quantify from field data. Thus, geological expertise must be included when choosing a value for this parameter. In the case discussed below, several different, lateral continuity options are included for the correlation range. These options reflect uncertainty inherent in incomplete geological knowledge

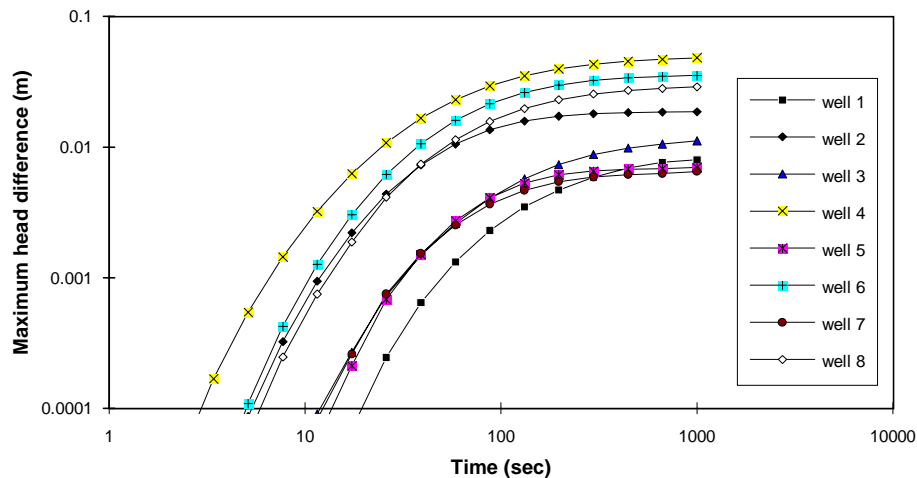


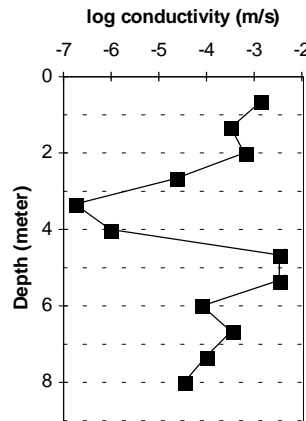
Figure 6.14: Maximum vertical head difference within observation wells (nests).

**Table 6.3:** Variogram parameters for variogram options of Gaussian model.

Variogram option	Correlation range of spherical variogram (m)			Realization
	hor - NS	hor - EW	Vertical	
Option 1	25	5	1.6	1 - 4
Option 2	10	5	1.6	5 - 8
Option 3	10	10	1.6	9 - 12
Option 4	5	5	1.6	13 - 16

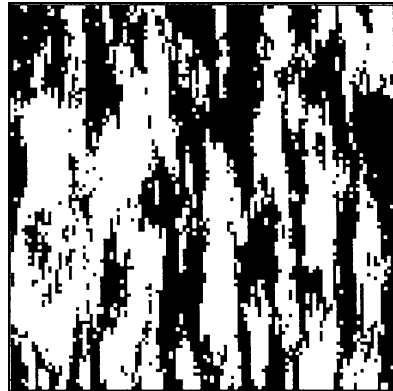
### 6.5.1 Description of the heterogeneity model

A spherical variogram is used to generate Gaussian conductivity distributions conditioned by the vertical (well) conductivity profile shown in Figure 6.15. The average conductivity is  $10^{-4}$  m/s while the standard deviation for the  $^{10}$ logarithmic conductivity is 1.25. Table 6.3 presents four options for the range length used to represent uncertainty with regard to lateral continuity. The minimum conductivity is approximately  $10^{-8}$  m/s, in other words 99% of the conductivities is larger than  $10^{-8}$  m/s. On the high end, all values above  $10^{-1}$  m/s (about 3% of all values), are set to  $10^{-1}$  m/s. Figure 6.16 shows an example

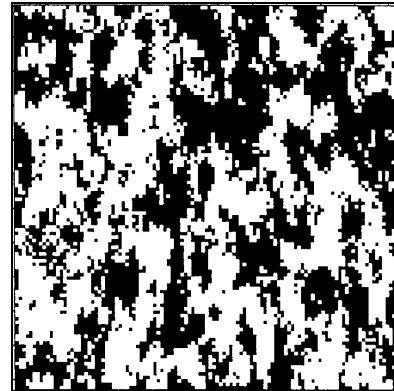
**Figure 6.15:** Conductivity profile used to condition Gaussian model.

of a conductivity pattern (a layer of a realization) for each of the different, lateral continuity, variogram options. Thus, sixteen (16) realizations (four for each of the four options), are available and reflect a broad spectrum of aquifer variability. For each option four different realizations reflect the variability remaining after fixing the variogram.

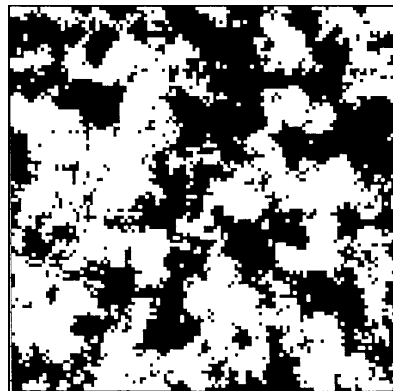
Variogram Option-1, Realization-1



Variogram Option-2, Realization-5



Variogram Option-3, Realization-9



Variogram Option-4, Realization-13

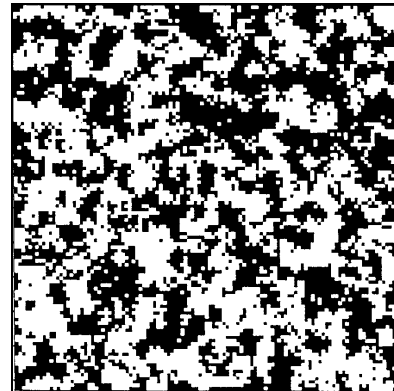


**Figure 6.16:** Gaussian random fields for hydraulic conductivity. The black area represents the 30% highest conductivity values. Variogram Options 1-4, Realizations 1, 5, 9, 13, respectively (also see Table 6.3).

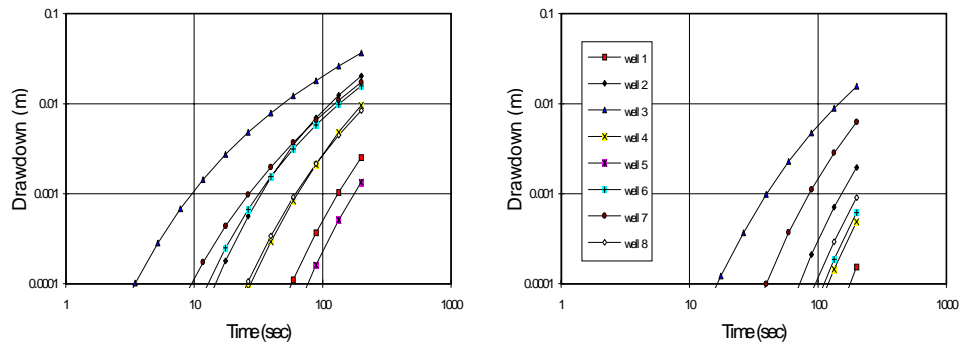
### 6.5.2 Results of pumping test model

For this case, both a modeled multi-well pumping test and a single-well pumping test have been evaluated. The evaluation of the multi-well pumping test is similar to what has been presented in previous sections of this chapter. This evaluation focuses on the possibility of establishing a relation between the multi-well pumping test response and heterogeneous high conductivity connections between the pumping well and observation wells. The purpose of evaluating a single-well pumping test is to assess the possibility of establishing a local, “near well”, transmissivity value. This “near well” transmissivity is an important parameter when calculating conductivity values using the borehole flowmeter method (see also Section 2.5.1).

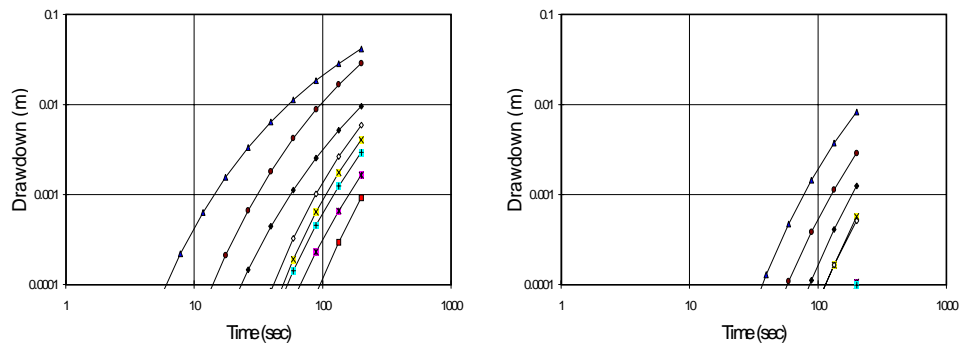
#### *Multi-well pumping tests*

Figure 6.17 shows the drawdown response for two circles of observation wells ( $R = 30$  m and  $R = 50$  m, see Section 6.2.3 and Figure 6.2) for three realizations. Early drawdown response at these radial distances exhibits the same variability of onset time as Case-2 of the previously discussed object model. In contrast to Case-1 of the object model, observation wells at a radial distance much larger than the correlation length of 50 meters, exhibit connections to the pumping well by continuous high conductivity flowpaths. For example, Realization-16 represents variogram Option-4 with the smallest (5 meters) lateral continuity (correlation length). Nevertheless, observation wells at a radial distance of 30 meters and 50 meters, show quite a variability of responses. This indicates that persistent heterogeneity is present and the aquifer does not act as an equivalent homogenous aquifer. Figure 6.16 provides an explanation of this concept. The black shaded area represents the highest 30% of conductivities; it forms continuous flowpaths with lengths occasionally exceeding 50 meters. This concept of connected flowpaths determining the pumping test response, is discussed in greater detail for single-

Realization-1 (variogram Option-1)



Realization-2 (variogram Option-1)



Realization-16 (variogram Option-4)

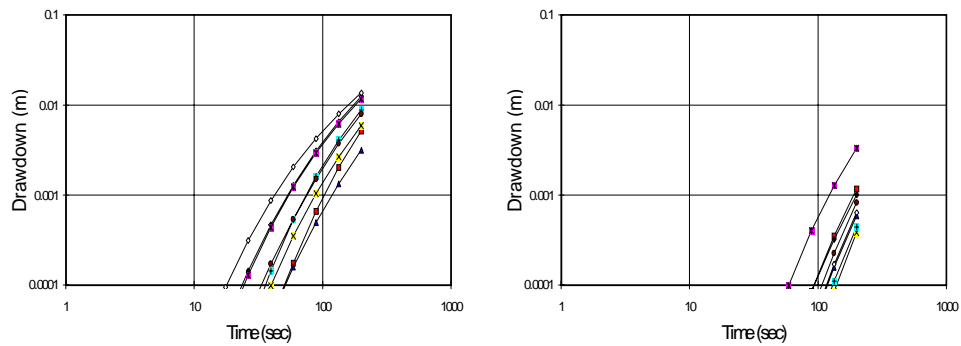


**Figure 6.17:** Drawdown response at a radial distance of 30 meters (left) and 50 meters (right) for Realizations 1, 2, and 16 of the Gaussian model

well tests conducted in a petroleum reservoir surrounded by four closed boundaries (appendix A).

Figure 6.17 shows that when a sufficient number of wells is available (e.g. sixteen (16) wells on two circles each with different radial distances), the drawdown response can be uniquely related to the variogram option. With a limited number of observation wells available, however, the discrimination among variogram options becomes less straightforward (Figure 6.18). For example, the drawdown response of Well-1 of Realization-4 of variogram Option-1, is practically duplicated by wells for the other

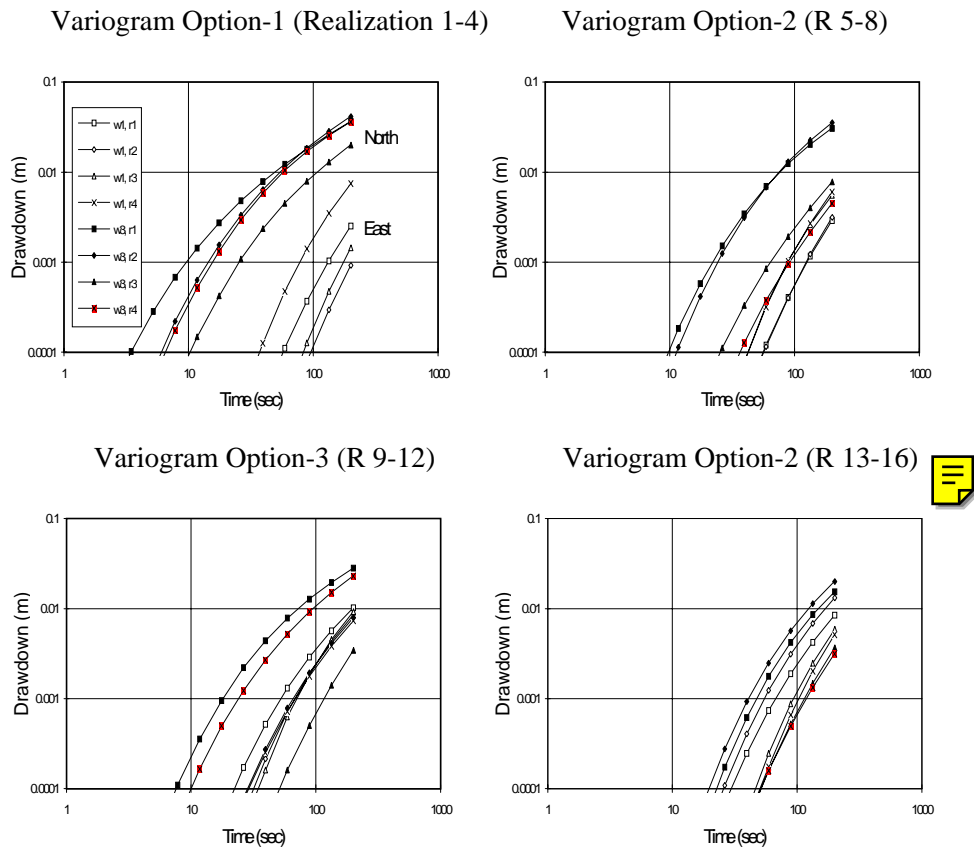


**Figure 6.18:** Drawdown response at Wells 1 and 3 (respectively east and north of the pumping well at a radial distance of 30 meters, see Figure 6.3).

realizations of other options. Thus, for significant uncertainty reduction with respect to the variogram option, it is obviously necessary to have drawdown data from more than one observation well.

#### *Single-well pumping tests*

Figure 6.19 shows for three selected realizations both the drawdown at the pumping well and the drawdown derivative (Cooper-Jacob slope). Similar to the Columbus field observations, the Cooper-Jacob slope varies significantly (see Section 4.4 and Young, 1995). Therefore, strictly speaking, the application of the Cooper-Jacob method is inappropriate and more complex models should be applied (see Section 2.5.1). As discussed in Section 4.4, however, the Cooper-Jacob method is useful in diagnosing conductivity variability around a pumped well. Moreover, in most practical applications, a single straight line will be fitted, assuming field data accuracy does not warrant a more detailed investigation. One of these practical applications is determining a transmissivity that is subsequently used to determine larger conductivities by pro-rating layer flow rates measured with the borehole flowmeter (see Section 2.5.3). These (infinite-) layer conductivities are subsequently used to determine the spatial variability of a heterogeneous conductivity field (e.g. Moltz et al. 1989, Rehfeldt et al., 1992).

It is important to assess the uncertainty and error introduced by the transmissivity variability around the pumped well, which for all realizations has exactly the same conductivity profile (Figure 6.15). The minimum and maximum Cooper-Jacob slope are, respectively 0.05 m/s and 0.15 m/s. The pumping rate is 0.003 m<sup>3</sup>/s. Thus, the transmissivity ranges from 3.3 10<sup>-3</sup> m/s to 1 10<sup>-2</sup> m/s. The true transmissivity (the sum of the individual layer conductivities) of the well is 1 10<sup>-2</sup> m/s. Thus, for the same vertical profile of conductivity, the surrounding heterogeneity introduces an uncertainty (error) of a factor of 3 in transmissivity as determined from a single-well pumping test. The lower pumping test transmissivity value concurs with (see Section 2.4.1) a power-exponent weighted sum of the well conductivities. A power-exponent of 0.3 correctly relates, in this case, the point-support-scale conductivities to the single-well test transmissivity. This is the same value that relates the small-scale, borehole flowmeter conductivities to the transmissivity value obtained from the large-scale, multi-well pumping test (Section 5.3).

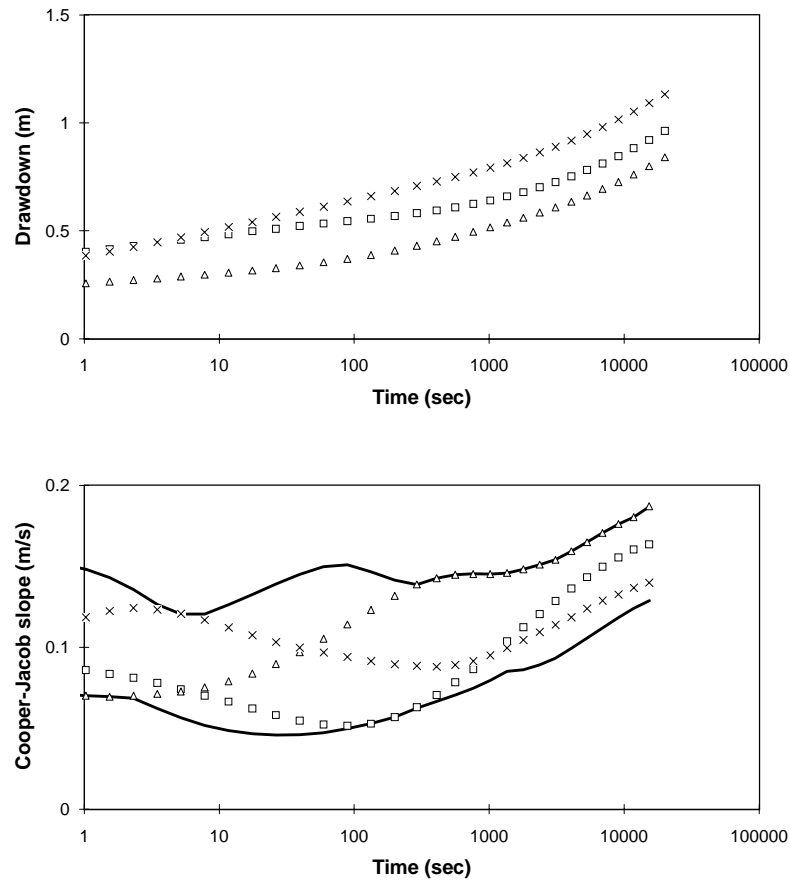


**Figure 6.19:** Results of a single-well test for Gaussian model. Upper diagram: Cooper Jacob (semi-log) plot for 3 selected realizations. Lower diagram: Evolution of the derivative (Cooper-Jacob slope) during the test (solid lines denote upper and lower limit of slope for all 16 realizations).

The higher pumping test transmissivity value is the arithmetic summation of the well's conductivity profile.

These findings indicate that borehole flowmeter conductivities obtained by arithmetic proportioning of a pumping test transmissivity (Moltz et al., 1989; Rehfeldt et al., 1992), must be treated with care. These measurements are an excellent indicator for heterogeneity, but do not represent the point-support-scale. Within a single-well,

conductivity contrasts are measured with an accuracy related to the borehole flowmeter's sensitivity. However, comparing borehole flowmeter values from different wells potentially introduces an error. This error is introduced by the impact of heterogeneity on the interpretation of the single-well test used to determine the borehole flowmeter conductivities. As shown above the true point-support-scale conductivity, can be underestimated for this case by a factor of 3. Thus, when using borehole flowmeter conductivities for a spatial analysis, these values should not be considered as point-support-scale conductivity measurements.

### 6.5.3 Results of tracer test model

For each of the sixteen realizations of the Gaussian model, eight, two-well tracer tests were modeled. As discussed in Section 6.2.3, the pumped well and the injection wells, respectively, coincide with the pumped well of the modeled pumping test and with the observation wells in a circle at radial distance 30 meters (also see Figure 6.2). Figure 6.20 shows the results for injection Well-1 (for locating that well, see Figure 6.2) over sixteen realizations. The time of first (5%) breakthrough varies from 30 days to 200 days.

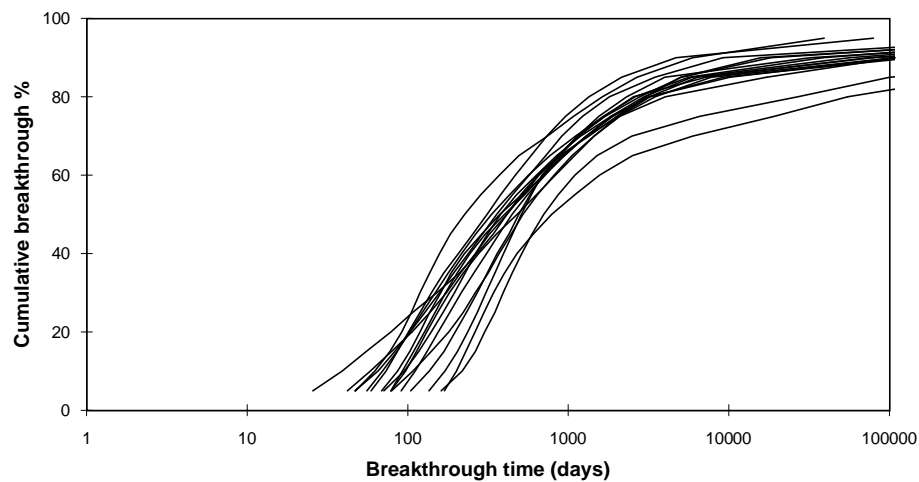


**Figure 6.20:** Tracer test results for Well-1 to central pumping well for 16 realizations.

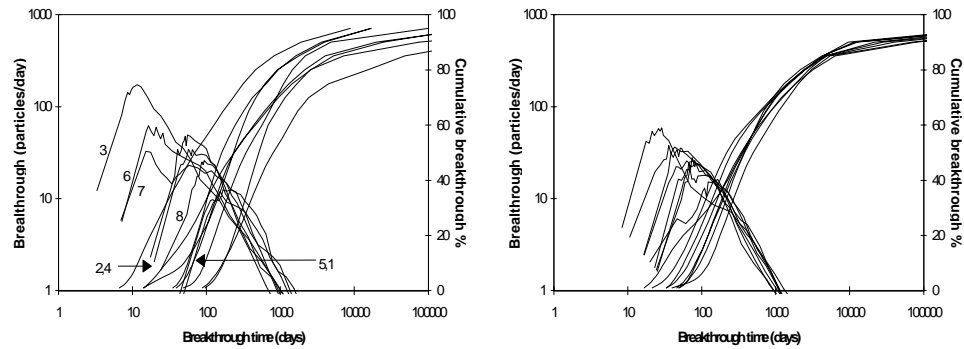


**Figure 6.21:** Concentration and cumulative breakthrough for 8 wells at  $R = 30$  m (Left: Realization-1, variogram Option-1; Right: Realization-16, variogram Option-4; horizontal axis depicts breakthrough time in days)

The tail end of the cumulative breakthrough curve also shows considerable variation. For most of the realizations 75% of tracer breakthrough occurs between 800 and 2,000 days. Some of the realizations show a substantial amount of tracer residing for a very long time in the system, and 75% of tracer breakthrough is only reached at 7,000 days.

Figure 6.21 shows comparable variability of tracer response for eight different, two-well tracer tests within two single realizations. Realization-1 (Figure 6.21, left) represents variogram Option-1, the strongly anisotropic, spatial, conductivity distribution. Note that the wells showing relatively rapid breakthrough, are wells in the direction of the anisotropy (Wells 3, 6 and 7). However, not all wells in a similar direction compared to the anisotropy, show the same early breakthrough (compare for example the breakthrough of Wells 3 and 7, and Wells 2/4, 6 and 8). Thus, a significant difference occurs with respect to the connection between the injection well and the pumping well for those wells having a symmetric position with respect to both the pumping well and the spatial structure. Note that both Wells 6 and 7 exhibit a double or prolonged peak. Well-6 is in a symmetric position with respect to Well-2; apparently no high conductivity connection occurs between this well and the pumping well, in turn causing the breakthrough to be later and more dispersed than the breakthrough in Well-2. The connection between Well-6 and the pumping well causes earlier, but more dispersed, tracer breakthrough than the breakthrough in the symmetrically equivalent wells (Wells 2, 4 and 8). Apparently the

connection between Well-6 and the pumping well is characterized by a higher conductivity than the connections between these last three wells (Wells 2, 4 and 8) and the pumping well. Realization-16 (Figure 6.21, right) represents variogram Option-4, an isotropic, short-range, spatial, conductivity distribution. The peak travel time variation is limited to only 0.5 log-cycle. Two of these wells show a prolonged peak, while the other six wells have an essentially similar response.

The response of Realization-1 (Figure 6.21, left) represents, to some extent, the pattern of breakthroughs observed in the field for the large-scale, 5-spot, tracer test conducted at the test site (see Section 3.4.3). Initial and peak breakthroughs vary from several days (for Well-3) to ten (10) days (Wells 6 and 7) with more than 50 days for other wells. The response of Realization-16 (Figure 6.21, right) clearly does not match the breakthrough pattern observed in the field during the 5-spot tracer test conducted at the test site. The first well shows tracer breakthrough at 20 days, and breakthrough for all other wells comes later and relatively uniformly within a short time span (between 50 and

**Table 6.4:** Breakthrough data and dispersivities for Realization-1, Wells 1-8.

Well	$T_{\text{peak}}$	$C_{\text{peak}}$	$T_{5\%}$	$T_{15\%}$	$T_{50\%}$	$T_{15\%}/T_{5\%}$	$T_{50\%}/T_{5\%}$	$\alpha_L$	$\phi_{\text{eff}}/\phi_{\text{bulk}}$	dd-bt
1	150	12	129	204	505	1.5	3.9	6	1.2	657
2	55	50	47	64	162	1.4	3.5	3	0.4	167
3	12	180	9	14	70	1.5	7.4	3	0.1	48
4	60	33	53	79	238	1.5	4.5	6	0.5	320
5	160	11	126	211	804	1.7	6.4	10	1.3	883
6	18	60	20	42	237	2.0	12	>15	0.1	160
7	18	30	27	66	234	2.5	8.8	>15	0.1	133
8	95	25	77	112	343	1.4	4.4	3	0.8	308

$T_{\text{peak}}$  = breakthrough time of peak of tracer concentration (days)

$C_{\text{peak}}$  = concentration of peak of tracer breakthrough (particles)

$T_{n\%}$  = time of cumulative breakthrough of n% of tracer (days)

$\alpha_L$  = longitudinal dispersivity (m)

$\phi_{\text{bulk}}$  = bulk porosity

$\phi_{\text{eff}}$  = effective porosity

dd-bt = drawdown breakthrough (days), i.e. drawdown exceeds 0.01 m (see Figure 6.17)

75 days).

Dispersivities are estimated by comparing the tracer test type-curves (Figure 6.3) and the modeled breakthrough (Figure 6.21, left diagram). Accurate determination of dispersion values is difficult for many of the tracer tests results (breakthrough curves 2, 4, 3, 6 and 7). This problem of estimating dispersion is similar to what is usually encountered when interpreting field data, and in a way the problem confirms the realism of the heterogeneous models.

Table 6.4 presents an overview of the values determined from the breakthrough curve. The effective porosity is directly calculated from the time of peak breakthrough. For this calculation, a peak breakthrough time for the homogeneous case of approximately 125 days is assumed (see also Figure 6.9). The values larger than 1 for the ratio effective porosity divided by bulk porosity (Table 6.4 second column from the left) are obviously unrealistic. These are caused by misreading of the (unclear) peak breakthrough time. The dispersivity values are estimated by visually comparing the modeled curves with the type-curves. Note the good coherence between the time of peak breakthrough and the time of 15% cumulative breakthrough (also see Figure 6.4). Neither the ratio  $T_{15\%}/T_{5\%}$  nor the ratio  $T_{50\%}/T_{5\%}$  ranks the dispersivity perfectly. Only an order of magnitude can be estimated for dispersivity. The last column of Table 6.4 confirms that the time of drawdown breakthrough from a multi-well pumping test, is an excellent estimator for effective porosity.

In summary, the breakthrough curves are not very well characterized by dispersion. Effective porosity does not at all appear to be an overall aquifer property. The tracer tests involving different well-pairs in the same aquifer realization, exhibit large differences in effective porosity. Effective porosity appears to be the most important parameter to assess (high hydraulic conductivity) inter-well connections determining the tracer breakthrough characteristics.

As previously demonstrated for the facies model and the object model, drawdown breakthrough is very distinctive for tracer breakthrough. The last two columns of Table 6.4 confirm the relation between drawdown breakthrough and tracer breakthrough for Realization-1 of the Gaussian model. Figure 6.22 shows that this relation holds very well

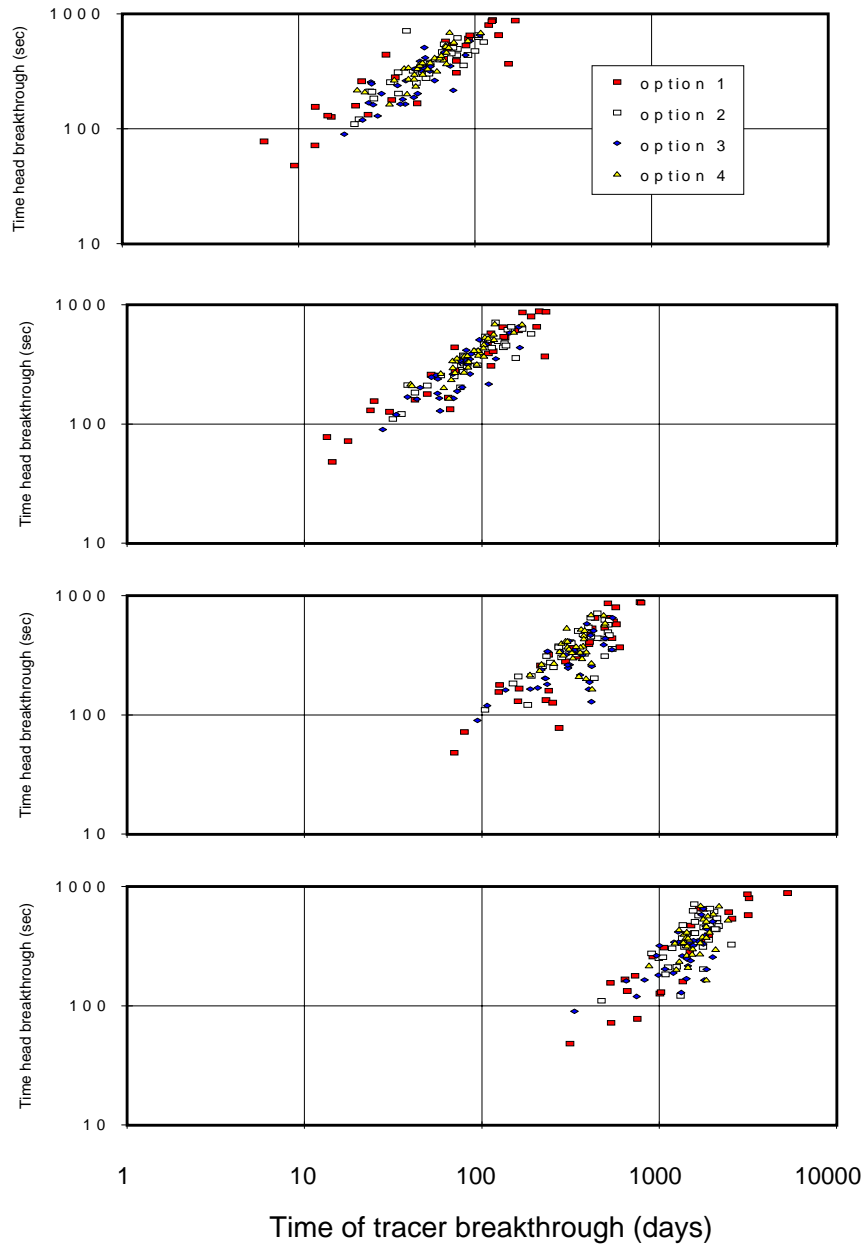


**Figure 6.22:** Head (drawdown) breakthrough versus tracer breakthrough at respectively 5%, 15%, 50% and 75% cumulative breakthrough.

for the 128, two-well tracer tests investigated for the 16 realizations of Gaussian model. For the lower percentiles of tracer breakthrough (5% and 15% cumulative) the correlation appears to be very good. For the higher percentiles (the tail of the breakthrough distribution, i.e. 50% and 75% cumulative breakthrough) the correlation is still there, but less perfectly. Initial breakthrough time ranges from six (6) days to 170 days, covering nearly 1.5 cycle of log-time. Late breakthrough (75% cumulative) ranges from 300 to 6,000 days. A significant number of tracers tests exhibit residence times of 2,000 days or more for the last 25% of tracer injected. These cases especially occur for the highly anisotropic variogram Option-1. The scatter of drawdown versus tracer breakthrough, gives an error of roughly 0.25 cycle of log-time when the drawdown breakthrough is used to predict tracer breakthrough. Thus, drawdown behavior is not an ideal predictor of transport. However, knowing the drawdown breakthrough greatly reduces the uncertainty range of tracer breakthrough by a factor of 6.

For all 128 tracer tests, Figure 6.23 explores in more detail the relation between the time of cumulative breakthrough respectively 5% and 50% (also see  $T_{5\%}/T_{50\%}$  column in Table 6.4). The log-time lag (ratio) between these two cumulative breakthrough times,

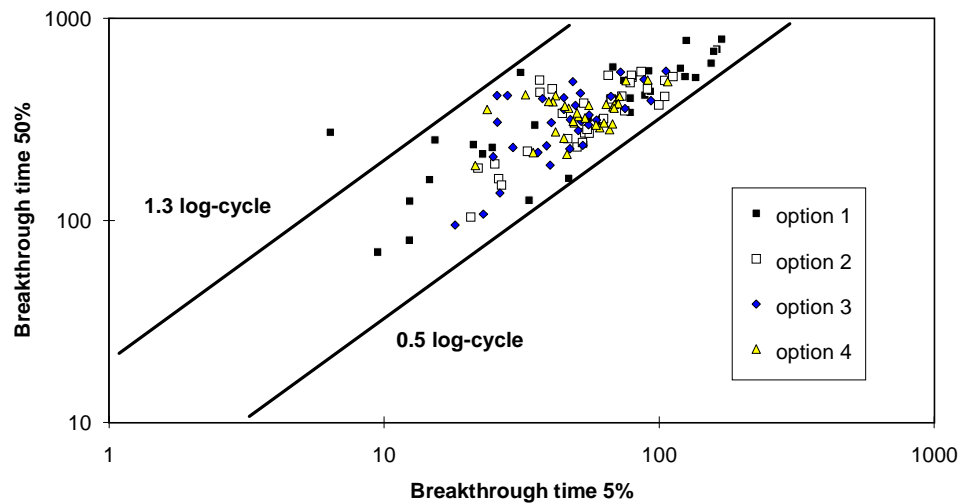


**Figure 6.23:** Dispersion of time lag between 5% and 50% cumulative breakthrough.

ranges from a quarter log-cycle (small dimensionless dispersivity) to three-quarters of a log-cycle (see also Figure 6.4). If the differences between breakthrough curves are only caused by a difference of effective porosity, all points would be on the same line. The diagonal lines in Figure 6.23 are these lines of equal time lag, and thus, equal dispersivity. From Figure 6.4 it can be inferred that the 0.5 log-cycle time lag represents a dispersivity of two meters (2 m) (dimensionless dispersivity of 0.07), while the 1.3 log-cycle log-time lag respectively represents a dispersivity between 15 meters and 30 meters (dimensionless dispersivity between 0.5 and 1). These estimates concur well with the estimates from the type-curve analysis presented in Table 6.4.

Macro-dispersivities (discussed in Section 2.4.2) can be calculated on the spatial conductivity distribution parameters used as input for the Gaussian model (Equation 2.5). Note, however, that these calculations are only approximations, because the distribution parameters greatly exceed the small conductivity range values for which the theory has been derived. The values calculated are:

- macro-dispersivity of 75 m for range 25 m (Option-1)
- macro-dispersivity of 30 m for range 10 m (Option-2 and Option-3)
- macro-dispersivity of 15 m for range 5 m (Option-4)

Only the calculated macro-dispersivity value for Option-4 is observed as an upper limit value for some tracer tests modeled for realizations of this specific option. None of the other calculated macro-dispersivities matches with results derived from the modeled tracer tests. One reason is the large range of conductivity values, larger than is justified based on theoretical considerations (also see section 2.4). Additionally the flow field is not linear and does not cover a sufficient amount of macro-dispersion lengths for the first three options. Thus, as expected from the theory, macro-dispersion is not a particularly useful parameter in describing transport for the type of problem as described in this section.

Figure 6.24 shows the vertical distribution of tracer breakthrough at the central well for all modeled, 128, two-well tracer tests. Note that the vertical conductivity profile of this well is exactly identical (the “conditioning well”) for all realizations. Additionally, the ensemble of all grid conductivities statistically matches this well (same average and standard deviation). For all realizations nearly all tracer breakthrough occurs at the two

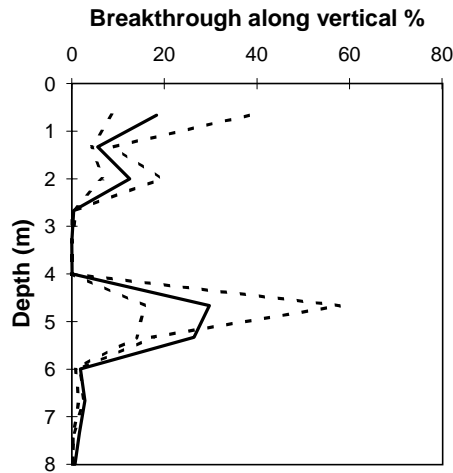


**Figure 6.24:** Percentage of tracer breaking through at different depth intervals. Solid line is average for 128 tests (in 16 realizations). Dashed lines denote extreme cases.

high conductivity intervals (depth of 1-3 meters and depth of 4-6 meters). On the average the lower interval is twice as productive as the higher interval. The maximum case for the upper interval (minimum case for the lower interval) indicates 60% of tracer breakthrough in the upper interval with 40% in the lower interval. Conversely, the maximum case for the lower interval indicates 80% of tracer breakthrough in the lower interval and only 20% in the upper interval. For both the upper and lower intervals, there is a factor of about 3 between the minimum and maximum cumulative breakthrough.

## 6.6 A NESTED-FACIES GAUSSIAN MODEL

The Gaussian models discussed above are a global approximation for conductivity heterogeneity. Only the range and, to a much more limited extent, the variogram type and anisotropy offer the possibility of relating a model to a certain type of sedimentological heterogeneity. The previously discussed facies model is a conceptualization of the architectural elements (facies geometry) of the sedimentological model (Figure 6.5). This

model, however, lacks conductivity variability within its architectural elements. In the next sections, models are presented based on a combination of the facies model and the Gaussian model of conductivity variability. This approach represents two nested-scales of heterogeneity; the first scale represents geometrical sedimentological information, while the second (smaller) scale represents conductivity variability within the sedimentological facies. This variability of small-scale, within facies, conductivity values is obviously smaller than the variability of the global distribution of conductivity values discussed in Section 6.5.

### 6.6.1 Description of the heterogeneity model

The four previously presented, lateral continuity options (Table 6.3) are now used to represent the four different architectural elements (facies) that occur in the facies model (Figure 6.5). The lateral continuity parameters (i.e., correlation length, spatial anisotropy) remain the same. However, the conductivity distribution is now tailored for each facies. Each individual facies conductivity distribution is significantly narrower than the global conductivity distribution described in Section 6.5. Table 6.5 gives a comprehensive overview of the parameters for the nested-facies Gaussian model. The conductivity distributions for individual facies are inferred from the borehole flowmeter measurements (see Chapter 5).

In practice, the model is composed of four independent Gaussian grids that cover the whole model. For each grid cell the conductivity value is selected from one of the

**Table 6.5:** Variogram parameters for different facies of the nested facies model.

Facies	Range of spherical variogram (m)			<sup>10</sup> log K (m/s)	
	hor - NS	hor - EW	Vertical	average	std. dev.
Channel	25	5	1.6	-3	0.75
Pointbar	10	5	1.6	-4	0.75
Braided	10	10	1.6	-3.5	1.5
Chute Channel	5	5	1.6	-2	0.5

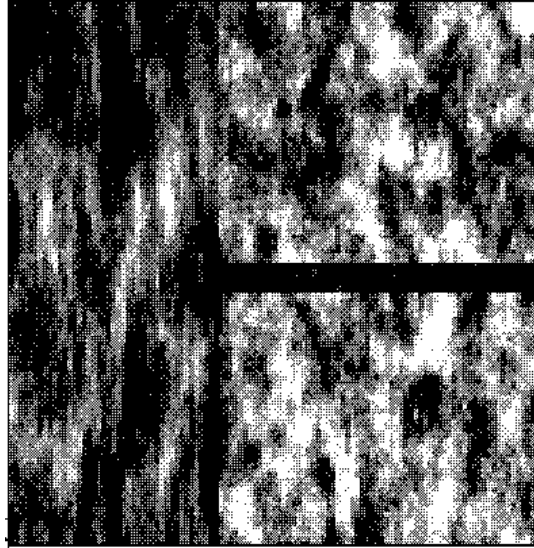
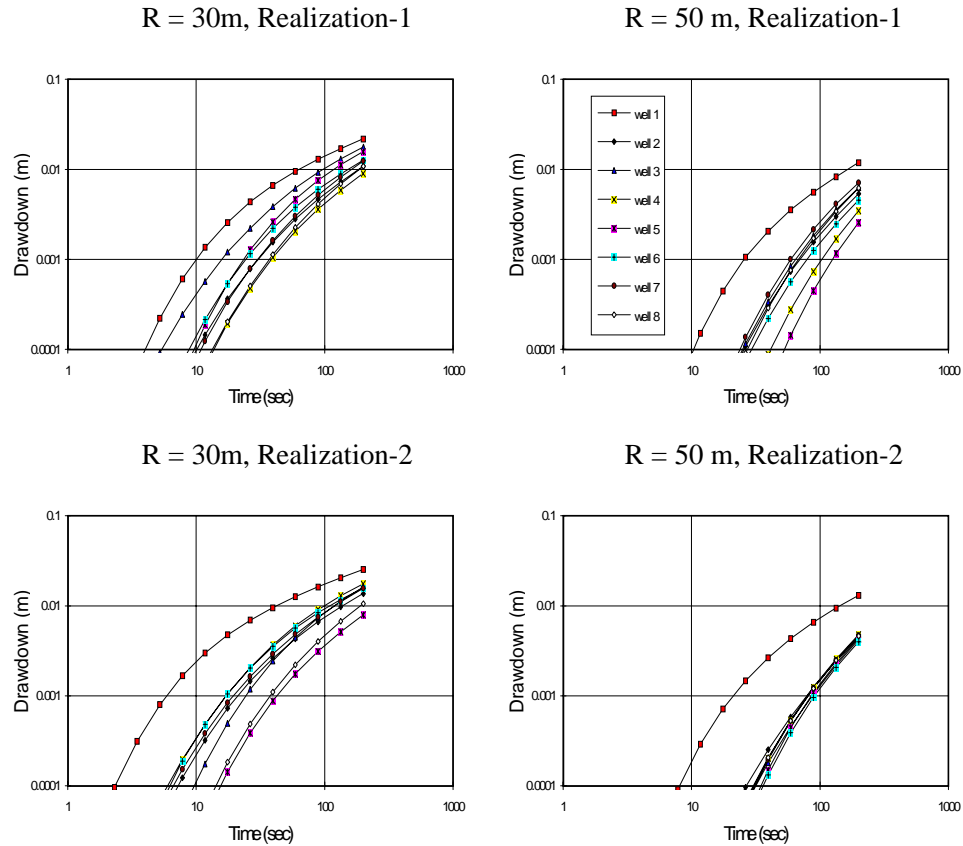


**Figure 6.25:** Example of conductivity (K) distribution for Layer-1 of the nested-facies model. Logarithmic gray-scale: black for  $^{10}\log K = -1$ , white for  $^{10}\log K = -7$  (K in m/s, also see Table 6.5 for distribution parameters of  $^{10}\log K$ ).

Gaussian grids dependent on the facies of that cell. Figure 6.25 shows an example of Layer-1 of this model. For each realization of the nested-facies model, a new realization is used for each of the Gaussian conductivity fields representing the four individual facies (see Table 6.5). For each facies, four realizations were available (see also Table 6.3). Therefore, a total of four realizations could be made for the nested model.

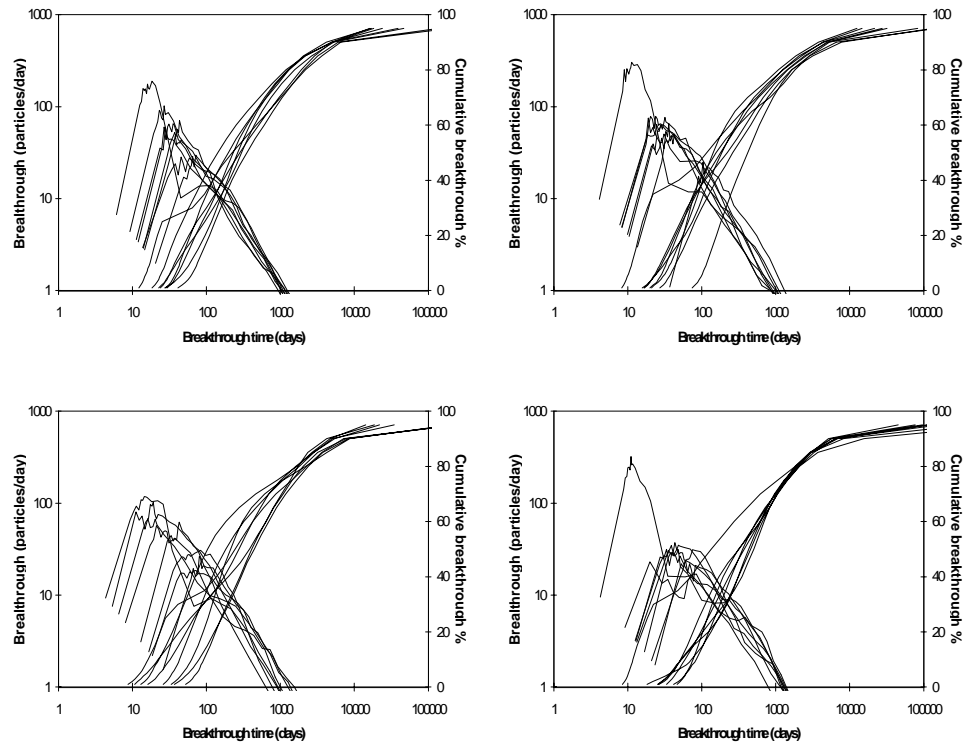
### 6.6.2 Results of pumping test model

Figure 6.26 shows the drawdown response for two circles of observation wells ( $R = 30$  m and  $R = 50$  m, see Section 6.2.3 and Figure 6.2) for two realizations of the nested model. The early drawdown response at these radial distances, exhibits the same variability of onset time as the previously discussed object model and Gaussian model. The onset times are close to those seen for Case-2 of the object model (Figure 6.13). The extremely early onset times observed in the Gaussian model (Figure 6.17), are similar to



**Figure 6.26:** Drawdown for wells at radial distance 30 meters (left) and 50 meters (right) for Realizations-1 and -2 of the nested-facies Gaussian model.

those observed in the nested-facies Gaussian model. However, the consistently observed, relatively late, onset times for the Gaussian model (around 100 seconds at  $R = 30$  m) are not observed for the nested model; the latest onset time for the nested model at  $R = 30$  m, is 20 seconds. In all four realizations of the nested model, Well-1 which is located in the chute channel, shows the earliest response. This is consistent with the pure facies model, although for that model the early onset for the homogeneous, high conductivity, chute channel is earlier (Figure 6.5) than that of the nested model (Figure 6.26). The relatively late onset times of the nested model (around 10 seconds at  $R = 30$  m) are earlier than the



**Figure 6.27:** Breakthrough curves for four realizations (clockwise from upper left: Realizations 1, 2, 3, and 4) of the nested-facies Gaussian model. Each diagram presents concentration cumulative breakthrough curves for 8 two-well tracer tests (also see Section 6.2.3 and Figure 6.2). Horizontal axis depicts breakthrough time in days.

late onset times observed in the facies model for the homogeneous pointbar wells. Thus, the heterogeneity within the relatively small, highly conductive, chute channel diminishes its function as a high hydraulic conductivity connection. In comparison to the homogeneous pointbar, heterogeneity on the relatively large, low conductivity pointbar, also creates connections with a relatively high hydraulic conductivity.

### 6.6.3 Results of tracer test model

For each of the four realizations, eight two-well tracer tests were modeled. As discussed in Section 6.2.3, the pumped well and the injection wells, respectively, coincide with the pumped well of the modeled pumping test and with the observation wells on a circle at a radial distance of 30 meters (also see Figure 6.2). Figure 6.27 shows for all four realizations the cumulative RTD of the tracer injected as a slug. Well-1 located in the chute channel, appears to be the first well showing breakthrough for each realization. Except for Realization-4, the breakthrough at Well-1 significantly precedes the breakthrough in the other wells. For the remaining three realizations, the other wells show a fairly similar response. The time of peak breakthrough falls within 0.5 log-cycle. Only Realization-4 shows significant, separate, peak, breakthrough times for each of the eight wells. This rapid early breakthrough is, in part, similar to the breakthrough of tracer injected in Well-1 in the facies model. None of the curves shows the long tail end (extended breakthrough beyond 1,000 days of last 25% of tracer) observed for some realizations of the Gaussian model (see Figure 6.20, and Figure 6.21). In contrast to the Gaussian models (discussed in Section 6.5), several well-pairs show double or prolonged peaks of breakthrough. This indicates the presence of several different heterogeneity systems, rather than one system with a single unique type of heterogeneity (such as the Gaussian models).

In comparison with the large-scale 5-spot tracer test conducted at the test site, all realizations show the correct pattern of a first breakthrough at less than 10 days, followed by a cascade of breakthroughs between 10 and 100 days. This breakthrough pattern is similar to the breakthrough pattern of the facies model and, obviously, the result of the underlying geological structure. The variability between the realizations is still significant, and allows one to address the uncertainty for breakthrough at different wells.

Figure 6.28 confirms the previously observed correlation between drawdown breakthrough and tracer breakthrough. The correlation for 50% and, especially, 75% is significantly worse than similar correlations for the Gaussian model. Figure 6.29 explores in detail the relation (ratio) between the time of, respectively, 5% and 50% cumulative breakthrough for all 32 tracer tests. For S-shaped, two-well tracer test, cumulative breakthrough, type-curves, this ratio of these breakthrough times (the log-time lag), is

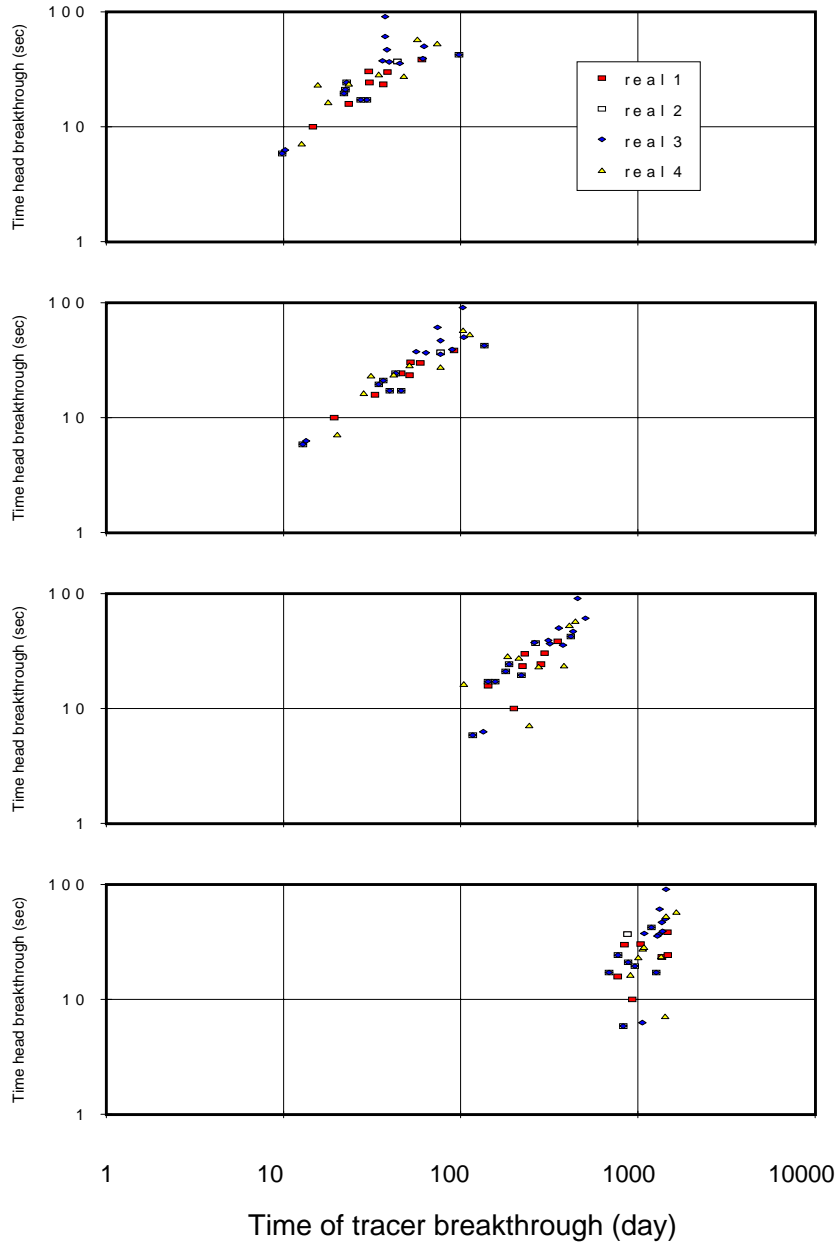


**Figure 6.28:** Head (drawdown) breakthrough versus tracer breakthrough at respectively 5%, 15%, 50% and 75% cumulative breakthrough.

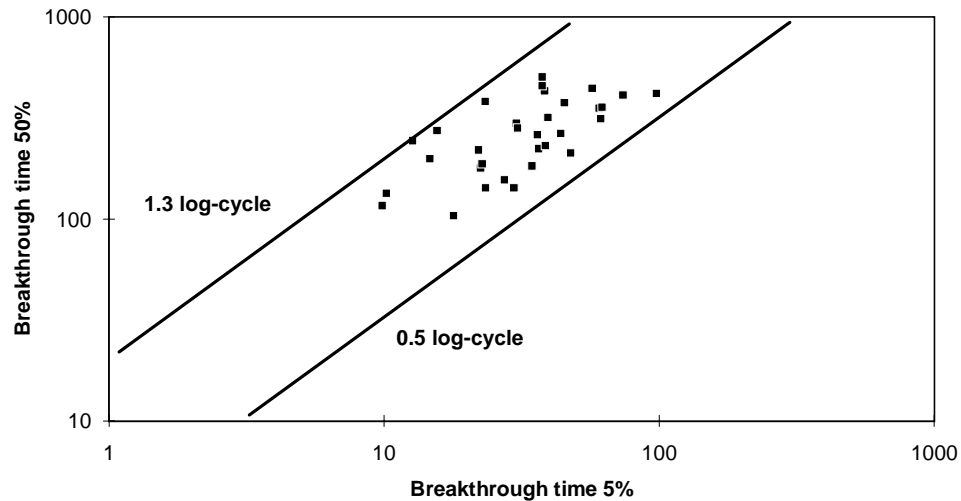


**Figure 6.29:** Dispersion of time lag between 5% and 50% cumulative breakthrough.

indicative of dispersion (also see Section 6.2.4). Based on this measurement, the dispersive behavior of the nested model is similar to the dispersive behavior of the Gaussian model. Thus, dispersion is an incomplete characterization of the nested model. It does not reveal prolonged peaks that are the result of different heterogeneity systems.

Figure 6.30 shows the vertical distribution of tracer breakthrough in the pumping well for all 32 tracer tests modeled for four realizations. Similar to the Gaussian models (see also Section 6.5.3 and Figure 6.25), this vertical distribution is largely constrained by the vertical conductivity profile of the production well. Breakthrough occurs mainly in the upper high conductivity zone (1-3 meters) and in the lower conductivity zone (7-8 meters). Contrary to the Gaussian models, the range between the extreme cases (maximum breakthrough in upper zone and maximum breakthrough in lower zone) is much smaller. Thus, the fixed arrangement of architectural elements largely dominates the vertical distribution of tracer production.

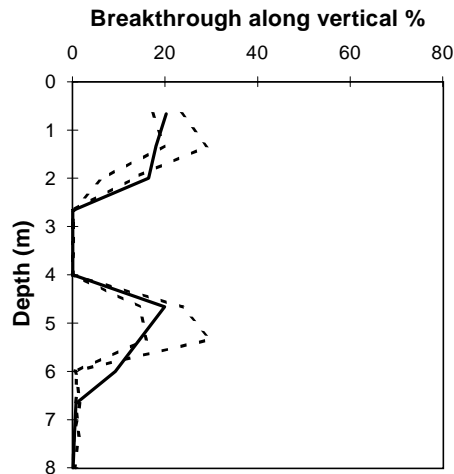


**Figure 6.30:** Percentages of tracer breakthrough at different depth intervals. The solid line is an average for 32 tests (in 4 realizations). Dashed lines denote extreme cases.

## 6.7 DISCUSSION AND CONCLUSIONS

Pumping tests in a heterogeneous confined aquifer were modeled and analyzed in conjunction with two-well (pumping and re-injection) tracer tests. Four different types of heterogeneity models were developed for this aquifer, inspired by the field data collected for the Columbus aquifer at the 1-HA test site. The heterogeneous aquifer models are, respectively: a deterministic facies model; a simple geostatistical model for facies objects; a Gaussian model for hydraulic conductivity; and a nested model combining the deterministic facies model and the Gaussian model.

The modeled pumping test differs from the actual tests conducted in the field, because a confined aquifer was modeled. This choice was made because it allows one to better isolate effects due to heterogeneity. Moreover, the initial response of an unconfined aquifer, largely resembles the response of an equivalently confined aquifer (Boulton, 1954; Neuman, 1972; Streltsova, 1972). Therefore, conclusions based on analyzing the early part of the modeled drawdown-curve, can be applied with reasonable confidence to

an unconfined case, like the Columbus aquifer. The two-well tracer test was modeled to assess tracer transport between the pumped well (from the pumping test) and individual observation wells. The choice for a two-well test was motivated by a potentially simple analysis of tracer breakthrough, as well as an analysis of tracer pathways between two wells. The modeled two-well tracer test differs in layout from the 5-spot tracer test conducted at the Columbus 1-HA test site; however, these results can be compared with reasonable confidence with the Columbus field data.

It can be concluded that detailed multi-well pumping tests are a useful tool to predict tracer transport and/or to characterize preferential flowpaths for a large ensemble of model realizations. The only measurement required is the time when drawdown due to pumping, exceeds a given threshold (i.e., the onset time of drawdown, or the time of drawdown breakthrough). For all heterogeneity models analyzed, it is shown that early drawdown breakthrough coincides with early tracer breakthrough. For the deterministic facies model and the Boolean object models, it is shown that one or more highly conductivity elements are responsible for both the early drawdown breakthrough and the early tracer breakthrough. For the Gaussian and nested model, it can, therefore be inferred that similar high conductivity connections (pathways) cause early drawdown and tracer breakthrough. The differences in onset time of drawdown, can result in wrongly determined apparent storage coefficients; this is especially so when an interpretation method is used that does not explicitly cater to conductivity heterogeneity.

Dispersion seems to be a less useful parameter for the entire variety of models investigated using tracer tests. Primarily a standard value between 5 and 10 meters is found, and this is unrelated to the actual spatial distribution of heterogeneity. When more dispersion becomes apparent, it is impossible to decently fit a dispersion type-curve, since a double peak occurs. Consequently, dispersion is a very questionable parameter to characterize the results of a two-well tracer test, much less an aquifer. This problem of estimating dispersion is similar to what is usually encountered when interpreting field data; in a way this problem confirms the realism in heterogeneity models.

Effective porosity, however, appears to be a useful parameter to characterize tracer flow between two wells in the heterogeneous models. Effective porosity determines the onset and peak of tracer breakthrough. Effective porosity is the fraction of bulk porosity which is an active part of the flow system. Traditionally, it is seen as the “so called”

connected pore space; in other words, it is the pore volume, excluding fully isolated and dead end pores. However, if interpretations are based on a homogeneous isotropic model, the results of the tracer tests for the heterogeneous models, indicate that redistribution of flow due to heterogeneity causes an apparent reduction of effective porosity. It is shown for all models that it is this onset and the peak of tracer breakthrough; hence, effective porosity is predicted with reasonable accuracy using drawdown breakthrough. For field practice, effective porosity allows one to estimate the aquifer's volume that actively contributes to the outflow of a well given a certain time span. If that active portion is the aquifer volume directly connected by high conductivity pathways, and if it can be estimated, then conversely the inactive unconnected portion of the aquifer can also be estimated as being its complement. These estimates are very important when designing pump-and-treat cleanup systems, and/or for evaluation of hydrochemistry along flowpaths in active flow-systems.

The simple facies model containing a few relevant facies elements, already appears useful for obtaining similar trends in tracer breakthrough as observed in the field data of the Columbus 1-HA test site. The Gaussian model has both realizations for the hydraulic behavior which reasonably concur with trends inferred from field data, and other realizations that do not. The Gaussian model provides a good means to estimate the variation (uncertainty) of possible breakthroughs, especially when no specific sedimentological data are available and one has to rely on rough estimates of spatial continuity. For the investigated options, no relation is observed between the spatial continuity parameters and the dispersion length. The latter is no surprise, because the scale of the spatial correlation is not negligible with respect to the scale of the modeled, two-well tracer tests.

The combination of a facies model and the Gaussian model (the nested model) is largely dominated by the sedimentological trend. First breakthrough always occurs in the same well, while for the other wells the time range of later breakthroughs is smaller. This points to the fact that when the possible geometry of the sedimentological structures is well described, reducing uncertainty is much better achieved by specific sedimentological insights about a trend (or the occurrence of major conductive facies elements), than by taking extra measurements of local conductivities.

Of all the realizations shown, several could fit Columbus, but a lot do not match with the field observations. Thus, the geostatistical modeling exercise shown in this chapter, is a way to screen a sufficient number of models on their resemblance with observed field data. Ideally an *a priori* large uncertainty (for example, 20 realizations of which 16 are Gaussian and 4 nested), can be reduced by retaining only those models fitting a detailed, multi-well, pumping test. Obviously some error is always involved, and as a result uncertainty can not be eliminated, but can be considerably narrowed. Hence, a small(er) ensemble of realistic heterogeneous models is retained for further analysis and predictions.

## **CHAPTER 7**

### **CONCLUSIONS AND PERSPECTIVE**

## 7.1 SUMMARY OF RESULTS

This dissertation addresses the problem of adequately describing the hydraulic behavior of a heterogeneous aquifer, specifically the flow towards a well. Typically for a subsurface problem, the quantity of available data versus the number of unknowns, is very limited. Therefore, an adequate hydrogeological description still encompasses a range of possible aquifer responses. Thus, a broad approach has been followed to obtain a more or less, reliable estimation of the range of possible aquifer responses within a limited spectrum of sedimentological options. This broad approach includes the following methods: sedimentological analysis; multi-well and single-well pumping tests; tracer experiments; geostatistics; and numerical modeling of groundwater flow. Any application of only one of these methods can lead to a strongly biased and erroneous estimate of the range of aquifer responses. Thus, this dissertation aims at integrating and combining several direct and indirect methods to identify the aquifer's structure and to analyze the associated groundwater flow and solute transport behavior.

The final objective of this research is to characterize a heterogeneous aquifer in order to better describe contaminant flow; many of the findings are also applicable to the recovery of oil from heterogeneous reservoirs. When groundwater is contaminated, an assessment of risk for migration is imminent. In addition, options need to be evaluated for containment and/or removal; for example options may be pumping or destruction by injecting (bio)chemical agents. All of this requires sound knowledge of how constituents of groundwater, flow in subsurface formations. Migration must be predicted accurately and agents must be distributed properly in the subsurface to do their reactive work.

This dissertation is based on field studies specifically focused on flow towards a well. An extensive program of pumping tests and tracer tests was conducted at the 1-HA test site (Columbus, Mississippi, USA). Based on these field data, it is shown that pumping tests can be the backbone of hydraulic information about heterogeneity. Subsequently, heterogeneity models are used to replicate the pumping test data and tracer test data collected in the field. Consequently, this dissertation shows how conventional pressure drawdown measurements (pumping tests) can be diagnostic in predicting solute (contaminant) transport. It stresses the importance of adequate field measurements before developing highly sophisticated, computer models. There seems to be sufficient scope to

update pumping test, field techniques in order to attain a more accurate, diagnostic, predictive tool for flow in heterogeneous aquifers. The model results for pressure drawdown in heterogeneous aquifers, indicate that these field techniques must have the objective and capability to measure pressure drawdown, precisely, locally, and systematically distributed in space. If these requirements are met, then they have a large potential to resolve aquifer heterogeneity and to contribute to better assessment of contaminant flow.

Within the framework of hydrogeological research, aquifer models with different degrees of complexity have been used. For the homogeneous aquifer (Figure 7.1A) a single fixed value applies to the hydraulic conductivity ( $K$ ). For the composite aquifer,

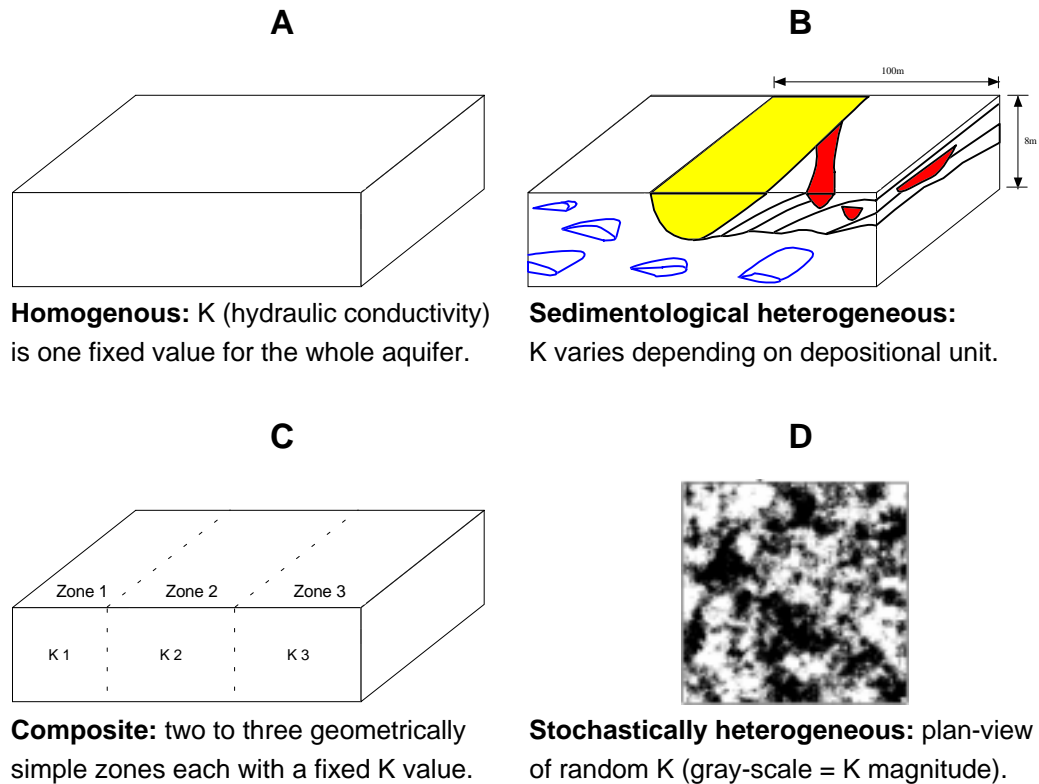


**Figure 7.1:** Homogeneous, composite, sedimentologically heterogeneous, and stochastically heterogeneous aquifer models.

fixed values apply to a couple of geometrically simple zones like: a strip model (see Figure 7.1C); circular zones; layers; or regular fracture patterns. For the heterogeneous aquifer (Figure 7.1B), different property values apply for the relevant sedimentological units. For the stochastic aquifer (Figure 7.1D) the conductivity varies according to a specific statistical distribution. Conductivity values often range over several orders of magnitude (i.e., differing by a factor of 1,000).

Only for the homogeneous case (see Figure 7.1A) is it relatively straightforward to make predictions about contaminant flow and transport. For example, when a slug of non-reactive contaminant is released in a homogeneous aquifer given an uniform flow field, it will become an ellipsoid plume with an increasing size and a decreasing maximum concentration that follow known functions of time and space (Domenico and Schwartz, 1990). The homogeneous case, however, is purely a model for mathematical convenience. When comparing this with the more realistic heterogeneous case, it becomes clear that contaminant flow will be impacted by the structures which coincide with contrasts of hydraulic properties. A contaminant release may, for example, shoot in a highly conductive streak, resulting in a very erratic plume shape, along with unpredictable concentrations. Thus, it is very important to assess the aquifer's heterogeneity in order to accurately describe movement of contaminants. For most real-life heterogeneous aquifers, no unique assessment can be made; in fact, due to heterogeneity, flow behaves chaotically. Therefore, it is very important to conduct risk assessment including aquifer heterogeneity, for example, to evaluate the possible range of impacts of a contaminant release.

### 7.1.1 Reject Null Hypothesis: No single model describes a heterogeneous aquifer

Models are a description of reality based on limited data and schematization. Within the framework of this dissertation, the purpose of a heterogeneous aquifer model is to obtain a robust prediction of groundwater flow and solute (contaminant) transport. The null hypothesis of this dissertation is:

#### **Null Hypothesis:**

If one of the models (modeling methods) depicted in Figure 7.1 fits to a limited set of field data (for example, a pumping test), then we have obtained an aquifer description that is reliable for a variety of predictions pertinent to the behavior of that aquifer.

For the pumping tests analyzed (see Section 4), it was found that several models identified in Figure 7.1, can explain the same pumping test data. Thus, a high-degree of non-uniqueness occurs; for example, the theoretical drawdown-curve of several different composite models, will fit the same set of limited field data; or several realizations of the stochastic model will have the same pumping test response which is, in turn, very similar to the pumping test response of the sedimentological model. However, large differences are observed for tracer test response for different models that have the same pumping test response for a limited set of data points. Thus, the fact that a model makes it possible to fit a limited set of field data (e.g. pumping test data), does not at all imply that this model is the only one possible, and/or that it is the most appropriate model for a variety of hydrogeological applications (such as tracer transport, or contaminant transport). Therefore, the Null Hypothesis can be rejected.

### 7.1.2 Hypotheses: Heterogeneity can be derived from pumping test results

Rejection of this Null Hypothesis leads to two other hypothesis about dealing with multiple models (see Figure 7.1) and pumping tests:

**Hypothesis-1:**

If different composite models can be found which fit the data of an aquifer's pumping test, then that heterogeneous aquifer can be characterized by reconciliation of the different composite models, along with its known sedimentological or other geological features.

**Hypothesis-2:**

If the aquifer's pumping test data show a spatial variability that can not be fit with a homogeneous or composite model, then heterogeneity is a likely cause and these pumping test data can be used to predict contaminant flow which is predominantly a function of heterogeneity.

In order to fully explore these hypotheses, extensive research on various pumping tests in heterogeneous aquifers was conducted.

Chapter 2 provides an overview of recent trends in sedimentology to quantitatively assess geometry and hydraulic properties of sedimentological units. In order to more fully include sedimentological concepts in pumping test interpretation, the last part of Chapter 2 reviews recent trends in pumping test analysis that specifically aim at resolving zonal composite models in relation to sedimentological heterogeneity. The most important conclusion is that there is no single data type that "does the ultimate" in describing flow in a heterogeneous aquifer. In other words, one should combine all possible (and economically feasible) information, ranging from geological information found in simple driller's logs to sophisticated measurements such as the borehole flowmeter.

In Chapter 3 this data collection approach is implemented. Results are presented from a field testing program conducted at the 1-HA test site at Columbus Air Force Base and an overview is presented of specific sedimentological data for the 1-HA test site. In a fairly conventional manner, pumping tests were conducted to determine the hydraulic conductivity of the "average aquifer". Less conventionally, the pumping tests were repeated for many locations that are relatively close together and in the same aquifer. These experiments were supplemented with borehole flowmeter measurements that specifically aim at revealing the heterogeneous character of the aquifer. Tracer tests were conducted to investigate the effect of heterogeneity, as well as to demonstrate whether

results from pumping tests could be used to understand the impact of heterogeneity on solute transport.

Chapter 4 discusses a conventional (type-curve) interpretation of the pumping tests in the heterogeneous Columbus aquifer. The following options for type-curves and methods are used for interpretation of the test conducted at the 1-HA test site:

- 1- Theis curves for a homogeneous confined aquifer;
- 2- Neuman delayed yield curves for a homogeneous unconfined aquifer;
- 3- curves for a radial composite aquifer (Butler, 1988);
- 4- curves for a linear composite (strip) aquifer (Butler and Liu, 1991);
- 5- the Cooper-Jacob Straight Line (CJSL) method applied to different time segments of the tests; this is a simplified version of the derivative method (see, for example, Ehlig-Economids, 1988);
- 6- the Kazemi method for a double porosity fractured aquifer.

From Chapter 4 it emerges that interpretation "problems" (such as fitting problems and/or inconsistency of resulting parameters) should not be discouraging, but rather can be used to better characterize heterogeneity and its effects on fluid flow. It is shown that perfect curve-fitting, without an appropriate conceptual (sedimentological) model, may defeat the purpose of properly understanding the performance of a heterogeneous aquifer. In general it is concluded that the composite aquifer curves (see above Option-3 and Option-4) and the application of the CJSL method for different time segments, are relatively successful at resolving lateral heterogeneity in a manner consistent with the sedimentological information for the 1-HA test site. This demonstrates that Hypothesis-1 makes sense.

Additionally, the research in Chapter 3 combined with the results of Chapter 4, show how variability of early-time drawdown response, related to highly conductive connections between wells, could be related to the variability of storage coefficients. This variability of the storage is actually a variability of the diffusivity ( $T/S$ ), but is in conventional interpretation mostly reflected in variability of  $S$ , the storage. The reason is that most drawdown curves follow during early-time a Theis curve representing the local situation between a given pumping and observation well. In the case of a highly conductive lense, this implies a high transmissivity ( $T$ ) and thus a high diffusivity. During

late-time, drawdown curves reflect the average aquifer. For most conventional interpretations, the T value is largely based on the late-time and therefore fixed at a lower (average) level than locally around the well where a finite high conductivity lense occurs. As a consequence the storage value, which is mostly based on the early- time, becomes lower when a highly conductive lense occurs. The highly conductive connections were confirmed using tracer test results. This demonstrates the validity of Hypothesis-2.

### 7.1.3 Hypothesis: Describing real variability requires a combination of models

From rejection of the Null Hypothesis it follows:

#### **Hypothesis-3:**

If the objective is to make reliable, risk based, predictions using heterogeneous models, then one can not assume that a single conceptual model is perfect, and it is essential to use a range of possible concepts for aquifer heterogeneity models.

This range of possibilities should include different concepts of modeling, for example: models based on sedimentological insight; models based on geostatistical techniques; and/or combinations of these two. From the resulting ensemble of models, a full range of possible model responses can be derived.

In order to explore this hypothesis, research was conducted in both theoretical and practical aspects of modeling heterogeneous aquifers. The ground work for the various models is laid in Chapter 2 and Chapter 5. Additionally, Chapter 2 provides a site-specific sedimentological model for the 1-HA test site. The coarse-grained pointbar model is adopted as a viable analog for the sedimentological structure(s) occurring at the 1-HA test site. This chapter also provides an overview of the various geostatistical techniques used for modeling heterogeneous formations.

Chapter 5 provides a geostatistical analysis of local-scale (borehole flowmeter) conductivity data collected in large numbers at the Columbus 1-HA test site. The conductivities measured range over four orders of magnitude (i.e., by a factor of 10,000). The problem of non-stationarity is addressed by employing knowledge about possible

distribution of sedimentological facies used to distinguish between zones that may have different spatial characteristics. Effective flow and transport parameters are calculated analytically using co-variance parameters obtained from this analysis. The obtained effective conductivity fits well with the conductivity range obtained by an analysis of the pumping tests using an equivalent, homogeneous, aquifer model. The co-variance parameters are also used to determine macro-dispersivity, the effective dispersion parameter.

Chapter 6 deals with flow and transport models based on geometries and spatial conductivity distributions that are either based purely on sedimentological concepts or on geostatistical distribution parameters (variogram). Pumping tests and tracer tests are modeled for a suite of heterogeneous models which conceptually represent the Columbus 1-HA test site. The heterogeneous models are:

- 1- a sedimentological model (also see Figure 7.1B);
- 2- a model of random (sedimentological) objects around the pumping well;
- 3- a Gaussian stochastic conductivity model based on variograms;
- 4- and a combination of the sedimentological model and the Gaussian model.

The sedimentological and the object models clearly demonstrate that high conductivity connections between pumping well and observation well, cause an anomalous early drawdown response. The latter results in anomalous low storage coefficients when conventional, pumping test, interpretation techniques based on a homogeneous model, are applied. The same high conductivity connections result in very early tracer breakthrough, when compared to a homogeneous model. The early breakthrough translates into a low effective porosity when conventional, tracer test, interpretation techniques based on a homogeneous model, are applied. Note the analogy between a low effective porosity and a low storage coefficient, both caused by a limited high conductivity portion of the aquifer that dominates flow patterns towards a well.

A stochastic Gaussian model was developed. This model is based on four different covariance parameters (variograms). Each variogram represents a different length pattern for the heterogeneities. In a way, these four different variograms represent four geological options. For the Gaussian model, sixteen (16) realizations were created, four for each geological (variogram) option. For each realizations eight, two-well, tracer tests were

modeled for combinations of pumping and observation wells subjected to a pumping test. Again it was found that the early-time, pumping test drawdown in an observation well appears to be an excellent indicator for the relative time of breakthrough during the tracer test. It is shown that “drawdown breakthrough time” (the time for which drawdown exceeds a certain threshold) is an excellent indicator of connectivity by high hydraulic conductivity lenses between wells. The Gaussian geostatistical model shows a full spectrum of degrees of connectivity expressed in the drawdown and tracer breakthrough. Therefore, it should be possible to find stochastic conductivity fields that, more or less, represent a specific pumping test response. Such a selection procedure allows one to constrain the ensemble of stochastic conductivity fields using field pumping test data. However, it was also found that it is impossible to systematically separate the hydraulic response for stochastic conductivity fields with significantly different variogram models. Therefore, one should be very cautious about applying inverse techniques based on a single variogram model

The combination of the sedimentological model and the Gaussian model is a sedimentological model filled in with stochastic conductivity values from a Gaussian stochastic random field differently defined per facies. For each facies specific covariance parameters are chosen that in a way could represent a typical length for the heterogeneity pattern of that facies (compare the geological options of the Gaussian model discussed above). Four realizations were made of this model. Also for this model pumping tests and two-well, tracer tests were modeled, and the relation between early-time drawdown and tracer breakthrough was investigated. A similar relation between drawdown breakthrough and tracer breakthrough as was found for the Gaussian model. However, the hydraulic behavior for individual wells is much more narrowly defined due to the imposed sedimentological framework.

Appendix A presents the results of oil reservoir studies using the same approach of integrating geostatistical models and pressure transient tests (pumping tests). This approach is applicable for the oil reservoir examples presented, even though field conditions, the spatial scale, and the economical scale are very different from similar studies presented in Chapter 6 for the Columbus 1-HA test site. Pressure diffusion through connected high-permeability pathways, is found to be very important for the well test response in a strongly heterogeneous reservoir with closed boundaries. This finding is

similar to the relationship established in the preceding chapters between tracer transport and multi-well test (interference) response.

In conclusion, this research indicates that employing a variety of heterogeneity models is a viable tool to realistically characterize the effect of heterogeneity on groundwater flow and transport. Thus, Hypothesis-3 appears realistic.

#### **7.1.4 Risk can more precisely be defined by constraining models**

##### **Work method:**

If it is impossible to do measurements that really determine and precisely define a heterogeneous aquifer model, then the aim must be to take measurements and interpretations of those measurements that constrain an ensemble of models and realizations by rejecting those that are contradicted by those measurements.

The constrained subset ensemble of models is a more precise predictor, for example, of risk associated with contaminant transport. The results presented in Chapter 6 indicate, in this respect, the potential of field techniques involving measurement of pressure drawdown that is precisely, locally, and systematically distributed in space. However, further field research and instrumentation development is required to confirm the applicability of such techniques.

## **7.2 SPECIFIC CONCLUSIONS AND OBSERVATIONS**

The following lists a number of specific conclusions and observations based on the work presented in this dissertation:

1. De Vries (1982) mentions in his book about the history of hydrological sciences in the Netherlands, that after 1900 a newly obtained theoretical basis and mathematical formulation of hydraulics allowed, for the first time, an appropriate scientific understanding of groundwater movement, and as a result, permitted better management of groundwater resources. It appears as if the current abundance of

mathematical and numerical hydrological concepts, does not provide a similar leap forward in advancing hydrological practices related to groundwater flow and contaminant transport modeling.

2. The delayed gravity drainage type-curves and the macro-dispersion concept, are two of the most sophisticated theoretical principles in the field of groundwater hydraulics. They both share this author's concern that successful practical applications are rare.
3. Stationarity of a hydraulic conductivity field is a critical assumption for the applicability of the macro-dispersion concept. For the Columbus aquifer this assumption appears to be invalid for both the MADE test site and the 1-HA test site. The boundaries between sedimentological facies with different hydraulic conductivities seem to govern a non-stationary trend of the hydraulic conductivity field. Given common sense knowledge about sedimentology, non-stationarity may be the rule rather than the exception for most other aquifers.
4. Freeze and Cherry (1979) remark that multi-well pumping tests are overly expensive and mostly unnecessary because a value for aquifer transmissivity can also be determined using a single well test. This remark can be misinterpreted as a denunciation of multi-well pumping tests. This dissertation shows, however, that such tests have a large potential when assessing aquifer heterogeneity and preferential pathways for solute (contaminant) transport.
5. The borehole flowmeter is an excellent tool to assess local-scale hydraulic conductivity variations. One should, however, not confuse this with the idea that a point measurement of hydraulic conductivity is conducted.
6. Delayed gravity drainage probably occurs during pumping tests at the Columbus 1-HA test site. Delayed yield from the unsaturated zone could occur, but seems unlikely given the very coarse nature of the aquifer. Flow through highly conductive lenses within a relatively low conductive matrix, is highly probable given the borehole flowmeter measurements clearly demonstrating the occurrence of such lenses. The lenses are rapidly drained during the early part of the test, while halfway through the test a delayed yield occurs from the remainder of the aquifer (the matrix) into the lenses. The delayed gravity drainage causing delayed yield from the unsaturated zone,

has approximately the same effect on the drawdown-curve as delayed yield from the matrix to highly permeable lenses. There is, however, an important difference between delayed gravity drainage and the delayed yield through lenses; in the latter case early-time drawdown can vary quite erratically, depending on whether or not a high conductivity lens connects the pumping and observation well.

7. Not only should one observe that a model fits a certain set of field data, but one should also observe that certain models do not fit a certain set of field data. Finding the answer to the following question can be very revealing: “Why do the field data not accommodate a certain model?”
8. Models are a convenient replacement of reality through simplifications. There is no such thing as a perfectly correct model, unless that model is reality. Thus, it is fruitless to search for a single correct model. Rather, one should investigate a multitude of models, and then should find out which aspects of these models are correct and which are incorrect. Subsequently, one should approximate reality through some inference.
9. The models of two-well tracer tests in heterogeneous aquifers, show that effective porosity appears to be the most important characteristic in assessing (high hydraulic conductivity) inter-well connections that determine the tracer breakthrough characteristics
10. Rather than seeing effective porosity in terms of drainable or connected pore space, the effective porosity from a field-scale tracer test, should be seen as the portion of the heterogeneous aquifer that forms the major flowpaths between wells.
11. A very clear relation was found between effective porosity (determined from field scale tracer testing) and early-time drawdown behavior (drawdown breakthrough).
12. It is tempting to speculate that, analogous to fractured aquifers, for sedimentary aquifers early-time drawdown behavior is mostly governed by a very small, but highly conductive, portion of the total (volumetric) aquifer storage. This results in very small storage coefficients when a conventional homogeneous pumping test analysis is conducted. The same highly conductive horizons are also responsible for relatively

rapid tracer breakthrough. Thus results in low effective porosity when a conventional homogeneous tracer test interpretation is conducted.

13. It is an ironic fact that the very same concepts used by petroleum reservoir engineers to recover oil left behind in the subsurface by nature, are applicable to recovery of its polluting deviates spilled into the subsurface by humanity.
14. It took the petroleum industry about a hundred years to develop costly techniques for recovery of at maximum 60-70% of oil-in-place from subsurface reservoirs. It is no surprise that similar hydrological methods (e.g., pump-and-treat), used to recover more than 99% of a subsurface contaminant, are often relatively unsuccessful and require further research.

### 7.3 GENERAL PERSPECTIVE

Using experimental field data from the Columbus 1-HA test site and a variety of heterogeneous aquifer models, it has been demonstrated that heterogeneity characterization can largely benefit from pumping tests. However, these pumping tests must be conducted and analyzed with the objective of describing heterogeneity. This implies that a pumping test must be designed and analyzed to challenge homogeneity, rather than to fit a theoretical type-curve based on a single homogeneous (or, at best, composite) model. From the field data it was concluded that early-time drawdown data can be used to identify high hydraulic conductivity lenses between the pumping and specific observation wells. Numerically modeled pumping tests for a variety of heterogeneous models, confirmed that differences of pressure drawdown are highly diagnostic for preferential flowpaths of tracer (i.e. contaminants). Currently used field techniques prohibit measurement at reasonable costs of pressure drawdown that is precisely, locally, and systematically distributed in space. However, this problem might be resolved for unconsolidated sediments by using a string of (semi-) permanent pressure transducers that can be installed using a reusable driving rod, similar to a Cone Penetrometer (CPT; see Huijzer, 1992).

Another focus is the data collection pertinent to sedimentary heterogeneity and its impact on the conductivity distribution. From the modeling of heterogeneous aquifers, it

appears that the sedimentological structure(s) at relevant scale, dominate the pumping test results and the tracer (contaminant) transport. The borehole flowmeter data provide insight into the conductivity distribution, along with some (minor) insight into the sedimentary heterogeneity. The spatial distribution of conductivity data alone, is not enough to build reliable heterogeneous models (this dissertation; Rehfeldt et al., 1992). Thus, a large scope exists for relatively inexpensive methods to collect sedimentological data that help to construct a three-dimensional heterogeneous model. Techniques, such as stratigraphic interpretation of CPT logs (Huijzer, 1992) in combination with borehole flowmeter measurements, may be an option to fill in this gap in data acquisition.

It is this author's opinion that compared to the limited options for acquisition of precise field data, numerical techniques and computer resources are by no means a bottleneck for developing reliable models for tracer (contaminant) flow in heterogeneous aquifers. It is, therefore, strongly recommended to focus further research on field techniques, rather than on desktop numerical techniques.

## **CHAPTER 8**

### **SEDIMENTAIRE HETEROGENITEIT EN PUTSTROMING: SAMENVATTING, CONCLUSIES EN PERSPECTIEF**

## 8.1 SAMENVATTING

Dit proefschrift behandelt stroming in heterogene aquifers, toegespitst op putstroming. Zoals voor ieder probleem dat zich beneden het aardoppervlak afspeelt, zijn er veel onbekende variabelen en relatief weinig data. Daarom kunnen ondergrondse stromingsproblemen meestal niet uniek worden opgelost en dient een mate van onzekerheid te worden geaccepteerd. Een realistische benadering om zo betrouwbaar mogelijke stromingsberekeningen te maken, behoeft dan ook een multi-disciplinaire aanpak waarbij de nadruk ligt op het verwerken van zoveel mogelijk (vaak kwalitatieve en indirecte) aardwetenschappelijke en hydraulische gegevens. De gebruikte gegevens en methoden in dit proefschrift zijn: sedimentologische analyse, pompproeven en putproeven, geostatistische analyse, tracer experimenten, en het numeriek modelleren van grondwaterstroming. Het geïsoleerd toepassen van één van deze methoden brengt het risico met zich mee van gelimiteerd en derhalve onjuist inzicht.

Het doel van het onderzoek was om methoden te ontwikkelen voor het beschrijven van heterogene aquifers en de invloed van aquifer heterogeniteit op de stroming van vervuild grondwater. Verscheidene resultaten zijn ook toepasbaar voor de winning van aardolie uit heterogene formaties. Indien vervuild grondwater wordt aangetroffen, dienen twee vragen met zo groot mogelijke nauwkeurigheid te worden beantwoord: (1) Hoe groot is het directe risico voor migratie, bijvoorbeeld naar een drinkwaterwinning, en (2) Wat zijn de opties voor verwijdering van de vervuiling (bijvoorbeeld door wegpompen of in-situ destructie met behulp van bacteriën)? In beide gevallen is precies inzicht vereist betreffende stromingsrichtingen en verblijftijden. Dit precieze inzicht kan alleen worden verkregen indien gegevens beschikbaar zijn omtrent de heterogene structuur van de doorlatendheid en porositeit van de aquifer.

Dit proefschrift richt zich op putstroming. De beschikbare veldgegevens bestaan voornamelijk uit pompproeven en tracer experimenten die werden verricht op een proefveld met een oppervlakte van 1 hectare. Dit proefveld (genaamd 1-HA) is gelegen op Columbus Air Force Base (in de VS, staat Mississippi), waar op verschillende locaties ook diverse andere experimenten werden verricht (zie bijvoorbeeld Rehfeldt et al., 1992).

In het eerste gedeelte van het proefschrift wordt aan de hand van deze veldgegevens aangetoond dat pompproeven zeer informatief kunnen zijn voor het analyseren van de

hydraulische heterogeniteit van een aquifer. In het tweede deel van het proefschrift worden modellen voor heterogene aquifers gepresenteerd om de essentie van de veldgegevens na te bootsen. Uit dit werk blijkt dat, voor een heterogeen aquifer, een gedetailleerd uitgevoerde conventionele pompproef goede informatie verschaft om vervuilingstransport te voorspellen. Dit benadrukt het belang van goede veldmetingen alvorens een geavanceerd model te ontwikkelen. Ook blijkt dat “precisie pompproeven” mogelijkheden bieden voor een meer gedetailleerde voorspelling van vervuilingstransport. Dit betekent dat veldmethoden moeten worden ontwikkeld om lokaal precisie metingen te verrichten van de stijghoogteverlaging (drukverlaging) als gevolg van een geringe onttrekking.

In hydrologisch onderzoek wordt gebruik gemaakt van aquifermodellen met verschillende gradaties van ingewikkeldheid (Figuur 7.1). Het homogene model heeft één enkele waarde voor de hydraulische parameters (bijvoorbeeld de doorlatendheid,  $K$ ) voor de gehele aquifer. Het composietmodel (of zonemodel) bestaat uit een aantal simple geometrieën (rechte lijnen, cirkels) die zones met verschillende hydraulische parameters afbakenen. Voor de meer heterogene modellen zijn de twee voornaamste opties: modellen, op basis van sedimentologische facies met verschillende hydraulische parameters en stochastische modellen die gebaseerd zijn op een specifieke ruimtelijke statistische distributie voor een hydraulische parameter.

Alleen voor het homogene model (Figuur 7.1) zijn simpele en betrouwbare methoden beschikbaar om voorspellingen te doen ten aanzien van het transport van vervuiling. Er bestaat, bijvoorbeeld, een formule voor het bepalen van het transport van een éénmalige lozing van een niet-reactieve stof in een homogeen aquifer waarvan de stijghoogtegradient constant is (Domenico en Schwartz, 1990). Deze formule toont dat de vervuiling zich als een ellips verspreidt. De assen van de ellips worden met de tijd groter en als gevolg daarvan nemen de concentraties gradueel af. Het homogene geval, echter, is een mathematische noodzaak om deze formules te ontwikkelen, maar heeft een twijfelachtig realiteitsgehalte. In werkelijkheid is het zeer wel mogelijk dat de vervuilende stof in een zeer doorlatende laag schiet. Als gevolg zal de vervuilingspluim zich niet als een ellips gedragen, maar een vingerachtige vorm aannemen. Zo kunnen dichtbij elkaar forse, onvoorspelbare, concentratieverschillen optreden. In de praktijk is het in de meeste gevallen vrijwel onmogelijk een éénduidige, simpele beschrijving van

een vervuilingsspluim te geven. De heterogeniteit veroorzaakt een chaotisch stromingspatroon. Juist hierom is het belangrijk rekening te houden met aquifer heterogeniteit en een risicoanalyse uit te voeren waarbij, in plaats van een éénduidige oplossing, een spectrum van mogelijke voorspellingen wordt beschouwd.

### **8.1.1 De Nul Hypothese “Er is een éénduidig model voor een heterogeen aquifer” werkt niet.**

Modellen zijn er om, gebaseerd op een gelimiteerde hoeveelheid gegevens, de werkelijkheid in een schematische vorm te beschrijven. In dit proefschrift zijn heterogene modellen gebruikt ten behoeve van een zo betrouwbaar mogelijke voorspelling van stof- of vervuilingstransport. De nul hypothese van dit proefschrift is:

#### **Nul-hypothese:**

Indien één van de modellen weergegeven in Figuur 7.1 een goede representatie is voor een gegeven set meetwaarden (bijvoorbeeld een pompproef), dan is dit model bruikbaar en betrouwbaar voor allerlei voorspellingen aangaande het gedrag van een aquifer

Uit de analyses gepresenteerd in hoofdstuk 4 van dit proefschrift blijkt dat meerdere van de modellen in Figuur 7.1 het mogelijk maken een *fit* te verkrijgen met één en dezelfde pompproef dataset. Eenduidigheid is dus ver te zoeken. Bijvoorbeeld: verschillende composietmodellen hebben een praktisch identieke pompproef respons; nog een voorbeeld: verschillende realisaties van een heterogeen stochastisch model hebben een identieke pompproef respons, die op haar beurt vrijwel identiek is aan de respons van een heterogeen sedimentologisch model. De tracer-test respons kan echter zeer verschillend zijn voor al de bovengenoemde modellen. Goede simulatie van een bepaalde pompproef respons door een gegeven model, betekent dus in het geheel niet dat het model een unieke representatie is voor de werkelijkheid. Het betekent evenmin dat het model betrouwbaar kan worden gebruikt om allerlei hydrogeologische processen (bijvoorbeeld het transport van vervuiling) te simuleren. Dus, de nul-hypothese dient te worden verworpen.

### 8.1.2 Hypothese: Heterogeniteit kan worden verwerkt in de pompproefanalyse

Het verwerpen van de nul-hypothese leidt tot twee hypothesen in relatie tot het verwerken van heterogeniteit in de analyse van een pompproef:

#### **Hypothese 1:**

Indien meerdere composietmodellen kunnen worden gevonden ter verklaring van dezelfde pompproefdata, dan kan uit deze modellen in samenhang met sedimentologische en andere geologische gegevens een heterogeen aquifermodel worden gedestilleerd.

#### **Hypothese 2:**

Als de pompproefdata ruimtelijke variabiliteit vertonen welke niet verklaard kan worden met een homogeen of composietmodel, dan is de waarschijnlijke oorzaak de heterogeniteit van de aquifer, en dit betekent dat pompproefdata kunnen worden gebruikt om het effect van de heterogeniteit op het transport van vervuiling te voorspellen.

Teneinde de aannemelijkheid van bovengenoemde hypothesen te onderzoeken, werd uitvoerig onderzoek verricht op het gebied van pompproeven in heterogene aquifers.

Hoofdstuk 2 geeft een overzicht van recent werk op het gebied van kwantitatieve sedimentologie. Dit werk is gericht op het verzamelen van data betreffende afmetingen en hydraulische parameters voor diverse sedimentaire eenheden. Het laatste gedeelte van hoofdstuk 2 behandelt recente ontwikkelingen op het gebied van pompproefanalyse. Speciale aandacht wordt besteed aan methoden om zonale analyse te doen in samenhang met sedimentologische gegevens. De belangrijkste conclusie is, dat er geen panacee is om stroming in een heterogeen aquifer te analyseren. Derhalve is het noodzakelijk om zo breed mogelijk informatie te verzamelen, variërend van simpele geologische informatie verkregen van boorbeschrijvingen tot geavanceerde technologie zoals de *borehole flowmeter* methode.

Hoofdstuk 3 laat de praktijk zien van de bovengenoemde brede aanpak van informatie verzamelen. Dit hoofdstuk behandelt de resultaten van een omvangrijke veldcampagne uitgevoerd op het 1-HA proefveld en presenteert tevens een overzicht van

de specifieke sedimentologische gegevens, beschikbaar voor deze locatie. Conventionele pompproeven werden verricht om op de gebruikelijke manier een “gemiddelde” aquifer doorlatendheid te bepalen. Minder gebruikelijk is het dat de pompproeven werden herhaald voor meerdere, dicht bij elkaar gelegen, lokaties op het 1-HA proefveld. Parallel aan het pompproefprogramma werden *borehole flowmeter* metingen verricht. Dit type metingen biedt, voor een verticaal boorgatprofiel, een gedetailleerd inzicht in de heterogeniteit en maakt het mogelijk de lokale variabiliteit van de doorlatendheid te bepalen. Uiteindelijk werden tracerproeven gedaan om het effect van de heterogeniteit op stoftransport te onderzoeken. Een ander oogmerk van deze tracerproeven was het aantonen dat de pompproefresultaten bruikbaar zijn voor nadere analyse van heterogeniteit en stoftransport.

Hoofdstuk 4 behandelt de meer conventionele (type-curve) analyse van de pompproeven die werden uitgevoerd op het 1-HA proefveld. De volgende methoden (type-curves) werden gebruikt voor de interpretatie van een pompproef:

- 1- Theis curves voor een homogeen *confined* aquifer;
- 2- Neuman *delayed yield* curves voor een homogeen *unconfined* aquifer;
- 3- curves voor een radiaal composiet aquifer (Butler, 1988);
- 4- curves voor een lineair composiet (*strip*) aquifer (Butler en Liu, 1991);
- 5- de Cooper-Jacob *Straight Line* (CJSL) methode, toegepast voor verschillende tijds intervallen; dit is een vereenvoudigde versie van de *derivative method* (Ehlig-Economides, 1988).
- 6- de Kazemi methode voor een *double porosity* aquifer bestaande uit gebroken gesteente.

Uit het in hoofdstuk 4 gepresenteerde materiaal, blijkt dat interpretatie “problemen” zoals een slechte fit of een spreiding van gevonden parameters voor verschillende observatieputten, verder dienen te worden geanalyseerd. Deze “problemen” blijken veelal te worden veroorzaakt door aquifer heterogeniteit en kunnen worden gebruikt ten behoeve van een betere beschrijving van een heterogeen aquifer. De conclusie lijkt gerechtvaardigd dat het klakkeloos fitten van een gecompliceerde type-curve, zonder een goed (sedimentologisch) concept voor de aquifer structuur, onverstandig is. Het laatste is

zeker het geval als het doel van de exercitie is het beschrijven van stoftransport gerelateerd aan aquifer heterogeniteit.

Om inzicht in de laterale heterogeniteit van de Columbus aquifer te verkrijgen, bleken, van de bovengenoemde interpretatiemethoden vooral de composiet type-curves (methode 3 en 4) en de *CJSL* methode voor verschillende tijdsegmenten (methode 5) het meest bruikbaar. Dit geeft aan dat hypothese 1 houdbaar is.

Ook blijkt uit de in hoofdstukken 3 en 4 gepresenteerde gegevens, dat de variabiliteit in de respons van de eerste fase van de pompproef is gerelateerd aan lenzen (tussen een gegeven pompput en een observatieput) met een hoge doorlatendheid ( $K$ ). Deze variabiliteit weerspiegelt feitelijk de diffusiviteit ( $KD/S$ ), maar vindt in geval van conventionele interpretatie vooral zijn weerslag in variabiliteit van de bergingscoëfficiënt ( $S$ ). De reden hiervoor is dat vrijwel iedere verlagingscurve gedurende de allereerste fase van de pompproef een Theis curve volgt. Deze curve is niet kenmerkend voor de gehele aquifer, maar voor het gelimiteerde gedeelte van de aquifer dat bijdraagt tot de putstroming tijdens dit deel van de test. Tijdens de latere fase van de test volgt de verlagingscurve een andere Theis curve, die representatief is voor de totale (gemiddelde) aquifer. Indien de interpretatiemethode is gebaseerd op de aanname van een lateraal homogeen aquifer, dan betekent dit dat de doorlatendheid voornamelijk wordt vastgelegd door het laatste gedeelte van de verlagingscurve, hetwelk in het algemeen weinig variatie vertoont voor de verschillende testen en observatieputten, omdat de gemiddelde aquifer in grote lijnen altijd hetzelfde is. Derhalve vindt de variabiliteit van de diffusiviteit als gevolg van lenzen met een hoge doorlatendheid vooral zijn weerslag in de variabiliteit van de bergingscoëfficiënt. Het feit dat deze variabiliteit van de bergingscoëfficiënt is gerelateerd aan lenzen (tussen pompput en een observatieput) met een hoge doorlatendheid, die ook sterk van invloed zijn op (versneld) stoftransport, werd onafhankelijk bevestigd door tracer-test resultaten. Dit bevestigt hypothese 2.

### 8.1.3 Hypothese: Een model voor heterogeniteit bestaat uit meerdere conceptuele modellen

De verwerping van de nul-hypothese leidt tot:

#### **Hypothese 3:**

Indien het doel van een heterogeen model is om een betrouwbare risico-analyse uit te voeren, is het zeer riskant aan te nemen dat er een enkel perfect conceptueel model is; om die reden is het essentieel om een scala van conceptuele heterogene modellen te analyseren.

Dit scala van modellen moet diverse conceptuele modellen (zie ook Figuur 7.1) omvatten, zoals bijvoorbeeld: een sedimentologisch model, een stochastisch model, en/of een combinatie van beide. Het resultaat is een verzameling van modellen en bijbehorende voorspellingen.

Aanzienlijk theoretisch en praktisch werk ten aanzien van het modelleren van heterogene aquifers werd verricht teneinde hypothese 3 verder te onderzoeken. Hoofdstukken 2, 5 en 6 vormen de basis voor de diverse modellen. In hoofdstuk 2 wordt tevens een sedimentologisch model specifiek voor het 1-HA proefveld gepresenteerd. Dit zogenaamde *coarse grained pointbar* model is een analogie voor de sedimentologie van het 1-HA proefveld. In hoofdstuk 2 is voorts een samenvatting opgenomen van een aantal geostatistische technieken die bruikbaar zijn voor het modelleren van heterogene aquifers.

Hoofdstuk 5 behandelt de geostatistische analyse van de *borehole flowmeter* doorlatendheidswaarnemingen, die in overvloedige mate zijn verricht in de putten van het 1-HA proefveld. De doorlatendheidswaarden bestrijken vier orden van grootte, met de grootste waarden meer dan 10.000 maal groter dan de kleinste. Op basis van het sedimentologische model is de dataset gesplitst in een aantal facies zones, waarvan wordt verondersteld dat de ruimtelijke statistische eigenschappen constant (stationair) zijn. Uit de aldus bepaalde covariantieparameters zijn effectieve hydraulische parameters berekend. De effectieve doorlatendheid stemt overeen met de resultaten van de pompproefanalyse voor een equivalent homogeen aquifer. De covariantieparameters zijn

ook gebruikt om macro-dispersiviteit, de effectieve parameter voor stoftransport, te berekenen.

In hoofdstuk 6 worden stromings- en transport modellen ontwikkeld op basis van de sedimentologische concepten en de geostatistische (covariantie) parameters. Voor deze modellen, die conceptueel het 1-HA proefveld representeren, zijn pompproeven en tracer-testen gemodelleerd. Deze modellen zijn:

- 1- een sedimentologisch model;
- 2- een model bestaande uit sedimentologische objecten in een willekeurige positie rondom de pompput (object model);
- 3- een stochastisch Gauss model voor de doorlatendheid;
- 4- en een combinatie van het sedimentologisch model en het Gauss model.

In deze modellen voor het 1-HA proefveld dient de centrale put als pompput. De verlaging werd geregistreerd voor hypothetische observatieputten gelegen op een aantal cirkels rondom de pompput. Voor ieder model zijn acht (8) tracer-testen gemodelleerd tussen combinaties van de pompput en individuele observatieputten op één bepaalde cirkel.

Het sedimentologisch model en het objectmodel demonstreren duidelijk dat een zeer doorlatende lens tussen de pompput en de observatieput abnormale verlagingen veroorzaakt gedurende de allereerste fase van een pompproef. Dit leidt tot abnormaal lage bergingscoëfficiënten, omdat dit verschijnsel niet volledig verwerkt kan worden in de pompproefanalyse, zoals eerder werd geconstateerd. De zeer doorlatende lenzen veroorzaken ook een zeer vroegtijdige doorbraak van tracer geïnjecteerd in de observatieput. Indien de tracer resultaten op conventionele wijze met een homogeen model worden geanalyseerd, leidt deze vroegtijdige doorbraak tot abnormaal lage waarden voor de effectieve porositeit. Hieruit blijkt een analogie tussen de lage bergingscoëfficiënten en de lage waarde voor effectieve porositeit, die voort komt uit het feit dat slechts een gering gedeelte van de heterogene aquifer actief deelneemt aan de putstroming.

Het voor het onderzoek ontwikkelde stochastische Gauss model is gebaseerd op vier verschillende covariantieparameters (variogrammen). Deze variogramparameters representeren verschillende typische lengtes voor conductiviteitspatronen. In zekere zin

vertegenwoordigen zij verschillende geologische (sedimentologische) opties. Zestien realisaties (vier voor iedere geologische optie) van het Gauss model werden gemaakt. Voor iedere realisatie werd een pompproef gemodelleerd. Tevens werden, voor iedere realisatie, acht tracer-testen gemodelleerd tussen verschillende combinaties van de pompput en equidistante observatieputten. Deze modellen bevestigen het verband tussen het allereerste gedeelte van de verlagingscurve (van de pompproef) en de doorbraaktijd van de tracer. De zogenaamde verlagingsdoorbraak (de tijd waarin de verlaging een bepaald drempelniveau bereikt), blijkt zeer indicatief voor het optreden van verbindingen tussen twee putten met een hoge doorlatendheid (connectiviteit). De 128 onderzochte putcombinaties voor de Gauss modellen laten een breed scala van connectiviteit zien. Dit betekent dat het mogelijk is een (of meer) realisatie(s) te vinden die in zekere mate representatief is (zijn) voor de pompproef respons. Een dergelijke selectieprocedure maakt het in principe mogelijk om pompproefdata te gebruiken om een deelverzameling van de verzameling van realisaties te bepalen die de pompproef data goed weergeeft. De verschillende Gauss modellen met verschillende covariantieparameters hebben vaak een overlappende pompproef (en tracer-test) respons. Derhalve blijkt het onmogelijk te zijn om de covariantieparameters te onderscheiden op basis van de pompproef en tracer-test data.

De combinatie van het sedimentologische model en het bovengenoemde Gauss model werd verkregen door verschillende doorlatendheidswaarden (verkregen uit een Gauss model) toe te kennen voor iedere grid cel van het sedimentologische model. Voor ieder facies is er een speciaal Gauss model met een individuele set covariantie parameters (de bovengenoemde geologische opties) en zijn vier realisaties beschikbaar. Aldus werden vier realisaties van het combinatiemodel gemaakt. Ook voor dit model werd een pompproef en een aantal tracer-testen gemodelleerd en een goede relatie gevonden tussen de allereerste verlagingsinzet (doorbraak) en de doorbraak van tracer. Over het geheel van de vier realisaties genomen, is spreiding van verlagingsdoorbraak en tracer doorbraak min of meer indentiek aan de gevonden spreiding voor het Gauss model. De respons van individuele putten is voor het combinatie model echter veel precieser gedefinieerd, omdat het model, alhoewel het stochastisch is, wordt overheerst door een zekere structuur (de onderverdeling in sedimentologische facies met ieder hun eigen Gauss model voor de doorlatendheid).

Analoog aan de bovengenoemde aanpak voor aquifers, werden *pressure transients* (pompproeven) bestudeerd voor een aantal geostatistische modellen van petroleumreservoirs. Ondanks het feit dat de ruimtelijke en economische schaal in grote mate verschillend zijn van die van aquifers, blijkt de methodologie van hoofdstuk 6 ook voor petroleumreservoirs in grote mate toepasbaar. De verspreiding van de verlaging door verbindingen met een relatief hoge permeabiliteit blijkt ook in dit geval bepalend te zijn voor het gedrag van de verlaging gedurende een pompproef.

In het algemeen kan worden geconcludeerd dat het onderzoeken van een aantal verschillende modellen voor heterogene aquifers (en petroleumreservoirs) waardevol is om een realistisch inzicht te verkrijgen in het effect van heterogeniteit op stroming en stoftransport. Derhalve is ook hypothese 3 houdbaar.

#### 8.1.4 Betere risico-analyse door inperking van variabiliteit

##### **Werkmethode:**

Indien het onmogelijk is om metingen te verrichten die een éénduidig model voor een heterogeen aquifer mogelijk maken, dan moet men streven naar het verrichten van metingen en interpretaties die de omvang van de verzameling van heterogene aquifers kunnen beperken, door middel van verwerping van de modellen (realisaties) die niet bij de metingen passen.

Uit het werk in dit proefschrift blijkt dat een gegeven pompproefresultaat kan worden gebruikt om stoftransport te voorspellen, zij het niet volledig éénduidig. Uit een verzameling van mogelijke heterogene modellen voor een aquifer, kunnen die modellen worden geselecteerd die de pompproefresultaten niet tegenspreken. Uit hoofdstuk 6 en de veldresultaten blijkt dat, om dit optimaal toe te passen, moet worden gestreefd naar een preciese, lokale, en ruimtelijk systematisch gespreide registratie van de verlaging. Dit laatste vereist de ontwikkeling van meer geavanceerde instrumentatie en meer veldonderzoek.

## 8.2 PUNTSGEWIJZE CONCLUSIES EN OPMERKINGEN

De navolgende lijst bevat specifieke conclusies en opmerkingen gebaseerd op het werk, gepresenteerd in dit proefschrift:

1. De Vries (1982) vermeldt in zijn boek over de geschiedenis van de hydrologie in Nederland, dat na 1900 het begrip van de wiskundige grondslagen der hydraulica sterk verbeterd. Dit toegenomen wetenschappelijk begrip van grondwaterstroming maakt dan, voor het eerst, een verantwoord beheer van grondwatervoorraden mogelijk. De huidige overvloed aan wiskundig inzicht en numerieke methoden lijkt, daarentegen, niet tot dezelfde grote sprong voorwaarts te leiden.
2. De *delayed gravity drainage* type curves en het macro-dispersie concept zijn twee zeer geavanceerde theorieën in het vakgebied van de grondwaterhydraulica. De auteur van dit proefschrift acht het bedenkelijk dat voor beide theorieën relatief weinig praktische toepassingen worden gerapporteerd.
3. Het macro-dispersie concept kan alleen worden toegepast indien de ruimtelijke distributie van doorlatendheidswaarden stationair is. Voor de Columbus aquifer is dit noch voor het MADE proefveld, noch voor het 1-HA proefveld het geval. De grenzen tussen sedimentaire facies (met een verschillende doorlatendheid) verstoren de stationariteit en het blijkt onmogelijk deze verstoring door middel van trendanalyse te verwijderen. Het lijkt erop dat deze sedimentologische non-stationariteit meer regel dan uitzondering is.
4. Freeze en Cherry (1979) stellen dat pompproeven met observatieputten te duur en meestal onnodig zijn, omdat een aquifer transmissiviteit ook kan worden bepaald met een veel simpelere (en goedkopere) putproef. Deze opmerking kan, ten onrechte, worden geïnterpreteerd als een verwerping van het gebruik van pompproeven met observatieputten. Uit dit proefschrift blijkt dat zulke testen vooral van grote waarde kunnen zijn om aquifer heterogeniteit en stoftransport te onderzoeken.
5. De *borehole flowmeter* is een uitstekend instrument om op kleine schaal de variatie van de doorlatendheid van een aquifer te bepalen. Dit moet echter niet worden

verward met het idee dat met dit instrument een preciese in-situ puntmeting van de doorlatendheid kan worden verricht.

6. De Columbus pompproeven zijn ongetwijfeld beïnvloed door *delayed gravity drainage*. Wellicht speelt ook de vertraagde bijdrage (*delayed yield*) vanuit de onverzadigde zone een rol, hoewel deze rol waarschijnlijk klein is, gegeven de grove textuur van de aquifer. Stroming via lenzen met een hoge doorlatendheid treedt zeker op. De *borehole flowmeter* metingen tonen duidelijk aan dat dergelijke lenzen bestaan. Gedurende de eerste fase van de pompproef worden deze lenzen snel ontwaterd. Halverwege de pompproef komt een vertraagde bijdrage (*delayed yield*) op gang vanuit het resterende, minder doorlatende, gedeelte van de aquifer (de matrix). De *delayed gravity drainage* en de vertraagde bijdrage vanuit de onverzadigde zone hebben beide min of meer hetzelfde effect op de verlagingscurve als de vertraagde bijdrage van de minder doorlatende matrix via lenzen met een hoge doorlatendheid. Er is echter een zeer belangrijk verschil: in het laatste geval vertoont het begin van de verlagingscurve een grote variabiliteit, welke afhankelijk is van het feit of de pompput en een observatieput al dan niet worden verbonden door een lens met een hoge doorlatendheid.
7. Het is onvoldoende om uitsluitend vast te stellen dat een bepaald model de veldgegevens goed reproduceert. Het is minstens zo belangrijk om vast te stellen waarom bepaalde modellen niet in staat zijn bepaalde veldgegevens te reproduceren. Het werkt zeer verhelderend om een antwoord te vinden op de vraag “waarom passen deze veldgegevens niet bij een bepaald model?”
8. Modellen zijn een handig surrogaat voor de werkelijkheid. Er bestaat echter niet zoiets als een perfect model - behalve als dit model de werkelijkheid is, en dan is het geen model meer. Derhalve is het heilloos om naar een enkel correct model te zoeken. Het is beter om een verzameling van modellen te onderzoeken en na te gaan in welke aspecten deze modellen correct zijn, en in welke incorrect. Op grond van een dergelijke aanpak kan men met aanvullende schattingen de werkelijkheid beter benaderen.

9. Voor een heterogeen aquifer laten de modellen voor tracer transport tussen een injectieput en een onttrekkingsput zien dat de effectieve porositeit verreweg de belangrijkste parameter is om het effect van verbindingen met een hoge doorlatendheid op de tracer doorbraak te beschrijven.
10. De effectieve porositeit, bepaald uit veldonderzoek via een tracer-test, moet niet worden gezien als een poriënvolume dat kan worden gedraineerd. Het is beter om een dergelijke effectieve porositeit te beschrijven als het gedeelte van een heterogeen aquifer dat de voornaamste stroompaden omvat.
11. Een duidelijke relatie is gevonden tussen de effectieve porositeit gevonden uit tracer-test resultaten (tracer doorbraak) en het verlagingsgedrag gedurende de allereerste fase van een pompproef (verlagingsdoorbraak).
12. Het is aanlokkelijk om te speculeren dat er een analogie is tussen aquifers bestaande uit zeer heterogene sedimenten en aquifers bestaande uit gebroken gesteente. In beide gevallen wordt de verlaging gedurende de allereerste fase van een pompproef gedomineerd door een zeer kleine maar zeer doorlatende fractie van het totale aquifervolume. Indien een conventionele interpretatie, gebaseerd op een homogeen model, wordt uitgevoerd, resulteert dit in een relatief kleine bergingscoëfficiënt. Dezelfde zeer kleine maar zeer doorlatende fractie van het aquifervolume is ook verantwoordelijk voor relatief snelle doorbraak van tracer gedurende een tracer-test. Dit laatste resulteert, indien een conventionele interpretatie wordt uitgevoerd, in zeer lage waarden voor de effectieve porositeit.
13. Het is een ironisch gegeven, dat dezelfde methoden die worden gebruikt door petroleum-reservoiringenieurs om door de natuur in de ondergrond achter gelaten olie te winnen, ook bruikbaar zijn om vervuilende aardoliederivaten, die door de mensheid in de ondergrond gemorst zijn, op te ruimen.
14. In de petroleum industrie is honderd jaar onderzoek verricht om uiterst kostbare technieken te ontwikkelen die het mogelijk maken om maximaal 60 tot 70% van de origineel aanwezige aardolie uit een ondergronds reservoir te winnen. Derhalve is het geen wonder dat hydrologische methoden gebaseerd op vergelijkbare extractie methoden voor het verwijderen van vervuild grondwater (bijvoorbeeld door het

simpelweg op te pompen), vaak nog matig succesvol zijn en nog veel nader onderzoek en ontwikkeling vereisen.

### 8.3 EPILOOG EN PERSPECTIEF

De veldgegevens van het Columbus 1-HA proefveld werden geanalyseerd met behulp van een scala van heterogene aquifermodellen. Het blijkt dat pompproeven een belangrijke bijdrage kunnen leveren aan een gedetailleerde beschrijving van een heterogeen aquifer. Hiertoe is het evenwel noodzakelijk om de mogelijke heterogeniteit te verdisconteren in de uitvoering en analyse van de pompproef. Dit betekent dat planning en analyse van de pompproef moeten worden gericht op heterogeniteit, en dat een goede fit met een analytisch homogeen (type curve) model niet automatisch als een bevredigend eind antwoord moet worden beschouwd. De veldgegevens tonen aan dat het allereerste gedeelte van de verlagingscurve sterk wordt beïnvloed door zeer doorlatende lenzen tussen de pompput en de observatieput. Uit een modelstudie voor een scala van heterogene modellen blijkt dat (subtiele) verschillen in stijghoogteverlaging (drukverlaging) kunnen worden gebruikt om voorkeurs stroompaden voor stoftransport (vervuiling) op te sporen. Dit kan echter alleen worden benut, als in tegenstelling tot de huidige methodieken voor pompproeven, de stijghoogteverlaging zeer precies, systematisch, en als een puntwaarneming wordt gemeten. Een mogelijke techniek is om een array van pressure transducers te gebruiken, die in een niet geconsolideerd aquifer geïnstalleerd kan worden met behulp van een drijftechniek zoals de Cone Penetrometer (CPT, zie Huijzer, 1992).

Ook moet het belang worden benadrukt van het meer intensief vergaren van sedimentologische gegevens en de relatie tussen die gegevens en de ruimtelijke variabiliteit van de doorlatendheid. Uit de modellen voor heterogene aquifers blijkt dat sedimentologische structuren grote invloed kunnen hebben op pompproef resultaten en op stoftransport. *Borehole flowmeter* gegevens verschaffen het nodige inzicht in de variabiliteit van de doorlatendheid en in mindere mate in de sedimentologische structuren. Puur statistisch inzicht in de ruimtelijke verdeling van de doorlatendheid is echter onvoldoende om een betrouwbaar heterogeen model samen te stellen (dit

proefschrift; Rehfeldt et al., 1992). Derhalve is er een goede markt voor een systematische, maar relatief goedkope methode om sedimentologische data te verzamelen ten behoeve van een gedetailleerd drie-dimensioneel model. Methoden zoals de stratigraphische interpretatie van CPT logs (Huijzer, 1992) in combinatie met de *borehole flowmeter* gegevens, lijken een goede optie om deze lacune te vullen.

De auteur van dit proefschrift is van mening dat, in vergelijking met de mogelijkheden om preciese veldgegevens te verzamelen, de numerieke methoden en de computermogelijkheden geenszins een beperkende factor zijn waar het gaat om het ontwikkelen van betrouwbare modellen voor stof (vervuilings) transport in heterogene aquifers. Verder onderzoek dient zich daarom vooral te richten op het verbeteren van hydrologische veldmethoden en niet op het verfijnen van hydrologisch bureau en computer werk.

**APPENDIX A**

**SCREENING OF GEOSTATISTICAL RESERVOIR MODELS  
WITH PRESSURE TRANSIENTS**

by J.C. Herweijer and O.R.F. Dubrule

## A.1 SUMMARY

A geostatistical reservoir study provides an ensemble of possible reservoir models, with a variability reflecting the uncertainty of the geology and fluid-flow properties. A production test links the static geostatistical model with dynamic fluid-flow data and thus provides possible means of validation and selection. We used a highly efficient 3D single-phase simulator to simulate pressure transients without compromising the fine-grid resolution typical for geostatistical models. This simulator was applied to Boolean and Gaussian geostatistical models that represent reservoirs consisting of heterogeneous fluviodeltaic deposits. Simulated buildup and interference tests were analyzed and related to 3D permeability and connectivity patterns. Effective well-test permeability was compared to 3D averages obtained from different volumes within the geostatistical model. The cases studied show that combining geostatistical models and well tests can reduce uncertainty with respect to geometrical connections and the permeability distribution. However, the study also confirms that well tests have a limited capability to assess lateral continuity precisely and uniquely. Simulation of an interference test has the potential to screen the geostatistical model for high-permeability connections between wells. This pragmatic integration of pressure transients and detailed heterogeneous reservoir models through forward simulation provides a simple means to evaluate these models. It allows testing a model based on small-scale (core-plug) permeabilities and qualitative geological information versus routine field measurements representing large-scale hydraulic behavior of a reservoir.

## A.2 INTRODUCTION

During the early stage of field development production tests are the only data providing information about fluid flow in oil reservoirs and about permeability in the wider volume surrounding a well. At the same stage, the construction of a geostatistical reservoir model is now a viable option. The main purpose of this model is to assess the uncertainty of reservoir performance resulting from the incomplete knowledge of the heterogeneous reservoir. Geologic data and core measurements are honored at the wells,

---

This appendix is based on paper SPE 28434 first presented at the 1994 SPE Annual Technical Conference (New Orleans, Sept. 25-28) and published in *Journal of Petroleum Technology*, November 1995.

and models are created between wells that are statistically similar to those inferred from geological analogs (Haldorsen and MacDonald, 1987; Budding et al., 1988; Alabert and Massonnat, 1990). These are static data, and subjecting the geostatistical model to verification on the basis of dynamic fluid-flow data (i.e. pressure transient production-tests) is a logical step. The pressure transient reaches far-away boundaries in a relatively short time. By investigating the well-test response of a geostatistical model the following three issues can be addressed quantitatively.

1. Validation of the geostatistical model. Does the pressure response of the model fit field data or at least the type curve obtained through conventional analysis?
2. Diagnosis of thief zones. Does the geostatistical model show preferential paths for pressure diffusion caused by continuous high-permeability interwell connections consisting of more than one sand body?
3. Scaling up. Can the relation between observed local-scale (core) permeabilities and the effective well-test permeability be explained (and possibly quantified) in terms of connectivity?

We show how these questions can be answered through simple single-phase pressure-transient simulations without compromising the very-fine-grid resolution inherent to geostatistical models. Examples are shown for Boolean and Gaussian geostatistical models that represent reservoirs consisting of heterogeneous fluviodeltaic deposits. Distinct characteristics of the drawdown derivative can be related to 3D permeability and connectivity patterns. Discrepancies between the effective well-test permeability and the average of core permeabilities can be resolved by evaluating connectivity within the 3D geostatistical model. This adds a 3D geostatistical component to standard well-test interpretation.

Combining geostatistical models with the simulation of single-phase pressure diffusion is an efficient and cost-effective tool for assessing hydraulic behavior in geologically heterogeneous reservoirs. It provides a simple means of evaluating the realism of geostatistical models with respect to transient buildups and the sensitivity of flow patterns to geostatistical parameters. Results of the geostatistical model that are incompatible with the pressure-transient interpretation can be rejected. Thus, forward simulation of pressure-transients, combined with standard interpretation methods, allows reservoir engineers to use available pressure-transient field data to reduce the uncertainty of a geostatistical reservoir model. This type of analysis is a logical precursor to use of the

geostatistical model as input to the multiphase simulation for prediction of reservoir production. In the case of multiphase reservoir simulation, however, the cumbersome procedure of scaling up is inevitable and may introduce bias and inaccuracies because of the loss of detail (Keijzer and Kortekaas, 1990; Giudicelli et al., 1992).

### A.3 SEDIMENTARY HETEROGENEITY AND PRODUCTION TESTS

In favorable cases, production tests can have a very distinct response to heterogeneity, but nonuniqueness may affect the geological interpretation in many instances. This is expressed by the fact that two or more different geometrically simple analytical type-curve solutions often can be fitted to the same set of field data. Good insight, however, is obtained by connecting simple type-curve models to a detailed sedimentological model (Herweijer and Young, 1990; Massonnat and Bandiziol, 1991; Massonnat et al, 1993). Type curves are available for representing very schematic sedimentological geometries (Bourgeois et al., 1993), such as a straight homogeneous channel with two parallel homogeneous levees.

Results from well tests in heterogeneous formations can also be used to estimate spatial-continuity parameters (channel size, for example) that are subsequently used as input to a geostatistical model (Alabert and Massonnat, 1990). This is an efficient and suitable method for partially incorporating well-test results into the geostatistical model, but the model does not necessarily reproduce the well-test results. The geostatistical-inversion method, "simulated annealing", has been applied to obtain a geostatistical model that is exactly compatible with a well test (Deutsch, 1992; Sagar et al., 1993). This method involves a trial-and-error convergence toward a desired objective. In theory, 100,000 iterations may be needed to reach the objective. For each iteration the model well-test response has to be compared with the desired response. Because simulating a well test for each iteration is impossible, the desired objective is formulated as an average permeability that should be similar to the well-test permeability. This limits application of this method to cases for which an average permeability correctly represents the well-test response. As discussed later, this assumption is not always valid and other criteria, such as connectivity, need to be added.

Interference tests have, in theory, a large potential for detecting the impact of heterogeneity on interwell connectivity (e.g., connected sand bodies acting as a thief

zone). Herweijer's and Young's (1990) tracer experiment in a shallow aquifer provides evidence of the relationship between interference-test results and thief sands. In this case, a clear relation could be established between the nonuniform interference response and early tracer breakthrough. However, many practical considerations prohibit extensive interference testing in oil reservoirs. A geostatistical model, however, allows such an interference/connectivity exercise to explore the hydraulic connections in the model, and the results can be compared with field data (e.g., water breakthrough) during oil production.

#### A.4 SIMULATION OF WELL TESTS FOR GEOSTATISTICAL MODELS

A prerequisite for the proper simulation of well tests for a detailed geostatistical model is to retain the fine- grid resolution. Thus, very large grids should be used. For this work, we used a highly efficient fully-implicit, backward-in-time, finite difference simulator, designed exclusively for simulation of transient single-phase flow. Routinely, grids of 100,000 to 200,000 cells were simulated on a standard workstation, requiring CPU time of approximately 0.5-2 hours per run. The simplicity of single-phase flow also limits the effort in preparing data and monitoring results. Other than the spatial distribution of permeability and porosity, input is limited to the same data that are needed for a conventional type-curve analysis. The linearity of the single-phase flow equations practically eliminates severe numerical problems. To obtain a pressure derivative signature for single phase flow, simulating a single constant-rate test is sufficient. By virtue of the linearity of the single-phase flow equations, the response to a multiple rate history can be obtained by time superposition.

Geostatistical models are generated on a regular Cartesian grid. Radially expanding grids require scaling up of permeabilities, and the objective of investigating the behavior of the raw detailed geostatistical model would be missed. Therefore, a regular grid size with sufficient resolution to represent the spatial detail is maintained. The grid is refined around the well, and a very small inner gridblock with a very large vertical permeability represents the wellbore. We successfully tested the well test simulator on its ability to reproduce a broad range of type curves generated with conventional techniques.

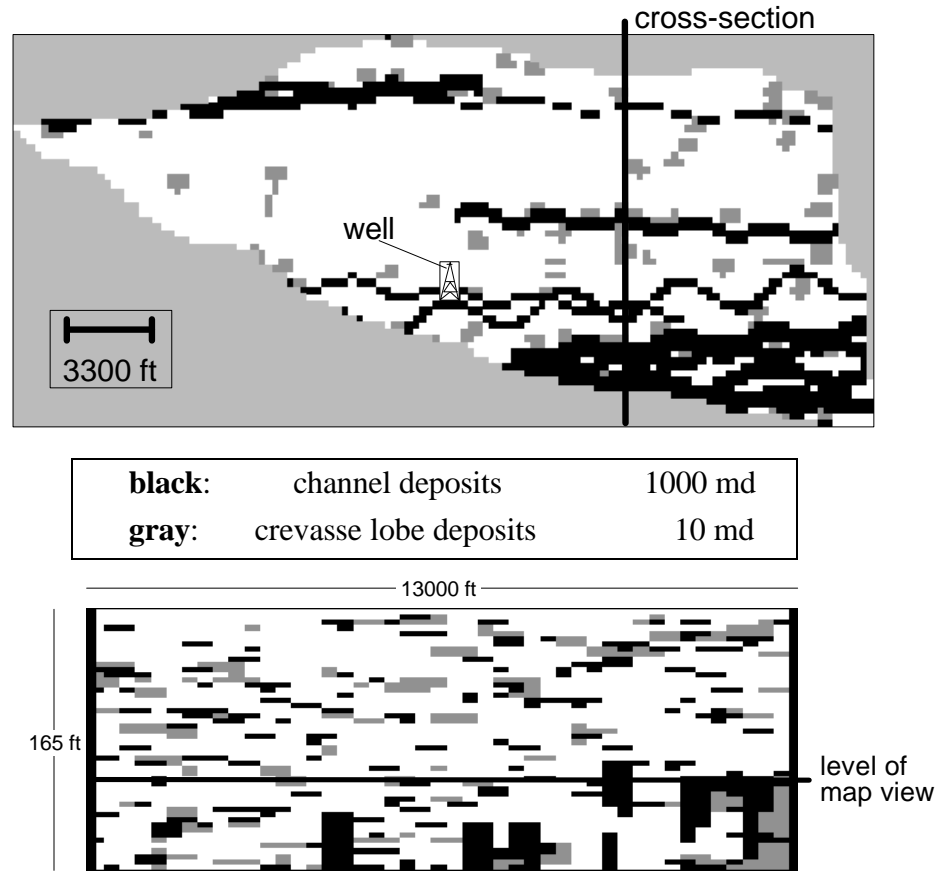


**Figure 1:** Object geostatistical model for a reservoir consisting of fluviodeltaic deposits; map view (upper) and cross section (lower)

## A.5 APPLICATIONS

The following sections present two cases that cover the application of pressure-transient simulation to reservoir characterization in a dynamic fluid-flow context. The first case pertains to an object-based model of a fluvial-deltaic reservoir. We show how the geostatistical model can be validated with a simulated well-test response. The same pressure-transient simulation is used to generate an interference-test response for a given (hypothetical) well pattern. This interference-test response allows the detection of preferential hydraulic connections between the wells, information that subsequently can be

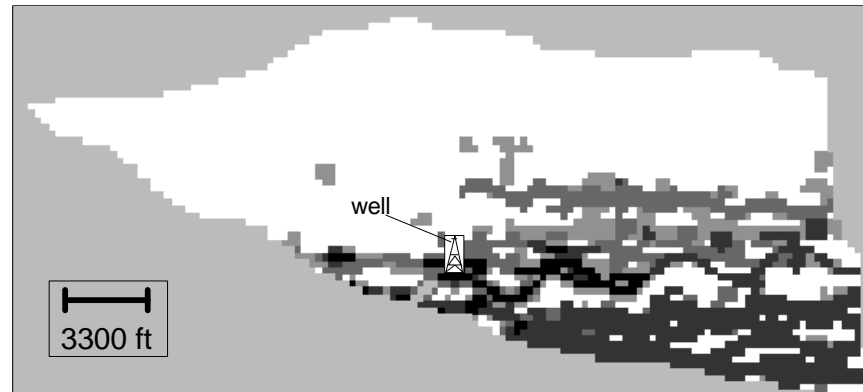


**Figure 2A:** Map view of pressure buildup during well test (at 0.3 hr).

used to diagnose connected sand bodies acting as thief zones. The second case pertains to a hypothetical reservoir interval for which a well test and core permeability data are available. A grid-based (Gaussian) geostatistical model is used to create multiple realizations for several geological options. Using volume averages and connectivity calculations for the geostatistical model, we assessed the relationship between the average core permeability and the well-test result.

### A.5.1 Case 1: A reservoir modeled using object techniques

Figure 1 shows a plan view and a cross section through an object-based 3D geostatistical model of a fluvial-deltaic reservoir. The model is generated with the following procedure: (1) sand bodies (objects) are randomly positioned in space; (2) sand-body size is selected from a geological database of possible sand-body dimensions; and (3) an objective function is optimized through an iterative procedure to fulfill such criteria as a match of the geological well data and geological constraints on the spatial arrangement of sand bodies (areal variations of net/gross, constraints of proximity between channels and crevasse lobes). The geostatistical model of Figure 1 consists of channel sands and crevasse lobes. The crevasse lobes are systematically juxtaposed to the channels or at a very close distance from them. The net sand percentage is about 25%. We assigned the following horizontal permeability values: 1,000-md for channels, 10-md for the crevasse lobes, and 0.01-md for the background shale. Vertical permeabilities are 100-md for the channels and 0.1-md for the crevasse lobes.

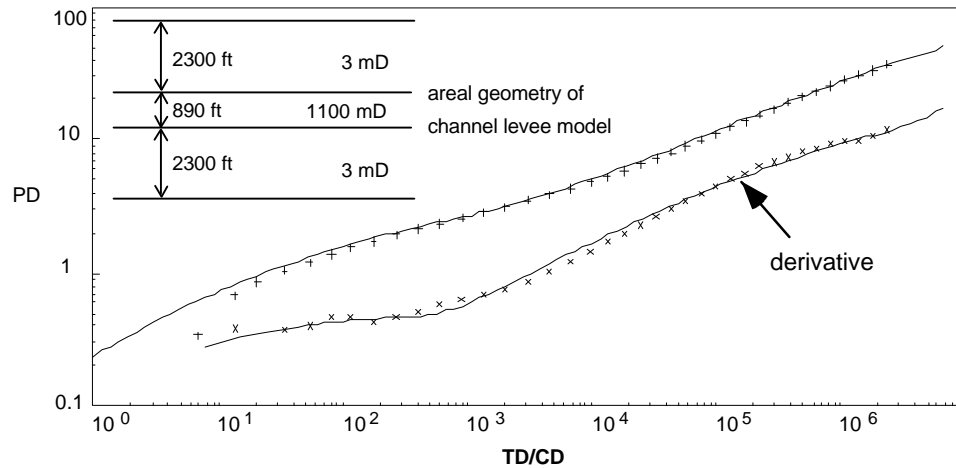


**Figure 2B:** Buildup/derivative plot for pressure; well test results simulated for heterogeneous model matched with a channel-levee type curve.

#### A.5.1.1 Analysis of the well-test response

Figures 2A through 2C show the results of a well test performed in the meandering channel penetrated by the well indicated in Figure 1. Figure 2A shows that pressure buildup is correlated strongly with the heterogeneity pattern and more pronounced in the southeast (lower right) corner of the reservoir. By use of channel/levee type-curves (Bourgeois et al., 1993), the buildup curve (Figure 2B) can be interpreted with a model consisting of a 1,100-md, 886-ft-wide channel bordered by two parallel low-permeability (3-md) levees. Figure 2C shows the geometry from this interpretation. The channel dimensions in the type-curve model are representative of the dimensions of the meandering channel in the geostatistical model. Note that a number of examples also exist where the type-curve interpretation may result in unrealistic channel dimensions (Massonnat et al., 1993). The low-permeability levees, however, represent the reservoir unit that is connected to this meandering channel through a limited number of moderate-permeability (10-md) crevasse lobes embedded in low-permeability (0.01-md) shale. Such connections are apparent in the cross section of the reservoir (Figure 1B). This example shows how a geostatistical model can be validated with an observed well-test response. The example also settles the apparent discrepancy between local-scale (core) permeabilities for the crevasses (10-md) versus an effective well-test permeability (3-md) of the parallel levees.

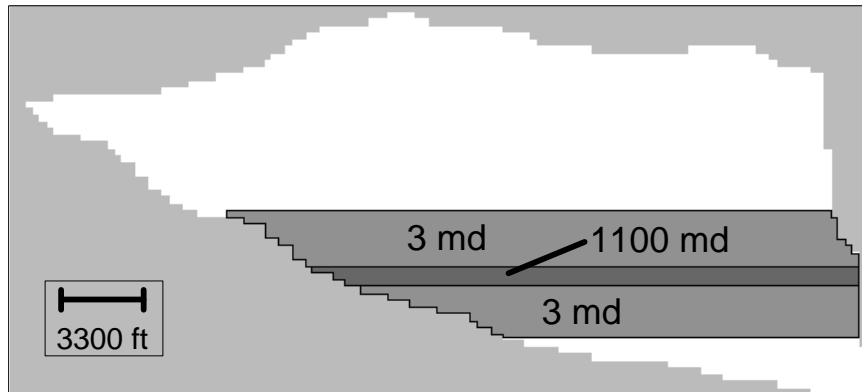


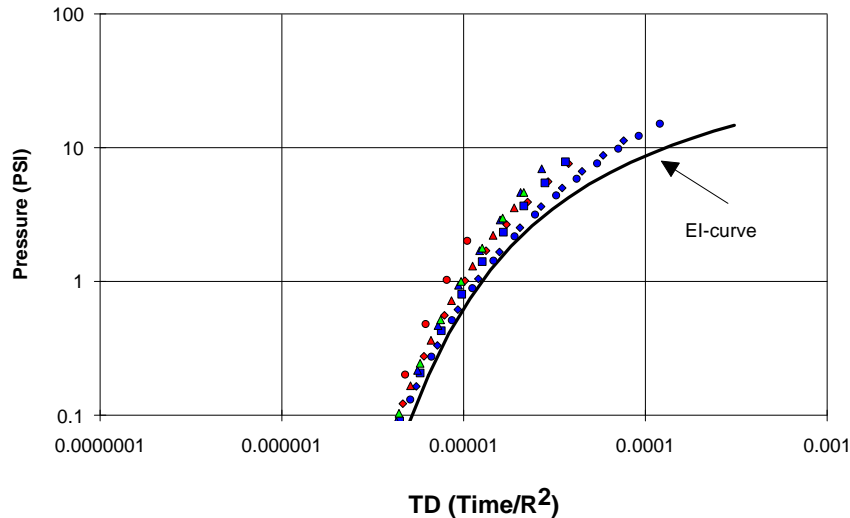
**Figure 2C:** Map view of geometry corresponding with matched channel-levee type curve of Figure 2B.

As discussed later in more detail, the effective well-test permeability obtained from the late-time well-test response can be largely influenced by connectivity. The 3-md value is a convolution of the true permeability of the crevasses (10-md), their limited occurrence parallel to the main channel within the background shale (0.01-md), and the geometrical pattern that lets them function as "bottle neck" connections between clusters of channel sands.

#### *A.5.1.2 Use of interference test to explore connectivity in a geostatistical model*

For an interference test that involves a single production well and multiple monitoring wells, the dimensionless interference responses of individual wells are identical for the case of a homogeneous reservoir. However, heterogeneity between the produced well and individual wells where interference is monitored may cause dissimilar interference responses (provided that porosity and fluid properties are constant). This dissimilarity is expressed in the onset of the interference response; the later part of the interference response reflects overall reservoir properties. Herweijer and Young (1990) give evidence that the dissimilar interference response is a useful characterization of connectivity and its effect on interwell flow patterns.

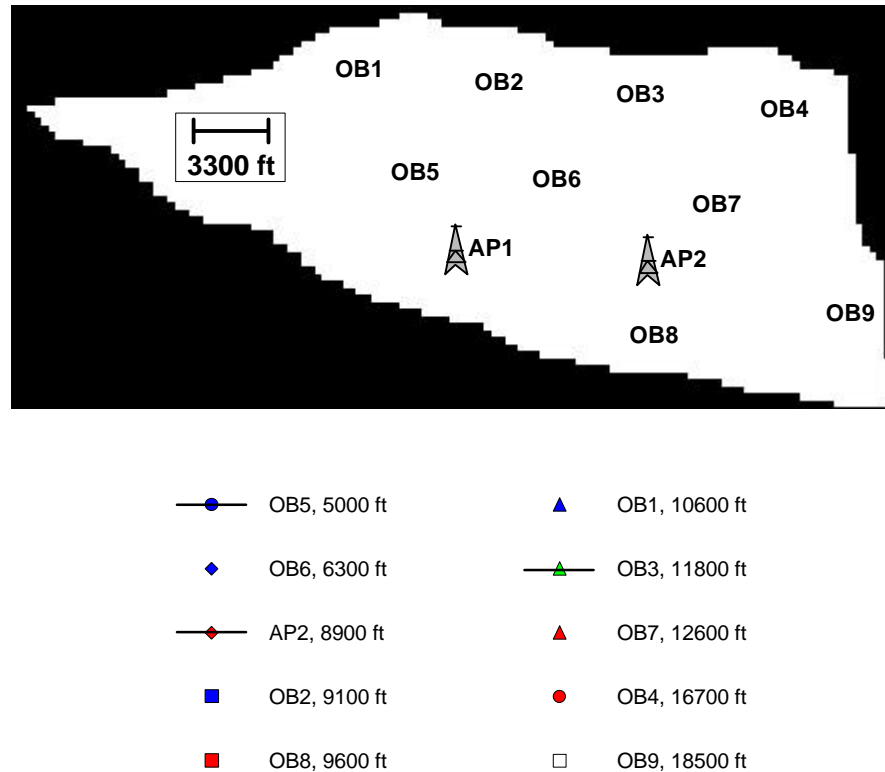
In oil reservoir engineering practice, systematic fieldwide interference testing is often impractical. In the context of heterogeneous geostatistical reservoir models, however, a simulated interference test can be applied to investigate the hydraulic



**Figure 4A:** Interference drawdown resulting from producing Well AP1; homogeneous model. See Figure 3 legend for well identification.

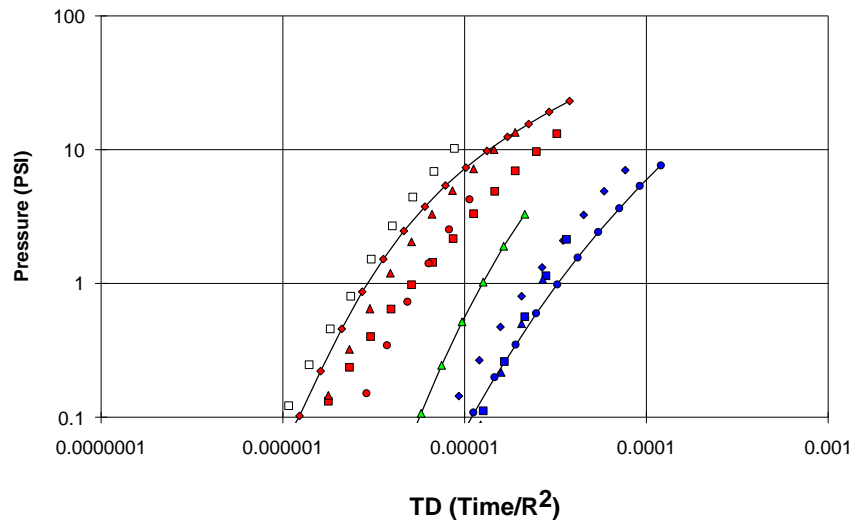
connectivity between wells. With this method, model realizations can be screened (and ranked) with respect to an important reservoir performance parameter directly related to connectivity, such as the breakthrough of injected water. The next section will discuss an application of a simulated interference test to the investigation of connectivity. This application pertains to the Boolean geostatistical model of a fluvial-deltaic reservoir (Figure 1), discussed earlier. Figure 3 shows a hypothetical well pattern for which the interference data were recorded during the same simulation that yielded the well test shown in Figure 2A through 2C. Production at Well AP1 is interrupted (for 7 days) and buildup is recorded for a set of hypothetical development wells (Well OB1 through Well OB9).

Figure 4A shows results for a completely homogeneous reservoir, disregarding the heterogeneity caused by the fluvial channels. Simulated pressures for Well AP2 and the Wells OB1 through OB9 are practically similar and are identical to the analytical solution for a homogeneous infinite reservoir (exponential/integral solution). The small deviations are caused by the boundary effects of the simulated case, which are not included in the analytical solution. Figure 4B shows simulated pressures for the heterogeneous case in Figure 1, thus including the fluvial channels. Owing to the different diffusivity caused by heterogeneous geometry and permeability, the buildup curves are scattered (shifted) over



**Figure 3:** Well pattern for simulated interference test; production stops at Well AP1. Distances in feet are distances from Well AP1.

more than one log-cycle of dimensionless time. Well OB5 is very close to the production well, Well AP1, but is the most poorly connected (the buildup curve ranks last on the dimensionless plot). Several wells that are much further away (e.g. Well AP2 and OB8) show a much earlier interference that translates into a much better connectivity. The reason is the direction of the fluvial channels, which favors connectivity to those wells, although they are not necessarily in exactly the same channel. Note also the earlier response in Well OB3 (relatively far away from the production well), which indicates a better connectivity compared with Well OB6 (relatively close to the production well in the same radial direction). Thus, the simulated interference test provides useful and nontrivial information about the effect of heterogeneity on fluid flow in the reservoir.



**Figure 4B:** Interference drawdown resulting from producing Well AP1; heterogeneous model. See Figure 3 legend for well identification.

### A.5.2 Case 2: Horizon modeled with a Gaussian image

Consider a drillstem test in a reservoir interval that is characterized by the permeability profile in Figure 5. Core permeabilities average 40-md (geometrical average). The question now arises about what can we expect for the effective well-test permeability. The assumption is that the permeability distribution can be represented by a spatial Gaussian field with a geometric mean of 40-md and a standard deviation of two orders of magnitude. Note that with such a distribution, 16% of the permeability values will be larger than ( $>$ ) 5,000-md. These unrealistically large values are all truncated to 5,000-md.

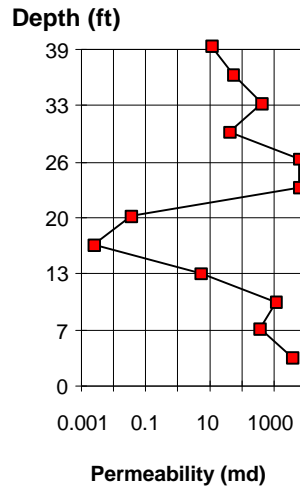


**Figure 5:** Well “core” data used to condition geostatistical model Case 2

Table 1 shows four options for the variogram parameters ranging from a large, anisotropic lateral continuity to a relatively short isotropic lateral continuity. Geologically, these options can be translated into a channelized valley fill, where the channels are either fairly continuous or relatively discontinuous as a result of rapid changes in their position and quick erosion after deposition. Figure 6 shows permeability patterns for different geological (lateral continuity) options. For each of the four geological (lateral continuity) options, the geostatistical model was run four times without changing the statistical parameters. Thus, within an option, the difference between realizations quantifies the

**Table 1:** Case 2 variogram parameters and well-test results

Option	Correlation Length (ft)			Well-Test Results		
	Horizontal North-South	Horizontal East-West	Vertical	Early-Time Permeability (md)	Late-Time Permeability (md)	Slope*
1	820	165	8.2	300 - 500	225 - 250	2
2	330	165	8.2	300 - 500	250 - 300	1 - 2
3	330	330	8.2	500 - 800	250 - 400	0
4	160	165	8.2	400 - 600	200 - 400	1 - 2

\* Number of realizations (per option) with largely sloping unstabilized derivative

**Table 2:** Core permeability averages for Case 2

Option	Average	Permeability (md)
1	Geometric average	40 md
2	Power average exponent $1/3$	420 md
3	Average $k_{\text{geo}}(1+1/6 \cdot \sigma_{\ln k}^2)$	180 md
4	Geological scenario A	180 md
5	Geological scenario B	920 md
6	Arithmetic average	1,200 md

uncertainty remaining after fixing the variogram. Between the options, extra variability is introduced by changing the in geostatistical (variogram) parameters. The model is a 12-layer, 3,675-ft closed square with 33-ft-long gridblocks.

#### A.5.2.1 The average permeability from "core" data

Table 2 lists several options to assess average permeability from the "core" data for the example well shown in Figure 5. The geometric average ( Option 1) is the widely used conservative choice that theoretically represents linear flow through a rectangle filled with random permeabilities that exhibit no spatial continuity. The power average (Option 2) with averaging exponent  $1/3$  follows the 3D generalization of Option 1 with the inclusion of spatial correlation (Desbarats, 1992a). The third expression was also derived for linear flow in spatially correlated media with a correlation length much smaller than the area of interest (Gutjahr et al., 1978; Dagan, 1979).

Geological averaging Scenarios A and B follow guidelines on mixing geometric and arithmetic averages based on lateral continuity inferred for geological facies (Weber

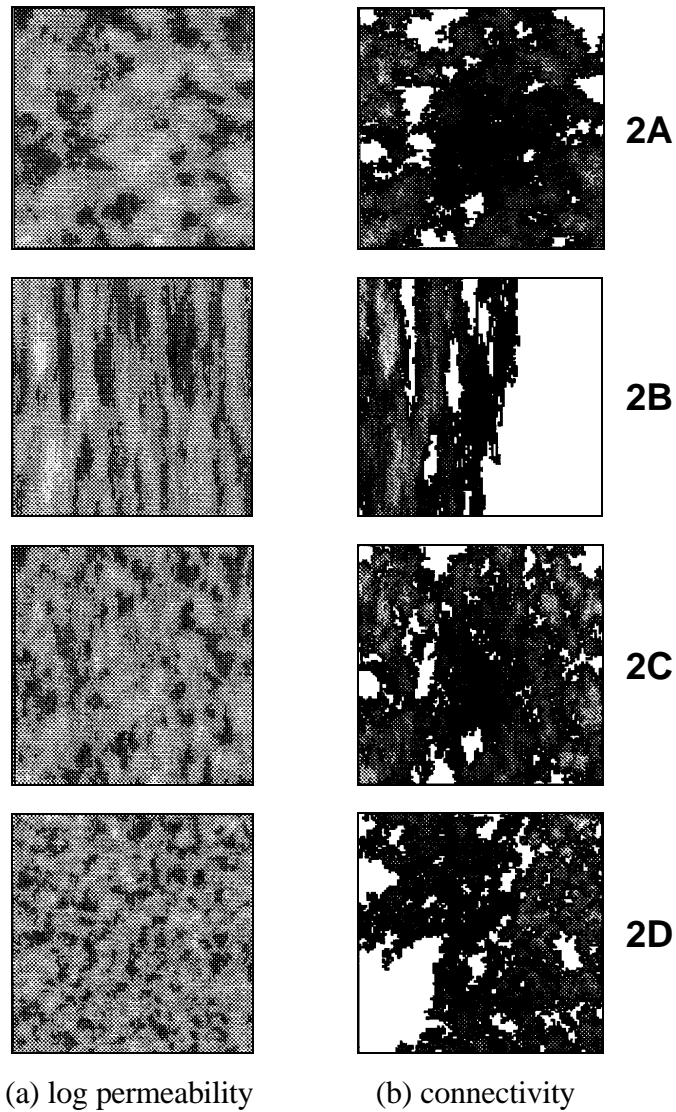


**Figure 6:** Maps (3675 ft by 3675 ft) for Cases 2A through 2 D of (a) permeability (dark is high) and (b) connectivity at 500-md threshold (dark is short connectivity length -- i.e., well connected).

and van Geuns, 1990). Scenario A (Option 4) splits the sequence in two zones (3.3 to 13 ft and 23 to 39 ft). Geological scenario B (Option 5) splits the sequence in three zones (3.3 to 13 ft, 23 to 27 ft, and 30 to 39 ft). Plugs within the zones are geometrically averaged, and the zone averages are arithmetically averaged (weighted by the zone thickness). This

represents an assumption, which has to be supported by geological evidence, of perfect lateral continuity for these zones.

Note that the expressions and methods applied to obtain the average permeabilities in Table 2 are not derived for transient radial flow in a bounded reservoir with a large permeability variation. Thus, comparing average permeabilities and effective well-test permeability is not justified theoretically. The comparison is useful in practice, however, because the well test is the only measure of large-scale effective permeability. The wide range of average values in Table 2 indicates that the choice of the averaging technique may be crucial when comparing core and well-test permeabilities. Therefore, this case offers large scope for use of a geostatistical model and well-test simulations to assess systematically the relationship between well-test permeability and the observed core permeabilities.

#### *A.5.2.2. Results of simulated well tests for Case 2*

Figure 7 shows the full range of variation of the pressure-derivative curves for the 16 realizations investigated for Case 2 (only four curves are plotted, all other curves fall in between). All realizations show an increasing trend of the pressure derivative until a unit slope (after 10 hours) indicates the full effect of the four reservoir limits. When interpreted with conventional type curves, the following models can be fitted: radial homogeneous with two intersecting limits, radial composite, and channel/levee (Bourgeois, 1993). All realizations represented by composite models show an early-time pressure-derivative stabilization that indicates a relatively high near-well permeability, and a late-time pressure-derivative stabilization that indicates a lower permeability. Some of the pressure-derivative curves for different geologic (lateral continuity) options overlap, whereas other realizations of the same geological option are significantly different.

Table 1 gives an overview of the permeability ranges for the early- and late-time stabilizations. All late-time stabilizations represent permeabilities between 200- and 400-md. This implies that sufficient paths exist in various radial directions to allow the pressure at the well to feel the boundaries before all the low-permeability zones are investigated. As a consequence, the effective well-test permeability represents the permeability along these paths (200- to 400-md) and does not represent low-permeability zones. Note that 38% of the total sand volume has a permeability greater than (>) 200-md and 33% has a

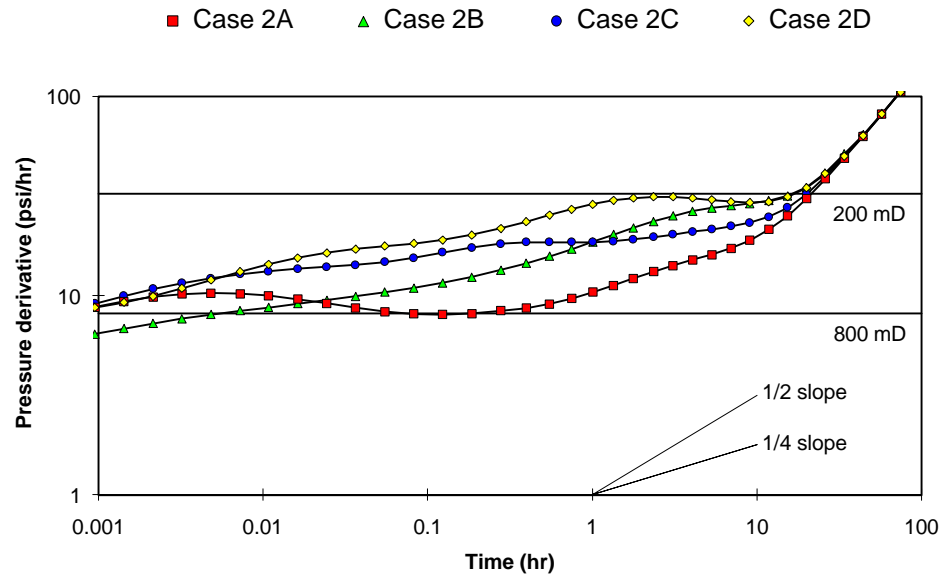


**Figure 7:** Pressure derivative for four selected realizations

permeability greater than ( $>$ ) 400-md. Apparently, a fraction in this range suffices to yield all flow to the well during the well test.

Early-time stabilizations yield a much larger variation of permeabilities, ranging from 300- to 800-md. The highest value for the near-well permeability (800-md) originates from the more strongly spatially correlated and spatially isotropic Option 3. This is in agreement with geological averaging Scenario B for the well core data (Table 2). As mentioned earlier, this scenario assumes perfect lateral continuity for the two high-permeability core-plugs at 23- and 26-ft (Figure 5). This condition is apparently matched by one of the realizations of Option 3, which yields an early-time stabilization of 800-md.

Several realizations show a nonstabilized constantly sloping derivative. This can be characterized by two idealized models: a model of relatively small concentric rings with decreasing permeability or a channel/levee model with a relatively small channel. Most of these nonstabilized, constantly sloping derivatives occur for the anisotropic geologic (lateral-continuity) Options 1 and 2 (Table 1). For these cases, linear flow is the most likely, and logical, explanation of this pressure-derivative signature. Note, however, that practically stabilized derivatives also occur for the strongest anisotropic geological option (Option 1). Thus, a constantly sloping, nonstabilized derivative cannot be considered to be a unique derivative signature for strong channelized anisotropy. The other option with a

constantly sloping derivative occurs is Option 4 (very limited, isotropic lateral continuity). In this case, the most likely suitable idealized model consists of multiple concentric rings, none of which are persistent enough to dominate radial flow for a sufficient time to result in derivative stabilization.

#### *A.5.2.3 Average permeability and influence of connectivity*

Most well-test responses simulated for Case 2 allow determination of a near well permeability (on the basis of early-time derivative stabilization), and a far-field permeability (on the basis of late-time derivative stabilization). The question arises whether these effective well-test permeabilities can be linked to trends of a 3D volume average of the permeability field. The following section illustrates the relationship among effective well-test permeability, the 3D volume permeability average of the permeability field, and connectivity. The analysis is limited to the four cases shown in Figure 7 (Cases 2A through 2D), chosen across the different geologic (spatial continuity) options (Figure 6 and Table 1).

For each of these four cases, the underlying permeability field is averaged as follows. Within a rectangular averaging zone, the permeabilities are geometrically averaged for each layer individually, and the individual layer results are arithmetically averaged. The procedure is repeated for several rectangular zones with an increasing size. The purpose of this averaging procedure is to test to what extent the trend in the pressure derivative from the well test is caused by trends in the permeability field\*. Figure 8 shows the trend of permeability with radial distance calculated as discussed earlier. Note that the plot is scaled to a time scale similar to that used for the drawdown derivative plot (Figure 7). We conducted the radial-distance to time conversion using the conventional radius-of-influence formula, assuming a 500-md effective permeability.

---

\* Personal communication with B. Noetinger, Institute Francais du Petrole, Pau, France.

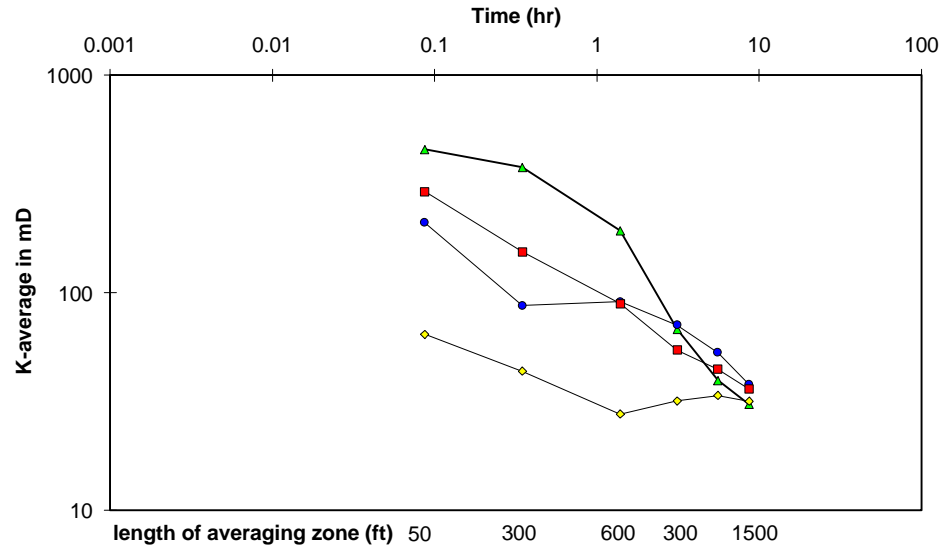


**Figure 8:** Three-dimensional average permeability (see Figure 7 for legend)

To some extent the trends for the average permeability reflect the derivative trends shown in Figure 7. All averages show a trend from a high near-well permeability to a low far-field permeability. Case 2B shows the largest permeability contrast that persists for the largest zone, a phenomenon that is corroborated by the sloping derivative that has the lowest values of all derivatives at the beginning of the well test. The averages within a 656-ft zone around the well properly rank Case 2A through 2C with respect to the permeability level that is associated with the early-time (0.1 hour) derivative stabilization (Table 1 and Figure 8).

To understand the differences in derivative signature for the cases selected (2A through 2D) further, the connectivity (Alabert and Modot, 1993) of permeability field was studied. Figure 6 shows maps of vertically averaged permeability and connectivity for a 500-md threshold for the four selected cases of Figure 7. Connectivity ( $1/\text{length}$ ) for a 500-md threshold implies that cells below this threshold are voided, and subsequently the shortest path to the well is calculated for each remaining cell. This connectivity fully explains the differences in derivative signature. All four selected cases show a complete connectivity at a 250-md threshold and virtually no connectivity at a 1,000-md threshold (Figure 6 does not show either of these connectivity thresholds). The 500-md connectivity threshold is a logical choice given the 300- to 900-md range of average permeabilities that is calculated from the well data alone (Table 2).

Case 2A and 2C (Figure 6) show complete connectivity at the 500-md threshold level, which explains the radial flow pattern and the well-test permeability greater than 500-md. Case 2A shows a slightly larger zone of high connectivity values directly surrounding the well. This explains the lower stabilization level of the derivative for this case compared with the derivative belonging to Case 2C (Figure 7). Note, however, that crossflow may also be the cause. The connectivity for Case 2B (Figure 6) corroborates the sloping derivative representing bilinear flow. A highly connected "channel" zone occurs that is indirectly connected to one side and unconnected (at the 500-md level) to the other side of the reservoir. Case 2D shows that one corner of the reservoir is totally unconnected (at the 500-md level), causing a transition to a lower (<500-md) permeability stabilization halfway through the test.

#### *A.5.2.4 Discussion Case 2*

A simple geostatistical model realistically reproduces common discrepancies between core permeabilities and effective well-test permeabilities. Connectivity appears to be a major parameter. Buildup occurring during the transient well test is related to a minority portion of the high-permeability connected sands, which contributes most of the flow during the limited timespan of the well-test (before the boundary effect becomes obvious). As a consequence, most of the low-permeability sands are not investigated; therefore, the effective well-test permeability is higher than expected from volume averaging. The case described involves closed boundaries, and the results presented are expected to be sensitive to boundary conditions.

A simple 3D average (geometric horizontal followed by arithmetic vertical) approximately predicts the near-well effective well-test permeability. In combination with maps of connectivity for different permeability thresholds, the full well-test response can be predicted. These criteria could be used to apply geostatistical inversion of well tests (Deutsch, 1992; Sagar et al., 1993) to 3D cases with high-permeability contrasts as discussed earlier. Note, however, that further research is required to generalize the approach we have suggested.

## A.6 CONCLUSIONS

1. The single-phase pressure-transient simulation is an excellent tool for getting an early understanding of the complex relationship between sedimentological heterogeneity and fluid flow in a reservoir.
2. A 3D geostatistical model can be validated using well-test data (or indirectly by use of the interpretation results). The potential exists to narrow the uncertainty range through rejection of realizations that do not fit field-observed well-test results (or interpretations).
3. Realizations with the same lateral-continuity parameters may have very different well-test responses. However, realizations with very different lateral-continuity parameters may have very similar well test responses. Thus, the use of well tests to assess lateral continuity uniquely is limited. We stress that the range of lateral-continuity parameters should be considered when a geostatistical model is systematically compared with a well-test response.
4. Pressure transients can be used to screen a geostatistical model to determine high permeability connections, consisting of more than one sand-body, that act as a thief zone.
5. For a geostatistical model of a highly heterogeneous reservoir with closed boundaries, the effective well-test permeability was assessed successfully for early-time with a spatial volume average of permeabilities within a "zone of influence" (geometric within layers, followed by vertical arithmetic) and with a permeability related to a connectivity threshold for late-time (before boundary effects are visible).
- 6.. Combining the geostatistical model with a simulated well test allows the discrepancy between core permeabilities and effective well-test permeability to be explained quantitatively in terms of connectivity.

**NOMENCLATURE**

- $c_D$  = dimensionless compressibility  
 $k_{geo}$  = geometrical average of permeability, L<sup>2</sup>, md  
 $p_D$  = dimensionless pressure  
 $r$  = radial distance between wells, L  
 $t$  = time, t  
 $t_D$  = dimensionless times  
 $s_{ink}$  = standard deviation of distribution of natural log of permeability

**ACKNOWLEDGMENTS**

We thank the management of Elf Aquitaine Production for permission to publish this paper and recognize the contributions of the following colleagues: Pierre Biver and Francois Petit of Elf for the Boolean model of Case 1; Jean Luc Bouteaud de la Combe of Elf, Kirk Hird of Amoco, and Robert Bissell of Elf, for fruitful discussions and their careful review of this manuscript; and the Commission of European Communities for funding the work of the first author within the framework of the JOULE I research program.

**SI METRIC CONVERSION FACTOR**

md x 9.869 233	E - 04 = $\mu\text{m}^2$
ft x 3.048	E - 01 = m
psi x 6.894 57	E + 00 = kPa

## REFERENCES

- Ababou, R., 1991, Identification of effective conductivity tensor in randomly heterogeneous and stratified aquifers, Proceedings of the 5th Annual Canadian American Conference on Hydrogeology, September 18-20, 1990, Calgary, NWWA, Dublin (Ohio).
- Ababou, R., and Wood, E.F., 1990, Comment on - 'Effective groundwater model parameter values - Influence of spatial variability of hydraulic conductivity, leakance and recharge, by J.J. Gomez Hernandez and S.M. Gorelick': Water Resources Research, v. 26, p. 155-157.
- Ababou, R.; Bagtzoglou, A.C.; and Wood, E.F., 1994, On the condition number of covariance matrices in Kriging, estimation and simulation of random fields: Mathematical Geology, v. 26, no. 1.
- Adams, E.E., and Gelhar, L.W., 1992, Field study of dispersion in a heterogeneous aquifer - 2-Spatial moments analysis: Water Resources Research, v. 28, no. 12, p. 3293-3307.
- Akindunni, F.F., 1987, Effect of the capillary fringe on unconfined aquifer response to pumping numerical simulations: Waterloo, Ontario, Canada, University of Waterloo, M.Sc. Thesis.
- Alabert, F.G., 1989, Constraining description of randomly heterogeneous reservoirs to pressure test data - A Monte Carlo study: SPE paper 19600 presented at the 1989 SPE Annual Technological Conference and Exhibition, San Antonio, Tex., October 8-11, 1989.
- Alabert, F.G., and Massonat, G.J., 1990, Heterogeneity in a complex turbiditic reservoir - Stochastic modelling of facies and petrophysical variability: SPE paper 20604 presented at the 1990 SPE Annual Technological Conference and Exhibition, New Orleans, La., September 23-26.
- Alabert, F.G., and Modot, V.M., 1992, Stochastic models of reservoir heterogeneity - Impact on connectivity and average permeabilities: SPE paper 24893 presented at the 1992 SPE Annual Technological Conference and Exhibition, Washington, D.C., October 4-7.
- Alpay, O.A., 1972, A practical approach to defining reservoir heterogeneity: Journal of Petroleum Technology, July.
- Arya, A., 1986, Dispersion and reservoir heterogeneity: Austin, University of Texas, Ph.D. dissertation.
- Barker, J.A., and Herbert, R., 1982, Pumping tests in patchy aquifers: Ground Water, v. 20, no. 2, p. 150-155.
- Boggs, J.M., and Adams, E.R., 1992, Field study of dispersion in a heterogeneous aquifer- 4-Investigation of adsorption and sampling bias: Water Resources Research, v. 28, no. 12, p. 3325-3336.
- Boggs, J.M.; Young, S.C.; Benton, D.J.; and Chung, Y.C., 1990, Hydrogeologic characterization of the MADE site: Electric Power Research Institute Interim Report EN-6915, Standford, Calif..
- Boggs, J.M.; Young, S.C.; Beard, L.M.; Gelhar, L.W.; Rehfeldt, K.R.; and Adams, E.R., 1992, Field study of dispersion in a heterogeneous aquifer - 1- Overview and Site Description: Water Resources Research, v. 28, no. 12, p. 3281-3291.
- Boulton, N.S., 1954, The drawdown of the water-table under non-steady conditions near a pumped well in an unconfined formation: *in* Proceedings Institute Civil Engineering, Part 3, p. 564-579.
- Boulton, N.S., 1963, Analysis of data from non-equilibrium pumping tests allowing for delayed yield from storage: *in* Proceedings Institute Civil Engineers, v. 26, p. 469-482.
- Bourdet, D.; Ayoub, J.A.; and Pirard, Y.M., 1989, Use of pressure derivative in well test interpretation: SPE Formation Evaluation, June.
- Bourgeois, M.J.; Daviau, F.H.; and Bouteaud de la Combe, J.L., 1993, Pressure behavior in finite channel-levee complexes: SPE paper 26461 presented at the 1993 SPE Annual Technological Conference and Exhibition, Houston, Tex., October 3-6, 1993.
- Bryant, I.D., and Flint, S.S., 1993, Quantative clastic reservoir geological modeling - Problems and perspectives, *in* The Geological model of hydrocarbon reservoirs and outcrop analogues: Special Publication of the International Association of Sedimentologists, no. 15, p. 3-20.

- Budding, M.C.; Eastwood, K.M.; Herweijer, J.C.; Livera, S.E.; Paardekam, A.H.M.; and Regtien, J.J.M., 1988, Probabilistic modeling of discontinuous reservoirs: Proceedings 17th Annual Convention of the Indonesian Petroleum Association, Jakarta, October 25-27, 1988.
- Burrough, P.A., 1983a, Multiscale sources of spatial variation in soil I - An application of fractal concepts to nested levels of soil variation: *Journal of Soil Science*, v. 34, p. 577-597.
- Burrough, P.A., 1983b, Multiscale sources of spatial variation in soil II - A non-Brownian fractal model and its application in soil survey: *Journal of Soil Science*, v. 34, p. 599-620.
- Butler, J.J., Jr., 1986, Pumping tests in non-uniform aquifers - A deterministic/stochastic analysis: Stanford, Calif., Stanford University, Ph.D. dissertation.
- Butler, J.J., Jr., 1988, Pumping in non-uniform aquifers - The radially symmetric case: *Journal of Hydrology*, v. 101, p. 15-30.
- Butler, J.J., Jr., 1990, The role of pumping tests in site characterization - Some theoretical considerations: *Ground Water*, v. 28, no. 3, p. 394-402.
- Butler, J.J., Jr., and Liu, W., 1991, Pumping tests in non-uniform aquifers - The linear strip case: *Journal of Hydrology*, v. 128, p. 69-99.
- Collinson, J.D., and Thompson, D.B., 1989, *Sedimentary Structures*: Unwin Hyman, p. 160.
- Cooper, H.H., and Jacob, C.E., 1946, A generalized graphical method for evaluating formation constants and summarizing well-field history: *Transactions of the American Geophysical Union*, No. 217, p. 626-534.
- Dagan, G., 1979, Models of groundwater flow in statistically homogeneous porous formations: *Water Resources Research*, v. 15, no. 1, p. 47-63
- Dagan, G., 1986, Statistical theory of groundwater flow and transport - Pore to laboratory, laboratory to formation, and formation to regional scale: *Water Resources Research*, v. 22, no. 9, p.120S-134S.
- Dagan, G., 1989, *Flow and transport in porous formatio*: Berlin, Springer Verlag.
- Damsleth, E.; Tjolsen, C. B.; and Omre, K. H., 1990, A two stage stochastic reservoir model applied to a North sea reservoir: SPE paper 20605 presented at the 1990 SPE Annual Technological Conference and Exhibition, New Orleans, La., September 23-26.
- Davis, J.M.; Colarullo, S.J.; Philips, F.M.; and Lohmann, R.C., 1991, Alluvial aquifer heterogeneities in the Rio Grande Valley - Implications for groundwater contamination: New Mexico Water Resources Research Institute Technical Completion Report, No. 256, 111 p.
- Desbarats, A.J., 1987, Numerical estimation of effective permeability in sand-shale formations: *Water Resources Research*, v. 23, no. 2, p. 273-286.
- Desbarats, A.J., 1990, Macro-dispersion in sand-shale sequences: *Water Resources Research*, v. 26, no. 1, p. 153-163.
- Desbarats, A.J., 1991, Reply to comment on 'Macro-dispersion in sand-shale sequences': *Water Resources Research*, v. 27, no. 1, p. 141-143.
- Desbarats, A.J., 1992a, Spatial averaging of hydraulic conductivity in three-dimensional heterogeneous porous media: *Mathematical Geology*, v. 24, no. 3, p. 249-267.
- Desbarats, A.J., 1992b, Spatial averaging of transmissivity in heterogeneous fields with flow towards a well: *Water Resources Research*, v. 28, no. 3, p. 757-767.
- Desbarats, A.J., 1994, Spatial averaging of hydraulic conductivity under radial flow conditions: *Mathematical Geology*, v. 26, no.1, p. 1-21.
- Desbarats, A.J., and Srivastava, R.M., 1991, Geostatistical characterization of groundwater flow parameters in a simulated aquifer: *Water Resources Research*, v. 27, no. 5, p. 687-698.

- Deutsch, C.V., 1992, Annealing techniques applied to reservoir modeling and the integration of geological and engineering (well test) data: Stanford, Calif., Stanford University, Ph.D. dissertation.
- Deutsch, C.V., and Journel, A.G., 1992, GSLIB - Geostatistical software library and user's guide: Oxford University Press.
- Domenico, P.A., and Schwartz, F.W., 1990, Physical and chemical hydrogeology: New York, John Wiley & Sons, 824 pp.
- Doyle, J.D., and Sweet, M.L., 1995, Three-dimensional distribution of lithofacies, bounding surfaces, porosity, and permeability in a fluvial sandstone - Gypsy sandstone of Northern Oklahoma: American Association of Petroleum Geologists Bulletin, v. 79, no. 1, p. 70-96.
- Earlougher, R.C., 1977, Advances in well test analysis: New York/Dallas, Society of Petroleum Engineers of AIME.
- Ehlig-Economides, C., 1988, Use of the pressure derivative for diagnosing pressure-transient behavior: Journal of Petroleum Technology, October, p. 1280-1282.
- Ehlig-Economides, C.; Joseph, J.A.; Ambrose, R.W., Jr.; and Norwood, C., 1990, A modern approach to reservoir testing: Journal of Petroleum Technology, December, p. 1554-1563.
- Emanuel, A.S.; Behrens, R.A.; and Hewett, T.A., 1987, Reservoir performance prediction methods based on fractal geostatistics: SPE paper 16971 presented at the 1988 SPE Annual Technological Conference and Exhibition, Dallas, Tex., September 27-30.
- Eype, R., and Weber, K.J., 1971, Mini permeameters for consolidated and unconsolidated sand: American Association of Petroleum Geologists Bulletin, v. 55, no. 2, p. 307-309.
- Fasanino, G.; Molinard, J.E.; Marsily, G. de; and Pelce, V., 1986, Inverse modeling in gas reservoirs: SPE paper 15592 presented at the 1986 SPE Annual Technological Conference and Exhibition, New Orleans, La., October 5-8.
- Faust, C.R., and Mercer, J.W., 1984, Evaluation of slug tests in wells containing a finite-thickness skin: Water Resources Research, v. 20, no. 2, p. 504-506.
- Fielding, C.R., and Crane, R.C., 1987, Application of statistical modeling to the prediction of hydrocarbon recovery factors in fluvial reservoir sequences: St. Lucia, Australia, The Society of Economic Paleontologists and Mineralogists, Department of Geology and Mineralogy, University of Queensland.
- Freeze, R.A., and Cherry, J.A., 1979, Groundwater: Englewood Cliffs, NJ, Prentice-Hall.
- Freyberg, D.L., 1986, A natural gradient experiment on solute transport in a sand aquifer - 2-Spatial moments and the advection and dispersion of nonreactive tracers: Water Resources Research, v. 22, no. 13, p. 2031-2046.
- Fried J.J., 1979, Groundwater pollution: Elsevier.
- Frind, E.O.; Sudicky, E.A.; and Schellenberg, S.L., 1987, Micro-scale modeling in the study of plume evolution in heterogeneous media: Stochastic Hydrology and Hydraulics, v. 1, p. 241-262.
- Garabedian, S.P.; LeBlanc, D.R.; Gelhar, L.W.; and Celia, M.A., 1991, Large-scale natural gradient tracer test in sand and gravel, Cape-Cod, Massachusetts - 2-Analysis of spatial moments for non-reactive tracer: Water Resources Research, v. 27, no. 15, p. 911-924.
- Gelhar, L.W., 1982, Analysis of two-well tracer tests with a pulse input: U.S. DOE Report no. RHO-BW-131, Richland, Wash., Rockwell International.
- Gelhar, L.W., 1986, Stochastic subsurface hydrology - From theory to applications: Water Resources Research, v. 22, no. 9, p. 135S-145S.
- Gelhar, L.W., and Axness, C.L., 1983, Three-dimensional stochastic analysis of macrodispersion in aquifers: Water Resources Research, v. 19, no. 1, p. 161-180.

- Gelhar, L.W., and Collins, M.A., 1971, General analysis of longitudinal dispersion in non-uniform flow: *Water Resources Research*, v. 7, no. 6, p. 1511-1521.
- Gelhar, L.W.; Welty, C.; and Rehfeldt, K.R., 1992, A critical review on field-scale dispersion in aquifers: *Water Resources Research*, v. 28, no. 7, p. 1955-1974.
- Giudicelli, C.B.; Alabert, F.G.; Massonat, G.J.; and Corre, B., 1992, Anguille marine, a deep-sea fan reservoir offshore Gabon - From stochastic modeling towards history matching: SPE paper 24894 presented at the 1992 SPE Annual Technological Conference and Exhibition, Washington, D.C., October 4-7.
- Goggin, D.J.; Chandler, M.A.; Kocurek, G.A.; and Lake, L.W., 1986, Patterns of permeability in Eolian deposits: SPE paper 14893 presented at the SPE/DOE 5th Symposium on Enhanced Oil Recovery, Tulsa, Okla., April 20-23, 1986.
- Gomez Hernandez, J.J., 1991, A stochastic approach to the simulation of block conductivity fields conditioned upon data measured at a smaller scale: Stanford, Calif., Stanford University, Ph.D. dissertation.
- Gomez Hernandez, J.J., and Cassiraga, E.F., 1992 [1993], Theory and practice of sequential simulation, *in* Armstrong, M., and Dowd, P., eds., *Proceedings of Geostatistical Simulation Workshop*, Fontainebleau, France, May 27-28: Kluwer.
- Goode, D.J., and Konikow, L., 1990, Apparent dispersion in transient groundwater flow: *Water Resources Research*, v. 26, no. 10, p. 2339.
- Goode, D.J., and Shapiro, A M., 1991, Comment on 'Macro-dispersion in sand-shale sequences' by A. J. Desbarats: *Water Resources Research*, v. 27, no. 1, p. 135-139.
- Gringarten, A.C., 1982, Flow-test evaluation of fractured reservoirs, *in* Narasimhan, T.N., ed., *Recent Trends in Hydrogeology*: Boulder, Colo., The Geological Society of America.
- Gutjahr, A.L.; Gelhar, L.W.; Bakr, A.; and McMillan, J.R., 1978, Stochastic analysis of spatial variability in subsurface flows - 2- Evaluation and application: *Water Resources Research*, v. 14, no. 5, p. 953-959.
- Haas, A., and Dubrule, O., 1994, Geostatistical inversion - A sequential method of stochastic reservoir modelling constrained by seismic data: *First break*, v. 12, no. 11, p. 561.
- Haldorsen, H.H., and Lake, L.W., 1982, A new approach to shale management in field scale simulation models: SPE paper 10976 presented at the 1982 SPE Annual Technological Conference and Exhibition, New Orleans, La., September 26-29.
- Haldorsen, H.H., and MacDonald, C.J., 1987, Stochastic modeling of reservoir facies (SMURF): SPE paper 16751 presented at the 1987 SPE Annual Technological Conference and Exhibition, Dallas, Tex., September 27-30.
- Haley, J.L.; Hanson, B.; Enfield, C.; and Glass, J., 1991, Evaluating the effectiveness of groundwater extraction systems: *Ground Water Monitoring Review*, Winter 1991, p. 119-124.
- Hemker, C.J., 1984, Steady groundwater flow in leaky multiple-aquifer systems: *Journal of Hydrology*, v. 72, no. 3-4, p. 355-374.
- Hemker, C.J., and Maas, C., 1987, Unsteady flow to wells in layered and fissured aquifer systems: *Journal of Hydrology*, v. 90, p. 231-249.
- Herweijer, J.C., 1989, WELPLAN - A computer program for geostatistical analysis and optimization of a well network: Memorandum to S.C. Young, TVA, Norris, Tenn.
- Herweijer, J.C.; Luijn, G.A. van; and Appelo, C.A.J., 1990, Calibration of a mass transport model using environmental Tritium: *Journal of Hydrology*, v. 78, p. 1-17.

- Herweijer, J.C.; Hocker, C.F.W.; and Williams, H., 1990, The relevance of dip profiles from outcrops as reference to the interpretation of SHDT dips, *in* Hurst, C.A., and Lovell, M.A., Geological application of wireline logs: Geological Society Special Publication, no. 48, p. 39-43.
- Herweijer, J.C., and Young, S.C., 1991, Use of detailed sedimentological information for the assessment of aquifer tests and tracer tests in a shallow fluvial aquifer: Proceedings of the 5th Annual Canadian American Conference on Hydrogeology, Calgary, September, 18-20, 1990. NWWA, Dublin (Ohio).
- Hewett, T.A., 1986, Fractal distributions of reservoir heterogeneity and their influence on fluid transport: SPE paper 15386 presented at the 1986 SPE Annual Technological Conference and Exhibition, New Orleans, La., October 5-8.
- Hocker, C.F.W.; Eastwood, K.M.; Herweijer, J.C.; and Adams, J.T., 1990, The use of SHDT data in sedimentological studies: American Association of Petroleum Geologists Bulletin, v. 74, no. 2, p. 105-118.
- Huijzer, G.P., 1992, Quantitative penetrostratigraphic classification: Amsterdam, Free University, Ph.D. dissertation.
- Isaaks, E.H., and Srivastava, R.M., An introduction to applied geostatistics: Oxford University Press.
- IFP (Institute FranHais de Petrole), 1990, HERESIM: integrated model for computer aided reservoir description: Rueill, France, Institute FranHais de Petrole.
- Indelman, P., and Dagan, G., 1993a, Upscaling of permeability of anisotropic heterogeneous formations -1- The General Framework: Water Resources Research, v. 29, no. 4, p. 917.
- Indelman, P., and Dagan, G., 1993b, Upscaling of permeability of anisotropic heterogeneous formations -2- General structure and small perturbation analysis: Water Resources Research, v. 29, no. 4, p. 925.
- Indelman, P., and Dagan, G., 1993c, Upscaling of conductivity of heterogeneous formations - General approach and application to isotropic media: Transport in Porous Media, v. 12, no. 2, p. 161.
- Jacob, C.E., 1963, Determining the permeability of water table aquifers: U.S. Geological Survey Water Supply Professional Paper 1563-I.
- Johnson, N.M., and Dreiss, S., 1989, Hydrostratigraphic interpretation using indicator geostatistics: Water Resources Research, v. 25, no. 12, p. 2501-2510.
- Jordan, D.W., and Pryor, W.A., 1992, Hierarchical levels of heterogeneity in a Mississippi River meander belt and application to reservoir systems: American Association of Petroleum Geologists Bulletin, v. 76, no. 10, p. 1601.
- Joseph, P.; Hu, L.Y.; Dubrule, O.; Claude, D.; Crumerolle, P.; Lesseur, J.L.; and Soudet, H.J., 1993, The Roda deltaic complex (Spain) - From sedimentology to reservoir stochastic modeling, *in* Eschard, R., and Dolignez, B., Subsurface reservoir characterization from outcrop observations: Paris, Technip.
- Journel, A.G., and Huijbregts, C., 1978, Mining Geostatistics: London, Academic Press.
- Journel, A.G., and Alabert, F.G., 1988, Focusing on spatial connectivity of extreme-valued attributes - Stochastic indicator models of reservoir heterogeneities: SPE paper 18324 presented at the 1988 SPE Annual Technological Conference and Exhibition, Houston, Tex., October 2-5.
- Journel, A.G.; Deutsch, C.V.; and Desbarats, A.J., 1986, Power averaging for block effective permeability: - SPE 15128.
- Jussel, P., 1992, Modeling solute transport in homogeneous aquifers: Zurich, Eidgenossische Technische Hochschule (ETH), Ph.D. dissertation, p. 323. [In German].

- Jussel, P.; Stauffer, F.; and Dracos, T., 1994a, Transport modeling in heterogeneous aquifers - 1-Statistical description and numerical generation of gravel deposits: *Water Resources Research*, v. 30, no. 6, p. 1803.
- Jussel, P.; Stauffer, F.; and Dracos, T., 1994b, Transport modeling in heterogeneous aquifers - 1-Three-dimensional transport model and stochastic numerical tracer experiments: *Water Resources Research*, v. 30, no. 6, p. 1819.
- Keijzer, J.H., and Kortekaas, T.F.H., 1990, Comparison of deterministic and probabilistic simulation models of channels sands in the Staffjord reservoir Brent field: SPE paper 22342 presented at EUROPEC90, The Hague, October, 1990.
- King, P.R., 1989, The use of renormalization for calculating effective conductivity: *Transport in Porous Media*, v. 4, p. 37-58.
- King, P.R.; Muggeridge, A.H.; and Price, W.G., 1993, Renormalization calculations of immiscible flow: *Transport in Porous Media*, v. 12, p. 237-260.
- King Hubbert, M., 1941, Discussion of papers by Messers. Jacob and Guyton: *Transactions of the American Geophysical Union*, v. 22, p. 770-772.
- Koltermann, C.E., and Gorelick, S.M., 1992, Paleoclimatic signature in terrestrial flood deposits: *Science*, v. 256, p. 1775-1782.
- Kruseman, G.P., and Ridder, N.A. de, 1990, Analysis and evaluation of pumping test data: International Institute for Land Reclamation and Improvement, Publication 47, The Netherlands, Wageningen.
- LeBlanc, D.R.; Garabedian, S.P.; Hess, K.; Gelhar, L.W.; Quadri, R.D.; Stollenwerk, K.G.; and Wood, W.W., 1991, Large-scale natural gradient tracer test in sand and gravel (of) Cape-Cod, Massachusetts - 1-Experimental design and observed tracer movement: *Water Resources Research*, v. 27, no. 15, p. 895-910.
- Leeder, M.R., 1973, Fluvial fining-upwards cycles and the magnitude of paleo channels: *Geological Magazine*, v. 110, p. 265-276.
- Levey, R.A., 1978, Bed-form distribution and internal stratification of coarse grained pointbars(of) Upper Congaree River, S.C., in Miall, A.D., ed., *Fluvial Sedimentology*: Canadian Society of Petroleum Geologists, p. 105-127.
- Liu, W., and Butler, J.J., Jr., 1990, Software for the evaluation of analytical and semi-analytical solutions for pumping induced drawdown in complex geologic settings: *Kansas Geological Survey Computer Program Series 90-4*, p. 52.
- Lorenz, J.C.; Heinze, D.M.; Clark, J.A.; and Searls, C.A., 1985, Determination of widths of meander-belt sandstone reservoirs from vertical downhole data (of) Mesaverde group, Piceance Creek Basin, Colorado: *American Association of Petroleum Geologists Bulletin*, v. 69, no. 5, p. 710-721.
- Mackay, D.M.; Freyberg, D.L.; Roberts, P.V.; and Cherry, J.A., 1986, A natural gradient experiment on solute transport in a sand aquifer - 1-Approach and overview of plume movement: *Water Resources Research*, v. 22, no. 13, p. 2017-2029.
- Mandelbrot, B.B., 1967, How long is the coast of Britain - Statistical self-similarity and fractional dimension: *Science*, v. 156, p. 636-638.
- Marsily, G. de, 1986, *Quantitative hydrogeology*: London, Academic Press, 440 pp.
- Marsily, G. de; Lavedan, G.; Boucher, M.; and Fasanino, G., 1984, Interpretation of interference tests in a well field using geostatistical techniques to fit the permeability distribution in a reservoir model, in Verly, G., et al., *Geostatistics for natural resources characterization - Part 2: The Netherlands*, Reidel Publishing, p. 831-849.

- Massonat, G.J., and Bandiziol, D., 1991, Interdependence between geology and well test interpretation: SPE paper 22740 presented at the 1991 SPE Annual Technological Conference and Exhibition, Dallas, Tex., October 6-9.
- Massonat, G.J.; Norris, R.J.; and Chalmette, J.C., 1993, Well test interpretation in geologically complex channelized reservoirs: SPE paper 26464 presented at the 1993 SPE Annual Technological Conference and Exhibition, Houston, Tex., October 3-6.
- Matheron, G., 1967, Composition des permeabilites en milieux poreux heterogene - Methode de Schwydlar et regles de ponderation: *Revue de l'Institut FranHais de Petrole*, v. 22, p. 443-466.
- Matheron, G., and Marsily, G. de, 1980, Is Transport in Porous Media always diffusive? - A counter example: *Water Resources Research*, v. 16, no. 5, p. 901-917.
- Matheron, G.; Beucher, H.; Fouquet, C. de; Galli, A.; Guerillot, D.; and Ravenne, C., 1987, Conditional simulation of fluvio-deltaic reservoirs: SPE paper 16753 presented at the 1987 SPE Annual Technological Conference and Exhibition, Dallas, Tex., September 27-30.
- McDonald, M.G., and Harbaugh, A.W., 1988, A modular three-dimensional finite difference groundwater flow model: *in* Techniques Of Water Resource Investigations of the U.S. Geological Survey, Book 6, Chapter A1.
- McGowen, J.H., and Garner, L.E., 1971, Physiographic features and stratification types of coarse grained pointbars - Modern and ancient examples: *Sedimentology*, v. 14, p. 77-111.
- Miall, A.D., 1988, Reservoir heterogeneities in fluvial sandstones - Lessons learned from outcrop studies: *American Association of Petroleum Geologists Bulletin*, v. 72, no. 6, p. 682-697.
- Mishra, S.; Parker, J.C.; and Singhal, N., 1989, Estimation of soil hydraulic properties and their uncertainty from particle size distribution data: *Journal of Hydrology*, v. 108, p. 1-18.
- Molz, F.J.; Morin, R.H.; Hess, A.E.; Melville, J.G.; and Guven, O., 1989, The impeller meter for measuring aquifer permeability variations - Evaluation and comparison with other tests: *Water Resources Research*, v. 25, no. 7, p. 1677-1683.
- Molz, F.J., and Young, S.C., 1993, Development of and application of borehole flowmeters for environmental assessment: *The Log analyst*, v. 34, no. 1, p. 13-23.
- Montadert, L., 1963, La sedimentologie et l'etude detaillee des heterogeneite's d'un reservoir: *Revue l'Institut FranHais de Petrole*, v. 18, p. 241-257.
- Muskat, M., 1949, *Physical principles of oil production*: New York, McGraw-Hill.
- Muto, G.R., and Gunn, J., 1986, A study of late Quaternary environments and early man - Phase I final report (with) project narrative and appendices A-D: U.S. Army Corps of Engineers, Mobile and Nashville Districts.
- Naff, R.L., 1991, Radial flow in heterogeneous porous media - An analysis of specific discharge: *Water Resources Research*, v. 27, no. 3, p. 307-316.
- Narasimhan, T.N., and Ming Zhu, 1993, Transient flow of water to a well in an unconfined aquifer - Applicability of some conceptual models: *Water Resources Research*, v. 29, no. 1, p. 179-191.
- Neuman, S.P., 1972, Theory of flow in unconfined aquifers considering delayed response of the water table: *Water Resources Research*, v. 8, no. 4, p. 1031-1045.
- Neuman, S.P., 1974, Effect of partial penetration on flow in unconfined aquifers considering delayed gravity response: *Water Resources Research*, v. 10, no. 2, p. 303-312.
- Neuman, S.P., 1975, Analysis of pumping test data from anisotropic unconfined aquifers considering delayed gravity response: *Water Resources Research*, v. 11, no. 2, p. 329-342.

- Neuman, S.P., 1982, Statistical characterization of aquifer heterogeneities - An overview: Boulder, CO, Geological Society of America, Special Paper 189.
- Neuman, S.P.; Winter, C.L.; and Newman, C.M., 1987, Stochastic theory of field-scale Fickian dispersion in anisotropic porous media: *Water Resources Research*, v. 23, no. 3, p. 453-466.
- Noetinger, B., 1994, The effective permeability of a heterogeneous medium: *Transport in Porous Media*, v. 15, no. 2, p. 99.
- Nwankor, G.I.; Gillham, R.W.; Van der Kamp, G.; and Akidunni, F.F., 1992, Unsaturated and saturated flow in response to pumping of an unconfined aquifer - Field evidence of delayed drainage: *Ground Water*, v. 30, no. 5, p. 690-700.
- Oert, B. van, 1988, Lessons learned in North Sea oil field developments: *Journal of Canadian Petroleum Technology*, v. 27, no. 6, p. 123-132.
- Olea, R.A., 1984, Systematic sampling of spatial functions: Kansas Geological Survey, Series on Spatial Analysis, v. 7.
- Oliver, D. S., 1990, The averaging process in permeability estimation from well-test data: *SPE Formation Evaluation*, September, p. 319-324.
- Parfit, M., and Richardson, J., 1993, Trouble waters run deep, *in* Water, the power, promise, and turmoil of North America's fresh water: National Geographic, Special Edition, v. 184, no. 5A.
- Pirson, S.J., 1983, *Geologic well log analysis*: Houston/London, Gulf Publishing Company..
- Poeter, E., and Townsend, P., 1991, Multiple indicator conditional simulation of a section of the unconfined aquifer, Hanford site, Washington, USA: Proceedings of the 5th Annual Canadian American Conference on Hydrogeology, Calgary, September 18-20, 1990, NWWA, Dublin (Ohio).
- Prickett, T.A., 1965, Type-curve solution to aquifer tests under water table condition: *Ground Water*, v. 3, no. 3, p. 5-14.
- Prickett, T.A.; Naymik, T.G.; and Lohnquist, C.G., 1981, A 'Random Walk' solute transport model for selected groundwater quality evaluations: Illinois State Water Survey (ISW), Bulletin 65.
- Ptak, T., and Teutsch, G., 1994, Forced and natural gradient tracer tests in a highly heterogeneous porous aquifer - instrumentation and measurements: *Journal of Hydrology*, v. 159, p. 79.
- Ravenne, C., and Beucher, H., 1988, Recent development in description of sedimentary bodies in a fluvio deltaic reservoir and their 3D conditional simulations: SPE paper 18310 presented at the 1988 SPE Annual Technological Conference and Exhibition, Houston, Tex., October 2-5.
- Reading, H.G. 1986, *Sedimentary Facies and Environments*: Blackwell, p. 36-37.
- Rehfeldt, K.R.; Gelhar, L.W.; Southard, J.B.; and Dasinger, A.M., 1989a, Estimates of macro-dispersivity based on analyses of hydraulic conductivity variability at the MADE site: Interim Report EN-6405, Electric Power Research Institute.
- Rehfeldt, K.R.; Hufschmied, P.; Gelhar, L.W.; and Schaefer, M.E., 1989b, Measuring hydraulic conductivity with the borehole flowmeter: Electric Power Research Institute Topical Report, EN-6511, Stanford, Calif..
- Rehfeldt, K.R.; Boggs, J.M.; and Gelhar, L.W., 1992, Field study of dispersion in a heterogeneous aquifer - 3-Geostatistical analysis of hydraulic conductivity: *Water Resources Research*, v. 28, no. 12, p. 3309-3324.
- Reeves, M.; Ward, D.S.; and Runkle, G.E., 1984, SWIFT II self-teaching curriculum - Illustrative problems for the Sandia Waste Isolation Flow and Transport model for fractured media: Sandia National Laboratories, NRC FIN No. A1166, Chapter 3, p. 28-37.
- Reineck, H.E., and Sing, I.B., 1980, *Depositional Sedimentary Environment*: Berlin, Springer-Verlag.

- Ridder, N.A. de, and Wit, K.E., 1965, A comparative study of the hydraulic conductivity of unconsolidated sediments: *Journal of Hydrology*, v. 3, p.180-206.
- Sagar, R.K., 1993, Reservoir description by integration of well-test data and spatial statistics: Tulsa, Okla., University of Tulsa, Ph.D. dissertation.
- Sagar, R.K.; Kelkar, B.G.; and Thompson, L.G., 1993, Reservoir description by integration of well-test data and spatial statistics: SPE paper 26462 presented at the 1993 SPE Annual Technological Conference and Exhibition, Houston, Tex., October 3-6.
- Sanchez Villa, 1993, Personal communication.
- Schad, H., and Teutsch, G., 1994, Effects of the investigation scale on pumping tests in heterogeneous porous aquifers: *Journal of Hydrology*, v. 159, p. 61.
- Streltsova, T.D., 1972, Unsteady radial flow in an unconfined aquifer: *Water Resources Research*, v. 8, p. 1059-1066.
- Streltsova, T.D., 1988, *Well Testing in Heterogeneous Formations - An Exxon Monograph*: New York, John Wiley & Sons, 413 pp.
- Sudicky, E.A., 1986, A natural gradient experiment on solute transport in a sand aquifer - 2-Spatial variability of hydraulic conductivity and its role in the dispersion process: *Water Resources Research*, v. 22, no. 13, p. 2031-2046.
- Swanson, D.C., 1993, The importance of fluvial processes and related reservoir deposits: SPE paper 23722, *Journal of Petroleum Technology*, April, p. 365-377.
- Tetzlaff, D.M., and Harbaugh, J.W., 1989, *Simulation of clastic sedimentation*: New York, Van Nostrand Reinhold.
- Teutsch, G.; Hoffmann, B.; and Ptak, T., 1990, Non-parametric stochastic simulation of groundwater processes in highly heterogeneous porous formations: *Proceedings of the International Conference and Workshop on Transport and Mass Exchange Processes in Sand and Gravel Aquifers*, Ottawa Canada, October 1-4, 1990.
- Theis, C.V., 1935, The Relation between the lowering of the piezometer surface and the rate and duration of discharge of a well using ground-water storage: *Transactions of the American Geophysical Union*, v. 16, p. 519-524.
- Vries, J.J. de, 1982, *Anderhalve eeuw hydrologisch onderzoek in Nederland (150 years hydrological research in the Netherlands)*: Amsterdam, Rodopi. [In Dutch].
- Warren, J.E., and Price, H.S., 1961, Flow in heterogeneous porous media: *Society of Petroleum Engineers Journal*, September, p. 153-169.
- Warren, J.E., and Skiba, F.F., 1964, Macroscopic dispersion: *Society of Petroleum Engineers Journal*, September, p. 215-230.
- Warrick, A.W., and Myers, D.E., 1987, Optimization of sampling locations for variogram calculations: *Water Resources Research*, v. 23, no. 3, p. 496-500.
- Webb, E.K., and Anderson, M.P., 1993, Simulation of preferential flow in three-dimensional heterogeneous random fields with realistic internal architecture: Accepted for publication in *Water Resources Research*.
- Weber, K.J., 1980, Influence of fluid flow of common sedimentary structures in sand bodies: SPE paper 9247 presented at the 1980 SPE Annual Technological Conference and Exhibition, Dallas, Tex., September 21-24.
- Weber, K.J., and Geuns, L.C. van, 1989, Framework for constructing clastic reservoir simulation models: SPE paper 19582, *Journal of Petroleum Technology*, October, 1990, p. 1248.

- Weerts, H.J.T., and Bierkens, M.F.P., 1993, Geostatistical analysis of overbank deposits of anastomosing and meandering fluvial systems - Rhine-Meuse delta (in) The Netherlands: Sedimentary Geology, v. 85, p. 221-232.
- Wietzerbin, L., 1994, Modelisation et parametrisation d'objets naturels de formes complexes en trois dimension - Application a la simulation syochastique de la distribution d'heterogenetes au sein de reservoirs petroliers: Nancy, France, Institute National Polytechnique de Lorraine, Ph.D. dissertation.
- Wietzerbin, L., and Mallet, J.L., 1993, Parameterization of complex 3D heterogeneities - A new CAD approach: SPE paper 26423 presented at the 1993 SPE Annual Technological Conference and Exhibition, Houston, Tex., October 3-6.
- Wu, T.H., S.K. Vyas, and Chang, N.Y., 1973, Probabilistic analysis of seepage: Journal of Soil Mechanics and Foundation Division, Proceedings of the American Society of Civil Engineers, v. 99, no. SM4.
- Young, S.C., 1991a, A site characterization methodology for aquifers in support of bioreclamation activities - Volume I-Well network design, well equations and aquifer multi- and single-well tests: Tyndall AFB, Fla., US Air Force Engineering and Services Center.
- Young, S.C., 1991b, A site characterization methodology for aquifers in support of bioreclamation activities - Volume II-Borehole flowmeter technique, tracer tests, geostatistics, and geology: Tyndall AFB, Fla., US Air Force Engineering and Services Center.
- Young, S.C., 1995, Characterization of high-K pathways by borehole flowmeter and tracer tests: Ground Water, v. 33, no. 2, p. 311-318.
- Young, S.C., and Pearson, H.S., 1990, Application of an electromagnetic borehole flowmeter to predict three-dimensional solute transport in a heterogeneous aquifer: Proceedings of the 83rd Annual Meeting of the Air and Water Management Association, Pittsburgh, Penn., June 24-29, Paper 90-8.3.
- Young, S.C., and Waldrop, W.R., 1989, An electromagnetic borehole flowmeter for measuring hydraulic conductivity variability, *in* Conference on New Field Techniques for Quantifying the Physical and Chemical Properties of Heterogeneous Aquifers, Proceedings: Dallas, Tex., Water Well Journal Publishing Company, p. 497-508.
- Young, S.C.; Herweijer, J.C.; and Benton, D.J., 1991, Geostatistical evaluation of a three-dimensional hydraulic conductivity field in an alluvial aquifer: Proceedings of the 5th Annual Canadian American Conference on Hydrogeology Calgary, September 18-20, 1990, NWWA, Dublin (Ohio).
- Zijl, W., and Nawalany, M., 1993, Natural groundwater flow: Boca Raton, Fla., Lewis Publishers.

**ACKNOWLEDGMENT**

I would like to show my appreciation to the following persons and organizations who contributed to this dissertation:

Professor J. J. de Vries (Free University, Amsterdam) who enthusiastically supervised the work that led to this dissertation, and always urged me to see the general (and historical) perspective of research results; the late professor N. A. de Ridder whose able enthusiasm to integrate the reality of field data with the abstraction of mathematical methods has been an example for this dissertation and my professional life as a hydrogeologist; professor G. de Marsily (Université Pierre et Marie Curie, Paris VI) who offered many ideas and suggestions during the research period in France and who later acted as *referent*; Professor G. Teutsch (Universität Tübingen) who also acted as *referent*; S.C. Young (formerly at Tennessee Valley Authority) who allowed me to share in the Columbus effort and with whom I co-authored several papers that contain some of material presented in this dissertation; S. Livingston who helped to improve the English manuscript.

Many colleagues with whom I cooperated in project teams contributed to my formation. I would like to highlight the following persons: D. Ward (GeoTrans) helped me to further understand the theory and mechanics of groundwater flow modeling; C. Hemker provided advice and critical reviews with respect to pumping test interpretation and groundwater modeling efforts; A. Haas (Elf Aquitaine Production) finally taught me the “easy way” of applying geostatistics; and K. Hird (Amoco) shared his extensive experience in reservoir engineering with me.

The Tennessee Valley Authority management is thanked for allowing me to work with the data collected at the Columbus one-hectare test-site and for funding some project work that was integrated in this dissertation. I am grateful to the European Union Fossil Energy Research (Joule) program for funding a two-year research period, part of which was used to finalize the research for this dissertation. My appreciation also goes to the management of Elf Aquitaine Production for hosting me during that two year tenure.

My parents have been instrumental and very supportive of my academic endeavors. They gave me, amongst many other benefits, very liberal opportunities for education, and supported the idea that school and study ought to be gratifying and enjoyable. My mother shepherded with her patience and enthusiasm, my early scientific training in school and she exemplified a practitioner of exact sciences. My father stimulated thinking about the intertwining of society, politics, and technology. My sisters (Marga, Rosien and Paula), aunt (C.J. Sniijders) along with other relatives and friends, provided indispensable practical and emotional support during the many years of study.

Geraldine, Leonora, and Philemon, you are still very young and for you it has not been easy to understand why delightful activities, such as our weekly trip to the swimming pool, swinging, and bed-time reading, sometimes had to suffer because I was working on more “important” matters like running computers, writing papers, and producing graphs.

Karin, from the moment that we met, you have been living also with this dissertation. That part has not always been easy. Much thanks for all your love and patience.

**DANKWOORD**

Graag wil ik de volgende personen en instanties bedanken die onontbeerlijk zijn geweest voor het tot stand komen van dit proefschrift:

Professor J. J. de Vries, die mij sterk gestimuleerd heeft bij het tot stand komen van dit proefschrift, en gedurende alle fasen van het werk een kritische begeleider is geweest, benadrukkend dat onderzoeksresultaten in een algemeen (en ook historisch) perspectief geplaatst moeten worden; Wijlen professor N.A. de Ridder, wiens wijze lessen en bedachtzaam commentaar een grote inspiratie zijn geweest voor dit proefschrift (en het professionele bestaan als hydrogeoloog) en van wie ik heb geleerd om bij het gebruik van mathematische en computermethoden vooral niet uit het oog te verliezen waar het in de (veld) realiteit om gaat; professor G. de Marsily (Université Pierre et Marie Curie, Paris VI), die gedurende de onderzoeksperiode in Frankrijk altijd beschikbaar was met grondig commentaar en suggesties, en als referent zijn oordeel over dit proefschrift heeft geveld; professor G. Teutsch (Universität Tübingen), die ook als referent is opgetreden; S.C. Young (voorheen verbonden aan de Tennessee Valley Authority), die altijd bereid was me in het werk op het Columbus proefveld te betrekken en met wie ik samen verscheidene artikelen heb geschreven waarvan gedeelten in dit proefschrift zijn verwerkt; S. Livingston, die geholpen heeft om het Engels te perfectioneren.

Mijn dank gaat ook uit naar de vele collega's met wie ik in projectgroepen nauw en leerzaam heb samengewerkt, in het bijzonder: D. Ward (GeoTrans), die mij verder begrip heeft bijgebracht betreffende de theorie en praktijk van het modelleren van grondwaterstroming; C. Hemker die vele kundige adviezen verstrekke aangaande pompproeven en grondwatermodellen; A. Haas (Elf Aquitaine Production), die mij er uiteindelijk van heeft overtuigd dat geostatistiek ook op een simpele manier kan worden toegepast; K. Hird (Amoco), die mij behulpzaam is geweest met zijn brede kennis van olie-reservoir engineering.

Het management van de Tennessee Valley Authority ben ik dank verschuldigd voor het mogelijk maken van mijn participatie in het werk op het Columbus proefveld en voor de incidentele financiële steun voor het werk aan dit proefschrift. Het Joule (fossiele energie) onderzoeksprogramma van de Europese Unie wordt bedankt voor de financiële ondersteuning van de twee-jarige onderzoeks periode, die gedeeltelijk gebruikt is om het onderzoek voor dit proefschrift af te ronden. Voorts dank ik het management van Elf

Aquitaine Production (Pau, Frankrijk) voor de ter beschikking gestelde faciliteiten gedurende deze laatste periode van het onderzoek.

Mijn ouders hebben grote steun verschaft bij de totstandkoming van dit proefschrift. Ik waardeer het enorm dat zij altijd het belang hebben ingezien van intellectuele vorming, en het feit dat vreugde en voldoening een belangrijke component daarvan zijn. Mijn moeder gaf een voorbeeld als beta georiënteerd academica, en heeft met veel geduld bijgedragen aan mijn scholing, variërend van wiskunde tot Grieks en Latijn. Mijn vader heeft mijn denken aangaande de rol van technologie en onderzoek in samenleving en politiek gestimuleerd. Mijn zussen (Marga, Rosien en Paula), tante (C.J. Snijders), en vele andere familieleden en vrienden bedank ik voor de steun die ik heb mogen ontvangen gedurende vele jaren van studie.

Geraldine, Leonora en Philemon, jullie zijn nog zeer jong en hebben wellicht moeite te begrijpen waarom zulke leuke activiteiten zoals onze wekelijkse gang naar het zwembad, schommelen en voorlezen, soms hebben moeten lijden omdat ik moest werken aan “belangrijkere zaken” zoals computerprogrammeren, artikelen schrijven en het maken van grafieken.

Karin, vanaf het moment dat wij elkaar hebben ontmoet, heb je ook min of meer met dit proefschrift geleefd. Dat gedeelte is zeker niet eenvoudig geweest. Daarom geweldig bedankt voor je liefde en geduld.

**CURRICULUM VITAE**

Joost Christiaan Herweijer was born in Utrecht (The Netherlands) on 18 January 1957. In 1978 he obtained a BS degree in Geology at the State University of Utrecht. Between 1977 and 1980 he worked part-time as field assistant for the geothermal research program conducted by TNO Groundwater Survey. In 1983 he obtained the Doctorandus degree Hydrogeology (Free University Amsterdam) with major second subject Exploration-Geophysics (State University Utrecht). His graduate study covered field investigations and a numerical model to assess the fate and transport of groundwater pollution resulting from manure disposal. From 1982 to 1985 he was self-employed at Groundwater Data Systems. Subsequently he worked as research petroleum geologist for Royal Dutch Shell Exploration and Production Laboratory. Between 1988 and 1992 he worked as hydrogeologist for GeoTrans Inc. (USA) on numerical models and other aspects of groundwater contamination cases. From 1992 to 1994 he was exchange scientist (in the framework of the European Union research program), hosted by the petroleum engineering research laboratory of Elf Aquitaine (Pau, France). He is currently group modeling manager and principal hydrogeologist at Water Management Consultants (Denver, USA), working on a variety of water resources projects and environmental impact studies in the USA, South-America, and Europe.

Joost Christiaan Herweijer is op 18 januari 1957 geboren te Utrecht. In 1978 behaalde hij het kandidaatsexamen Geologie 4 aan de Rijks Universiteit Utrecht. Gedurende de periode 1977 tot 1980 was hij als werkstudent (veldassistent) betrokken bij geothermisch onderzoek verricht door de Dienst Grondwater Verkenning van TNO. In 1983 behaalde hij het doctoraalexamen hydrogeologie (Vrije Universiteit Amsterdam) met groot bijvak exploratie-geofysica (Rijks Universiteit Utrecht). Het afstudeeronderwerp betrof veldonderzoek en een numeriek model ter beschrijving van grondwatervervuiling als gevolg van overbemesting op de Veluwe. Vanaf 1982 tot 1985 was hij eigenaar van Groundwater Data Systems. Daarna werkte hij als research petroleum geoloog bij het Koninklijke Shell Exploratie en Productie laboratorium (KSEPL). Vanaf 1988 tot 1992 werkte hij als hydrogeoloog bij GeoTrans Inc. (VS) aan numerieke modelstudies en diverse andere aspecten van grondwaterverontreiniging. Tussen 1992 en 1994 werkte hij als *exchange scientist* (in het kader van het Europees onderzoeks programma Joule) verbonden aan het *petroleum engineering* onderzoekslaboratorium van Elf Aquitaine Production (Pau, Frankrijk). Sinds 1994 is hij verbonden aan Water Management Consultants (Denver, VS), waar hij werkt als *group modeling manager* en *principal hydrogeologist* aan diverse water voorzienings projecten en milieu effect studies in de VS, Zuid-Amerika, en Europa.

# Boekbespreking

**Sedimentary Heterogeneity and Flow towards a Well; Assessment of Flow Through Heterogeneous Formations**, door: J.C. Herweijer

Op dinsdag 7 januari 1997 promoveerde Joost Christiaan Herweijer (Utrecht, 1957) aan de Vrije Universiteit op een proefschrift met de bovenstaande titel. Het promotie-onderzoek had ten doel om methoden te ontwikkelen voor het beschrijven van heterogene aquifers en van de invloed van heterogeniteit op de stroming van grondwater. Met name is onderzocht of het mogelijk is om op basis van pompproeven modellen te bouwen waarmee betrouwbare voorspellingen gedaan kunnen worden over het transport van verontreinigingen in sterk heterogene aquifers. Promotor was prof. J.J. de Vries; prof. G. de Marsily van de Université Pierre et Marie Curie, Paris VI en prof. G. Teutsch van de Universität Tübingen traden op als referenten.

Herweijer is geoloog; hij studeerde exploratiegeologie aan de Rijksuniversiteit Utrecht en hydrogeologie aan de VU. Hij werkte eerst enige tijd zelfstandig en daarna als research-petroleum-geoloog bij Shell, als grondwaterhydroloog bij GeoTrans Inc. (VS), als exchange scientist bij Elf Aquitaine (Fr) en momenteel als group modeling manager en principal hydrogeologist bij Water Management Consultants (VS).

Hoewel de serieuze belangstelling voor contaminant transport nog maar zo'n vijftien jaar geleden ontwaakte, is naar mijn inschatting aan geen ander onderdeel van de grondwaterhydrologie zoveel geld en aandacht besteed. De literatuur over het onderwerp is haast onafzienbaar. Dit is een sterke aanwijzing dat de theorie van het

stoftransport a) voor de praktijk erg belangrijk is, en b) rammelt. Voor een onderzoeker is dat weliswaar een uitdaging, maar het is moeilijk om nog een originele bijdrage te leveren, en dat is toch de eis die aan een promotie-onderzoek gesteld wordt.

Herweijer heeft de uitdaging aanvaard en hij is er inderdaad in geslaagd om een nieuw idee te lanceren en toepasbaar te maken: hij toont een verband aan (althans in freatische aquifers) tussen de snelheid waarmee een verstoring van de stijghoogte zich in de ondergrond voortplant en de snelheid waarmee een stof getransporteerd wordt. Hierdoor kan uit nauwkeurige stijghoogtewaarnemingen tijdens een pompproef informatie afgeleid worden over voorkeurswegen van grondwaterstroming. Dit idee is in het proefschrift ingebed in een meer algemene filosofie over het omgaan met veelsoortige gegevens om tot een zo klein mogelijke onzekerheid te komen. Met name benadrukt Herweijer - van een geoloog verwachten we ook niet anders - het belang van sedimentologische kennis en het gebruik daarvan om modellen van een heterogeen aquifer te bouwen. (Het woord aquifer is bij Herweijer consequent geslachtelijk onzijdig.)

De presentatie van het promotie-onderzoek is erg formeel: in een inleidend hoofdstuk begint Herweijer met het formuleren van een nulhypothese die - gesteld dat hij verworpen moet worden - drie andere hypothesen uitlokt die voldoende stof opleveren voor het verdere onderzoek. Zo'n opzet doet mij als technisch opgeleide hydroloog wat gekunsteld aan, vooral omdat de nulhypothese bij voorbaat tot falsificatie gedoemd was. In het eigenlijke proefschrift komen de hypothesen trouwens nauwelijks meer aan bod; dat gebeurt pas weer in een concluderend hoofdstuk, waardoor het vermoeden rijst dat ze wellicht naderhand opgesteld zijn. Is dit misschien de wetenschappelijke methode, die aan technische universiteiten

niet onderwezen wordt? Hoe het ook zij, ik zet me graag over zulke cultuurverschillen heen, want het proefschrift als geheel is zeer lezenswaardig.

Het onderzoek van Herweijer speelt zich af op de Columbus test site in Mississippi, die deel uitmaakt van een militair vliegveld. Onder contaminant hydrologen is deze locatie berucht, al is het niet om zijn buitensporige verontreiniging. (Protocollair werden Amerikaanse militaire vliegtuigen volgetankt tot ze overliepen. Hoe zou het met de voormalige Amerikaanse luchtmachtbasis Soesterberg gesteld zijn)? Zijn faam dankt Columbus aan het feit dat de stochastische theorieën voor stoftransport, die op bekende proeflocaties als Borden en Cape Cod heel behoorlijk werkten, hier volstrekt onderuit gingen. De reden is dat de ondergrond in Columbus veel heterogener is dan in Borden of Cape Cod. Stochastische theorieën moeten het hebben van ergodiciteit, wat wil zeggen dat de statistische eigenschappen op iedere plaats gelijk moeten zijn. In Columbus is een duidelijke geologische structuur aanwezig, zoals mooi blijkt op een luchtfoto (pagina 83). Aan de oppervlakte is een voormalige riviermeander te zien, met alle bijbehorende structurelementen. Op enige diepte (niet op de foto, dus) bevindt zich een ouder alluvium, dat opgebouwd is door een vlechtende rivier. Dit is het punt waarop de sedimentoloog van pas komt. Herweijer begint hoofdstuk 2 met een kort overzicht van sedimentologische kennis en begrippen die gebruikt kunnen worden om uit een beperkte hoeveelheid boringen een goed ruimtelijk beeld van een gebied op te bouwen. Deze kennis is vooral ontwikkeld binnen de olie-industrie. Het idee is dat sedimenten niet ad random afgezet worden, maar volgens systematische patronen, die in afgezwakte vorm als patronen in de hydraulische doorlatendheid worden teruggevonden. De geometrische wetmatigheden van zulke patronen zijn uitgebreid bestudeerd op plaatsen waar de sedimenten van

nature of in groeven dagzomen. Er zijn onder meer empirische formules afgeleid die een relatie leggen tussen de breedte en de diepte van een opgevlude rivierbedding. Zulke sedimentologische modellen zijn vanzelfsprekend onvolledig, maar ze bevatten toch veel te veel detail om een eenvoudige statistische karakterisering van de doorlatendheid te billijken. Hoofdstuk 2 gaat voort met een korte beschrijving van geostatistische methoden waarmee uit de sedimentologische gegevens driedimensionale modellen van de ondergrond opgebouwd kunnen worden. Aan de orde komen onder meer het werken met variogrammen, het genereren van Gaussische velden en het omgaan met geometrische objecten. Daarna komen bestaande technieken aan bod waarmee effectieve parameters voor stroming en transport geschat kunnen worden. Doorlatendheden, dus, en dispersiecoëfficiënten. Tenslotte beschrijft hoofdstuk 2 het gebruik van pompproeven onder heterogene omstandigheden. Dit is een belangrijke opmaat voor het feitelijke promotie-onderzoek. Herweijer wijst er terecht op dat juist de verschillen tussen gemeten tijd-stijg-hoogtelijnen en standaardkrommen voor het interpreteren van pompproeven interessante informatie opleveren over de heterogene aard van de ondergrond. Vooral aan de tijdafgeleide van de verlagingslijnen valt veel te zien. Het duurde even voordat ik het kon appreciëren. Ik heb heel wat pompproeven onder ogen gehad, maar het tijdafhankelijke deel van de waarnemingskrommen heb ik altijd gezien als een vervelende complicatie; een hindernis die je nu eenmaal moest nemen omdat er anders geen  $kD$ - en  $c$ -waarden berekend konden worden. Bergingscoëfficiënten beschouwde ik als afval, dat verder nergens toe diende. Herweijer grijpt juist de berekende bergingscoëfficiënten (en dan vooral onwaarschijnlijke uitkomsten) aan om conclusies te trekken over de heterogeniteit van de ondergrond. In afwijking van de klassieke toepassing van

pompproeven is dus niet het latere deel, maar juist het begin van de proef van groot belang. Naarmate een pompproef langer duurt betast hij een groter deel van zijn omgeving, waardoor lokale effecten uitdempenen. De verlagingslijnen gaan zich dan volgens de 'homogene' theorie gedragen, maar de informatie over heterogeniteiten verdwijnt.

We zijn inmiddels op een derde van het proefschrift, en tot nu toe is alleen reeds bestaande kennis gereproduceerd. Is dat erg? In een recent nummer van een engels-talig tijdschrift verbaasde de recensent van het proefschrift van Marc Bierkens zich over deze opzet van Nederlandse dissertaties. Het is in de Angelsaksische wereld kennelijk geen gebruik om eerst het werk van anderen te presenteren. Laten we dit nationale trekje vooral blijven koesteren! Een promovendus is jarenlang intensief bezig met zijn vak. Tegen de tijd dat hij zijn werk succesvol afrondt hoort hij tot de autoriteiten binnen zijn specialisme. Per definitie is zijn werk dan nog niet tot de studieboeken doorgedrongen. Wie anders dan juist hij is in staat om zo'n monografie te schrijven, waardoor het eigenlijke promotiewerk voor een breed publiek toegankelijk wordt? De afzonderlijke onderdelen van hoofdstuk 2 zijn niet nieuw, maar de manier waarop ze zijn samengebracht is dat wel. Door zijn overzichtelijke opzet en zijn schat aan referenties naar sleutel literatuur zou dit deel van Herweijers proefschrift zo als een syllabus voor een cursus over heterogene media kunnen dienen. Ik beveel dit hoofdstuk van harte ter lezing aan.

De rest van het proefschrift, de eigenlijke dissertatie, beschrijft in detail hoe de theorie van hoofdstuk 2 is toegepast op het proefterrein. De proeflocatie van Herweijer is niet de MADE-locatie waarover inmiddels veel gepubliceerd is in Water Resources Research. Het is een aangrenzend blok van

100 bij 100 m, dat dan ook heel prozaïsch aangeduid wordt als de 1-HA test site. Op basis van een uitgebreide sedimentologische beschrijving is een ruimtelijk netwerk van 37 waarnemingsfilters ontworpen volgens een door Herweijer geschreven computerprogramma, dat gebruik maakt van geostatistische technieken. De opzet was om het effect van heterogeniteiten maximaal in de waarnemingen tot uiting te laten komen. De filters werden in verschillende configuraties onderworpen aan pomp-, injectie-, flowmeter- en tracerproeven.

Hoofdstuk 4 is gewijd aan het interpreteren van de pompproeven en de tracerexperimenten. Hier demonstreert Herweijer hoe pompproeven gebruikt kunnen worden om mogelijke overgangen in doorlatendheid en voorkeurspaden voor grondwaterstroming op te sporen. Het is daarbij belangrijk om met meer dan één aquifermodel te werken. Herweijer gebruikt formules voor een homogene aquifer, voor vertraagde uitlevering, en voor cirkelvormige en rechte grenzen tussen gebieden met verschillende doorlatendheden. Verschillende formules kunnen perfecte fits opleveren, ook al vertegenwoordigen ze tegenstrijdige aannamen over de bodemopbouw. Vaker echter is de fit slecht. Dat moet niet als een mislukking gezien worden, maar juist als een interessante aanwijzing over heterogeniteiten. Vooral formules voor gezoneerde aquifers leveren, samen met sedimentologisch inzicht, veel informatie op over laterale heterogeniteit en voorkeurspaden. Herweijer laat zien dat de conclusies die hij uit de pompproeven trekt, consistent zijn met de resultaten van de tracerproeven. Dat is van praktische betekenis, want tracerexperimenten zijn veel moeilijker uitvoerbaar dan pompproeven, en ze duren véél langer. Intussen blijft het inzicht dat op deze manier verkregen wordt nog in belangrijke mate kwantitatief; er komt geen eenduidig beeld over de bodemopbouw tevoorschijn,

maar het scala van mogelijke beelden wordt sterk ingeperkt.

Als men een saneringssysteem moet ontwerpen voor een aquifer waarvan de opbouw onvoldoende bekend is, kan men op grond van statistische kentallen van de doorlatendheid alternatieve numerieke modellen bouwen om de pompstrategie te kiezen die de grootste kans van slagen heeft. Dit is vaker vertoond (al ken ik in Nederland geen praktische voorbeelden; alleen theoretische. Je zou toch denken dat het voor een bedrijf als de NS van economisch belang is om de pompstrategie bij saneringsoperaties te optimaliseren). Herweijer wil dit ook doen, maar dan rekening houdend met alle informatie die hij vergaard heeft. Dit werk wordt voorbereid met een geostatistische analyse van de data (hoofdstuk 5). Om bestaande opschalings-theorieën te mogen toepassen, moet uitgegaan worden van een verzameling 'puntgegevens' die statistisch gesproken stationair zijn. De verzameling data als geheel voldoet zeker niet aan de stationariteitseis; zoveel is op grond van geologisch inzicht bij voorbaat duidelijk. Herweijer verdeelt zijn data in subsets, overeenkomstig de verschillende sedimentologische eenheden. Logischerwijs is de kans dat nu aan de eis voldaan is veel groter, maar er is geen definitief bewijs voorhanden. De data zijn ook zeker geen puntgegevens: flowmetertests geven weliswaar een behoorlijk gedetailleerd inzicht in doorlatendheidscontrasten, maar ze hebben toch betrekking op een gebied van misschien wel 25 meter rondom de putten. Niettemin worden op deze basis kansverdelingen en variogrammen van de puntdoorlatendheid vastgesteld, waarna met verschillende alternatieve opschalingstechnieken effectieve stromings- en transportparameters voor de 1-HA test site berekend worden.

De tot nu toe beschreven werkzaamheden waren voorbereidingen voor het modelonderzoek, dat in hoofdstuk 6 gepresenteerd wordt. Hier bouwt Herweijer met MODFLOW vier verschillende numerieke modellen die 'geïnspireerd' zijn door de verzamelde gegevens. Het doel van deze exercitie is om na te gaan of op basis van de uitkomsten van de pompproeven het aantal mogelijke voorstellingen van de werkelijkheid sterk ingeperkt kan worden. Jammer genoeg blijkt het niet haalbaar te zijn om de gemeten verlagingslijnen en tracerdoorbraken te simuleren; Herweijer vermeldt althans dat hij daartoe geen poging gedaan heeft, omdat de beschikbare set gegevens daarvoor ontoereikend is (!). In de plaats daarvan komt een gestileerde voorstelling van de werkelijkheid, die toch wel veel trekken met de onderzoekslocatie gemeen heeft. De vier modellen zijn: een deterministisch model dat schematische versies van de belangrijkste sedimentologische eenheden bevat, ieder met een constante doorlatendheid; een eenvoudig geostatistisch 'objectmodel', waarin verschillende rechthoekige elementen met een relatief hoge doorlatendheid willekeurig in afmetingen en richting kunnen variëren; een Gaussisch model waarin de doorlatendheid van modelblok tot modelblok varieert; en een genest Gaussisch model, feitelijk het deterministische model, maar nu met variërende doorlatendheden binnen de sedimentologische eenheden. Met deze modellen worden pompproeven en tracerexperimenten nagebootst en de reacties worden kwalitatief vergeleken met de veldwaarnemingen. Het eerste, deterministische, model blijkt het karakter van de gemeten verlagingslijnen goed na te bootsen. Het toevoegen van doorlatendheidsvariëaties binnen de sedimentologische eenheden (vierde model) levert niet veel extra op. In de praktijk zal het vaak ontbreken aan gegevens die nodig zijn voor een deterministisch model. In die situatie is men wel aangewezen op modellen

van het type twee en drie. In het geval van de 1-HA test site blijkt het objectmodel, dat toch enigszins rekening houdt met de sedimentologische opbouw, het meest realistisch. Het Gaussisch model biedt een zeer grote variatie aan mogelijkheden, waarvan sommige wel en andere niet kwalitatief overeenstemmen met de bemeeten werkelijkheid. In principe zou men het aantal mogelijke Gaussische modellen moeten kunnen inperken door de modelresultaten te vergelijken met de metingen, maar dat blijkt toch niet goed te lukken. Verder blijkt het begrip dispersie in de gegeven heterogene omstandigheden van weinig nut te zijn. De moraal is dat de onzekerheid sterk afneemt naarmate er meer geologische informatie in het model verwerkt wordt, ook al is die niet zo precies. Zonder op het werk van Herweijer te willen afdingen moet ik zeggen dat ik dit resultaat niet verrassend vind. Wat me wel hevig intrigeert is dat er in alle modellen, realistisch of niet, een duidelijke relatie bestaat tussen het eerste moment waarop de verlaging in een peilbuis 'doorbreekt' en het moment waarop het front van de tracer aankomt. (Ik haalde dat aan het begin van deze boekbespreking al naar voren.) In Herweijers woorden: "It can be concluded that detailed multi-well pumping tests are a useful tool to predict tracer transport and/or to characterize preferential flowpaths for a large ensemble of model realizations. The only measurement required is the time when drawdown due to pumping exceeds a given threshold. For all heterogeneity models analyzed, it is shown that early drawdown breakthrough coincides with early tracer breakthrough". Deze claim gaat me wel wat te ver, of ik lees het verkeerd. De eerste doorbraak van de verlaging is een kwestie van seconden tot minuten, terwijl de eerste doorbraak van de tracer enkele tot vele dagen vergt. Ik denk dat men het zo moet opvatten: als in peilbuis A de verlaging  $x$  maal zo laat begint als in peilbuis B, dan zal de tracerdoorbraak in

peilbuis A ook  $x$  maal zo lang op zich laten wachten als de doorbraak in peilbuis B. Ik vind dit helemaal niet vanzelfsprekend. Hoe komt het? Is dit een toevallig resultaat voor de 1-HA test site of gaat dit overal op? Ik brand van nieuwsgierigheid naar een mathematisch onderbouwde verklaring, want dan vertrouw ik het pas. Maar waarschijnlijk ligt dat minder in de aard van een geoloog. Is het misschien iets voor een promovendus in een exactere discipline? Hoe dan ook, dit onderzoek werpt nieuwe vragen op, en dat is een betrouwbaar kenmerk van baanbrekend werk.

Het proefschrift heeft geen ISBN-nummer, maar vermeldt wel Herweijers e-mailadres: [jcherw@worf.omn.com](mailto:jcherw@worf.omn.com).

*Kees Maas*